RADC-TR-76-250
Final Technical Report
August 1976

HYBRID TROPO TRANSMISSION SYSTEM

Raytheon Company

Approved for public release;
distribution unlimited.

ROME AIR DEVELOPMENT CENTER
AIR FORCE SYSTEMS COMMAND
GRIFFISS AIR FORCE BASE, NEW YORK 13441

This report has been reviewed by the RADC Information Office (OI) and is releasable to the National Technical Information Service (NTIS). At NTIS it will be releasable to the general public including foreign nations.

This report has been reviewed and is approved for publication.

APPROVED: Olindo A. Tagliaferri

OLINDO A. TAGLIAFERRI
Project Engineer

APPROVED: Fred I. Diamond

FRED I. DIAMOND
Technical Director
Communications and Control Division

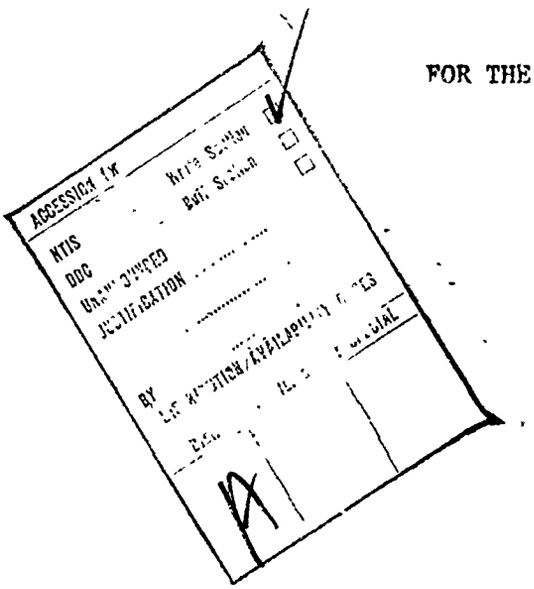

FOR THE COMMANDER: John P. Huss

JOHN P. HUSS
Acting Chief, Plans Office

Do not return this copy. Retain or destroy.

UNCLASSIFIED
SECURITY CLASSIFICATION OF THIS PAGE (When Data Entered)

REPORT DOCUMENTATION PAGE	READ INSTRUCTIONS BEFORE COMPLETING FORM
1. REPORT NUMBER: RADC-TR-76-250	2. GOVT ACCESSION NO. / 3. RECIPIENT'S CATALOG NUMBER
4. TITLE (and Subtitle): HYBRID TROPO TRANSMISSION SYSTEM.	5. TYPE OF REPORT & PERIOD COVERED: Final Technical Report. 15 May 73 - 29 Dec 75
	6. PERFORMING ORG. REPORT NUMBER: N/A
7. AUTHOR(s): Manfred Unkauf, Robert Bagnell	8. CONTRACT OR GRANT NUMBER(s): F30602-73-C-0273
9. PERFORMING ORGANIZATION NAME AND ADDRESS: Raytheon Company, Boston Post Road, Sudbury MA 01776	10. PROGRAM ELEMENT, PROJECT, TASK AREA & WORK UNIT NUMBERS: 65230436 / 04
11. CONTROLLING OFFICE NAME AND ADDRESS: Rome Air Development Center (DCCW), Griffiss AFB NY 13441	12. REPORT DATE: Aug 1976 / 13. NUMBER OF PAGES: 242
14. MONITORING AGENCY NAME & ADDRESS (if different from Controlling Office): Same	15. SECURITY CLASS. (of this report): UNCLASSIFIED / 15a. DECLASSIFICATION/DOWNGRADING SCHEDULE: N/A

16. DISTRIBUTION STATEMENT (of this Report)

Approved for public release; distribution unlimited.

17. DISTRIBUTION STATEMENT (of the abstract entered in Block 20, if different from Report)

Same

18. SUPPLEMENTARY NOTES

RADC Project Engineer: Olindo A. Tagliaferri (DCCW)

19. KEY WORDS (Continue on reverse side if necessary and identify by block number)

Troposcatter Communication
Digital Data Transmission
Hybrid Transmission

20. ABSTRACT (Continue on reverse side if necessary and identify by block number)

This document describes the design, development, laboratory testing, and over-the-air testing of a Digital Data Tropo Transmission System and Hybrid Tropo Transmission System (HTTS). Digital transmission was accomplished at data rates of 1.75, 3.5 and 7.0 Mbps by using the Raytheon Distortion Adaptive Receiver (DAR-IV) modulation/demodulation (modem) technique. Testing of the DAR-IV was performed using the RADC troposcatter media simulator and confirmed by actual over-the-air tests on the AN/MRC-98, AN/TRC-97 and AN/TRC-132 radio equipments

DD FORM 1 JAN 73 1473 EDITION OF 1 NOV 65 IS OBSOLETE

UNCLASSIFIED
SECURITY CLASSIFICATION OF THIS PAGE (When Data Entered)

298 250

in both modes. The test results showed that the DAR-IV technique has the potential to provide quality digital data transmission on both tactical and DCS troposcatter links. Within its multipath spread capabilities, the DAR-IV was shown to typically operate within 3 dB of theoretical. The extent of multipath spread accommodated was found to be approximately equal to the inverse of the transmission bit rate. Design improvements are identified to achieve greater multipath spread capacity at the higher data rates. Hybrid transmission was accomplished by using separate analog and digital subcarriers with conventional FDM/FM modulation for analog traffic of up to 60 voice channels. Testing in the hybrid transmission mode revealed that a dual subcarrier approach was feasible but somewhat inefficient in power utilization.

EVALUATION

The primary method of information transmission on military tropospheric scatter communication links is analog voice with Frequency Division Multiplex/Frequency Modulation (FDM/FM). This method of modulation is subject to gradual equipment degradations and is difficult to secure. Digitized voice with digital data transmission potentially simplifies equipment maintenance and permits cost effective encryption of the transmitted messages.

This report describes the development and test of a digital modulation/demodulation (modem) technique for both tactical and Defense Communication Systems (DCS) troposcatter channels.

This effort was carried out under Task 65230436 and is part of the Wideband Communications in TPO No. 10 Communications Transmission. The modem technique is based on the Distortion Adaptive Receiver (DAR) which operates as an adaptive matched filter to digital pulses that are randomly distorted by the multipath propagation. An experimental, quadruple diversity, simplex model of the DAR known as the DAR-IV was implemented at data rates of 1.75, 3.5 and 7 Mbps to permit testing over a wide range of tactical and DCS path conditions. Testing was performed at all data rates and diversity configurations on the RADC troposcatter media simulator and over-the-air evaluation performed on the RADC Experimental Troposcatter Range. Troposcatter radio equipments used were AN/MRC-98 (L band), AN/TRC-132 (C band) and AN/TRC-97 (C band). Measured performance was generally within 3 db of theoretical for the lower data rates typical of tactical channels. At the higher DCS data

rates, design improvements were identified as required to achieve greater multipath spread capacity.

The report would be beneficial to those involved in imposing performance requirements on both tactical and DCS troposcatter systems.

Olindo A. Tagliaferri

OLINDO A. TAGLIAFERRI
Project Engineer

TABLE OF CONTENTS

TABLE OF CONTENTS
(Continued)

TABLE OF CONTENTS
(Continued)

ILLUSTRATIONS

ILLUSTRATIONS
(Continued)

ILLUSTRATIONS
(Continued)

ILLUSTRATIONS
(Continued)

ILLUSTRATIONS
(Continued)

ILLUSTRATIONS
(Continued)

ILLUSTRATIONS
(Continued)

ILLUSTRATIONS
(Continued)

ILLUSTRATIONS
(Continued)

TABLES

1.0 INTRODUCTION

This report describes the major results of a program whose goal was to develop and test a low cost, high performance technique for digital data transmission on troposcatter channels and also to investigate hybrid techniques for combined digital and analog transmission. The heart of the digital transmission technique investigated is a concept called the Distortion Adaptive Receiver (DAR) invented by Raytheon for digital modulation and demodulation. This digital modem employs time-gated QPSK transmission pulses which minimize the effects of intersymbol interference and permit the implementation of a simple adaptive matched filter receiver.

The development and test of the DAR together with its additional circuitry for hybrid transmission was sponsored by RADC and DCA under Contract F30602-73-C-0273. The DAR experimental model developed provided transmitted data rates of 1.75, 3.5 and 7.0 Mbps without hardware changes by making use of the special properties of the technique. The emphasis in the digital modem development was the transmission of higher data rates, especially 7.0 Mbps, under troposcatter path conditions comparable to those anticipated for the future digital tropo upgrades of the Defense Communication System (DCS).

The experimental model of the DAR developed (known as the DAR-IV) was subjected to both laboratory channel simulator testing and over-the-air testing on two troposcatter test paths each 168 miles in length using the AN/MRC-98 (880 MHz) and AN/TRC-132 (4.8 GHz) radio equipments. Tests were run for non, dual, and quad path diversity and at data rates of 1.75, 3.5, and 7.0 Mbps. Although high path losses and radio equipment failures were encountered during the test program, sufficient data was obtained to demonstrate the high performance potential of the DAR-IV and its ability to transmit data rates up to 7 Mbps on relatively long troposcatter paths.

Additional testing of the DAR-IV modem was sponsored by TRI-TAC/ESD/RADC under Contract F19628-75-C-0103 to evaluate the potential of the technique for tactical applications of data rates of 2.3 Mbps or less. Extensive laboratory channel simulator testing was performed at the 1.75 Mbps data rates over a wide range of multipath profiles and fade rates. Over-the-air testing was also conducted using an 86 mile test path with the AN/TRC-97A radio equipment. Bit error rate over-the-air measurements were interleaved with RAKE multipath measurements to permit direct comparisons between over-the-air and simulator data. Agreement between both sets of measurements was excellent.

Section 2.0 of this report describes the DAR-IV experimental model developed together with its theory of operation. The theoretical performance of the DAR-IV was previously analyzed and reported in a Mathematical Model. Also described in this Section is the back-to-back performance of the DAR-IV and its departure from ideal.

Section 3.0 describes the media simulator test results obtained under both the DCS and tactical channel test conditions. Test results are compared with a performance prediction obtained via Monte Carlo simulation on the digital computer. The DAR-IV shows generally excellent agreement with theory and operation of the adaptive matched filter. The experimental results were used to develop a simple mathematical formula to predict the DAR's performance. This expression is presented in the conclusion of Section 3.

Section 4.0 describes the over-the-air test results on all three troposcatter paths employed using the AN/MRC-98, AN/TRC-132 and AN/TRC-97 radios. Test results are presented as "scatter plots" of 5 minute average bit error rate versus received signal level data points. Curves of ideal modem performance are also shown on the "scatter plots" to permit an evaluation of the level of performance achieved. For the AN/TRC-132, additional measurements of the error distribution histograms are also presented. The results show that the errors tend to occur in bursts and that typically 70% to 90% of the time intervals are error free.

Section 5.0 describes the additional circuitry developed for hybrid digital and analog transmission together with the test results obtained. The tests show it is possible to simultaneously transmit digital and FDM/FM analog signals on separate subcarriers over tropo. The advantage of the technique tested is low digital to analog crosstalk even with large multipath spread and intrinsic diversity gain for the digital signal. Conventional hybrid modulation schemes of data under voice or data over voice in an FDM/FM carrier would not exhibit these benefits. However, the hybrid transmission mode results in a 6 to 8 dB power loss which many DCS transmission links cannot afford.

2.0 THE DAR - GENERAL CHARACTERISTICS

2.1 Basic Operation

The operation of the DAR is illustrated with the aid of Figures 2-1 and 2-2. The transmitted pulse train employs digital PSK modulation of the carrier for optimum detector efficiency and a time gate is employed to provide a null zone or guard time between pulses.

If a narrow RF pulse of duration T is transmitted over the tropo channel, a distorted pulse of duration $T + \Delta$ will be received where Δ is the effective extent of the instantaneous channel impulse response (multipath duration). If a second RF pulse of the same shape but different RF phase is transmitted over the channel after a brief interval, the corresponding distorted received pulse will appear the same as the first one except that it will possess the same RF phase difference as the transmitted pulses. This situation is illustrated in Figure 2-1 for Binary Phase Shift Keying (BPSK) and the corresponding ideal matched filter implementation is also shown. If the dwell between transmitted pulses, Δ, is sufficiently long, the overlap between the distorted received pulses is negligible. Thus, the intersymbol interference between adjacent received pulses can be made negligible. Under these conditions, the matched filter receiver can make optimum use of all of the energy of the received pulse regardless of the distortion present.

This operation has an immediate implication of in-band frequency diversity. That is, as long as the instantaneous channel frequency response is not zero over the entire bandwidth used, some energy will reach the receiver and be optimally detected. Thus, a deep fade can occur only when all parts of the channel transmission bandwidth simultaneously fade. If the allotted bandwidth is larger than the channel "coherent bandwidth" (defined as the distance to the 1/e point of the channel frequency correlation function), then some diversity performance improvement will be realized. Said another way, the fading performance of the DAR will improve (due to in-band diversity) as the channel becomes more distorted within certain bounds (for example, as the path length is increased). A special band-spreading pulse shape can be used with the DAR to provide a reasonable flat transmission spectrum within the allowable radiated bandwidth and thus provides enhanced "in-band" or intrinsic diversity for any data rate.

The key to the implementation of the DAR is the generation of the reference pulse train (see Figure 2-1). This pulse train (at IF) has the identical complex pulse distortion as the received signal but the relative pulse to pulse phase shift (due to digital modulation) is zero, i.e., no digital phase modulation. Further, this reference pulse train must adapt to the time variant distortion of the channel and possess low noise. The technique used to achieve this reference signal is decision directed feed-

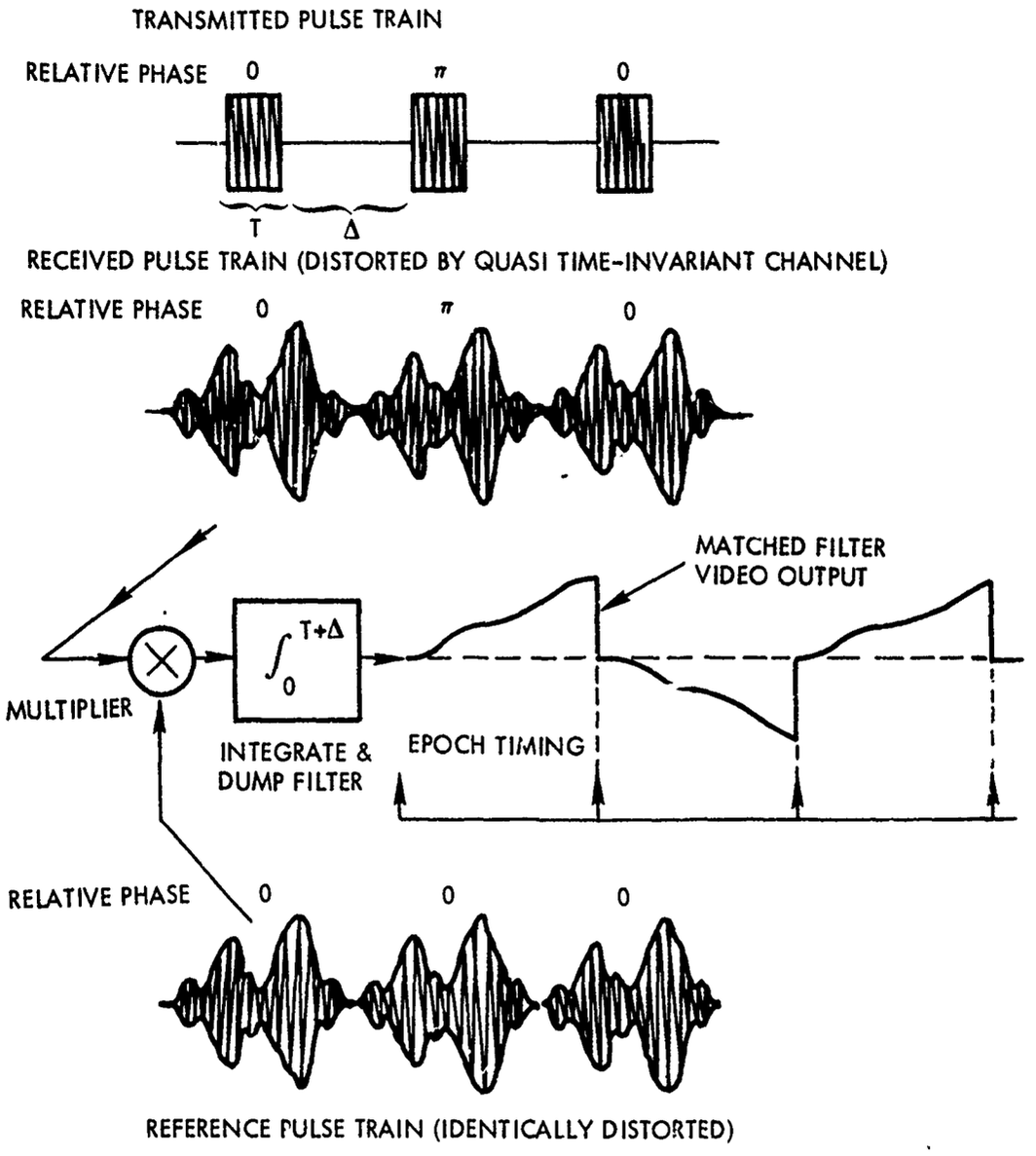

FIGURE 2-1 ILLUSTRATION OF IDEAL TRANSMISSION WAVEFORM AND IDEAL ADAPTIVE MATCHED FILTER RECEIVER

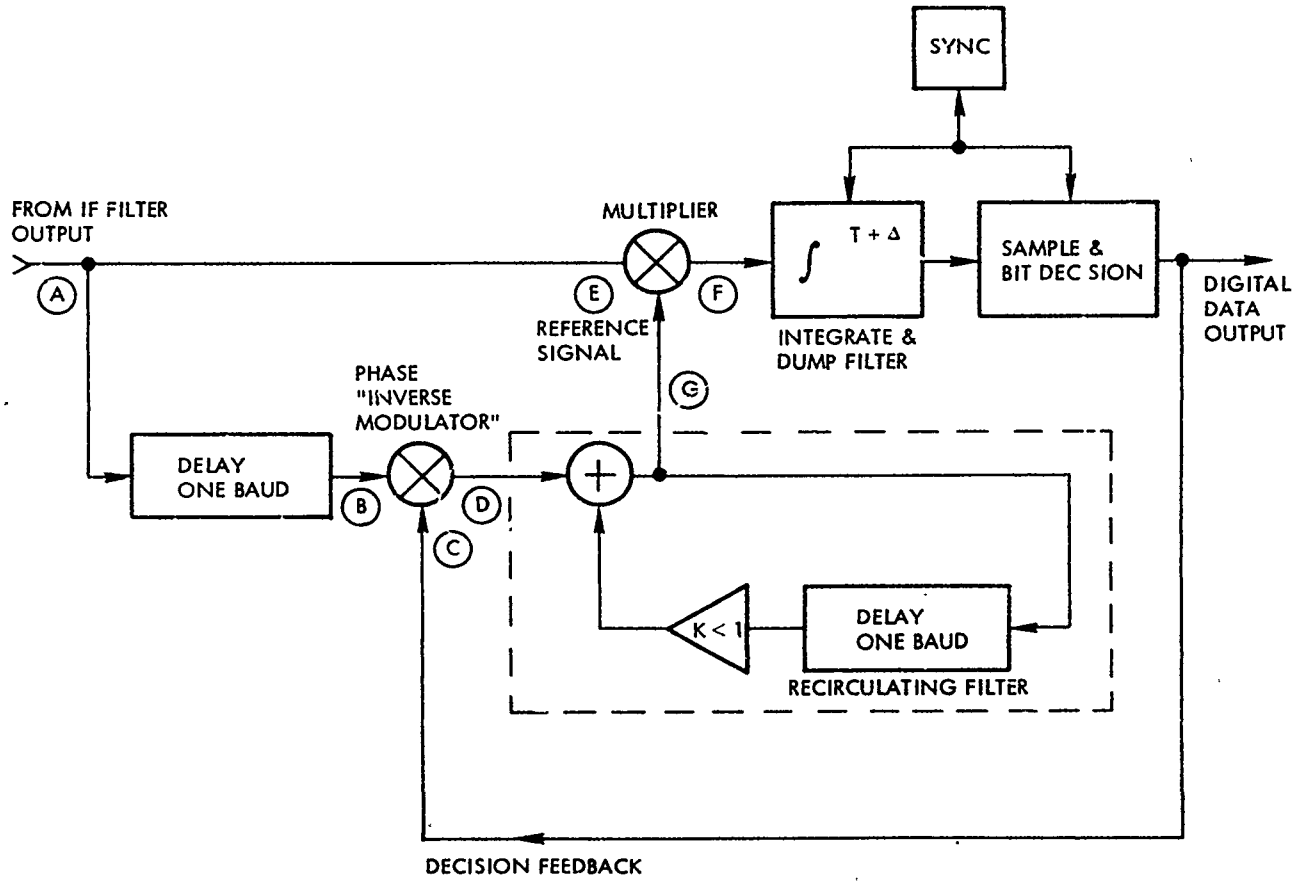

FIGURE 2-2 SIMPLIFIED DAR BLOCK DIAGRAM FOR BPSK TRANSMISSION

back and coherent filtering as illustrated in Figure 2-2 for BPSK modulation. While the concepts of decision feedback and coherent filtering are not new, their use in the fashion described herein is believed to be novel. The IF input to the DAR at Ⓐ consists of a train of distorted but nonoverlapping pulses with pulse to pulse relative phase modulation (impressed by the transmitted digital information). The desired reference signal is generated as follows: The input signal is delayed by approximately one baud ($T + \Delta_0$) of Figure 2-1 at Ⓑ to align in time with the digital decision performed on that same baud at Ⓒ . If it is assumed, for the moment, that the digital decisions are correct, then the effect of the decision feedback is to phase "inverse modulate" the received signal, i.e., to shift all 0 phase states by 0 and all π phase states by π such that all phase states are equal (modulo 2 π). The signal at Ⓓ then consists of a series of distorted pulses of identical phase state plus the thermal noise at the receiver input. It is possible to use this signal directly as a reference for the matched filter, but it would yield poor performance due to high noise and no immunity to occasional feedback errors. A recirculating, coherent filter is thus used to reduce the noise of the reference and to stabilize the reference against occasional errors in the decision process.

The coherent filter merely consists of a positive feedback loop composed of a precise IF delay line of one baud duration and a loop gain, K, slightly less than unity. This recirculatory loop coherently adds previous distorted pulses to the present pulse as $1 + K + K^2 + \cdots = 1/(1-K)$ while the noise is incoherently added and builds only in power as $1 + K^2 + K^4 + \cdots = 1/(1-K^2)$. The resultant signal to noise ratio of the output is thus improved over the input by a factor $X = (1 + K)/(1 - K)$. At a practical value of $K = 0.9$, a 13 dB improvement in signal to noise ratio results (a nearly noiseless reference for practical purposes). The filter "memory" is also approximately equal to X so that for $K = 0.9$, a memory of about 20 pulses results. Hence, in this example, the channel need only be quasi time invariant over a period of 20 pulses which is a condition more than satisfied by all troposcatter links of interest at megabit rates. The effect of a single decision feedback error in the memory period is to reduce the reference level by two pulse contributions which results in less than a 1 dB signal to noise degradation in the above example.

The reference signal at the coherent filter output at Ⓖ then serves as the reference to the classic matched filter receiver structure. The input signal at Ⓔ and the reference at Ⓖ are multiplied together to form a video signal at Ⓕ. An integrate and dump filter over the duration of the received baud is then used to optimally add all signal contributions over the baud. The integrate and dump filter is sampled at the appropriate instant as determined by a separate synchronization circuit and a digital decision is made on the sign of the filter output. The resultant decision is held over a baud interval and is also fed back to close the DAR feedback loop.

It should be noted that the DAR structure of Figure 2-2 is very simple. If the coherent filter of Figure 2-2 is replaced by a simple narrow-band filter, the resultant receiver structure is identical to that employed for QPSK demodulation.

Since the emphasis in digital troposcatter is on increasingly higher data rates, the transmission pulse should be coded into as many phase states as possible. Four, eight, or even larger phase state alphabets are possible, but the receiver complexity and degradation budget increase rapidly beyond four level phase shift keying (QPSK). The DAR implementation for QPSK pulses as illustrated in Figure 2-3 is not much more complicated than that for BPSK pulses. The operation of the QPSK demodulator is easily understood if the input signal is visualized as two BPSK signals (with identical pulse distortion) in phase quadrature. The upper and lower halves of Figure 2-3 are then just BPSK demodulators for the in-phase and quadrature components. The use of symmetrical phase shifters and a common coherent filter insure correct phase separation of the two components. Again, if the coherent filter is replaced by a bandpass filter, the receiver structure is that employed in a wide variety of coherent BPSK demodulators.

2.1.1 Diversity Operation

The DAR structure shown in Figure 2-2 and 2-3 for BPSK and QPSK modulation, respectively, lends itself quite naturally to optimum diversity combining. It is only necessary to use a separate DAR (one printed circuit board) for each diversity channel but with a common integrate and dump filter and common decision feedback.

Consider a DAR on a single diversity channel. The matched filter operation consists of multiplying the input signal plus noise times a reference signal. The reference signal has the same complex distortion as the input signal and a constant phase state determined by the decision feedback. The reference signal amplitude is also linearly related to the input signal amplitude. Hence, the multiplier output consists of a strictly positive or strictly negative contribution due to the (signal) x (reference) component and a noise term due to the input (noise x (reference). Diversity combining is achieved by adding this video signal to the corresponding video signal from all other diversity channels. A common integrate and dump circuit and decision circuit thus determines the bit state and common decision feedback is applied to all diversity channels. This operation is illustrated in Figure 2-3 for QPSK operation as employed by the quad diversity DAR-IV experimental model.

Note that each DAR contribution to the integrate and dump filter is essentially "weighted" by the DAR reference signal. But this reference signal is linearly related to the input signal amplitude on that diversity channel. Hence, if the noise level at each diversity input is

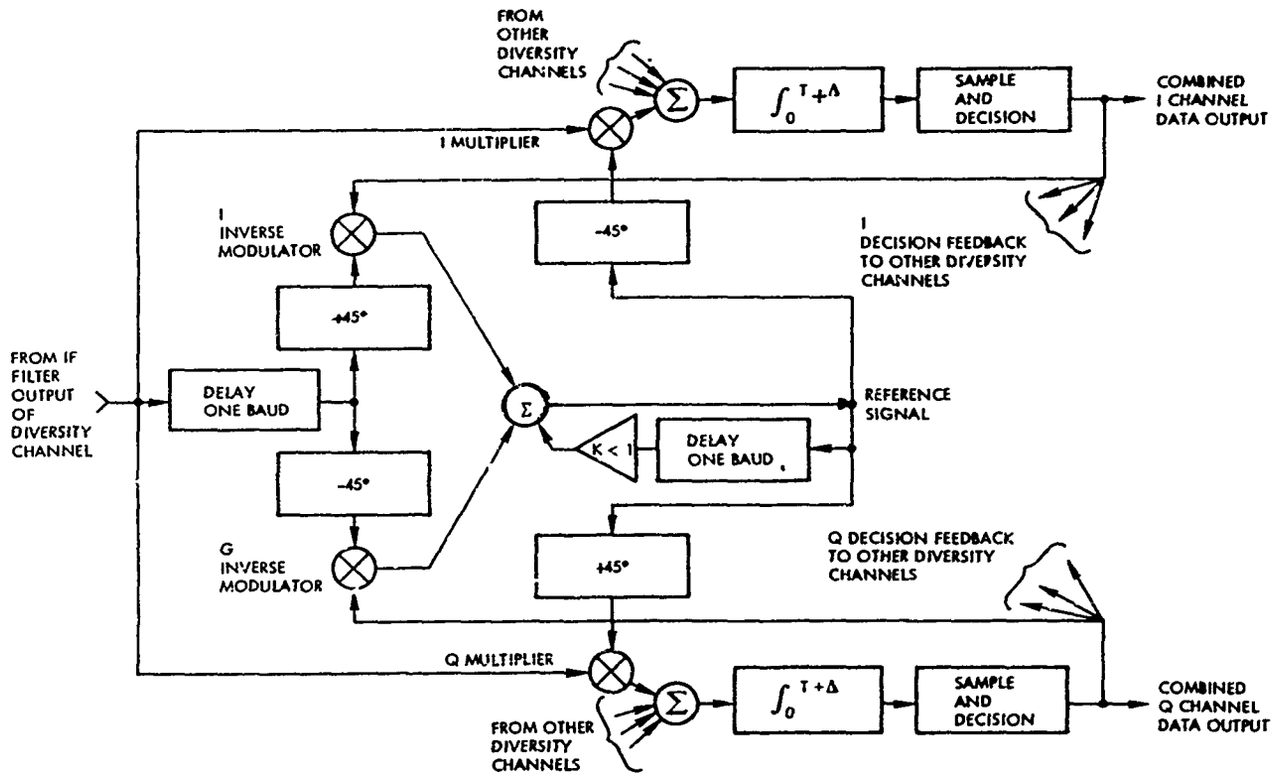

FIGURE 2-3 SIMPLIFIED BLOCK DIAGRAM OF DAR-IV QPSK RECEIVER UNIT

equalized (a normal condition), the per channel weighting can be considered as proportional to the channel signal level to noise power ratio. This weighting thus yields "maximal ratio" combining of all diversity signals and thus provides the maximum achievable combined signal to noise ratio. Optimum combining of diversity channels is thus achieved without additional circuitry. Optimum diversity combining is thus achieved by providing a separate adaptive matched filter unit (only one printed circuit board) for each diversity channel. Note that although the diversity signals are added at video, the combining operation is essentially predetection due to the linear nature of the detection process.

2.1.2 Variable Rate Operation

To be practical, the DAR-IV must accommodate different data rates with the minimum amount of alteration in the modem circuitry (especially in the more costly analog areas of the modem such as filters, delay lines, etc.). The DAR-IV accomplishes this objective with only a minor increase in circuit complexity.

The data rate of the DAR QPSK demodulator/diversity combiner illustrated by Figure 2-3 is determined by a pair of delay lines with a length of one baud. The obvious way to accommodate different data rates is to change the length of these delay lines. However, such a solution would be both costly and cumbersome. Instead, only one fixed delay line is employed for all rates and some simple digital logic manipulations are used to achieve the wide variety of rates.

At present, a large variety of external PCM and TDM multiplex equipment is in the Government inventory. This equipment generally has different output data rate and clock stability requirements when operated with the same traffic capacity. Hence, the design approach for the experimental DAR-IV was to employ a slightly higher transmission rate. The higher transmission rate also provides the necessary overhead capacity for integration of a digital service channel. Thus, fixed transmission rates of 1.75, 3.5, and 7.0 Mbps are used in conjunction with the single or parallel data modes of the DAR-IV to satisfy all data rate and interface requirements for N = 1, 2 and 4 where the nominal transmission rates are N x 1.544 Mbps.

The delay line in the DAR-IV unit is designed for the lowest 1.75/2 Mbps baud rate or approximately 1.14 usec. At each higher data rate, the delay line will thus contain exactly one, two, three, or four QPSK symbol(s). The only change in the DAR-IV is thus the clock rate in the timing recovery and integrate and dump circuitry. DAR operation is unaffected by the number of exact pulse intervals stored in the coherent filters and the change in rate is accomplished with maximum simplicity.

The operation of DAR-IV can be visualized as an adaptive matched filter to a symbol containing a string of one, two, three or four successive distorted pulses depending on data rate and diversity mode.

This variable rate operation is illustrated with the aid of Figure 2-4 for the transmitted waveshapes. At the N = 1 rate (1.75 Mbps) there is only one QPSK symbol (pulse) in each 1.14 usec basic baud interval. The number of QPSK pulses per basic baud interval increasing data rate until at the N = 4 rate with Q diversity there are exactly four QPSK pulses per interval. In each case, the integrate and dump decision interval is centered about only one QPSK pulse as determined by the recovered bit timing. Decision feedback, on a pulse basis, permits the simultaneous storing of up to four pulse intervals in the coherent filter of Figure 2-3. No change in the effective "memory" length results for operation at the different data rates.

In Figure 2-4, an asterisk is placed alongside the QPSK pulse in the basic baud interval which will (after decision feedback "inverse modulation") be used as the reference for the corresponding bit in the next basic baud interval. Differential data encoding (which is required by all decision feedback CPSK demodulators to resolve 180 deg phase ambiguity) is also performed between corresponding pulse pairs of adjacent baud intervals, also as indicated by the asterisks. At the error rates of interest, the degradation due to differential encoding is small (less than 0.4 dB between 10^{-5} and 10^{-8} BER).

2.1.3 DAR Plus Feedback Equalization

The previous description of the DAR operation assumed that the data rate and time gate duration of Figure 2-1 could be adjusted to prevent significant intersymbol interference. As the data rate is increased for a given tropo channel characterization, a point will be reached at which the time gate can no longer be adjusted to prevent intersymbol interference. The effect of this degradation on performance is to produce an irreducible error rate which cannot be overcome by increasing transmit power.

Figure 2-2 shows the basic DAR demodulator for binary PSK modulation. Intersymbol interference results when previous received pulses overlap the present pulse in the "integrate and dump" data decision interval. This intersymbol interference results in an amplitude fluctuation of the integrate and dump filter output which degrades the demodulators noise performance and can even cause errors in the absence of noise when the multipath dispersion is large. The overlap of adjacent pulses also causes some degradation in the reference signal at the output of the coherent filter (recirculating memory). However, if the gain of the recirculating memory is made large, the intersymbol interference degradation of the reference signal is

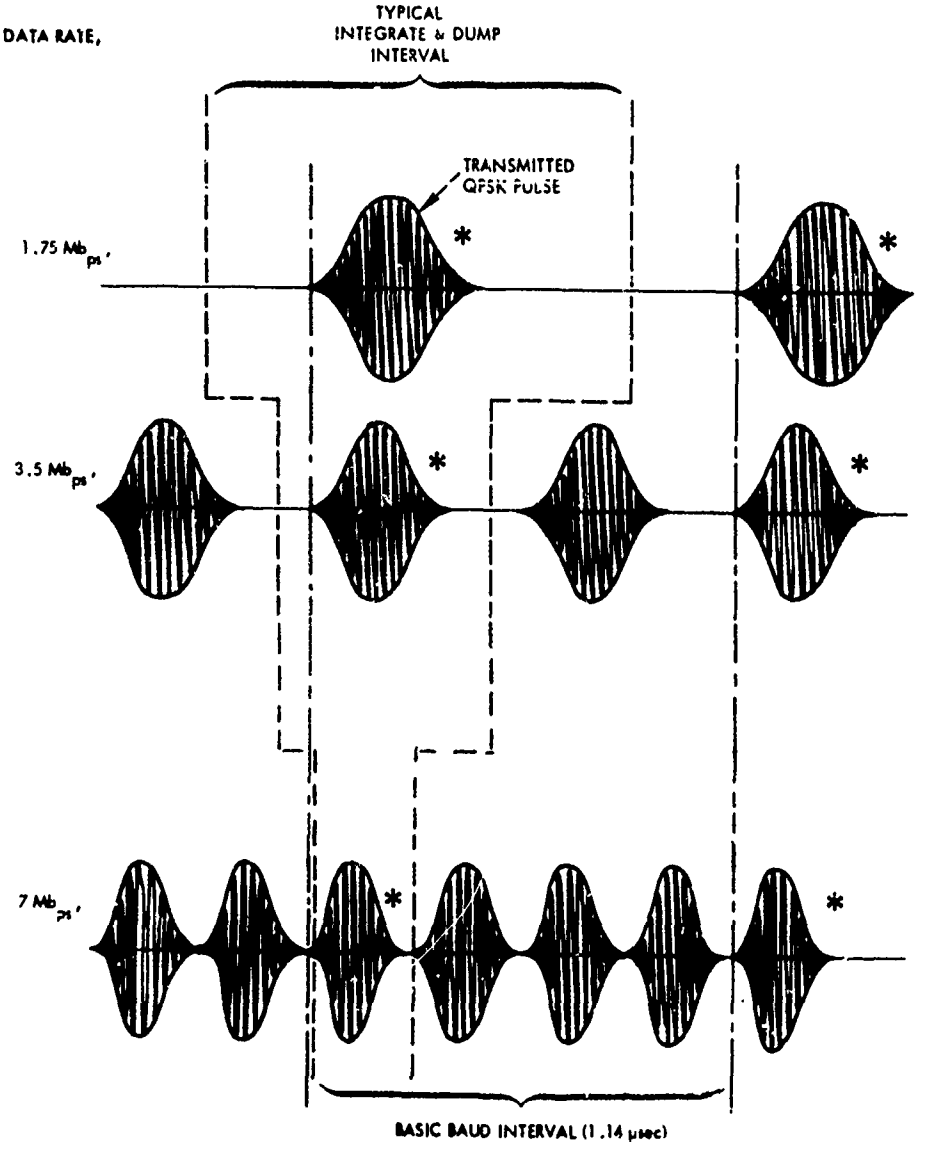

FIGURE 2-4 ILLUSTRATION OF MULTIPLE DATA RATE OPERATION OF DAR-IV WITHOUT NEED FOR SWITCHING OF ANALOG CIRCUITRY

largely eliminated. That is, the tails of the previous data bits cannot coherently build up in the recirculating loop since they are not multiplied by the correct decision feedback data (they are out of time-sequence with the "inverse-modulator" of the recirculating memory).

To adaptively remove the intersymbol interference at high data rates, a Decision Feedback Equalizer (DFE) can be added to the DAR modem. Figure 2-5 shows how the (DFE) function is incorporated with the DAR. An "error" signal is formed between the present decision (usually +1 or -1) and the analog voltage at the output of the "integrate and dump" filter. In the absence of intersymbol interference, this analog signal assumes values of approximately ± 1 due to automatic gain control action with zero mean noise perturbation. Thus, in this case, the average value of the error signal is zero.

When there is intersymbol interference from a previous bit, then the integrate and dump filter will fluctuate depending on the strength of the interference and the signs of the previous and present data bits. If the error signal is multiplied by the previous bit and the resultant signal averaged, the averaged signal will be non-zero whenever the previous bit introduces interference. This averaged signal is, in turn, multiplied by the previous bit in question, inverted in sign, and added to the output of the integrate and dump filter for the purpose of cancelling the interference from the previous bit. The feedback nature of the DFE causes this process to continue until the error signal becomes uncorrelated with the previous data state which is the only stable operating condition. At this time, the error due to the previous bit is reduced in the minimum mean-square sense.

The DFE technique can be applied to QPSK (four phase PSK) or higher phase alphabet signalling version of the DAR modulation technique. For higher phase alphabets, it is generally necessary to adaptively cancel the intersymbol created by previous bits even if they are on orthogonal phase states. The DFE can also be used to cancel the interference from more than one previous bit as dictated by the extent of multipath dispersion compared to a digital signalling interval.

2.2 Implementation of the DAR-IV Experimental Model

2.2.1 General

The major segment of hardware developed for this effort was an experimental model of the Distortion Adaptive Receiver (DAR) modem. This digital modem was required to provide digital data rates of 1.75, 3.5 and 7 Mbps with a capability of interface with standard troposcatter radios including the AN/MRC-98, the AN/TRC-132 and the AN/TRC-97A. The modem was also required to interface

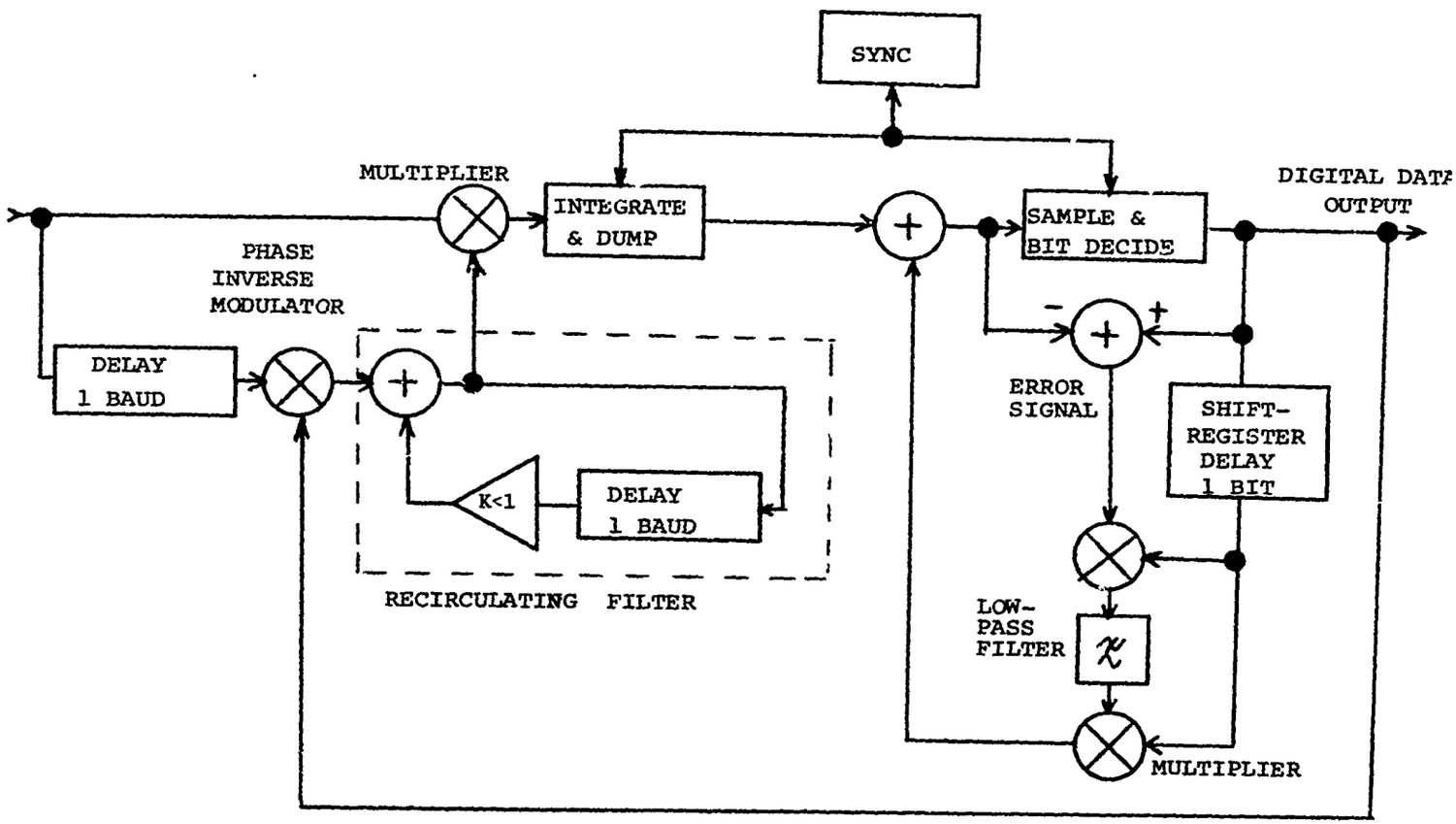

FIGURE 2-5 BASIC DEMODULATOR FOR BPSK ILLUSTRATED WITH ADAPTIVE INTERSYMBOL INTERFERENCE REMOVAL

with the radios using non, dual or quad explicit orders of diversity in addition to providing an interface for hybrid digital/analog transmission. A quad diversity implementation of the DAR known as the DAR-IV was implemented in a simplex configuration to meet these requirements.

While the objective of the experimental model was mainly to demonstate the tropo performance achievable with a sophisticated digital modem technique, it was deemed necessary to construct the model in a fashion similar to commercial grade test equipment to facilitate field testing. At the time of this writing, the DAR-IV experimental model has successfully completed nearly 8 months of uninterrupted laboratory and field testing under a wide variety of environmental conditions with no failures in the basic circuitry. The low complexity of the DAR-IV modem is a significant factor in achieving this high reliability operation.

Figure 2-6 shows a simplified block diagram of the DAR-IV transceiver which would normally be employed at one terminal of a communications link. In the present experimental model, the modulation and demodulation functions of the DAR-IV were packaged into separate, self contained units to provide simplex operation with the lowest hardware costs. In the block diagram of Figure 2-6, the QPSK modulator, and half of the mode control, interface and orderwire units were packaged in a "transmit unit" while the remainder of the functions comprise a "receive unit".

2.2.2 Description of the Experimental Model

2.2.2.1 Unit Descriptions

The DAR-IV simplex experimental model consists of two basic units, a Transmitter Electronics Bay and a Receiver Electronics Bay. Associated with each of these is a power supply and monitoring unit. Figure 2-7 is a photograph of the Transmitter Electronics Bay and its Power Supply/Monitor Bay and Figure 2-8 is a photograph of the corresponding receiver unit. In its normal transceiver configuration, the equipment form factor of Figure 2-8 can be used to contain both modulator and demodulator circuits since it is possible to share a number of the plug-in modules and power supplies between both functions.

The Transmitter unit of the simplex DAR-IV contains the following plug-in modules:

(a) Master Oscillator
(b) Digital Multiplexer
(c) Service Channel A/D Converter (CVSD)
(d) QPSK Modulator
(e) Tx Hybrid Translator (used only in Hybrid Mode)
(f) Mode Programmer

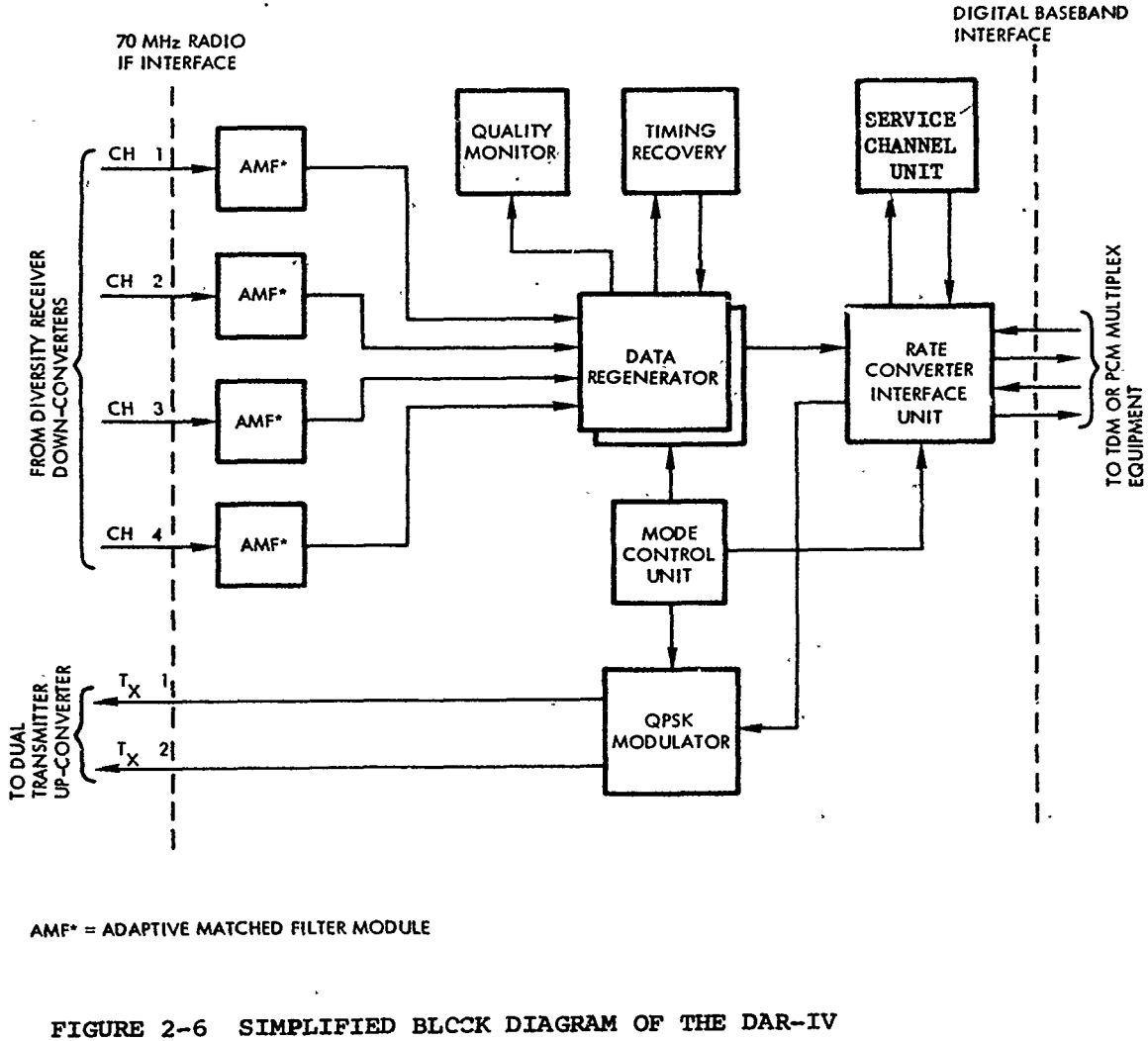

AMF* = ADAPTIVE MATCHED FILTER MODULE

FIGURE 2-6 SIMPLIFIED BLCCK DIAGRAM OF THE DAR-IV

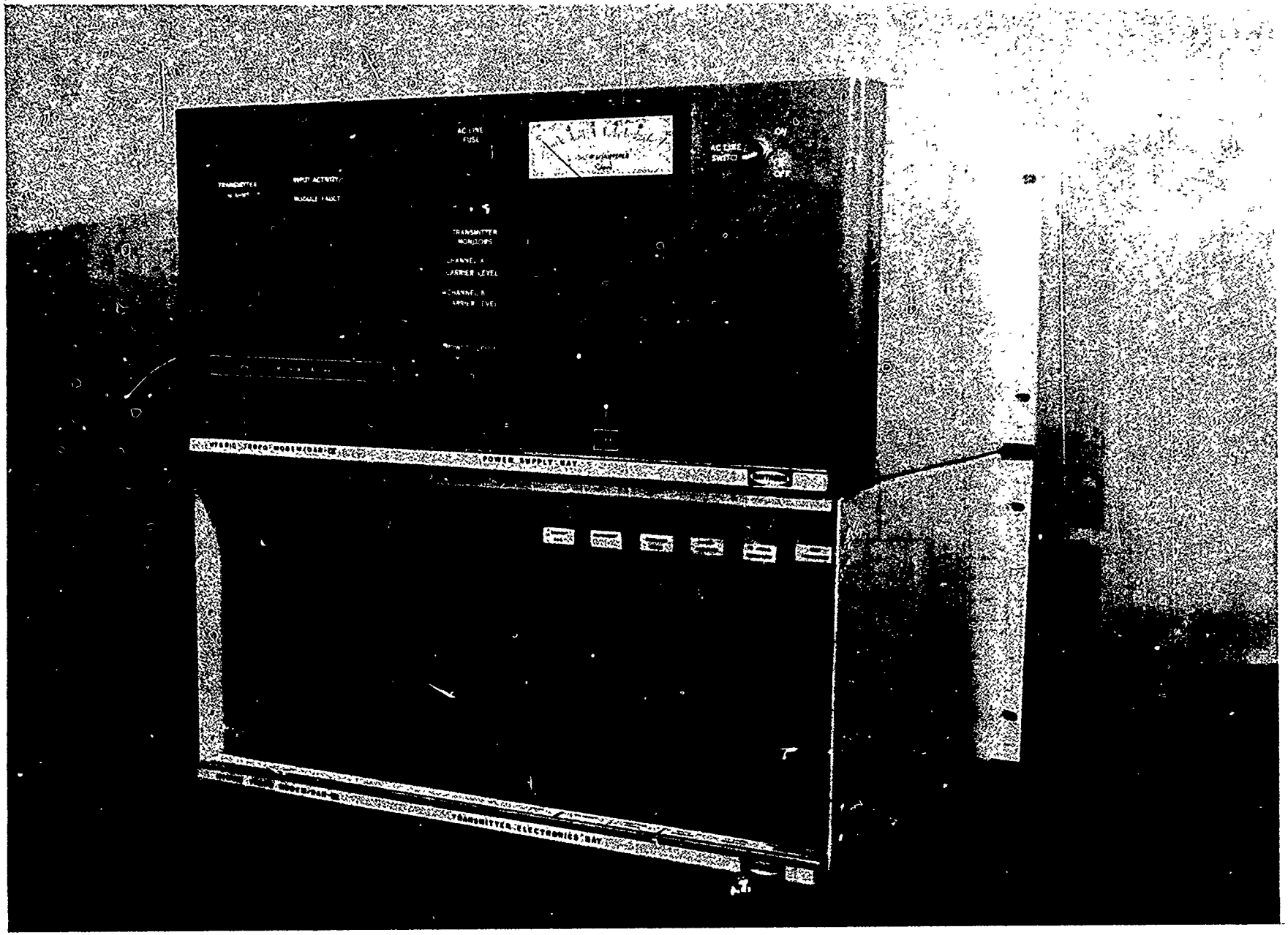

FIGURE 2-7 FRONTAL VIEW OF TRANSMITTER UNIT

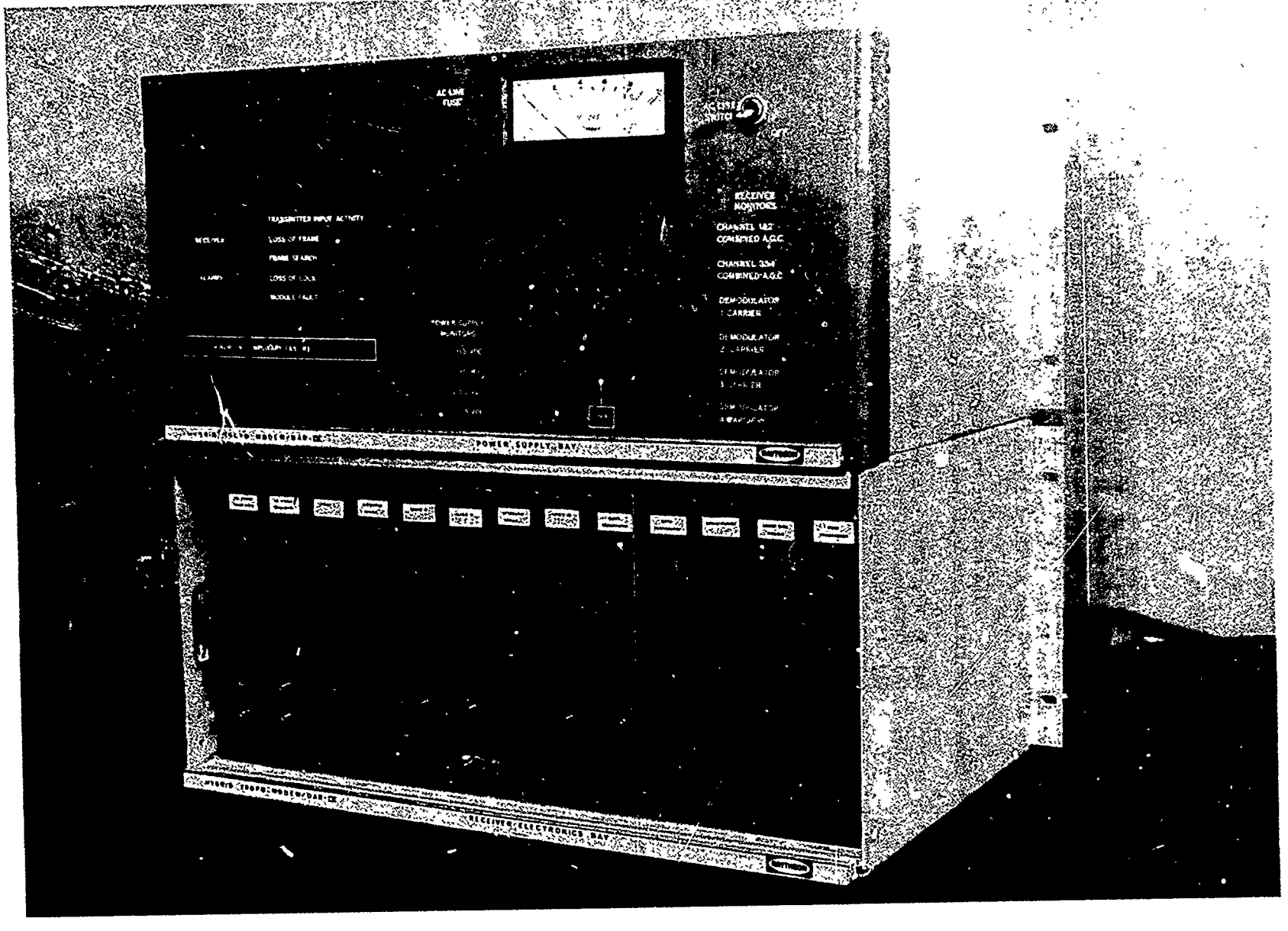

FIGURE 2-8 FRONTAL VIEW OF RECEIVER UNIT

Each individual module contains its own fault detection circuitry that activates an LED alarm on the module itself and on the display panel. The inputs to the transmit unit are the analog orderwire signal and the main digital traffic. The unit provides a clock output to synchronize the input traffic and two 70 MHz IF outputs for the two separate up-converter chains of the AN/MRC-98 and AN/TRC-132 radios.

The Receiver unit contains the following plug-in modules (module quantities are indicated parenthetically):

(a) Rx Hybrid Translator (used only in Hybrid mode)(2)
(b) QPSK Demodulator (4)
(c) Integrate and Dump (2)
(d) Clock Regenerator
(e) Data Regenerator
(f) Demultiplexer
(g) Service Channel A/D Converter (CVSD)
(h) Mode Programmer

The receiver unit has a 70 MHz input port for each of up to 4 explicit diversity channels. All of the IF processing including band-pass filtering, amplification, Automatic Gain Control (AGC), and adaptive matched filter detection is performed in a single plug-in module. It is practical to add any number of these plug-in modules desired to accommodate any order of explicit diversity without modification of the basic DAR-IV. The outputs of the receiver unit are the demodulated data signal, the recovered clock signal, and the received analog orderwire signal (after CVSD decoding). The integrate and dump filtering and data regeneration functions of the receive unit are duplicated to permit operation in a Dual plus Dual mode. This mode permits the simultaneous transmission of two separate data streams with half of the available explicit diversity applied to each and can be used to double the transmission bit rate of the DAR-IV for a given set of channel conditions.

Both transmit and receive units have a self contained power supply and fault monitoring system to permit operation at remote locations. The power supply unit contains the following:

(a) +15 V DC, -15 V DC, +5 V DC, -5 V DC power supplies
(b) LED power supply monitors.
(c) LED alarms indicating loss of input activity and a complete module fault.
(d) LED alarm indicating minor or temporary fault.
(e) Metering for transmitter carrier power on each channel output.
(f) Power supply metering for each DC supply voltage.

2.2.2.2 Equipment Specifications for DAR-IV Simplex Model

Orderwire Input/Output:	2 V p-p maximum in 600 ohms. CVSD sample rates of 125 Kb/s, 250 Kb/s, 500 Kb/s. Analog Frequency Response 300 Hz to 12 KHz.
Bit Rates Input/Output:	1.5934 MHz 3.1868 MHz TTL Compatible 6.3736 MHz Clock from Internal DAR-IV reference.
Bit Rates (Transmit):	1.75 Mb/s, 3.5 Mb/s, 7.0 Mb/s.
IF Output:	+3 dBm ±2 dB peak.
IF Input:	70 MHz, 50 ohms -20 to -70 dBm input levels. Bandwidths up to 12 MHz.
Demodulation:	Coherent matched filter detection. Maximal ratio combining. Automatic gain control over -20 to -70 dBm input range.
Clock Output:	TTL Clock Rates: 1.75 Mb/s with gaps for overhead to yield 1.5934 Mb/s rate. 3.5 Mb/s with gaps for overhead to yield 3.1868 Mb/s rate. 7.0 Mb/s with gaps for overhead to yield 6.3736 Mb/s rate.
Modulation:	Quadriphase - Phase Shift Keying with differential data encoding.

2.2.2.2 Equipment Specifications for DAR-IV Simplex Model (continued)

Modes Available:	1.75, 3.5 or 7.0 Mb/s QPSK. Non, Dual or Quad Diversity. Dual + Dual Diversity. Spectrum Spreading. Variable time gating on transmitter carrier.
Spectrum Spreading:	Internally Selectable codes. Ratios available: 5:1 @ 1.75 Mbps 3:1 @ 3.5 Mbps Codes available: 11111111 11101110 10101010 11001100
Time Gating:	Internally selectable. Transmitted pulsewidths available: 95, 190, 285, 380, 475, 570 nsec or continuous.
Dual + Dual Mode:	Internally selectable. This mode allows twice the data rates listed above to be transmitted by transmitting one-half of the data bits on each of the IF output channels. This allows twice the data rate with no increase in transmitted bandwidth.
Prime Power:	115 V AC, 50 - 60 Hz, 80 watts.

2.2.2.3 Transmitter Unit Implementation

The basic elements of the transmit unit of the DAR-IV simplex experimental model have been previously described. To fully understand the experimental results presented in the following sections, it is desireable to present some of the detailed implementation features

of the equipment. The transmit unit or DAR-IV modulator is relatively straightforward. However, the method of multiplexing the CVSD encoded orderwire signal with the main data stream and the details of the QPSK modulator coding and time-gating require additional clarification.

Orderwire Multiplexer

The function of the multiplex module is to combine the 125, 250 or 500 Kbps digitized orderwire signal with the main data traffic to achieve a corresponding 1.75, 3.5, or 7 Mbps transmission rate. The data rate clock from the master oscillator is received and passed through a count down and logic network to generate new clocks for framing, data and orderwire. The system frame is designed to consist of 56 bits/frame. The frame structure is that there are 51 data bits, 4 orderwire bits and 1 frame bit in each frame. The interleaving sequence is as follows:

6 Data, 1 CVSD 13 Data, 1 CVSD, 13 Data, 1 CVSD, 13 Data, 1 CVSD, 6 Data, 1 Frame

The frame word used is a three bit code (110). The clock logic generates the orderwire clock by generating a pulse every time there should be a CVSD bit as seen above. The frame generation logic generates a 110 code that fits sequentially with each bit appearing every 56 clock pulses. The data clock takes the basic data rate clock and deletes a pulse everywhere a non-data bit occurs in the above sequence. This is then sent to the rear panel as the clock output. When connected to a data test set, data bits only appear where there are clock pulses. The structure of this output clock is that the transitions occur at N times the 1.75 Mb/s rate, but the deletions lower the overall rate to the N times 1.5934 Mb/s.

These new clocks are used to clock out data and orderwire bits in the right sequence and at the appropriate time slots. The data and orderwire bits are brought into the multiplexer and combined with the framing bits to yield a smooth data rate of N times 1.75 Mb/s. This output data is then sent to the modulator.

As described above, the orderwire multiplex takes in data bits in blocks and is designed to interface directly with a data simulation test set such as the HP1930A. To employ this experimental model with an actual external traffic multiplex equipment or operational data, a smoothing buffer must be added to provide continuous input and output data streams. However, no loss in generality results from this configuration in the measurement of BER performance under test conditions.

QPSK Modulator

The primary function of the QPSK Modulator is to generate the modulated RF carrier for the DAR-IV modem. Figure 2-9 is a simplified block diagram of the basic modulator.

The first operation is to take the serial data stream from the multiplexer and convert it to two parallel data streams. These two data streams are then used as inputs to the differential encoder portion of the modulator. For reasons that will become more clear in the section describing the demodulator, the differential encoding takes on some unique characteristics. The standard differential encoder includes an interleaver which, depending on the data rate selected, determines which pairs of bits are used in the encoding process. For example, at 1.75 Mb/s, the first bit is encoded with the second, at 3.5 Mb/s, the first and third bits are used, at 7 Mb/s the first and fifth bits are used, and so on. The encoded data then goes to the phase modulators.

The 10.5 MHz clock from the encoder is received and directed to the time gate pulse generation scheme. This clock along with the pulse width code logic from the programmer board determines the width of the transmission pulse. This pulse width is programmable for 0 (no transmission), multiples of 95 nsec up to 570 nsec, and continuous transmission. Once this pulse has been generated, it is sent to some steering logic which in Quad diversity does nothing to the pulse and in Dual + Dual diversity alternates the pulses from one frequency diversity channel to the other. The output of the steering logic then controls a pair of RF switches, one on each channel. These switches gate the modulated signal on for the duration of the gate pulse.

The 70 MHz carrier from the master oscillator is received and fed to a quadrature hybrid. The outputs of the hybrid are each brought to a pair of phase modulators having the I and Q data on one port as described above. The data then binary phase shift keys each of the quadrature 70 MHz carriers and these two modulated carriers are then recombined to form a QPSK carrier. This carrier is then split into two paths each going through an RF switch for gating as mentioned previously. The gated signals are then filtered, amplified and sent out to the rear panel as the channel 1 and 2 QPSK outputs to the transmitter exciters.

The basic 10.5 MHz clock is derived from and synchronous with the 70 MHz IF carrier. Since all of the time gating, data clocks, and pulse coding functions are derived from the 10.5 MHz clock, all functions of the modulator are synchronous with the IF frequency. This procedure results in a very simple timing chain for the experimental equipment and greatly facilitates testing and trouble shooting of the equipment.

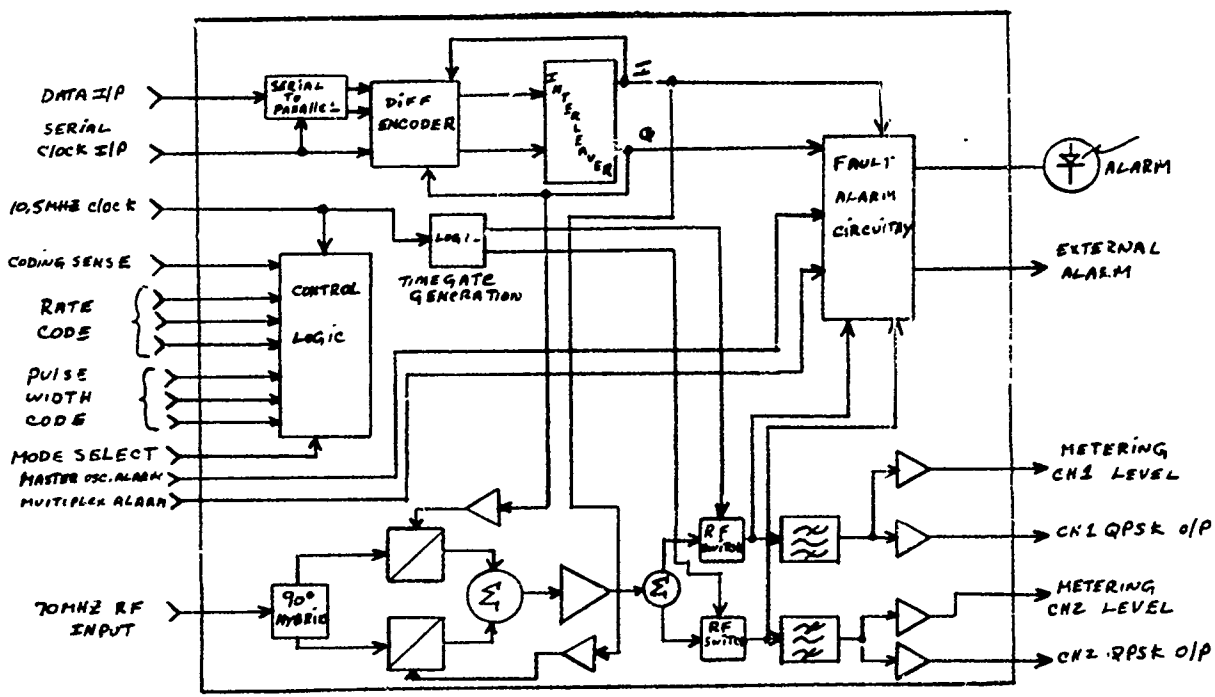

FIGURE 2-9 DAR-IV QPSK MODULATOR

2.2.2.4 Receiver Unit Implementation

This section deals with a more detailed description of the Receiver Unit of the DAR-IV at module level. Figure 2-10 is a functional block diagram of the Receiver Electronics Bay showing each module as well as its interconnection with the other modules and external equipment. It will be helpful to refer to Figure 2-10 occasionally while reading the module descriptions to more clearly understand the functions of the various modules.

QPSK Demodulator

Since the basic theory of operation of the demodulator was discussed previously, the primary intent here is to outline the implementation. The module consists of two sub-units. The first sub-unit contains the coherent filter which is placed inside a thermal oven. The units will be discussed separately. Figure 2-11 is a block diagram of the demodulator circuitry.

The input signal comes into the module and goes through a chain of amplifiers and voltage variable attenuators allowing the demodulator to handle signals within the range of -70 to -20 dBm. The signal is then split into two paths. The first path is through a surface acoustic wave delay line. This line provides 1, 2 or 4 bits of delay at 1.75, 3.5 or 7.0 Mb/s respectively. This delayed signal is then split into two paths where each signal is now inverse modulated by the recovered data and then combined in quadrature. This process yields a carrier with all digital modulation removed except for the complex pulse distortion. The carrier is then passed through the coherent filter to improve the signal to noise ratio. The output of the coherent filter which acts as the reference signal and is split into two carriers in-phase quadrature and used to demodulate the input signal. The outputs of the two data detectors are low pass filtered and sent out to the video combiner.

The function of the coherent filter is to reduce the noise on the reference signal and stabilize the recovered reference against occasional decision feedback errors. Figure 2-12 is a block diagram of the coherent filter. The Surface Acoustic Wave (SAW) delay lines together with their associated circuitry are placed in an "oven" for temperature regulation and precise maintenance of the delays. The SAW substrate material employed was Lithium Niobate ($LiNbO_3$) due to the availability of an appropriate design with this material. It is recommended that future implementations use a relatively temperature insensitive SAW material, ST-cut quartz. Using this alternate material, the need for oven regulation can be eliminated. The gain of the positive feedback recirculating filter loop is adjusted by means of a

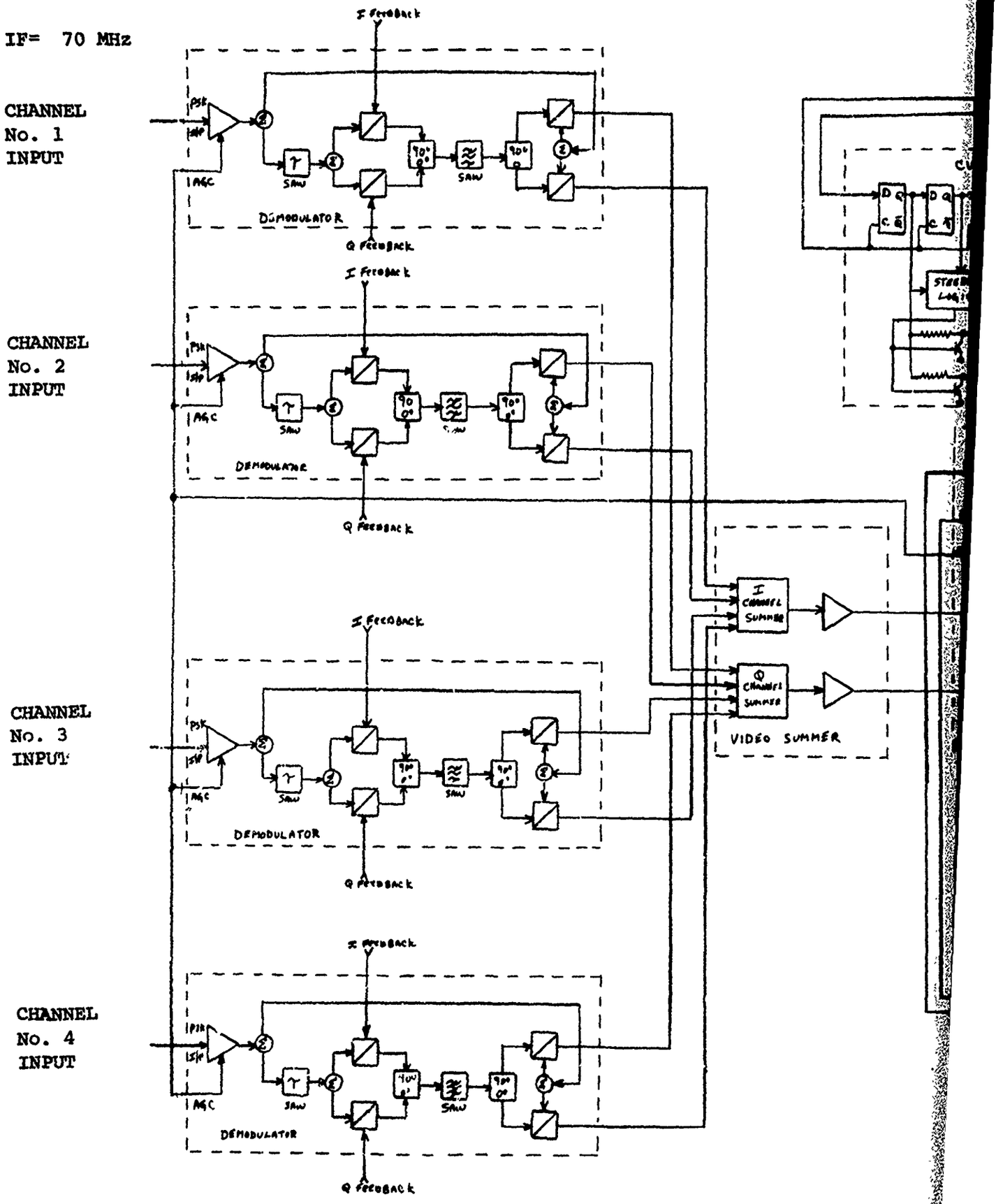
IF= 70 MHz
CHANNEL No. 1 INPUT
CHANNEL No. 2 INPUT
CHANNEL No. 3 INPUT
CHANNEL No. 4 INPUT
I Feedback
Q Feedback
AGC
SAW
DEMODULATOR
I CHANNEL SUMMER
Q CHANNEL SUMMER
VIDEO SUMMER

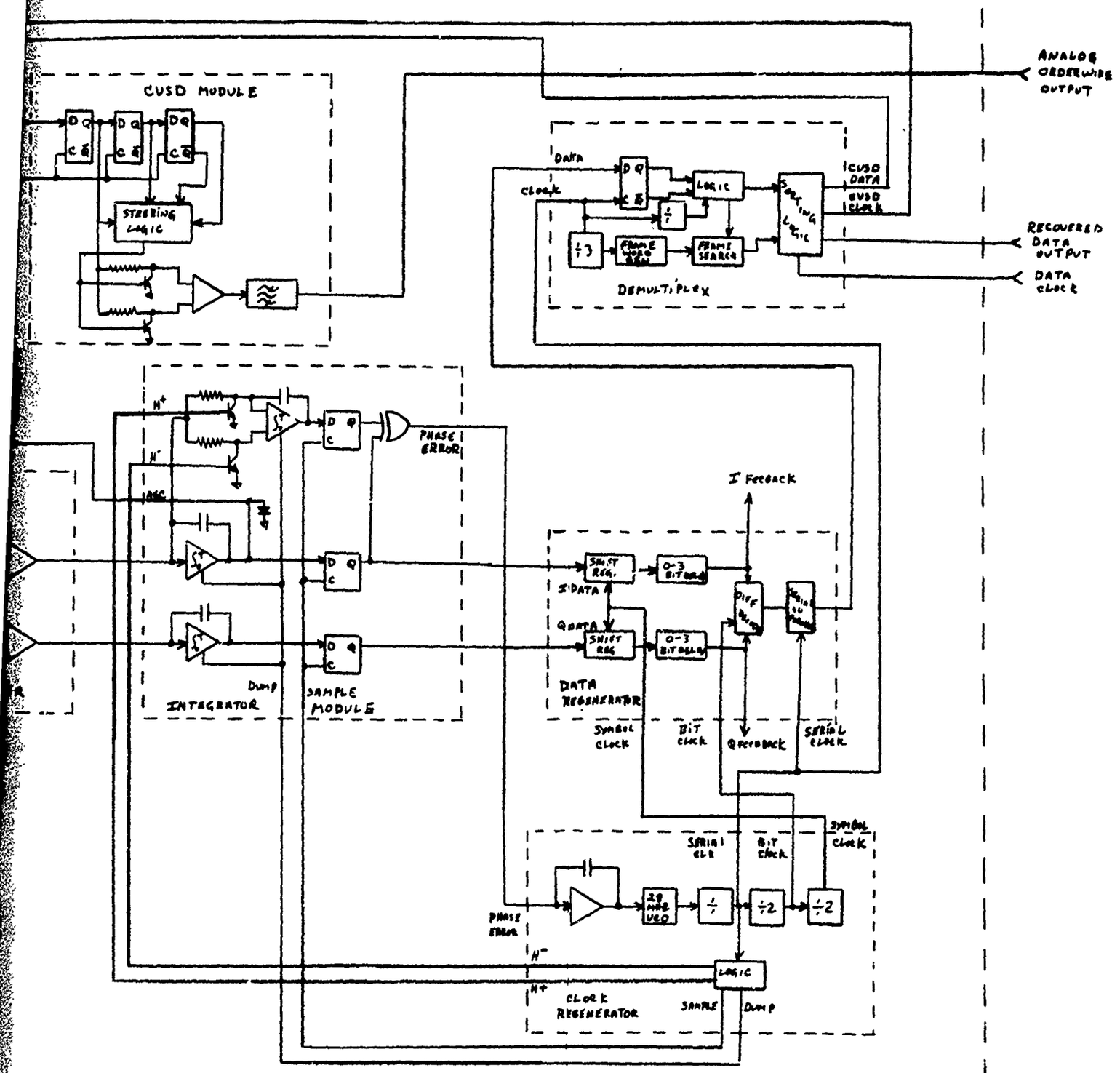

FIGURE 2-10 RECEIVER UNIT OVERALL DETAILED BLOCK DIAGRAM

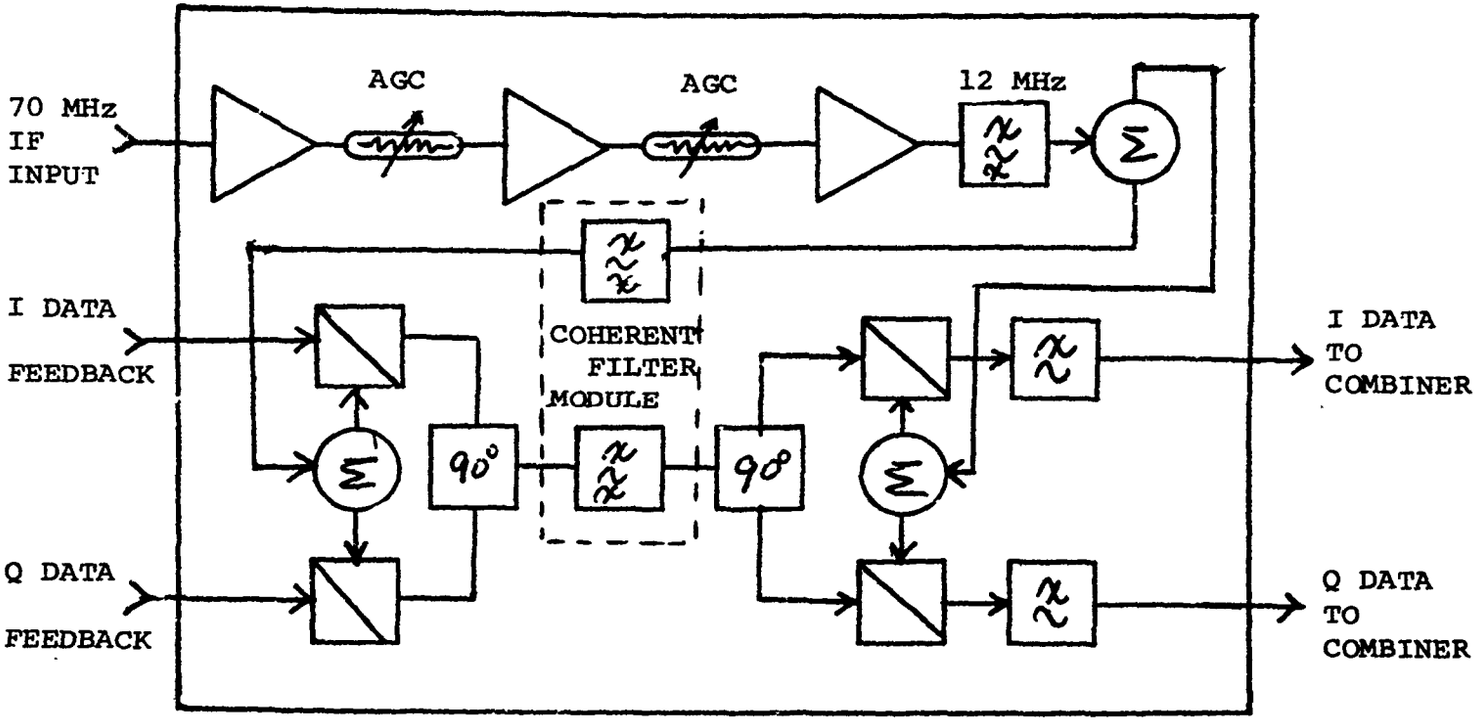

FIGURE 2-11 SIMPLIFIED DEMODULATOR IMPLEMENTATION

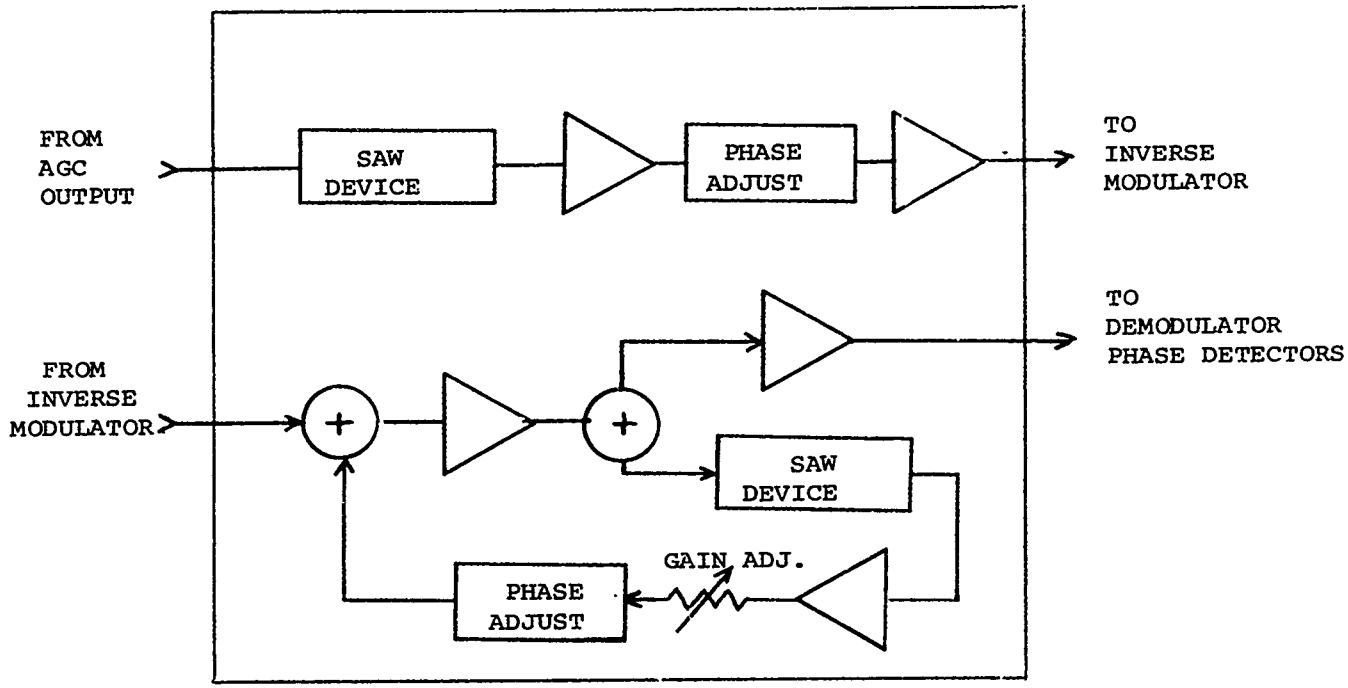

FIGURE 2-12 SURFACE ACOUSTIC WAVE DELAY LINE MODULE WITH RECIRCULATING COHERENT FILTER

potentiometer. Generally, the largest loop gain is employed at which stable operation can be guaranteed over a range of ambient conditions. Typically a loop gain of K = 0.9 to 0.93 is achievable. The SAW devices and their associated circuits have proven remarkably stable permitting operation of the experimental models over a period of months without need for circuit recalibration.

Figure 2-13 is a photograph of the demodulator plug-in module with RFI cover removed and with the cover of the "oven" removed to expose the SAW devices. The lower 1/3 of the module contains the temperature regulated recirculating filter loop and the two identical SAW delay lines. A single potentiometer, accessible from the front panel, permits adjustment of the filter loop gain. Field experience with this circuitry has demonstrated that a production version of the DAR plug-in demodulator can be fabricated without operator adjustments of any kind. This feature is desirable for optimum operation of a sophisticated digital modem in a tactical or remote environment.

Figure 2-14 shows the construction of the SAW delay line employed in the DAR-IV experimental model. The SAW device is reproducible, low cost, small size and rugged. If the SAW technology were not available, the construction of the DAR-IV at megabit rates would be impractical except for an implementation which employs high speed digital signal processing (sampled data) techniques throughout. However, at the present time, the high digital speeds would lead to significantly higher production cost, large power consumption, and lower reliability. The present SAW device has a delay of 1.1428 us, a center frequency of 70 MHz, and a 0.3 dB bandwidth of 4 MHz which was insufficient bandwidth as described in Section 3.2.4, page 3-31.

Video Combiner

The primary function of the video combiner is to take the analog data from the demodulators and linearly add these signals thus achieving maximal ratio combining (the amplitude weighting is performed during the demodulation process). The combined baseband signals are then sent to the integrate and dump filter for detection.

In the quad diversity configuration for example, the I and Q data inputs from the four demodulators are summed, amplified, and sent out to the integrator module number 2. The output of the integrator I channel is fed through this board to the AGC inputs of the four demodulators and the derived AGC control voltages from the four demodulators are commoned on this card so that all four demodulators see the same AGC control voltages.

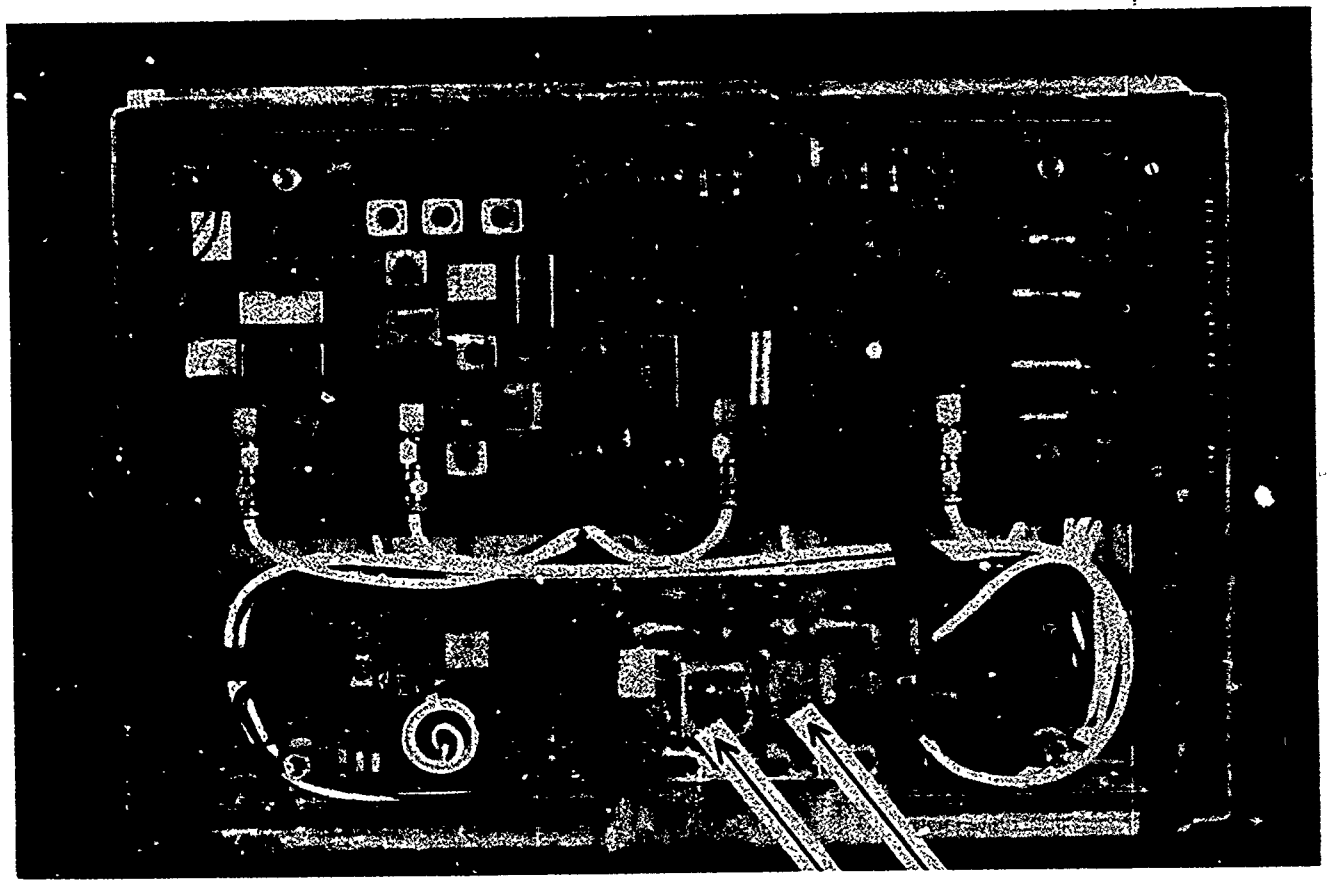

SURFACE ACOUSTIC WAVE
DELAY LINES

FIGURE 2-13 DEMODULATOR MODULE WITH "OVEN" COVER REMOVED TO EXPOSE SAW DELAY LINES

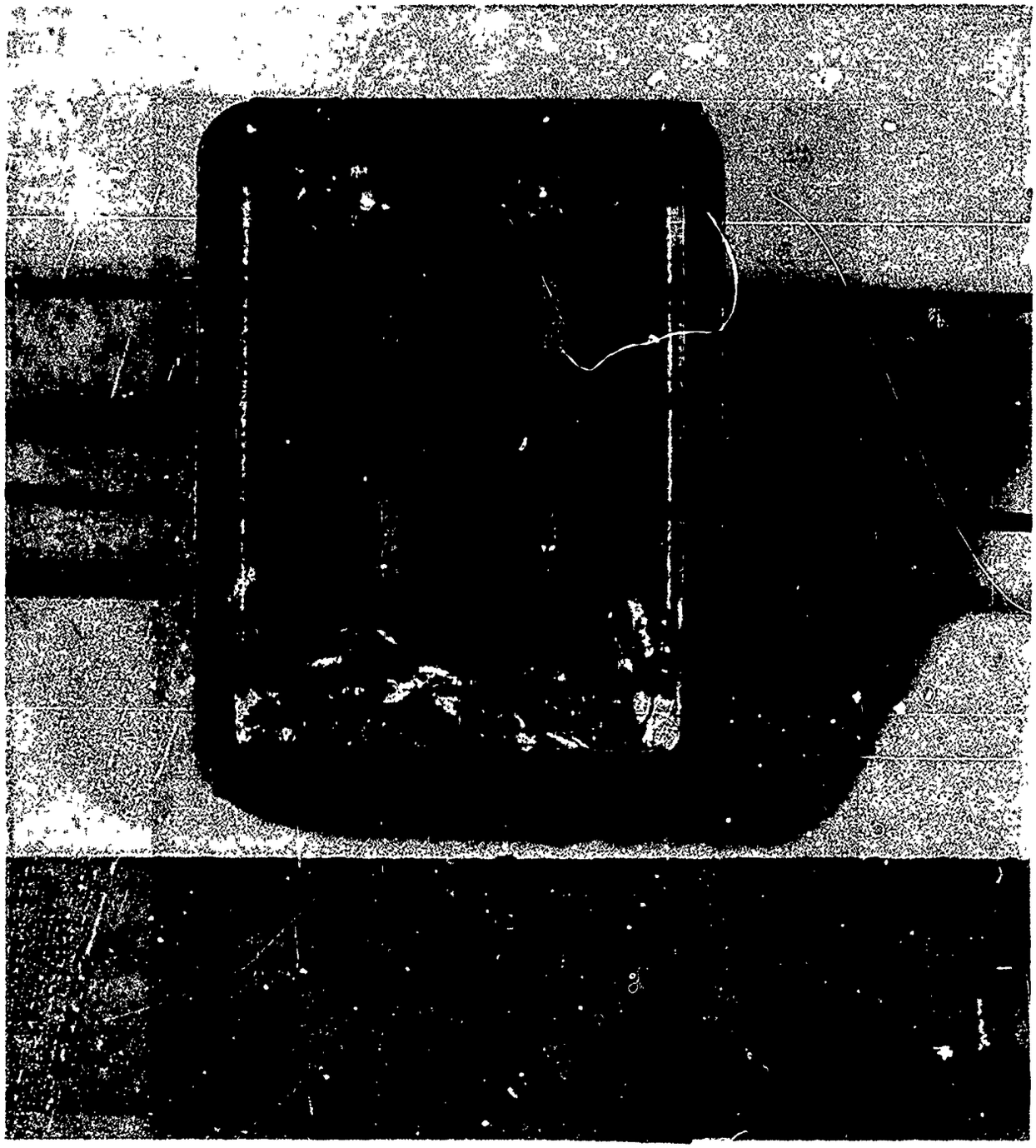

FIGURE 2-14 SURFACE ACOUSTIC WAVE (SAW) DEVICE USED IN DAR-IV

Integrator and Phase Error Estimator

This is a dual function module. One function is to perform integrate and dump filtering and detection of the raw demodulated data, and the other function is to derive bit timing information for the timing recovery loop.

Figure 2-15 is a block diagram representation of the integrator module. The combined I and Q channel information from the video summer is applied to a high speed integrate and dump circuit. The output of the integrator is then sampled and held and sent out to the Data Regenerator.

The phase error estimator circuit derives its information from the I channel data. The phase error information is derived by a standard early-late gate technique. The baseband signal from the I channel is sampled and integrated positively at the beginning of the symbol interval. The integrator is then disabled during the middle of the symbol and then integrated negatively for the last part of the interval. The effect of this technique is to center the data bit within the symbol interval. The output of the phase error integrator is then quantized and sampled in a manner similar to the data channels. This digitized form of the phase error is then correlated with the bit decision on the I channel and sent out to the Clock Regenerator module.

Data Regenerator

The primary function of the Data Regenerator is to take the digital data from the Integrator and perform the appropriate processing for the data feedback to the inverse modulator and supply a serial bit stream for the demultiplexer.

The digital data outputs from the integrator module are first put through one of four bit shift registers and then a four to one multiplexer chip. This process provides a 0, 1 or 3 bit delay in the data feedback to the inverse modulator to match the delay in the SAW device at the respective data rates of 1.75, 3.5, or 7 Mbps. The I and Q data after the 0 - 3 bit delay circuits is then reclocked and decoded in the differential decoder. The decoder contains the appropriate logic to decode the appropriate pairs of bits due to the complex encoding scheme described previously. The output of the differential decoder is then converted from a parallel to serial bit stream, retimed, and sent out to the demultiplexer module.

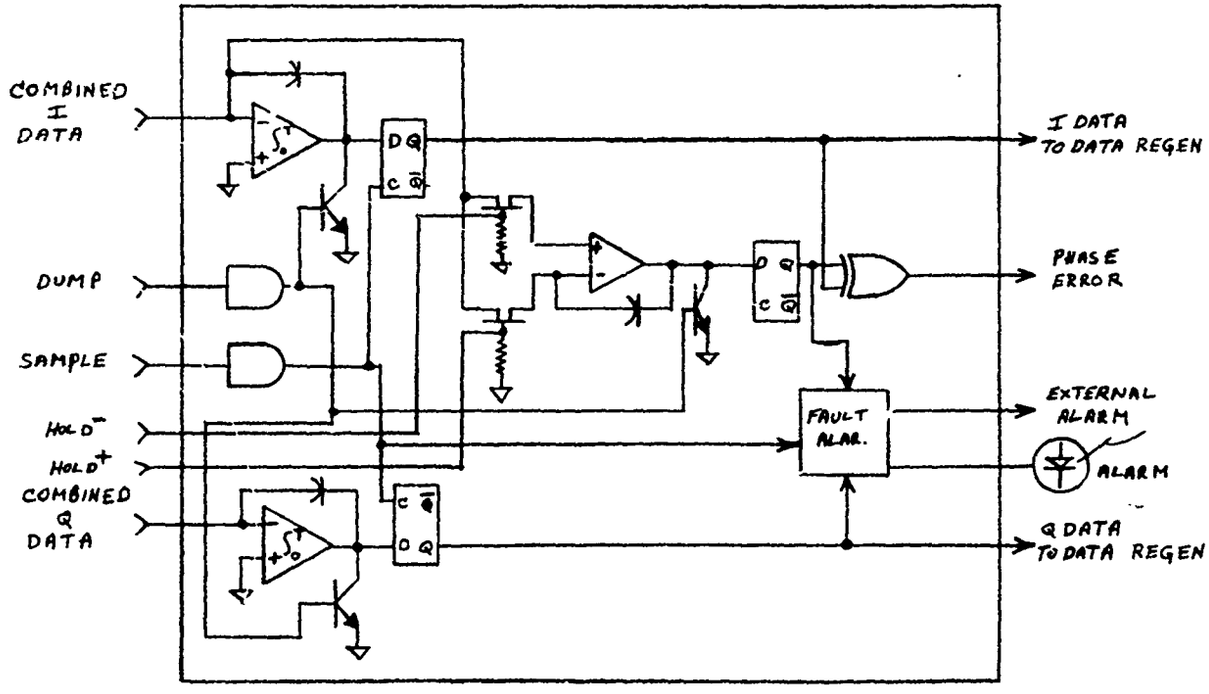

FIGURE 2-15 INTEGRATE AND DUMP FILTER

Demultiplexer

The primary function of this module is to take the received data from the data regenerator and separate the frame bits, the orderwire or CVSD data, and the original information. The clock and data from the Data Regenerator is used as inputs to the Demultiplexer. The received data stream is a composite of frame bits, orderwire or CVSD bits, and information bits. The structure is such that a frame period consists of 56 bits of which 51 are information, four are CVSD, and one is a frame bit. The arrangement of the frame interval as previously described is:

6 Data, 1 CVSD, 13 Data, 1 CVSD, 13 Data, 1 CVSD, 13 Data, 1 CVSD, 6 Data, 1 Frame

The Frame word is a three bit word composed of a 110 code. The basic idea is that the logic searches the received data stream and looks for the frame word 110. Once this has been determined, the locations of frame, information, and CVSD bits are now known. The clock goes through a series of dividers and logic to generate three separate clocks at the appropriate rates for the frame, CVSD, and information bits. Once frame lock has been achieved, the locations of the various types of bits are known and are picked out and directed to their correct destinations.

The CVSD data bits and clock are sent out to the orderwire module for processing. The data bits and clock are sent out of the modem and to the data test set receiver for error rate measurement, and the frame clock and bits are used internally by the demultiplexer to continually update the frame recognition circuitry. If the frame error rate exceeds a preset threshold, a frame search is reinitiated to relocate the frame bit. Note that this multiplex/demultiplex design was chosen to facilitate testing only and the parameters of a multiplex designed for a specific tactical or DCS application are likely to be different.

Clock Regenerator

This module completes the timing recovery loop and provides the basic timing and clock frequencies used throughout the receiver unit of the DAR-IV. Figure 2-16 is a block diagram of the clock regenerator module.

The error signal from the phase error estimator is passed through a lead/lag low pass filter which determines the loop time constants of the second order tracking loop. The output of the filter goes to a summer and to a comparator. The comparator digitizes the filtered error signal and is used as an input for the sweep circuit logic. The sweep logic also receives some control logic signals from the receiver

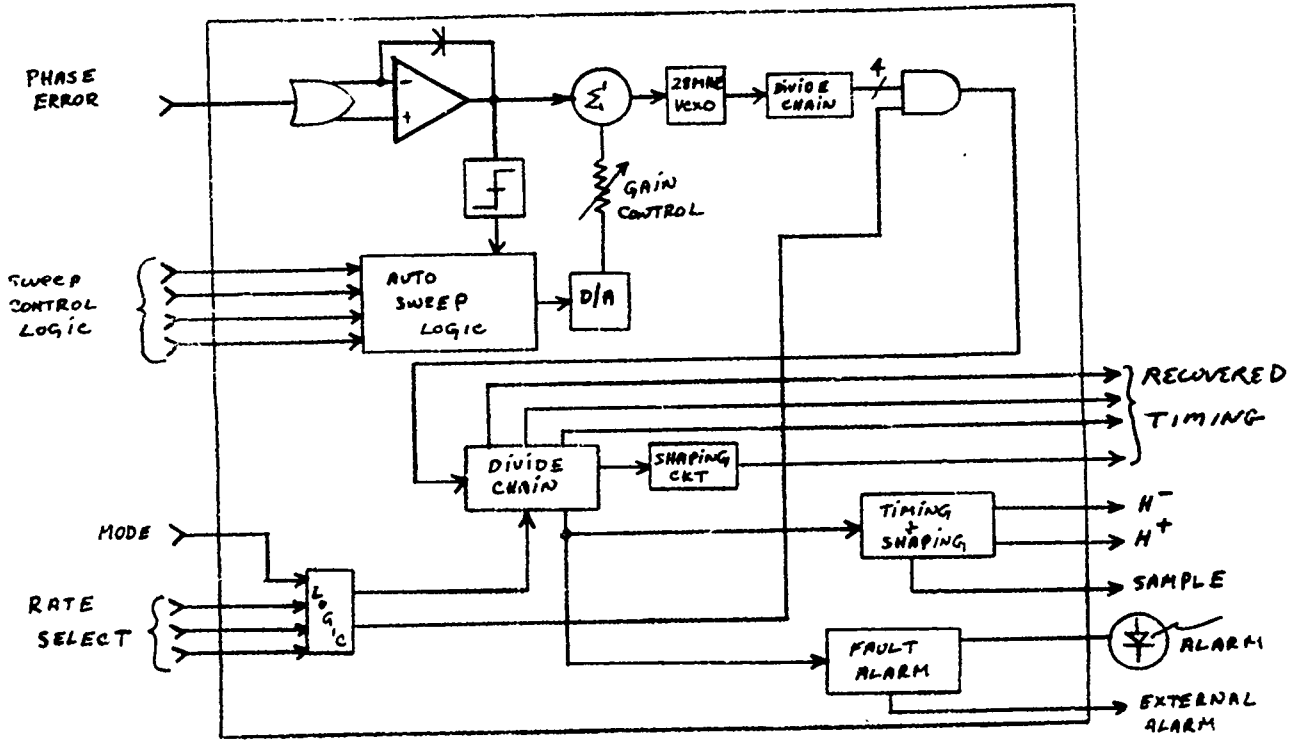

FIGURE 2-16 TIMING RECOVERY MODULE AND PROGRAMMABLE CLOCK DIVIDER

mode programmer. The digital command from the sweep circuit is D/A converted and summed with the filtered error signal from the phase error estimator and used as a control signal for a VCXO. This VCXO running at 28 MHz is the basic clock frequency for the receiver. The 28 MHz output is divided down to the fundamental data rate and symbol rate frequencies. The rate code logic from the mode programmer is used to gate the various divider chain outputs to be compatible with the desired data rate and mode of operation. The remaining circuitry is devoted to pulse shaping and phasing for the Dump, Sample and Hold pulses. These pulses have the same basic frequency as the baud rate but different relative phase or position than the clock pulses.

The sweep logic for automatic acquisition was rarely used during actual testing. The VCXO frequency stability is such that frequency offsets of several tens of Hertz can be accumulated over a period of days. However, the closed loop tracking bandwidth employed was on the order of 0.1 Hertz. An automatic sweep step search thus requires on the order of 100 x 10 sec. or 1000 seconds. It was found to be much easier to simply adjust the VCXO offset with a potentiometer until lock was observed on an oscilloscope. This procedure was normally necessary only at the start of a days testing. For military applications a rapid, automatic acquisition circuit is required. Such a circuit can be devised using a digital tracking loop with an adjustable tracking time constant or higher stability clocks can be employed to eliminate the need for a clock frequency search. If a stable station clock is supplied, it must have a minimum short term stability of 1 part in 10^8.

Orderwire Module

The function of the orderwire module in the receiver is essentially the opposite of that of the transmit orderwire. This module takes the digital CVSD data bits from the demultiplex module and reconstructs the analog waveform that the digits represent.

A standard implementation of the CVSD codec is employed. The CVSD data and clock are received from the demultiplexer. The data is applied to a 3 bit shift register and applied to a series of steering and control logic. The output of the logic is detected and amplified and passed through an active high pass/low pass filter configuration whose polarity is controlled by a set of differential switches driven by the received data. After passing through a gain control, the analog orderwire is made available at the rear panel of the Receiver Electronics Bay.

Adaptive Equalizer

When transmitting digital signals over a dispersive channel, one frequently encounters some degree of intersymbol inter-

ference. In the DAR-IV, when the delay spread exceeds the guard time between data bits, each received bit will be contaminated by some energy from the previous received bit. The effect of this interference is to reduce the available signal energy in the desired bit and hence increase the probability of error. The function of the adaptive equalizer is to determine the amount of intersymbol distortion present in the channel and then subtract off the energy from each data bit that came from the previous bit. Since the characteristics of the channel are time variable, the equalizer must be able to follow the changing characteristics, hence the name adaptive equalizer.

Figure 2-17 is a simplified block diagram of the equalizer used for the DAR-IV modem. The operation is described below.

The equalizer is essentially a negative feedback loop that generates an error signal and attempts to drive the error signal to zero.

The analog data from the I channel is applied to a summing junction. The other input to the summer is the negative feedback correction voltage which for the moment will be assumed to be zero. The output of the summer is applied to an eye detector or window detector. If intersymbol interference is present, the video signal will be either larger or smaller than normal and the eye detector output will indicate whether the signal is larger or smaller. At the same time, the output of the summer is sampled and a hard decision is made as to whether the received bit was a one or a zero. This is then delayed one bit interval and multiplied by the error signal from the eye detector. The process makes the error signal the same polarity regardless of whether the data bit was a one or a zero. The error signal thus generated will contain the in-phase component of the distortion which correlated with the I channel data and also contain the uncorrelated quadrature component. If this is now integrated, the in-phase components will add and the uncorrelated quadrature components will average to zero thus giving an estimate of the in-phase component of the distortion. The same procedure is used on the Q channel yielding an estimate of quadrature component of the distortion. The two components are now multiplied by the I and Q data decisions and appropriately combined to yield the correct form of the error signal. These are then converted to analog signals and fed back to the input summing junction. The closed loop operation then performs until the error signal is equal in magnitude to the distortion so that when the two signals are combined all that remains is the energy due to the present bit.

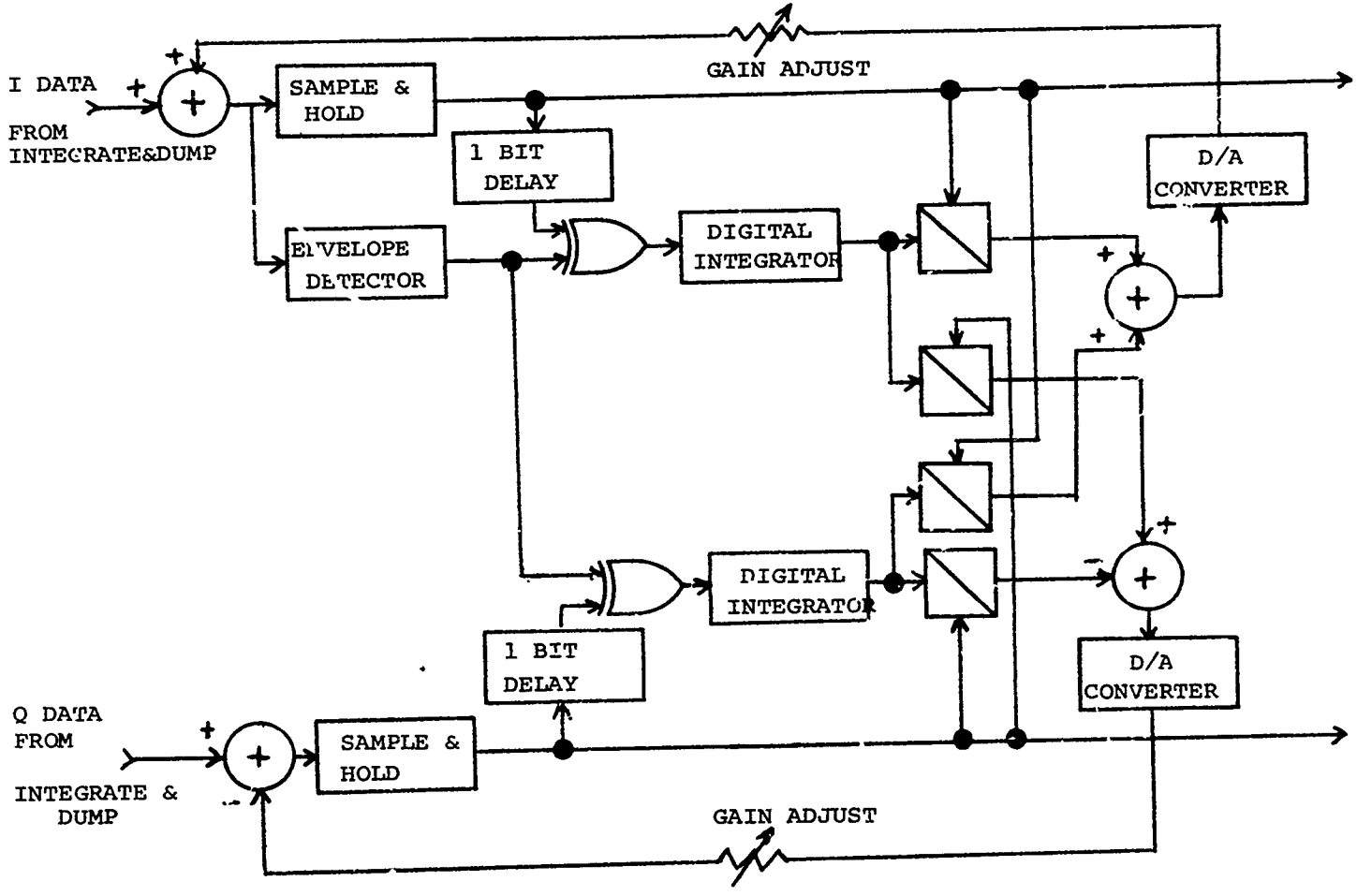

FIGURE 2-17 DETAIL BLOCK DIAGRAM OF DECISION FEEDBACK EQUALIZER

Performance

The adaptive equalizer was first tested at baseband only. In this case, intersymbol interference was introduced at baseband. Performance was found to be quite satisfactory.

The equalizer was then integrated with the DAR-IV modem. After final adjustment, it was discovered that, at best, no improvement in performance could be obtained. This was due to several factors. The first case was due to the limited memory of the DAR-IV recovered carrier filter. This would cause amplitude variations on the recovered data above and beyond those caused by the interference. These variations were not consistent with the interference and consequently would cause the equalizer to perform wrong corrections.

Secondly, the integrators in the equalizer were not leaky and would tend to saturate during severe multipath thus overcorrecting in many cases. Finally, the high switching speeds caused rather severe ringing on the D/A converter output which would distort the magnitude of the feedback voltage.

It is felt that none of the above problems are insurmountable and that an improved version can be built and used successfully.

2.3 Back-to-Back Performance of DAR-IV

The back-to-back performance of the DAR-IV is an important first step in the evaluation of this digital modulation technique on the fading, dispersive channel. The back-to-back performance establishes the implementation margin, dynamic range, bandwidth, and other features which will be necessary to properly interpret the fading channel performance.

Figure 2-18 shows the test set-up used to measure the BER performance versus the E_b/N_o per diversity channel. Four simulated back-to-back diversity signals were obtained by separating the IF modulator outputs into four equal strength paths and adding independent noise to each path. The Carrier to Noise Ratio (CNR) was adjusted by adjusting the IF signal level in the presence of additive Gaussian noise. For each value of CNR, the Bit Error Rate (BER) was recorded. The CNR was normalized to the equivalent "bit rate bandwidth" to yield the corresponding value of E_b/N_o.

The four independent noise sources were obtained by using high gain IF amplifiers with a nominal 20 MHz flat noise bandwidth centered at a 70 MHz. The source of a test data pattern and error detector was the HP-1930 A test set. A 2^{15} -1 bit test pattern was employed for all tests since it provides a high degree of data randomness with reasonable synchro-

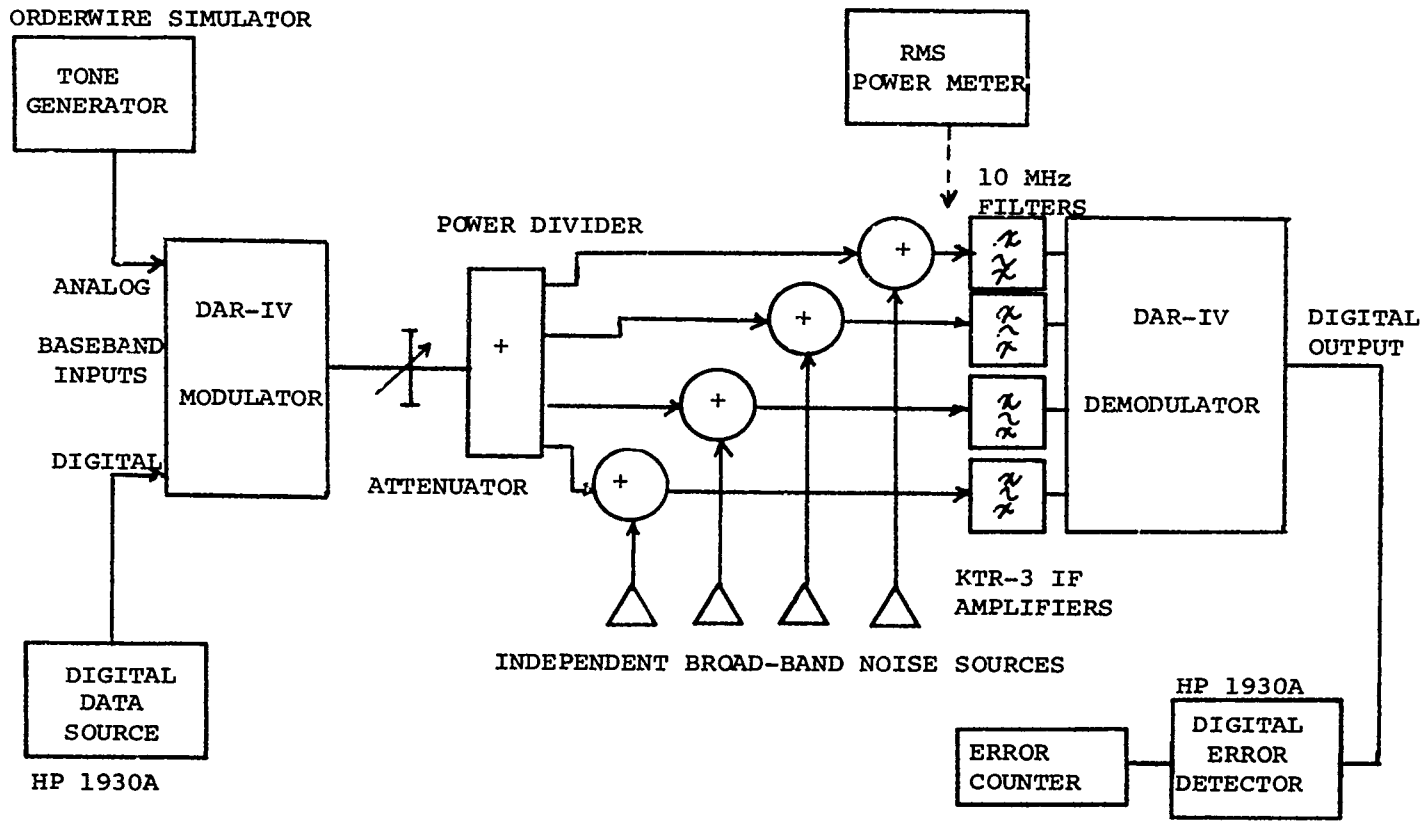

FIGURE 2-18 BACK-TO-BACK PERFORMANCE TEST SET-UP

nization behavior. The shortest and longest patterns of the HP-1930 A were also exercised at one data point to demonstrate the lack of pattern sensitivity in the error rate measurements-

The DAR-IV time gating was chosen to be representative of the over-the-air tests. In most tests, a nominal 50% pulse duty cycle was employed since it generally provides the best combination of spectral efficiency and multipath protection. The actual pulse duty cycles were determined by the DAR-IV options as previously described. At transmission rates of 1.75, 3.5 and 7 Mbps, the respective pulse durations were 475, 285, and 95 ns corresponding to duty cycles of 44%, 50% and 33%. Figure 2-19 shows a typical modulator output waveform at 1.75 Mbps and Figure 2-20 shows the corresponding $(\text{six } X/X)^2$ spectrum. A 10 MHz bandpass filter was placed before the DAR-IV input in the back-to-back tests to provide some representative pulse bandlimit and also to limit out-of-band noise power.

Figure 2-21 shows the back-to-back BER performance at 1.75 Mbps (solid lines) versus the theoretical performance of an ideal differentially encoded coherent PSK system (dashed lines). The performance is shown for non, dual and quad diversity operation.

In the non diversity case, all four input channels were tested and found to behave identically. The non diversity performance was found to be about 2.5 dB from ideal at 10^{-5} BER. This departure from ideal performance can be attributed to a number of implementation factors. One factor is the bandwidth of the recirculating filter employed in the adaptive matched filter unit. Although the basic SAW delay line has a 4 MHz 0.3 dB bandwidth, the positive feedback reduces the net bandwidth to between 3 and 4 MHz at 3 dB with Gaussian-like shape factor. Hence, some distortion will remain in the reference signal.

Non ideal compensation of delays and phase shifts also accounts for some of the loss. Since the present SAW delay lines are in an "oven" with a long thermal time-constant, fine grain adjustment of delay is difficult. As a result, some bias errors exist in the circuit implementation. In addition, misadjustment of the IF filters, and dc bias errors in the integrate and dump filter and channel video combiner contribute to the implementation losses. It is anticipated that the present 2.5 dB implementation loss can be lowered to about 1 dB through appropriate modifications to the present circuitry.

For non-fading channels, each doubling of the explicit order of diversity as shown in Figure 2-21 should produce an exact 3 dB reduction in required E_b/N_o for a given BER provided all channels have equal S/N. As shown in Figure 2-21, the experimental system provides approximately a 5 dB E_b/N_o reduction in going from non to quad diversity instead of the theoretical 6 dB. The primary contributor to this implementation degradation is imperfect weighting of the diversity channels due to errors in the tracking of the

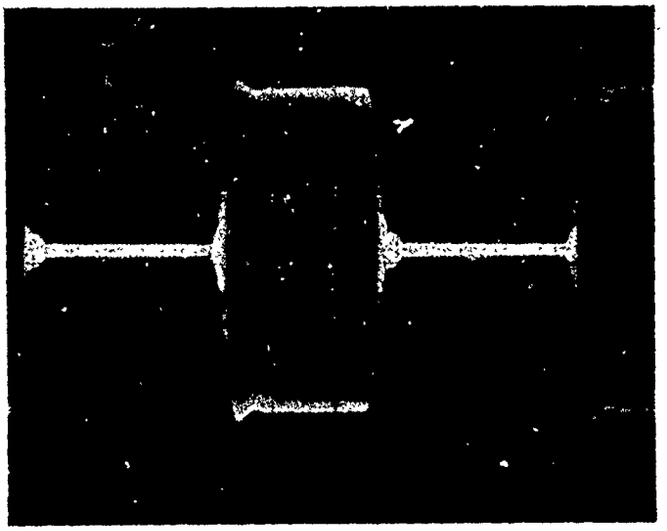

FIGURE 2-19

DAR-IV TRANSMISSION
WAVESHAPE
1.75 Mbps

44% Duty Cycle

200 nsec/Div.

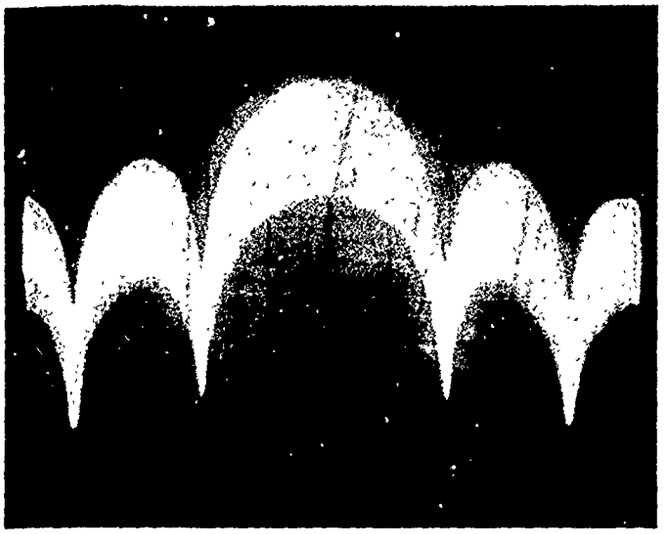

FIGURE 2-20

DAR-IV TRANSMISSION
SPECTRUM
1.75 Mbps

44% Duty Cycle

10 dB/CMx 1 MHz/Div.

FIGURE 2-21 1.75 MBPS DAR-IV BER PERFORMANCE FOR NON,DUAL, QUAD DIVERSITY

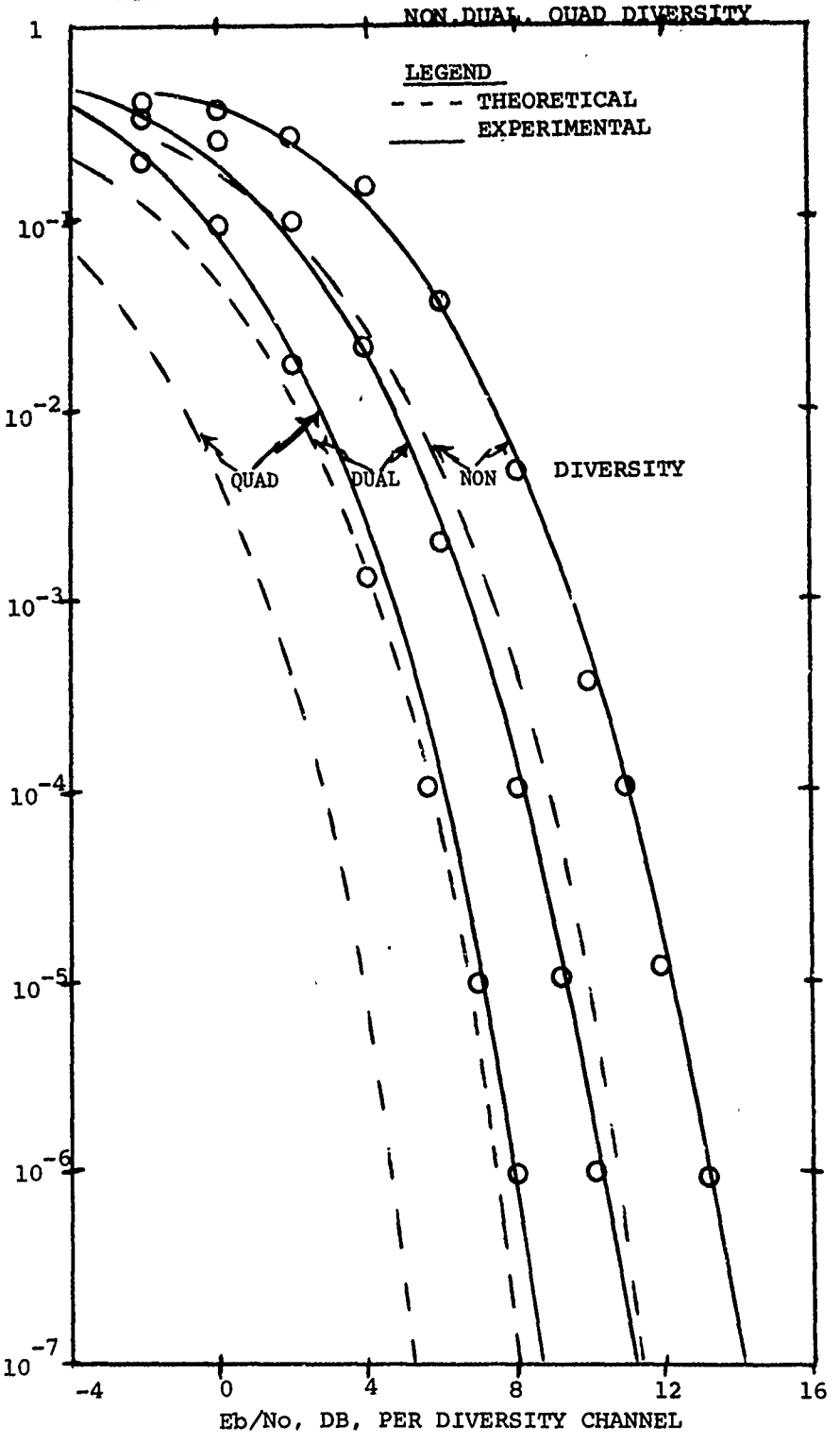

Automatic Gain Control (AGC) of each channel and dc bias errors in the video amplifier which linearly sums the matched filter outputs. Again, through appropriate design modifications, such as current controlled AGC attenuators, the present implementation loss can be significantly reduced. For the over-the-air experimental performance of the present model, an implementation loss of between 2.5 to 3.5 dB must be included at 1.75 Mbps depending on the order of diversity.

Figures 2-22 and 2-23 show similar back-to-back results for 3.5 Mbps and 7 Mbps, respectively. Within the experimental BER measurement accuracy (of approximately ± 0.5 dB in E_b/N_o), there is relatively little difference in back-to-back performance as a function of data rate. That is, with the possible exception of the SAW recirculating filter, the components of the modem are sufficiently broadband to accept a variety of range of data rates with very little difference in performance. (In some of the over-the-air results using spread-spectrum pulse coding, a SAW device bandwidth limitation is the present model is observed.)

The dynamic range of the modem was also examined in terms of the range of noise levels which could be tolerated for less than 1 dB degradation. Both signal and noise level were simultaneously varied at constant E_b/N_o and it was found that a range in excess of 18 dB exists over which the modem can be operated. Hence, the adjustment of "nominal" signal levels during modem installation is not critical but the median noise levels of all of the diversity channels should be made equal for optimum performance.

The lowest E_b/N_o at which the modem would retain bit-count-integrity was also examined for all operational modes of the modem. An E_b/N_o of -6 dB to -12 dB was measured depending on the order of explicit diversity. This lower limit on modem E_b/N_o operation was found to be very suitable for operation in the fading channel combined with a feature in the demultiplexer which inhibits a frame resynchronization search unless the low E_b/N_o condition persists.

The previous back-to-back performance results were for the DAR-IV experimental model with the "tail canceller" or Decision Feedback Equalizer (DFE) disabled. The back-to-back results with the DFE were similar to the results previously described in Figures 2-21 through 2-23 except that an additional implementation loss of 1 to 1.5 dB was observed. The resultant overall implementation loss (at 10^{-5} BER) was then approximately 3.5 to 5 dB depending on the order of explicit diversity when the DFE was employed. The extra DFE losses are created due to the fact that the DFE will make minor corrections for intersymbol interference even when none is present due to the presence of a noisy signal and quantization errors in the DFE loop. The DFE thus introduces a jitter or additional noise term and should, therefore, only be employed when intersymbol interference is likely to be a more important performance limitation than thermal noise. The noise

FIGURE 2-22 3.5 MBPS DAR-IV BER PERFORMANCE FOR NON, DUAL, AND QUAD DIVERSITY

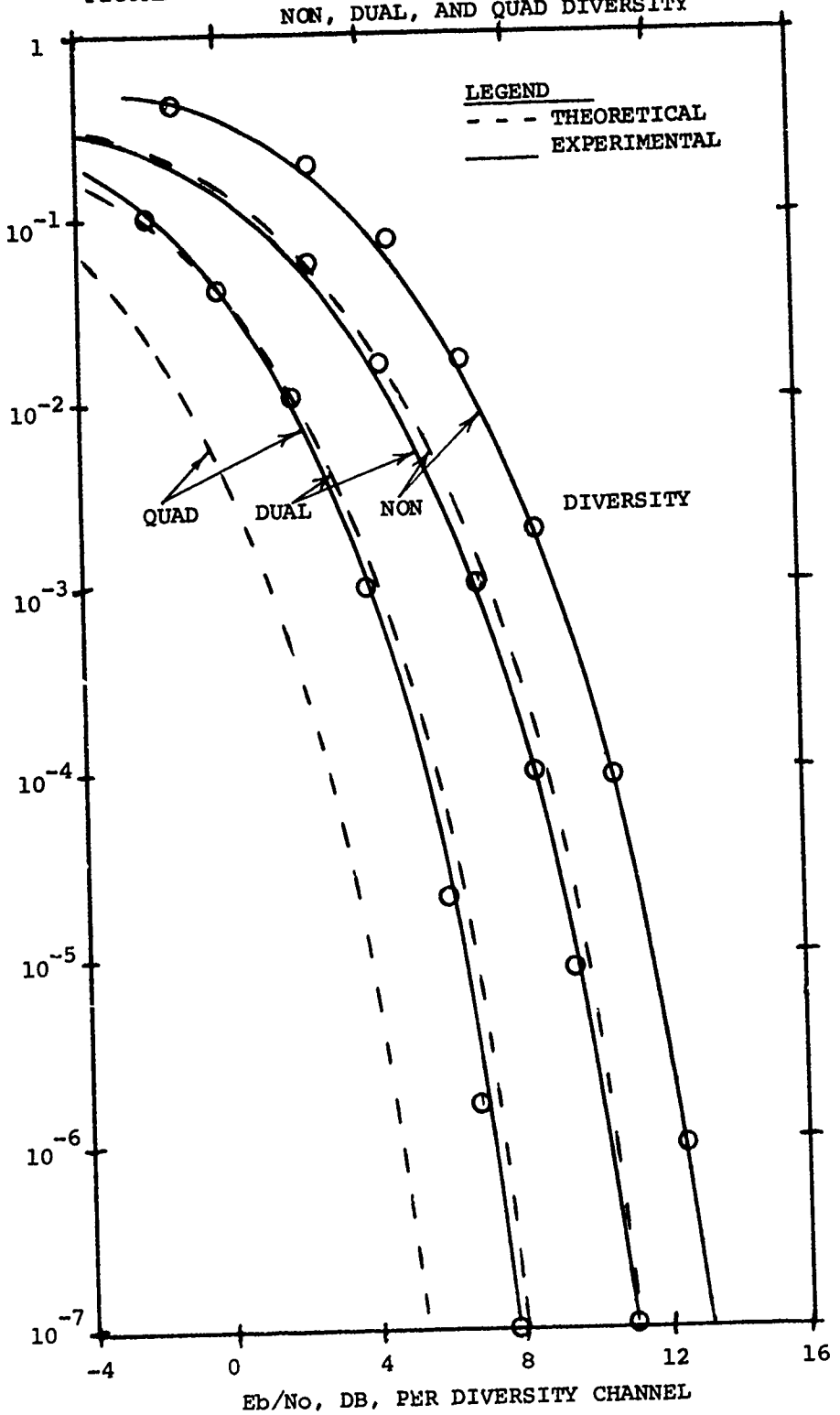

FIGURE 2-23 7 MBPS DAR-IV BER PERFORMANCE FOR NON, DUAL, AND QUAD DIVERSITY

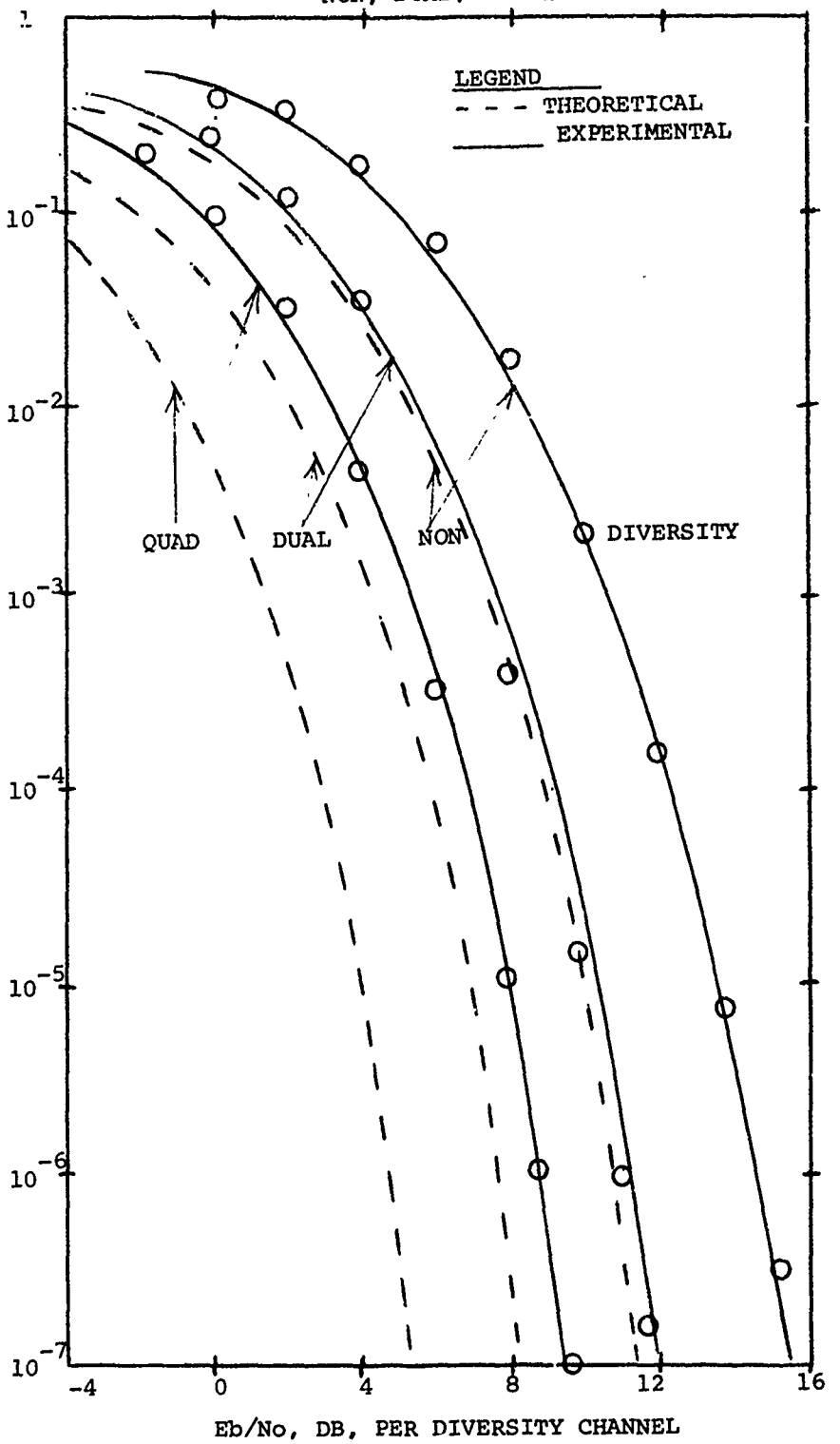

introduced by the present DFE implementation can also be improved in future DAR-IV designs through the use of longer averaging times and finer quantization. However, these improvements must be combined with expansion of the DAR-IV reference "memory" to be effective, as described in later sections.

The DAR-IV built has four Adaptive Matched Filter Modules which should all behave identically for proper diversity operation of the modem. Figure 2-24 shows the back-to-back BER performance for each modem at 1.75 Mbps superimposed on the same graph. Note that all matched filter units behave identically within the experimental measurement accuracy.

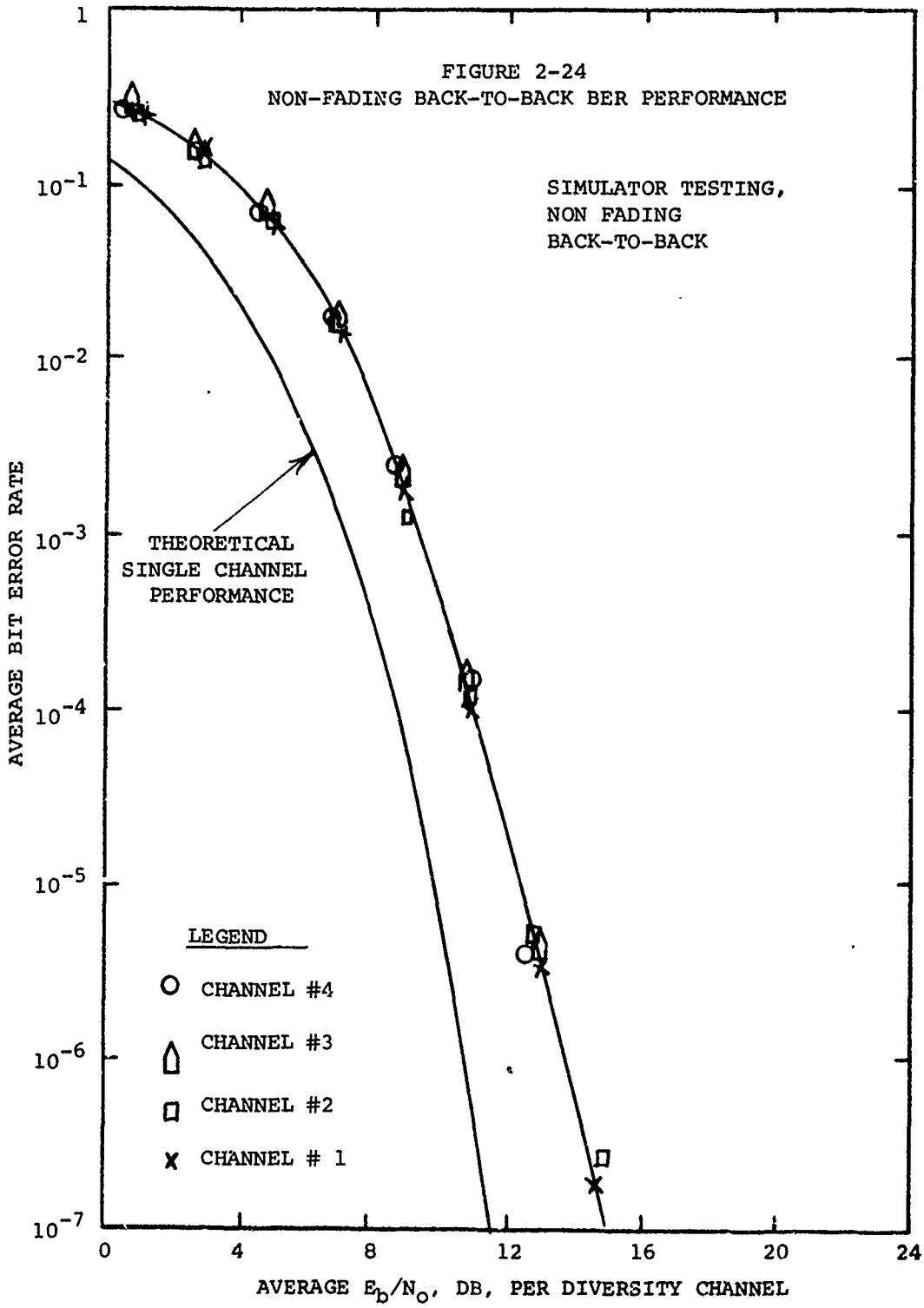

FIGURE 2-24
NON-FADING BACK-TO-BACK BER PERFORMANCE

3.0 DAR CHANNEL SIMULATOR TEST RESULTS

3.1 General

More than two months of channel simulator testing was performed with the DAR-IV experimental model to provide a performance baseline for over-the-air testing. The tests can be separated into two parts representing potential tactical and DCS application of the DAR-IV modem. The tactical channels are characterized by lower data rates (less than 2.3 Mbps) and a wide range of multipath dispersion. The DCS paths are likely to require higher data rates of up to 6.3 Mbps and a narrower range of multipath dispersion on many paths and more stringent bandwidth efficiency requirements.

Tactical simulator tests were performed on the Raytheon DAR-IV modem to determine its suitability for application to digital tactical troposcatter. The results described in Section 3.2 were obtained under a TRI-TAC (USAF) test program which was conducted by ESD/MITRE with Raytheon participation under contract F19628-75-C-0103. Operational tests were conducted using the RADC four channel troposcatter simulator at data rates of 1.75 and 3.5 Mbps and for non, dual, triple and quad explicit orders of diversity. The majority of tests performed were concentrated at 1.75 Mbps with dual diversity using multipath delay power spectra (channel characterizations) typical of the AN/TRC-97 on an 87 mile path with an equivalent 2.3 Mbps transmission rate.

Test results showed that the DAR-IV can provide very large performance improvements (on the order of 10 dB at 10^{-5} bit error rate) due to intrinsic diversity. Also, that the DAR provides significant intrinsic diversity improvement with even modest amounts of multipath dispersion and at all data rates of interest.

The DCS media simulator tests are described in Section 3.3. These tests were concentrated on the median and "worst case" multipath conditions for a 168 mile tropo path using the AN/MRC-98 radio at 880 MHz or the AN/TRC-132 radio at C-band. Tests were conducted at 1.75, 3.5 and 7 Mbps and for all orders of diversity. Emphasis in the test program was placed on the higher orders of diversity and higher data rates typical of the potential DCS applications. The test results show good agreement with theoretical predictions and verify the significant potential of the DAR-IV modem technique in satisfying future requirements of an all digital DCS.

Section 3-4 provides a performance summary of the simulator testing. Comparison of the results with theoretical shows that the DAR, after subtraction of implementation losses, provides ideal adaptive matched

filter performance within its design limits. A simple mathematical expression is fitted to these results which allows the prediction of the required E_b/N_o for a 10^{-5} average BER within ± 0.5 dB given only the channel rms multipath delay spread and the 3 dB bandwidth of the transmitted spectrum.

3.2 DAR Tactical Tropo Simulator Test Results

3.2.1 Test Conditions

The DAR-IV was tested over a wide range of simulated troposcatter channel conditions believed to represent both the typical and extreme operating conditions of a tactical troposcatter radio. The test conditions were based on a data rate of 2.304 Mbps and the channel multipath "profiles" (or delay power spectra) shown in Table 3-1. The multipath profiles were established in an ESD/RADC/MITRE over-the-air RAKE measurement program of the AN/TRC-97 on the 86 mile (Ontario Center to Verona, N.Y.) RADC test range. It was found that the typical multipath environment of an AN/TRC-97 on the 86 mile RADC test link was represented by profiles 2 and 3. To expand this typical operating region, an additional multipath profile labeled 2A was inserted between profiles 2 and 3.

The 1.75 Mbps rate of the DAR-IV was chosen for the tactical path simulation since it is nearest to the desired 2.304 Mbps rate. To permit comparison of the DAR-IV modem with alternative approaches, the multipath profiles of Table 3-1 were increased (scaled) by a factor of 2.304/1.75 = 1.3. Table 3-2 shows the resultant multipath profiles actually tested. Some additional testing of the DAR-IV with the unscaled multipath profiles of Table 3-1 was also performed at the 3.5 Mbps data rate.

Figure 3-1 shows the basic setup used for media simulator testing of the DAR-IV modem. A set of Hewlett Packard test data pattern generators (HP-1930A) were used to simulate random binary data and determine the occurrence of errors. In all the tests performed, a repetitive pseudo-random data pattern of approximately 2^{20} bits in length was employed which models random data to high accuracy.

The RADC four-channel troposcatter simulator was employed to create multipath propagation effects similar to those encountered on a real link. This simulator can provide up to four independently fading and multipath corrupted channels to examine the diversity performance of a modem. The channel simulator is basically transversal filter (or tapped delay-line filter) whose tap outputs are multiplied by weighted gaussian noise and linearly added. The noise weighting of the taps (or the average power of the signal from each tap) is adjusted to reflect the desired multipath delay power spectrum.

TABLE 3-1
MULTIPATH PROFILES FOR TRI-TAC TESTING

TAP NO.	PROFILE NO. 1	2	3	4	5	6
1	0	0	0	0	3	1
2	16	6	3	1	0	0
3	38	14	7	4	1	1
4		23	12	7	3	2
5		34	17	11	5	3
6			23	14	7	5
7			29	18	10	7
8				22	12	9
9				25	15	11
10				29	18	14
11					21	16
12					24	18
13					27	20
14						23
15						25
16						
Pav (dB)	0.1	1.1	2.5	4.0	5.5	6.6
$\overline{\tau}$ (μs)	0.103	0.127	0.167	0.214	0.325	0.360
$\Delta = 2\sigma$ (μs)	0.031	0.11	0.19	0.26	0.38	0.46

TABLE 3-2
SCALED MULTIPATH PROFILES FOR 1.75 Mbps

TAP NO.	PROFILE NO. 1	2	2A	3	4	5	6
1	0	0	0	0	3	1	8
2	11	4	3	2	0	0	1
3	28	10	7	5	1	1	0
4		17	13	8	3	2	0
5		24	18	12	5	3	1
6		32	24	16	7	5	2
7			30	21	10	7	4
8				25	13	9	5
9				29	15	11	6
10					18	13	8
11					21	15	9
12					24	17	11
13					27	19	13
14					30	21	14
15						24	16
16						26	18
Pav (dB)	0.34	1.8	2.5	3.4	5.5	6.6	7.7
$\overline{\tau}$ (μs)	0.108	0.144	0.164	0.20	0.323	0.365	0.511
$\Delta = 2\sigma$ (μs)	0.041	0.14	0.18	0.25	0.38	0.48	0.57

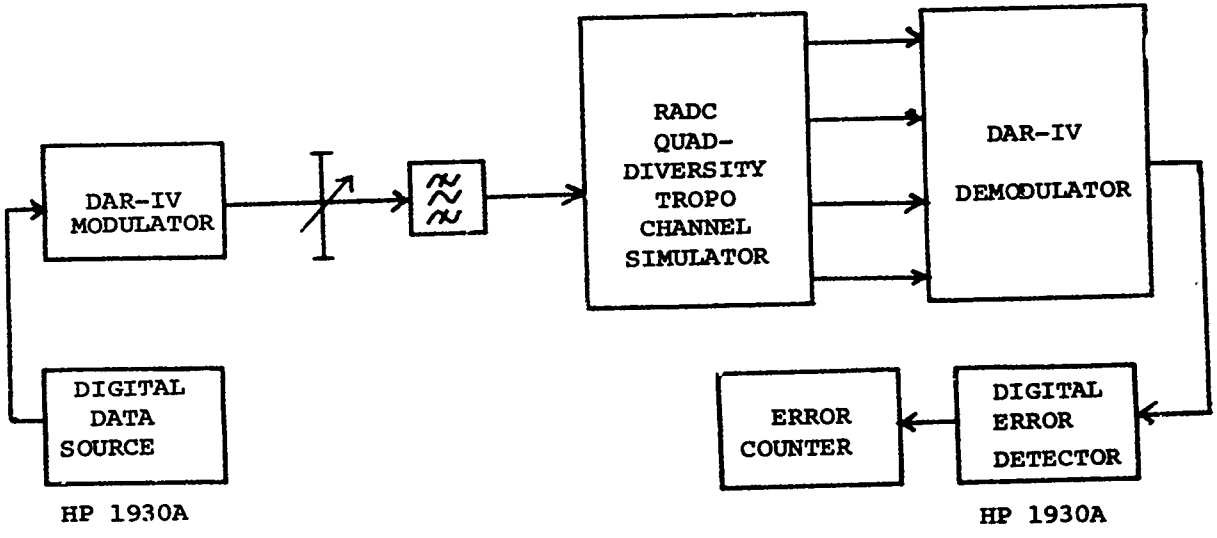

FIGURE 3-1 TROPO CHANNEL SIMULATOR TEST SET-UP OF DAR-IV

The multipath profiles of Tables 3-1 and 3-2 are shown in the form of "tap settings" for the RADC tropo channel simulator at a 0.1 us tap spacing. The profiles can be better visualized when plotted as shown in Figure 3-2. Here, each multipath profile (or delay power spectrum) is plotted on the same figure with the same area. That is, the average received power level from each profile shown is identical. Note the increase in time-dispersion for each profile. Figure 3-3 shows the same result plotted on a decibel scale. Here, the increase in multipath time dispersion for the large profile numbers is more clearly evident.

The RADC tropo channel simulator also has a capability to alter the fading rate (double-sided RMS Doppler spread) of the simulated channel over a wide range. Tests were performed for fade rates from 0.5 Hz to 10 Hz with no appreciable change in performance.

The first set of tests performed under the tactical modem evaluation program was the DAR-IV back-to-back performance. This set of tests established the basic "implementation margin" of the DAR-IV experimental model. These tests were then followed by a series of "flat fading" tests where the time dispersion of the multipath was zero and each diversity channel exhibited Rayleigh fading. A series of tests were performed to measure non, dual, triple, and quad diversity and also the sensitivity to fade rate. Under non-diversity conditions, all four channels of the DAR-IV were examined to determine the uniformity of the implementation margin.

The majority of the tests performed were for the frequency selective fading conditions described in Table 3-1 and 3-2. Tests were performed at fade rates (double sided rms Doppler spread) of 0.5 Hz and 5 Hz for all profiles. In each case, no significant difference in performance resulted indicating that the DAR-IV is not sensitive to fade rate over the range of fade rates typically encountered at C-band. The bulk of the tests were, therefore, performed at the 5 Hz fade rate to obtain more reliable statistical averages. At the start of each test, the channel simulator was reset so that the same instantaneous conditions of time-varying multipaths could be duplicated exactly for each bit error rate (BER) measurement. Non, dual, and quad explicit diversity tests were performed. Also, in selected cases, different conditions of transmission bandwidth, DAR-IV time gate duty cycle, and DAR-IV spread-spectrum pulse coding were tested.

3.2.2 Performance in Frequency-Flat Fading

A set of tests was next performed to evaluate the DAR-IV performance on the Rayleigh fading channel. This Rayleigh channel (or frequency-flat fading channel) is easily obtained by employing only one tap of the RADC channel simulator to represent each multipath profile (non-dispersive). The tests are useful to verify the dynamics of the DAR-IV as the ability to accommodate fading, bursts of noise or errors, fade

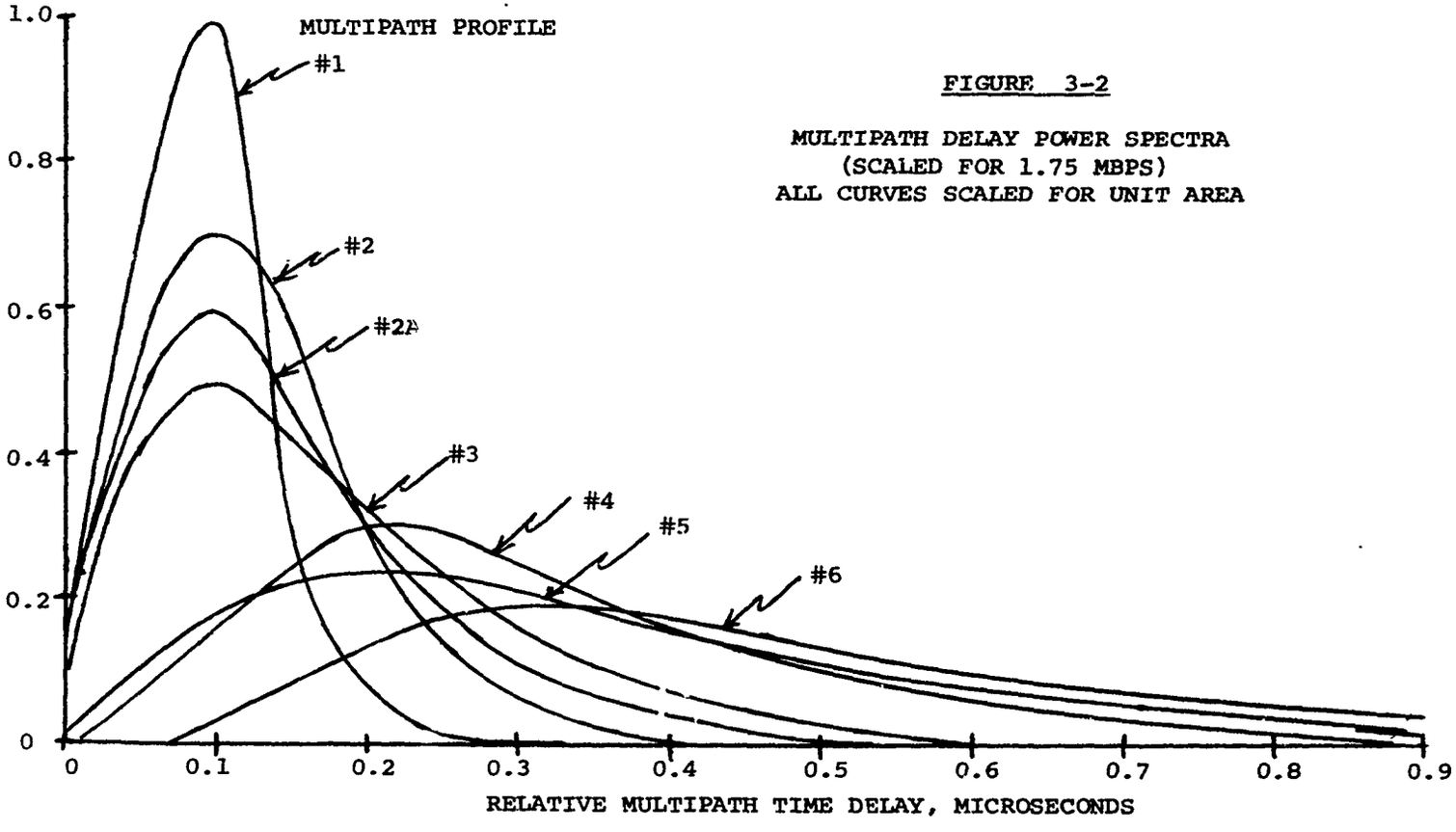

FIGURE 3-2

MULTIPATH DELAY POWER SPECTRA
(SCALED FOR 1.75 MBPS)
ALL CURVES SCALED FOR UNIT AREA

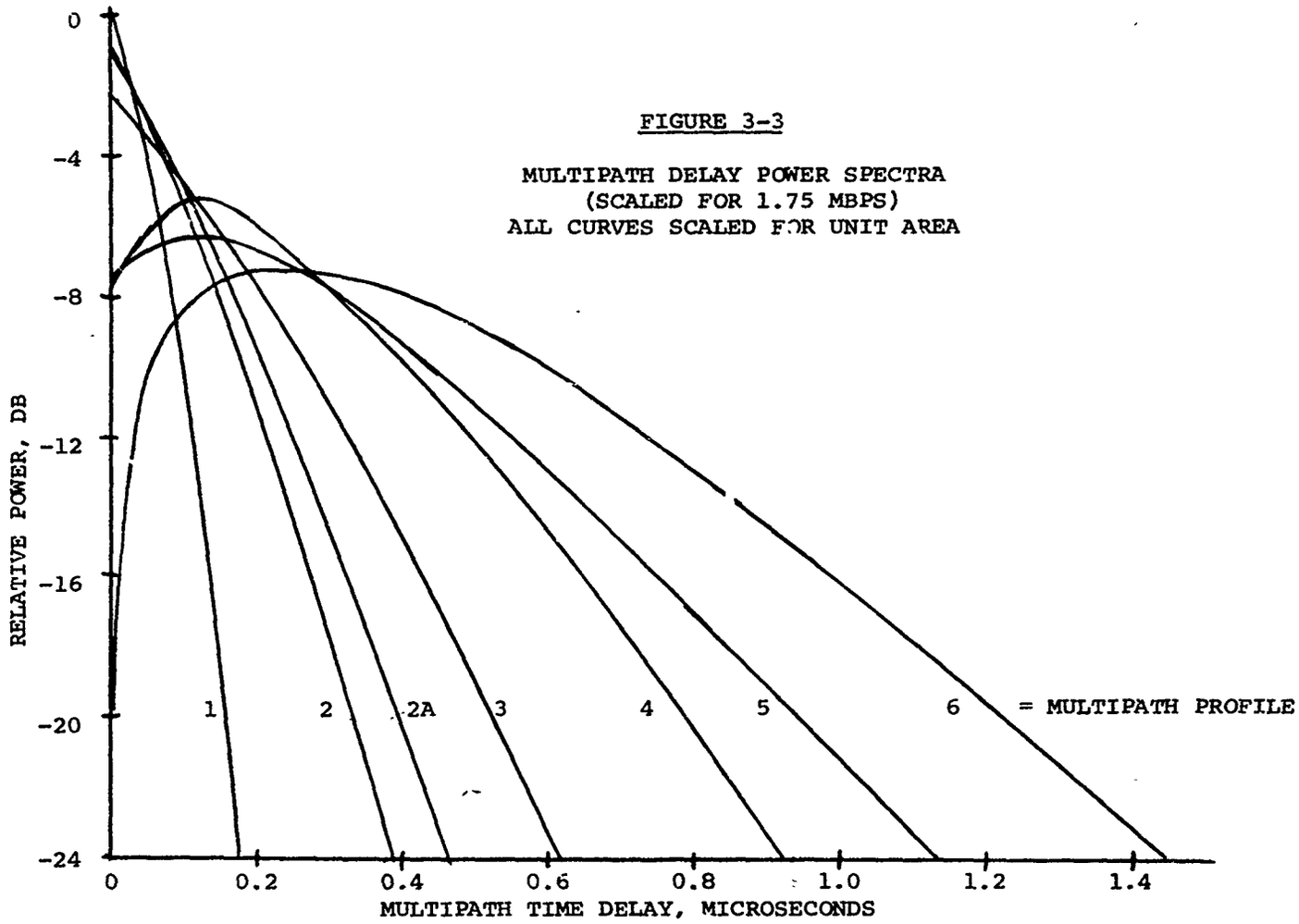

FIGURE 3-3

MULTIPATH DELAY POWER SPECTRA
(SCALED FOR 1.75 MBPS)
ALL CURVES SCALED FOR UNIT AREA

rates, dynamic range, and recovered timing stability.

Figure 3-4 shows the single channel (non-explicit diversity) performance of the DAR-IV for rapid, frequency-flat, Rayleigh fading. Data points for each of the four diversity channels of the experimental DAR modem are shown superimposed. The resultant dispersion in the data points is negligible and within the accuracy of the BER measurements. The implementation loss or departure from ideal DCPSK is 2.4 dB.

Figure 3-5 shows the sensitivity of the DAR-IV modem to fade rate (two-sided rms Doppler spread) from 0.5 Hz to 10 Hz. The results of this test showed no difference in the DAR performance over the range of the fade rates typical of a C-band troposcatter link. There was no indication of a bit count integrity loss problem even at the slowest fade rate.

Figure 3-6 shows the non, dual, and quad diversity performance of the DAR-IV on a single graph. Error rates as large as 0.4 can be measured without any apparent "threshold" phenomenon in the DAR. The DAR-IV reference memory is on the order of 10 symbols which is adequate to provide a low noise reference which is unlikely to produce significant error propagation effects. The measured performance is within 2.2 to 3 dB of the theoretical performance at average error rates of interest indicating that the DAR-IV is very accurate at realizing the ideal maximal ratio diversity combining characteristic. Also, very little "scatter" of the data points was obtained throughout all testing indicating that reasonable choices of averaging time were employed at each BER range.

3.2.3 Performance in Frequency-Selective Fading

3.2.3.1 1.75 Mbps Performance

The majority of tactical channel tests performed on the DAR-IV were at a data rate of 1.75 Mbps. The multipath delay power spectra of Table 3-2 were applied at this data rate. These multipath profiles are scaled up from those of Table 3-1 to represent equivalent performance at a data rate of 2.304 Mbps, which was employed as the comparison baseline in the tactical test program.

3.2.3.2 Rectangular Pulse Shape - 50% Duty Cycle

The first series of tests performed were for a nearly rectangular transmission pulse shape and a nominal 50% duty cycle transmit time gate (actually 44% as determined by quantized options within the DAR-IV model). The pulse bandlimiting results from the IF bandwidth of the present DAR-IV model (about 15 MHz) and the recirculating filter in the DAR-IV reference circuit (about 3 to 4 MHz). Hence, the

FIGURE 3-4

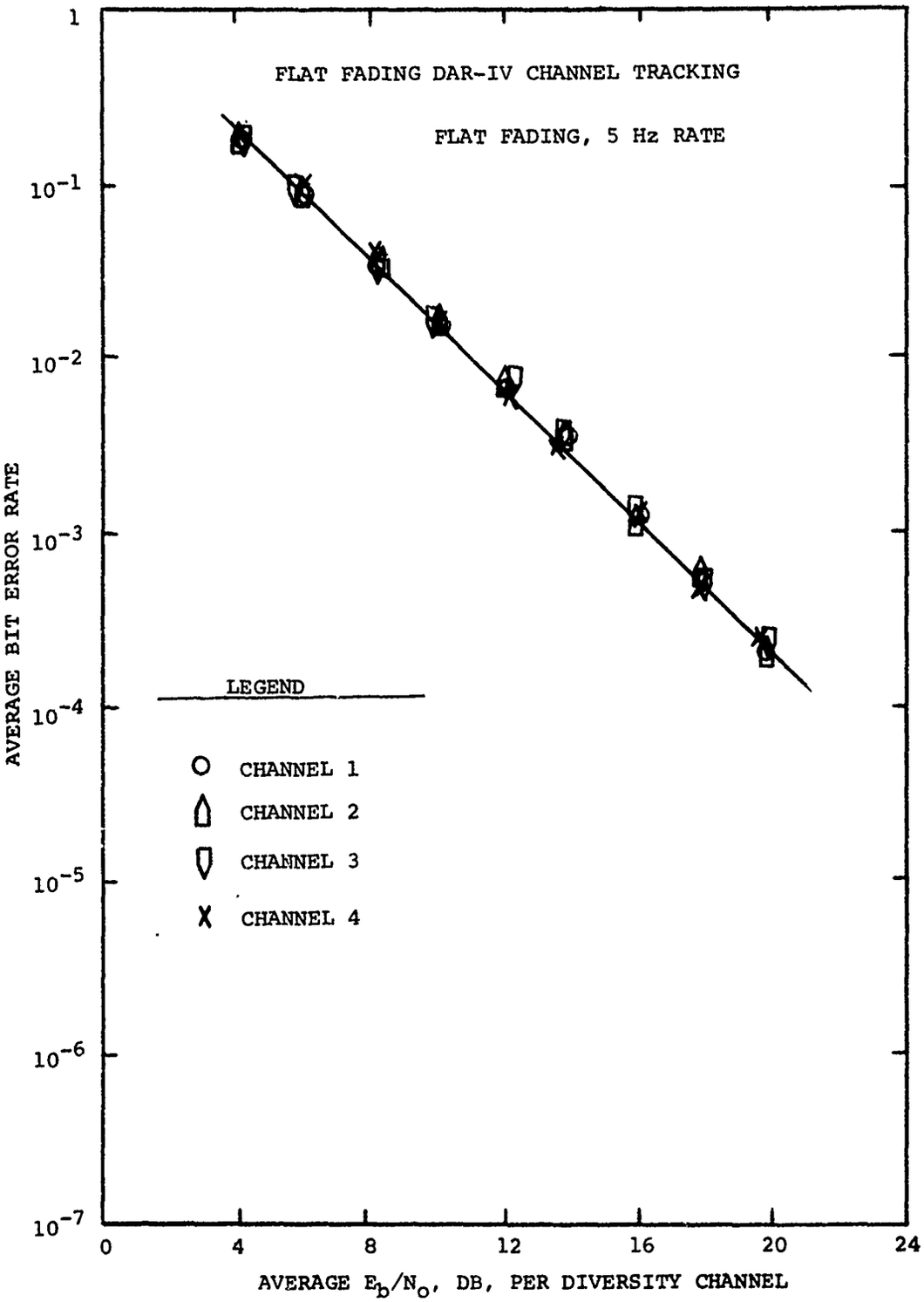
FLAT FADING DAR-IV CHANNEL TRACKING
FLAT FADING, 5 Hz RATE
AVERAGE BIT ERROR RATE
1
10^{-1}
10^{-2}
10^{-3}
10^{-4}
10^{-5}
10^{-6}
10^{-7}
LEGEND
CHANNEL 1
CHANNEL 2
CHANNEL 3
CHANNEL 4
0
4
8
12
16
20
24
AVERAGE E_b/N_o, DB, PER DIVERSITY CHANNEL

FIGURE 3-5

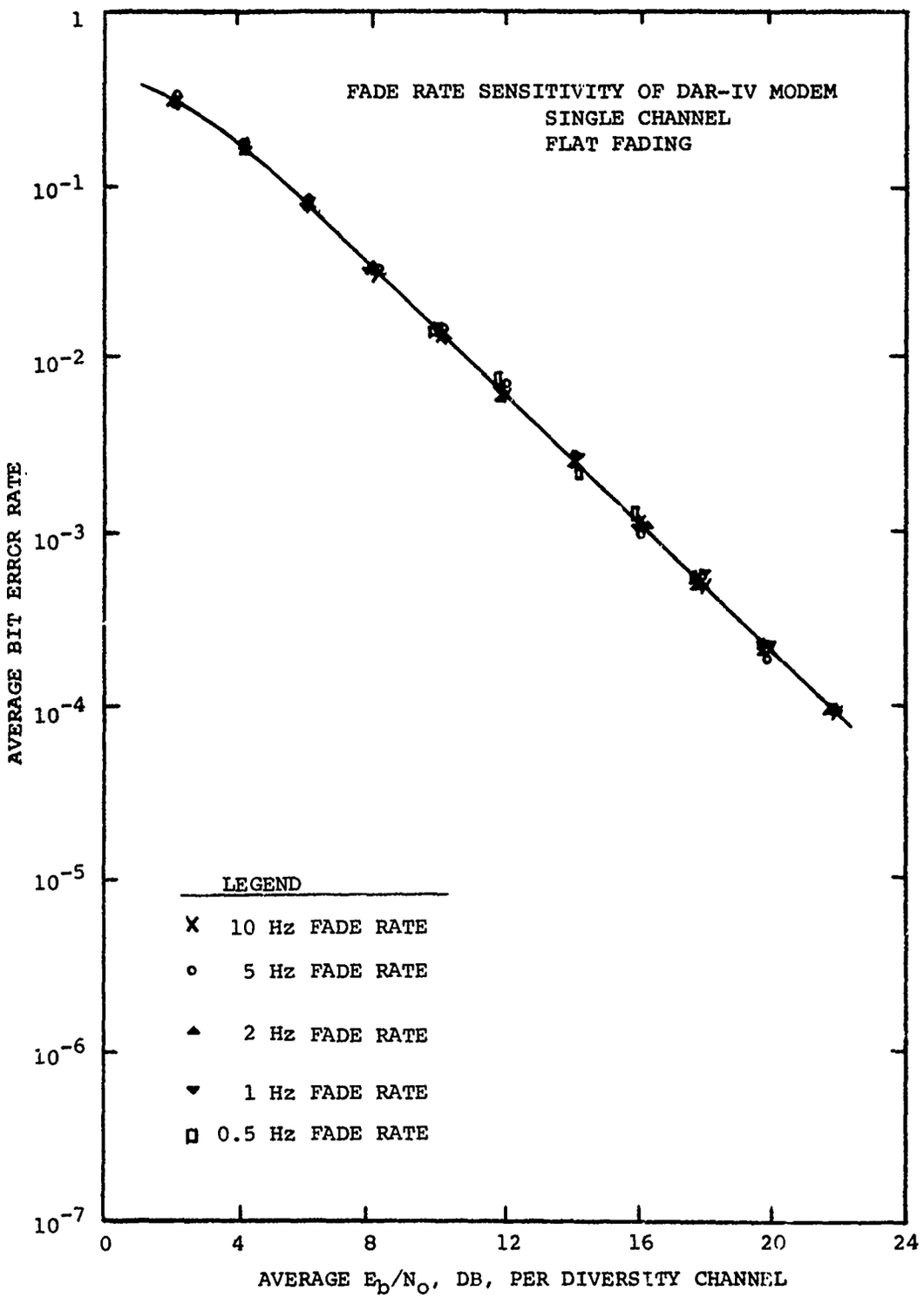
FADE RATE SENSITIVITY OF DAR-IV MODEM
SINGLE CHANNEL
FLAT FADING
AVERAGE BIT ERRCR RATE
1
10^{-1}
10^{-2}
10^{-3}
10^{-4}
10^{-5}
10^{-6}
10^{-7}
0
4
8
12
16
20
24
AVERAGE E_b/N_o, DB, PER DIVERSITY CHANNEL
LEGEND
10 Hz FADE RATE
5 Hz FADE RATE
2 Hz FADE RATE
1 Hz FADE RATE
0.5 Hz FADE RATE

FIGURE 3-6

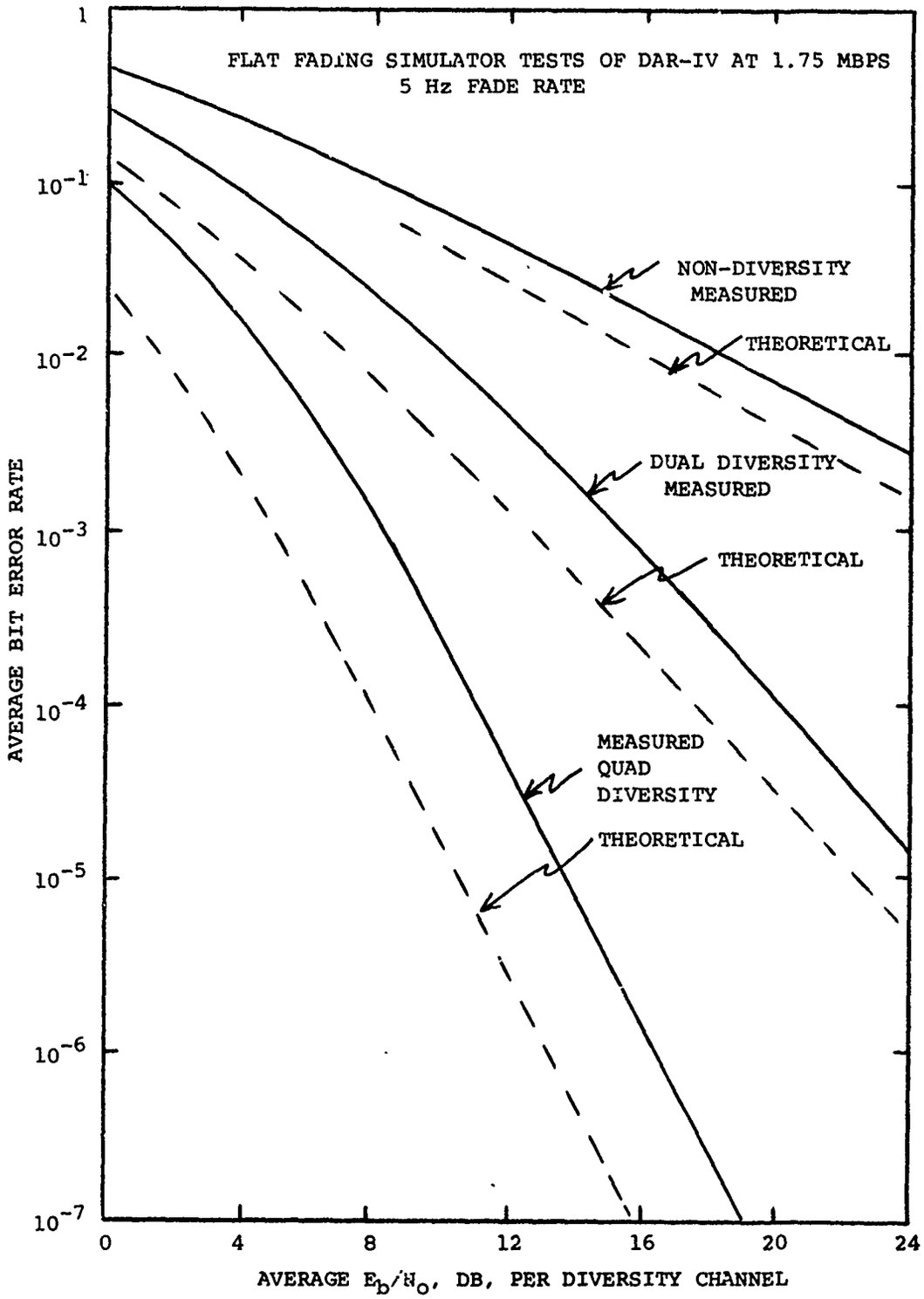
FLAT FADING SIMULATOR TESTS OF DAR-IV AT 1.75 MBPS
5 Hz FADE RATE
NON-DIVERSITY MEASURED
THEORETICAL
DUAL DIVERSITY MEASURED
THEORETICAL
MEASURED QUAD DIVERSITY
THEORETICAL
AVERAGE BIT ERROR RATE
1
10^{-1}
10^{-2}
10^{-3}
10^{-4}
10^{-5}
10^{-6}
10^{-7}
0
4
8
12
16
20
24
AVERAGE E_b/N_o, DB, PER DIVERSITY CHANNEL

pulse energy at frequencies significantly greater than 4 MHz does not contribute to performance in the present model.

Figures 3-7, 3-8, and 3-9 summarize the respective non, dual, and quad explicit diversity results of the selective fading tests. The improvement due to intrinsic diversity as the multipath spread increases is clearly evident in these figures. Also shown in Figures 3-7 and 3-8 are the respective ideal non diversity and dual diversity flat fading performance curves. Note that the intrinsic diversity benefit of the DAR-IV far outweighs its basic implementation loss and permits high quality (low BER) operation at lower values of E_b/N_o than required on flat fading channels.

Figure 3-7 shows the non-diversity performance measured (dark lines). The first test performed was for frequency flat fading, i.e., a simple Rayleigh fading channel with no multipath time dispersion. The performance of an ideal DCPSK modem on the flat fading channel is also shown (dashed line). At 10^{-3} BER, the DAR-IV is about 2.5 dB worst than the ideal channel which is only about a 0.3 dB increase over the back-to-back result. This implementation loss is not very large for a practical equipment and can be reduced to less than 1 dB by improvements to the present DAR-IV. These improvements include better quality mixers, a higher speed integrate and dump circuit, and higher stability d.c. amplifiers in the data regenerator/timing recovery circuits. While these improvements are relatively straight forward, the austere nature of the present program precluded this design iteration.

The next set of seven tests were for frequency selective fading indicated by the respective multipath profiles as previously described. As shown, the presence of multipath dispersion (or signal distortion) rapidly improves the performance of the modem. This performance trend continues until the multipath dispersion becomes significantly larger than the transmitter time-gate duration (off-interval). For the error rates of interest, an irreducible error rate phenomenon does not occur until multipath profile #4 is exceeded. For the non-diversity case, multipath profile #4 results in about 10^{-3} irreducible BER while profile #5 results in about 6×10^{-4}. Note that based on RADC RAKE measurements, the typical AN/TRC-97 multipath (8' antennas) on an 86 mile path will range between profiles #2 and #3 with only occassional days as bad as profile #4. Thus, even in a non-diversity mode, the DAR-IV modem technique provides reasonable power efficient performance.

The results for dual-explicit diversity as shown in Figure 3-8. The comments above describing the non-diversity performance are also valid here. Under conditions of flat fading, the dual diversity performance is within 2.5 to 3 dB of ideal DCPSK with maximal ratio combining at 10^{-3} BER. Thus, the DAR-IV explicit diversity combining action is within 0.3 to 0.5 dB of ideal maximal ratio combining.

FIGURE 3-7

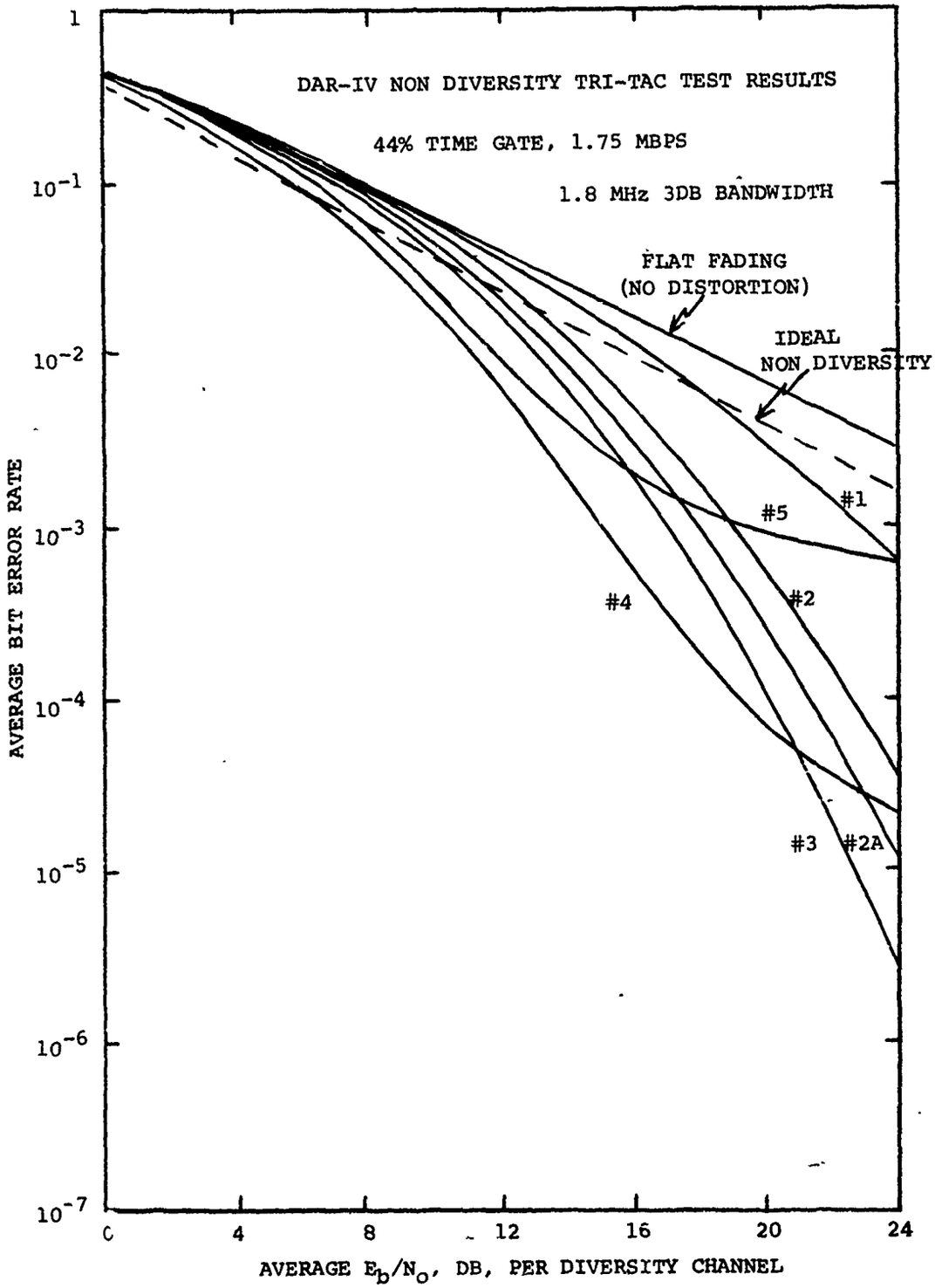
DAR-IV NON DIVERSITY TRI-TAC TEST RESULTS
44% TIME GATE, 1.75 MBPS
1.8 MHz 3DB BANDWIDTH
FLAT FADING
(NO DISTORTION)
IDEAL
NON DIVERSITY
#1
#2
#2A
#3
#4
#5
AVERAGE BIT ERROR RATE
1
10^{-1}
10^{-2}
10^{-3}
10^{-4}
10^{-5}
10^{-6}
10^{-7}
0
4
8
12
16
20
24
AVERAGE E_b/N_o, DB, PER DIVERSITY CHANNEL

FIGURE 3-8

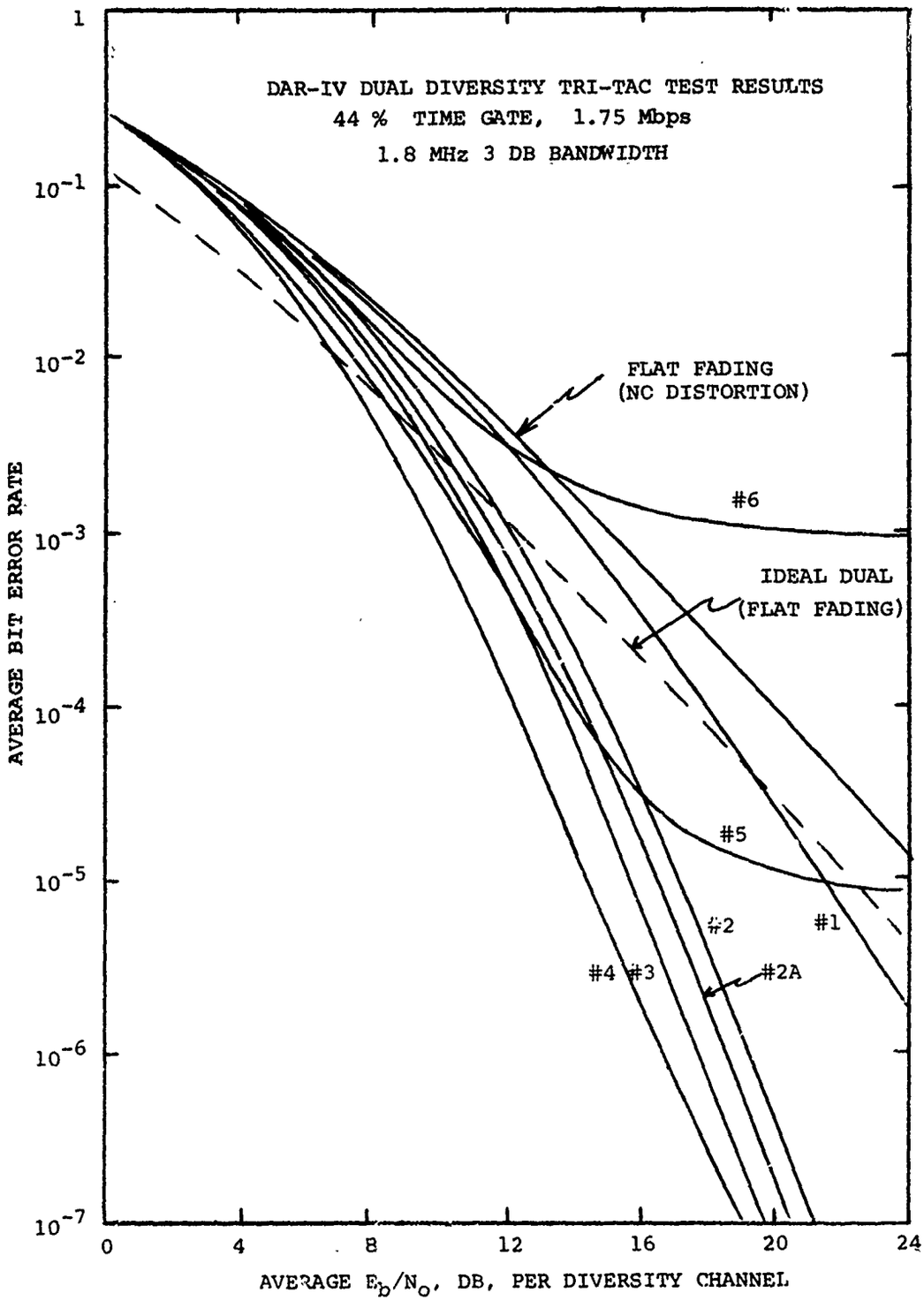
DAR-IV DUAL DIVERSITY TRI-TAC TEST RESULTS
44 % TIME GATE, 1.75 Mbps
1.8 MHz 3 DB BANDWIDTH
AVERAGE BIT ERROR RATE
1
10^{-1}
10^{-2}
10^{-3}
10^{-4}
10^{-5}
10^{-6}
10^{-7}
FLAT FADING
(NC DISTORTION)
#6
IDEAL DUAL
(FLAT FADING)
#5
#2
#1
#4 #3
#2A
0
4
8
12
16
20
24
AVERAGE E_b/N_o, DB, PER DIVERSITY CHANNEL

FIGURE 3-9

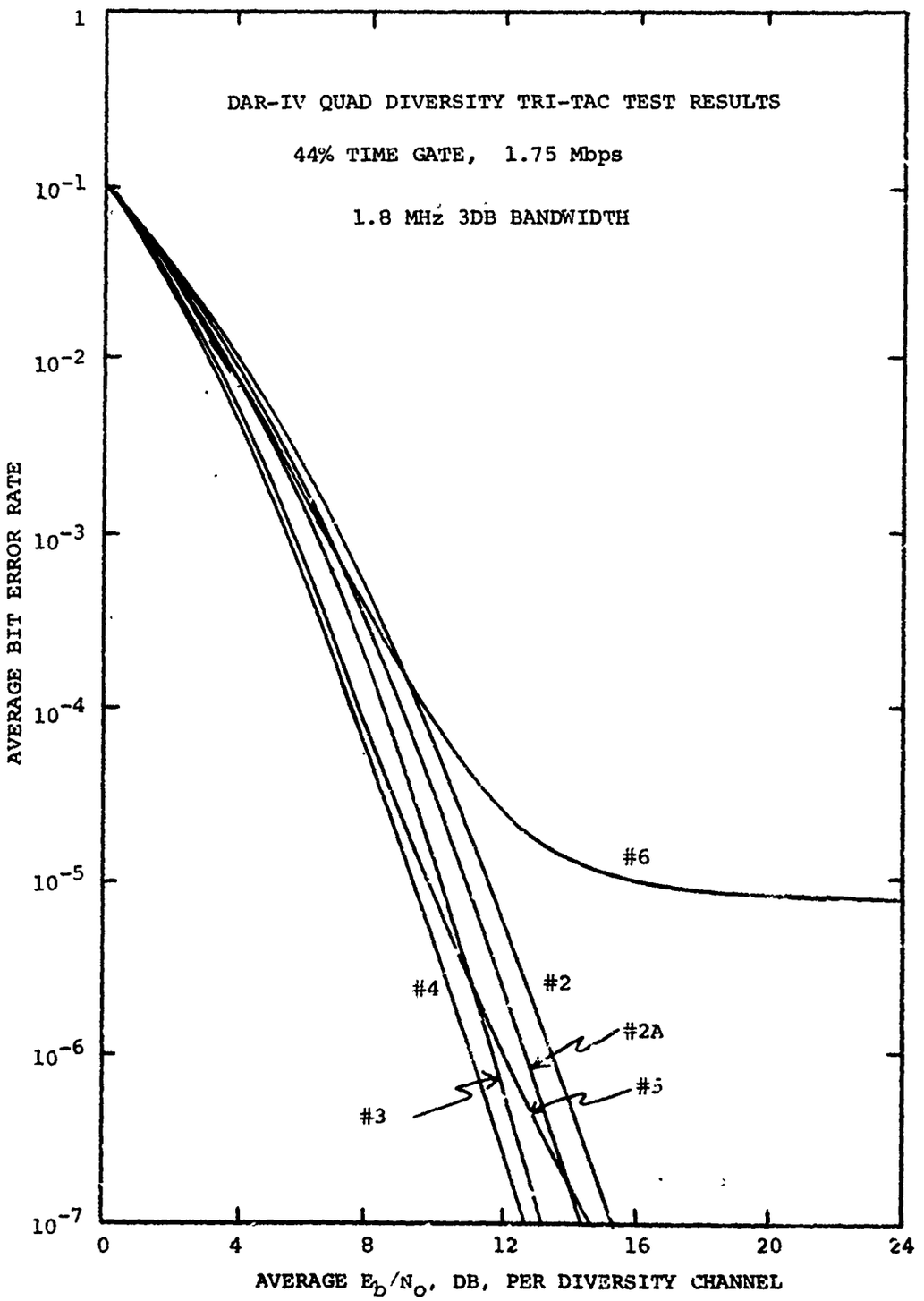
DAR-IV QUAD DIVERSITY TRI-TAC TEST RESULTS
44% TIME GATE, 1.75 Mbps
1.8 MHz 3DB BANDWIDTH
AVERAGE BIT ERROR RATE
1
10^{-1}
10^{-2}
10^{-3}
10^{-4}
10^{-5}
10^{-6}
10^{-7}
#6
#4
#2
#2A
#5
#3
0
4
8
12
16
20
24
AVERAGE E_b/N_o, DB, PER DIVERSITY CHANNEL

As the multipath dispersion increases, the performance of the modem rapidly improves. In the dual diversity case, no irreducible error rate effect is noticed until profile #5 which displays a 10^{-5} irreducible BER, and profile #6 which displays a 10^{-3} irreducible BER. Note that even at multipath profile #2, which represents only slight multipath dispersion, the DAR-IV results in a very large performance improvement of about 7 dB over the flat-fading case at 10^{-5} BER. For the still larger profile #4, this improvement is approximately 10 dB. Also, for profiles 2 through 4, the slopes of the BER versus E_b/N_o curves are proportional to about $[(SNR)^5]^{-1}$ or the equivalent fifth order diversity characteristic even though there are only two explicit diversity channels.

3.2.3.3 Filtered Rectangular Transmission Pulses

In the previous figures, the performance of the DAR on the RADC tropo channel simulator was described for rectangular transmission pulses with a 44% pulse duty cycle. Current troposcatter emission requirements require that 99% of the transmission power be contained within a certain bandwidth. In most applications including tactical and DCS, the spectral confinement is specified in multiples of 3.5 MHz depending on the data rate to be transmitted and the spectral resources available in the locality.

Figure 2-19 shows the 44% duty cycle rectangular QPSK pulse (at IF) used for the previous tests. The resultant $(\sin x/x)^2$ spectrum is shown in Figure 2-20. During a portion of the tactical modem evaluation tests, the DAR-IV signal at 1.75 Mbps was also filtered to provide an approximate 3.5 MHz spectral confinement. A four-pole Butterworth type filter with 4 MHz 3 dB bandwidth was used to filter the sidebands of the rectangular transmission pulse to provide the desired confinement. Figure 3-10 shows the bandlimiting filter characteristic and Figure 3-11 shows the pulse spectrum after filtering. Note that the pulse frequency sidelobes are now very small. Figure 3-12 shows the corresponding bandlimited transmission pulse (at IF).

Figure 3-13 shows the 1.75 Mbps performance of the DAR-IV with the previously described bandwidth limiting filtering and the 44% pulse duty cycle. Comparison of these results with the corresponding previous unfiltered results of Figure 3-8 reveals little difference. That is, in most cases, the effect of pulse bandlimiting is to reduce the performance at 10^{-5} BER by less than 0.5 dB. At higher error rates, the performance actually appears to improve (within a $\pm$0.5 dB measurement accuracy) due to a better match between the DAR-IV and the received pulse. The reason for this phenomenon is that the experimental DAR-IV modem tested has a limited bandwidth in the coherent reference signal recovery loop on the order of 3 or 4 MHz. Hence, it could not

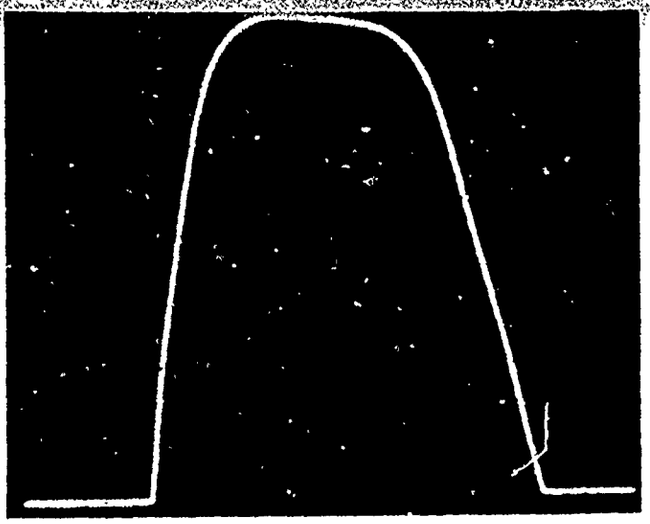

FIGURE 3-10

SPECTRAL CHARACTERISTIC OF BANDLIMIT FILTER

4-Pole Filter

4 MHz 3 dB Bandwidth

10 dB/Div. x 1 MHz/Div.

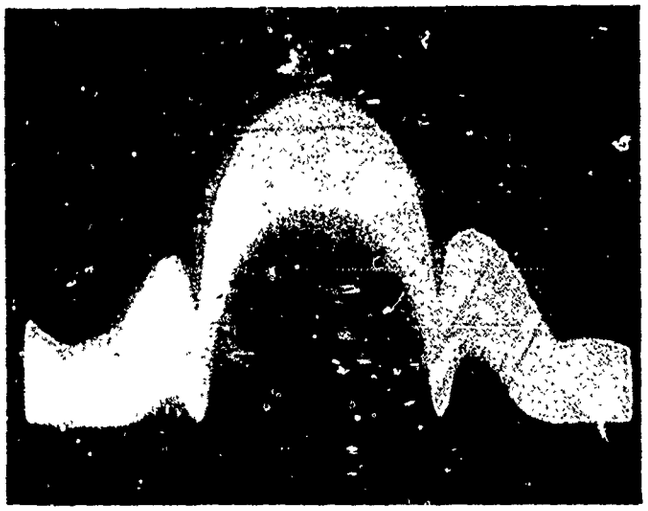

FIGURE 3-11

DAR-IV TRANSMISSION SPECTRUM

44% Duty Cycle

Filtered Pulse

4 MHz 3 dB Bandwidth

10 dB/Div. x 1 MHz/Div.

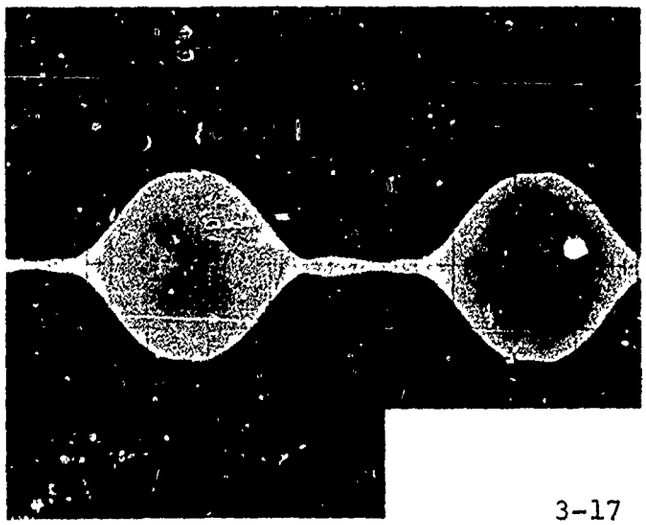

FIGURE 3-12

DAR-IV TRANSMISSION WAVEFORM

44% Duty Cycle

Filtered Pulse

4 MHz 3 dB Bandwidth

200 nsec/Div.

FIGURE 3-13

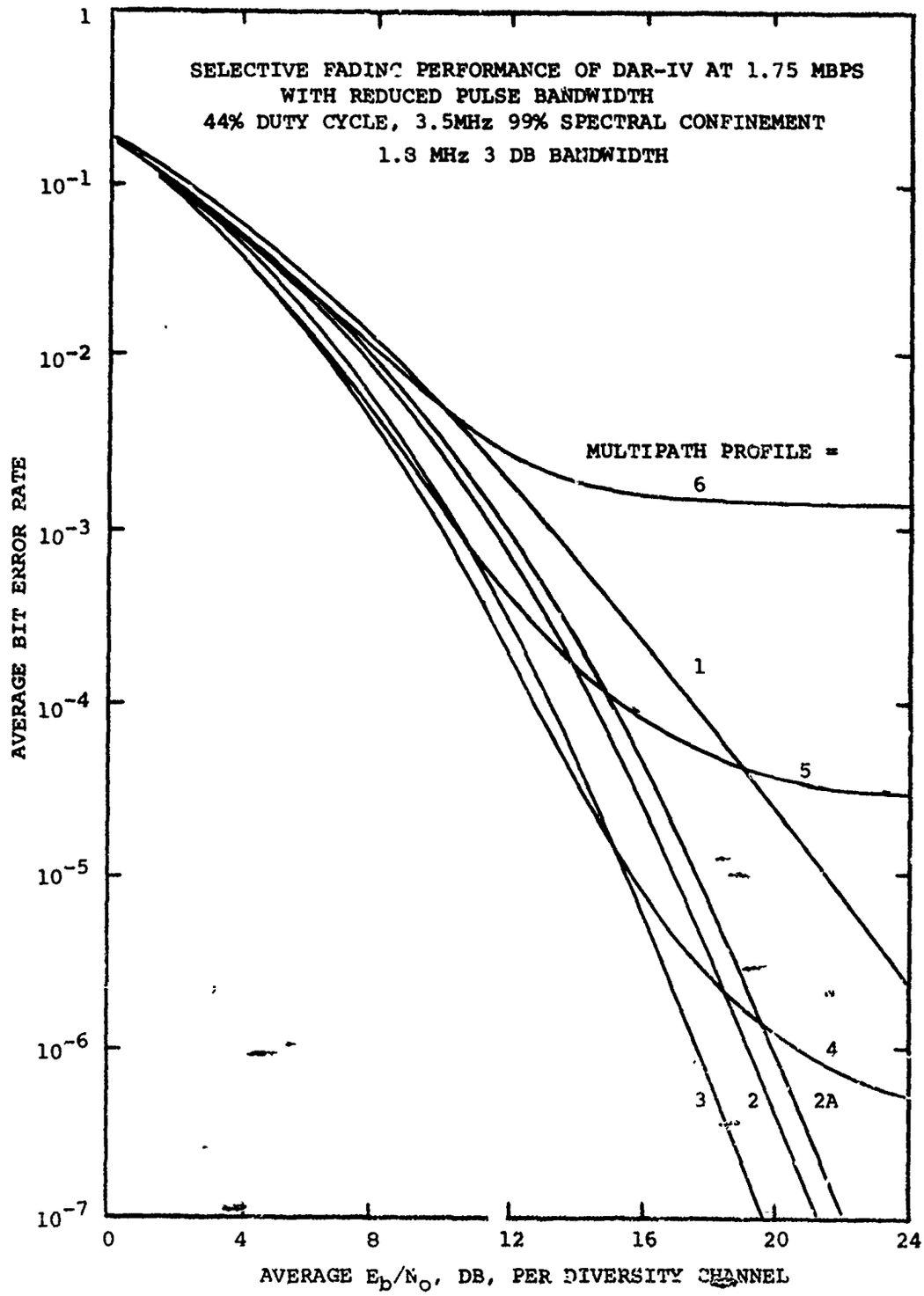
SELECTIVE FADING PERFORMANCE OF DAR-IV AT 1.75 MBPS
WITH REDUCED PULSE BANDWIDTH
44% DUTY CYCLE, 3.5MHz 99% SPECTRAL CONFINEMENT
1.8 MHz 3 DB BANDWIDTH
AVERAGE BIT ERROR RATE
1
10^{-1}
10^{-2}
10^{-3}
10^{-4}
10^{-5}
10^{-6}
10^{-7}
MULTIPATH PROFILE =
6
1
5
4
3
2
2A
0
4
8
12
16
20
24
AVERAGE E_b/N_o, DB, PER DIVERSITY CHANNEL

make effective use of the rectangular pulse sin x/x sidebands beyond this bandwidth resulting in an effective energy loss. The frequency components of the bandlimited pulse, however, are completely contained in the DAR-IV bandwidth and all signal energy is effectively utilized. The lower bandwidth of the DAR-IV experimental model is not an inherent feature but results due to the components chosen for the coherent reference recovery circuit. Much wider circuit bandwidths can be achieved by a suitable choice of component design.

Another effect is also apparent in the above comparison. The irreducible BER tends to occur at a BER about twice that of the unfiltered pulse. The reason for this phenomenon is that the filtered pulse has slightly greater residual intersymbol interference. Note that the exact pulse shape appears to play a relatively minor role in the level of intrinsic diversity achieved. Instead, as will be demonstrated later, the pulse rms bandwidth is the key factor in establishing this level of diversity gain.

Figure 3-14 shows the DAR-IV dual diversity 1.75 Mbps performance with still another choice of pulse shape and spectral confinement. Here, a narrower 25% duty cycle pulse is employed whose spectrum is limited by a 7 MHz bandwidth sharp cutoff filter. This pulse has lower duty cycle and, therefore, wider rms bandwidth than the previous pulse. As evidenced by comparison of Figure 3-14 with Figure 3-8, the wider bandwidth results in better performance through enhanced intrinsic diversity.

Figure 3-15 shows the typical dual diversity performance of the two bandlimited pulse shapes previously described for the multipath dispersion of multipath profile #2A. The high BER performance of the bandlimited pulses is as previously described. At low BER, the 3.5 MHz confined pulse provides somewhat lower intrinsic diversity gain than the simple rectangular pulse. Note, however, that the performance difference between the bandlimited and rectangular 44% duty cycle pulse is small even at low BER. The reason for this phenomenon is that the major intrinsic diversity gain results from the main lobe of the $(\sin x/x)^2$ pulse spectrum. The second sidelobe of the rectangular pulse $(\sin x/x)^2$ spectrum is down by about 13 dB and does not contribute greatly to the intrinsic diversity action of the modem. Hence, similar performance is achieved with or without filtering of the $(\sin x/x)^2$ spectrum beyond the central lobe.

The narrower 7 MHz bandwidth filtered pulse shows significantly greater intrinsic diversity improvement by about 2 dB. In this case, the main lobe of the $(\sin x/x)^2$ spectrum for the 285 ns pulse is nearly 70% wider than the main lobe of the 475 ns pulse. Since the main lobe of the spectrum contributes most to the intrinsic diversity, the

FIGURE 3-14

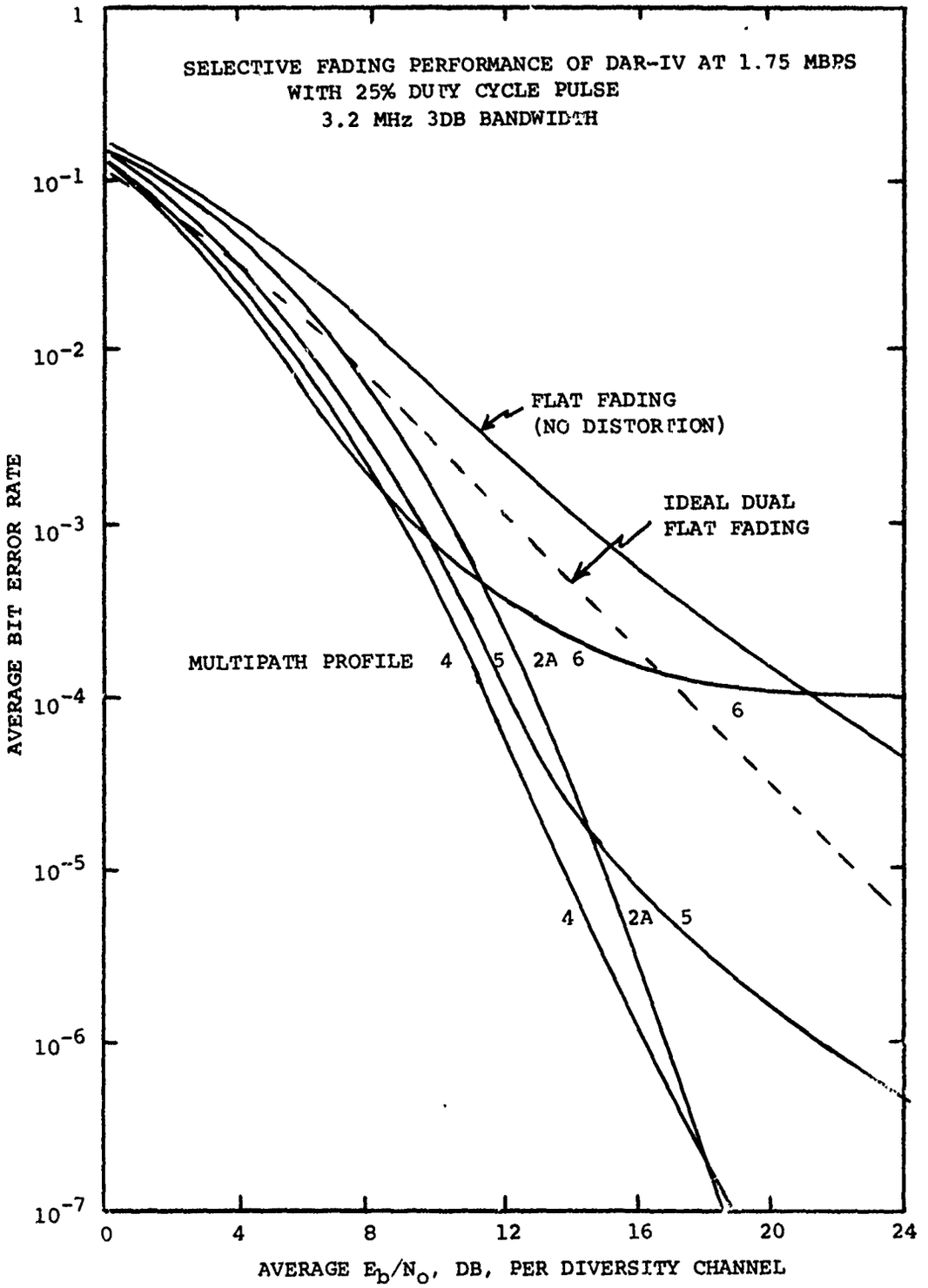
SELECTIVE FADING PERFORMANCE OF DAR-IV AT 1.75 MBPS
WITH 25% DUTY CYCLE PULSE
3.2 MHz 3DB BANDWIDTH
AVERAGE BIT ERROR RATE
1
10^{-1}
10^{-2}
10^{-3}
10^{-4}
10^{-5}
10^{-6}
10^{-7}
FLAT FADING
(NO DISTORTION)
IDEAL DUAL
FLAT FADING
MULTIPATH PROFILE 4 5 2A 6
6
4
2A
5
0
4
8
12
16
20
24
AVERAGE E_b/N_o, DB, PER DIVERSITY CHANNEL

FIGURE 3-15

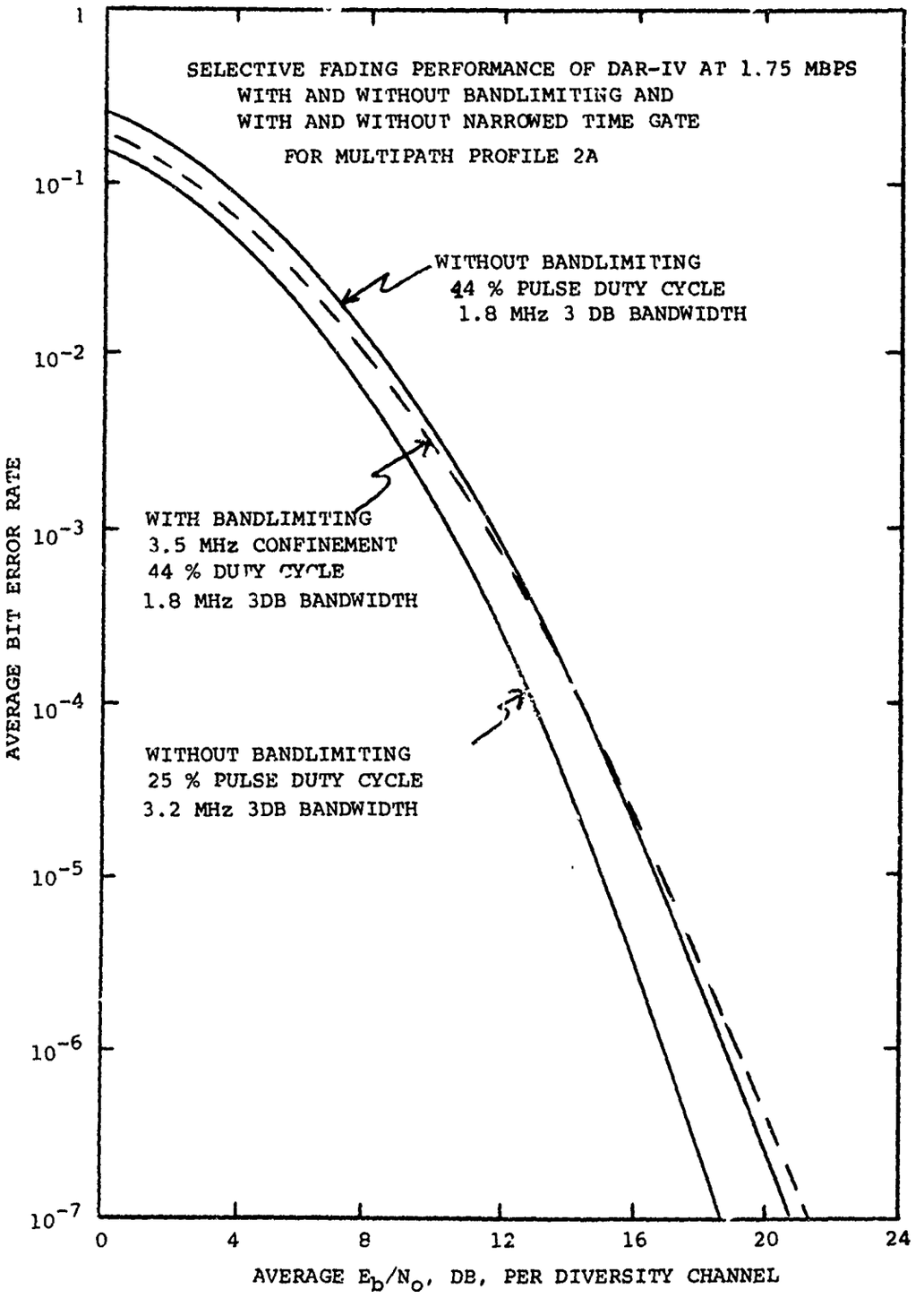
SELECTIVE FADING PERFORMANCE OF DAR-IV AT 1.75 MBPS
WITH AND WITHOUT BANDLIMITING AND
WITH AND WITHOUT NARROWED TIME GATE
FOR MULTIPATH PROFILE 2A
WITHOUT BANDLIMITING
44 % PULSE DUTY CYCLE
1.8 MHz 3 DB BANDWIDTH
WITH BANDLIMITING
3.5 MHz CONFINEMENT
44 % DUTY CYCLE
1.8 MHz 3DB BANDWIDTH
WITHOUT BANDLIMITING
25 % PULSE DUTY CYCLE
3.2 MHz 3DB BANDWIDTH
AVERAGE BIT ERROR RATE
1
10^{-1}
10^{-2}
10^{-3}
10^{-4}
10^{-5}
10^{-6}
10^{-7}
0
4
8
12
16
20
24
AVERAGE E_b/N_o, DB, PER DIVERSITY CHANNEL

performance of the narrower bandlimited pulse is superior. That is, the narrower pulse achieves a more uniform illumination of the RF bandwidth.

3.2.3.4 Filtered Spread Spectrum Transmission Pulses

The previous section showed the extra benefit provided by the DAR-IV due to intrinsic diversity. To maximize this type of diversity, it is necessary to employ a transmission pulse shape which fully "illuminates" the available transmission bandwidth. Fortunately, the DAR-IV design can adapt to essentially any transmission waveshape without modification of the demodulator. In fact, the present DAR-IV experimental model provides a number of different spread-spectrum phase codes which can be superimposed on the transmission pulse. This spread spectrum modulation is not intended for electronic counter - counter measure (ECCM) but rather to alter the pulse $(\sin x/x)^2$ spectrum to more uniformly illuminate the available RF bandwidth.

One spread spectrum code of interest is the 10001 code. That is, consider breaking up the previous 475 ns rectangular transmission pulse into five equal segments (or chips) of 100 ns duration each. The phase code then consists of reversing the phase of the first and last chips of the pulse. After passing this coded pulse through a 7 MHz sharp cutoff filter as shown in Figures 3-16 and 3-17, the pulse time waveform closely resembles a truncated sin x/x waveform consisting of the main lobe and the first sidelobe on either side as shown in Figure 3-18. The resultant pulse spectrum is very nearly rectangular (with Butterworth-like shaping) and uniformly illuminates most of the 7 MHz transmission band. The 7 MHz bandwidth filter represents the bandlimiting associated with an appropriately tuned Klystron power amplifier.

Figure 3-19 shows the non-diversity performance of the DAR with the 10001 spread spectrum pulse phase coding and 7 MHz bandlimiting. The flat fading (non dispersive) performance is shown as well as the selective fading for profiles #1 through #6. The rapid improvement with increasing multipath spread due to intrinsic diversity is clearly evident.

The intrinsic diversity performance of the DAR-IV can provide a very large performance benefit in non-diversity configurations. Between profiles #2 and #4, the DAR-IV requires 30 to 35 dB less E_b/N_o than on a flat fading channel. Also, for profile #3, the slope of the BER vs. E_b/N_o curve corresponds to fourth order effective diversity. That is, except for an increase of median energy, the DAR-IV modem at profile #3 leads to quad diversity performance for a troposcatter system with only one receiver.

Figure 3-20 shows the corresponding results for dual-explicit diversity. Also shown in Figure 3-20 is the ideal flat

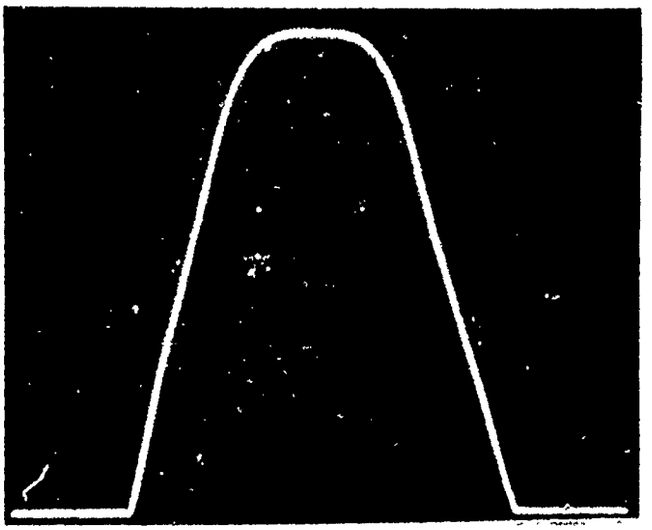

FIGURE 3-16

SPECTRAL CHARACTERISTIC
OF BANDLIMIT FILTER

4- POLE FILTER
7 MHz 3 DB BANDWIDTH

2 db/DIV x 2 MHz/DIV

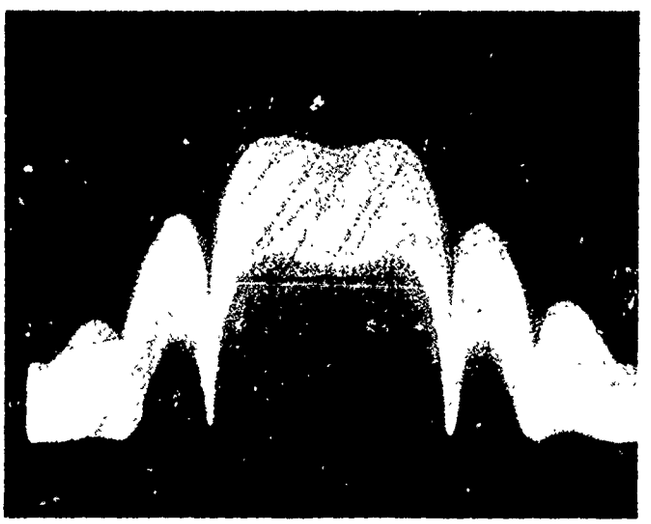

FIGURE 3-17

DAR-IV TRANSMISSION SPECTRUM

44% DUTY CYCLE
SPREAD SPECTRUM CODING
01110 PHASE CODE
7 MHz 3 DB BANDWIDTH

10 DB/DIV x 2 MHz/DIV

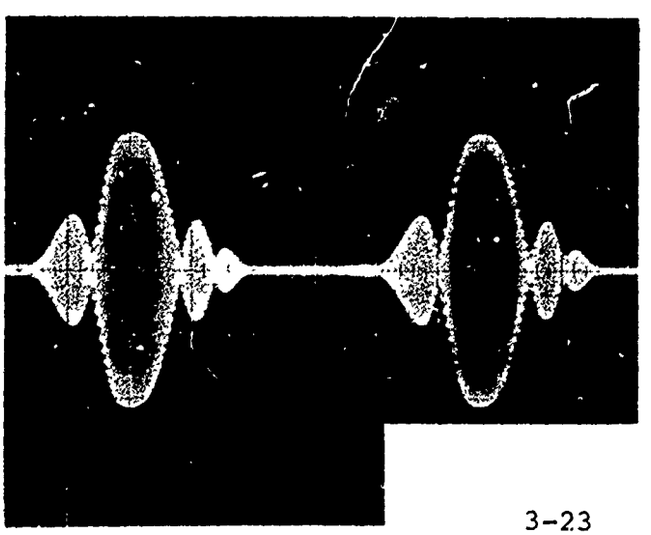

FIGURE 3-18

DAR-IV TRANSMISSION
WAVEFORM

44% DUTY CYCLE PULSE
01110 PHASE CODING
7 MHz 3 DB BANDWIDTH

200 nSEC/DIV

FIGURE 3-19

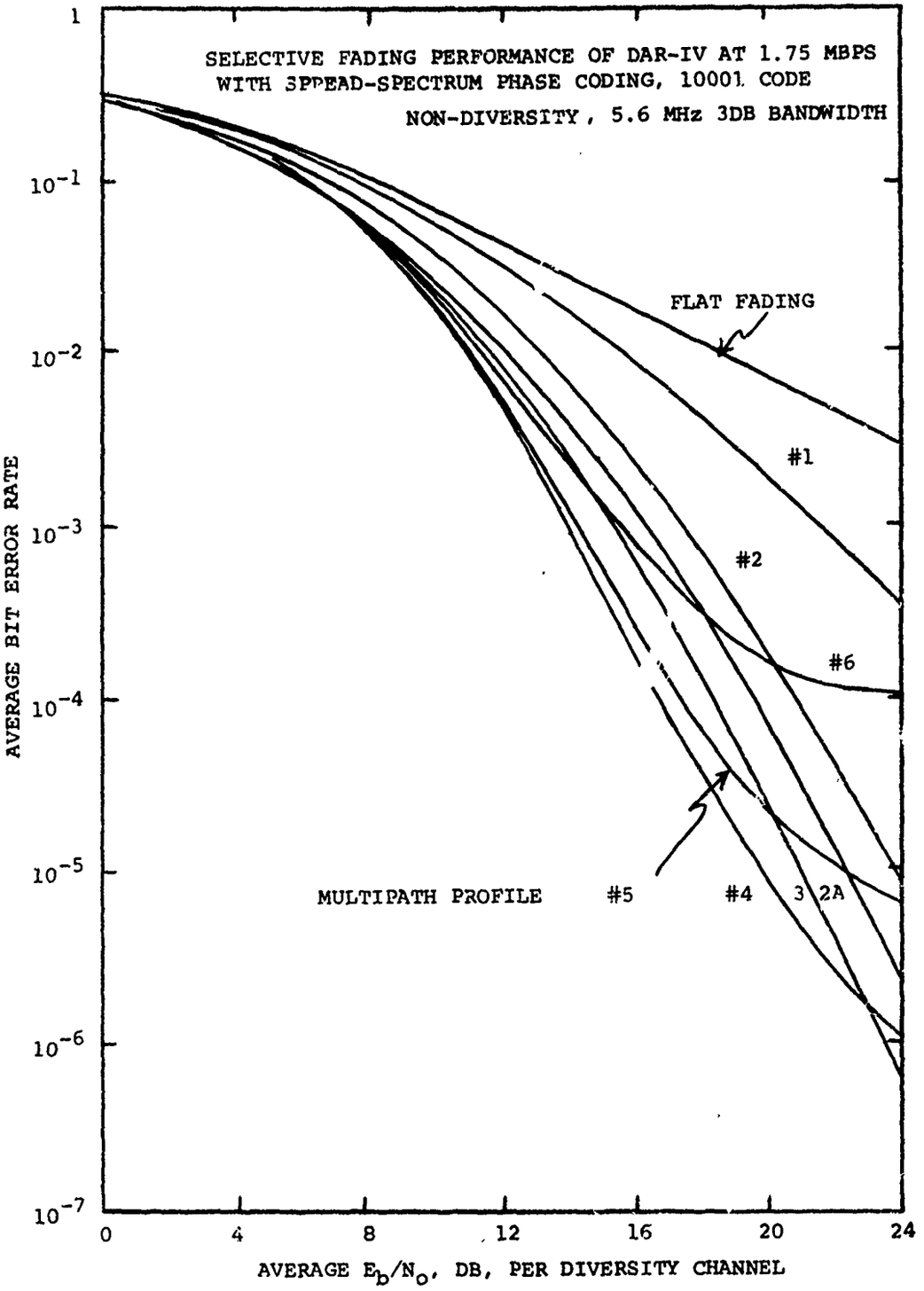
SELECTIVE FADING PERFORMANCE OF DAR-IV AT 1.75 MBPS
WITH SPREAD-SPECTRUM PHASE CODING, 10001 CODE
NON-DIVERSITY, 5.6 MHz 3DB BANDWIDTH
AVERAGE BIT ERROR RATE
1
10^{-1}
10^{-2}
10^{-3}
10^{-4}
10^{-5}
10^{-6}
10^{-7}
FLAT FADING
#1
#2
#6
MULTIPATH PROFILE
#5
#4
3
2A
0
4
8
12
16
20
24
AVERAGE E_b/N_o, DB, PER DIVERSITY CHANNEL

FIGURE 3-20

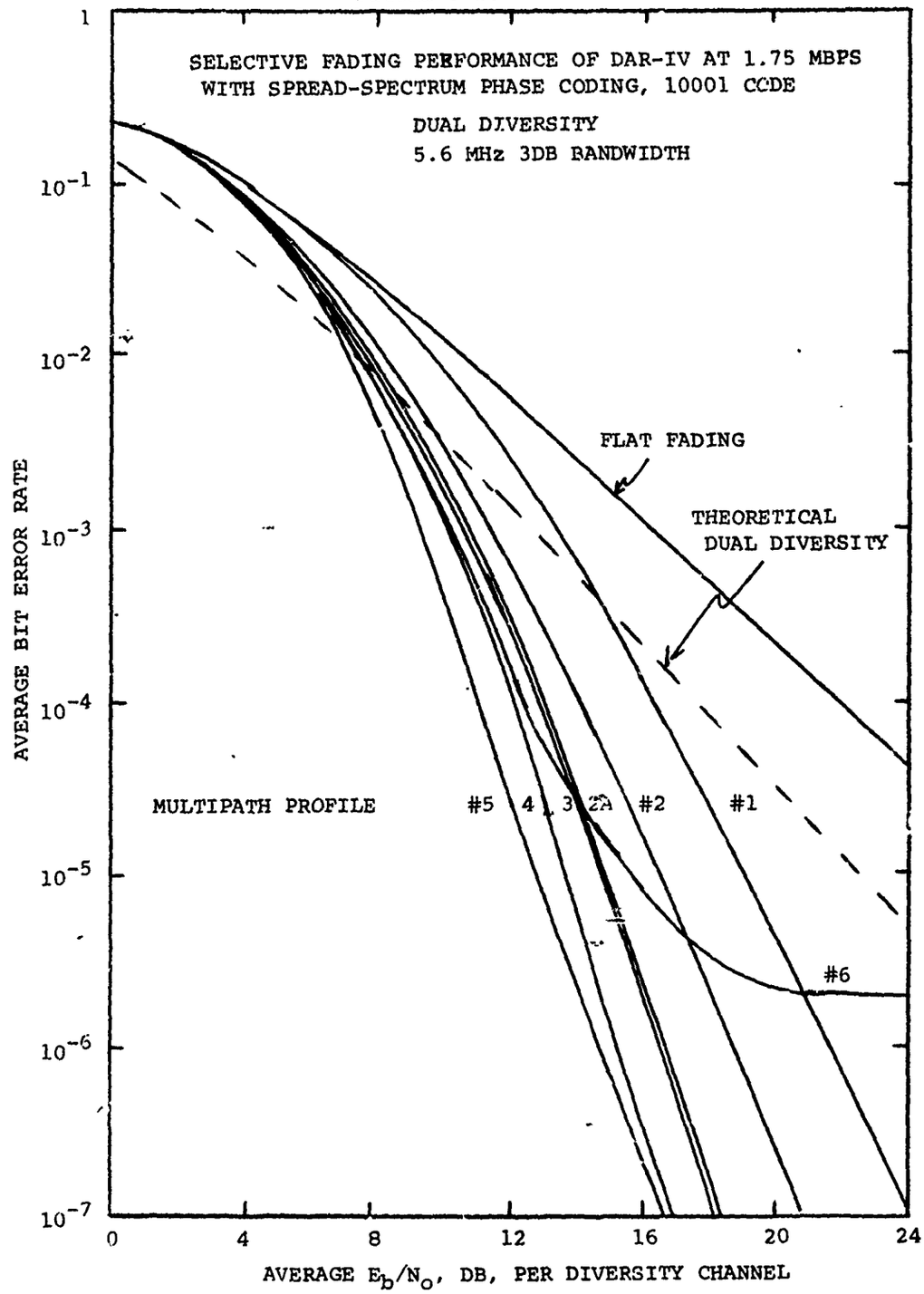
SELECTIVE FADING PERFORMANCE OF DAR-IV AT 1.75 MBPS
WITH SPREAD-SPECTRUM PHASE CODING, 10001 CODE
DUAL DIVERSITY
5.6 MHz 3DB BANDWIDTH
AVERAGE BIT ERROR RATE
1
10^{-1}
10^{-2}
10^{-3}
10^{-4}
10^{-5}
10^{-6}
10^{-7}
FLAT FADING
THEORETICAL
DUAL DIVERSITY
MULTIPATH PROFILE
#5
4
3
2A
#2
#1
#6
0
4
8
12
16
20
24
AVERAGE E_b/N_o, DB, PER DIVERSITY CHANNEL

fading, dual diversity performance. Comparison of these results and those of Figure 3-8 reveals the advantages of using spread-spectrum pulse coding where a larger transmitted bandwidth is permitted. Note that the pulse coding provides considerably larger intrinsic diversity gain for the same multipath delay spread. For example, at 10^{-5} BER, the use of spread spectrum pulse coding reduces the required E_b/N_o with profile #3 from 16 dB to about 14 dB. Also, the irreducible error rate phenomenon is lowered by more than two orders of magnitude so that a BER of less than 10^{-5} is easily obtained even in the largest multipath dispersion of profile #6.

Actually, as shown in Figures 3-11 and 3-17, the pulse 3 dB bandwidth is increased from approximately 1.8 MHz to 5.6 MHz or a factor of 3 to 1. Intuitively, the increase in intrinsic diversity should show a corresponding improvement. However, the bandlimited nature of the present DAR-IV recirculating filters does not permit all of the energy of the spread spectrum pulse to be efficiently utilized. Comparison of the flat fading performance of Figures 3-20 and 3-8 shows that the demodulator implementation loss increases from 2.5 dB in the uncoded case to more than 5 dB in the coded case. This extra loss is due entirely to reference signal bandlimiting.

The recirculating filter illustrated in Figure 2-2 is used to "clean-up" the adaptive coherent reference signal in the DAR matched filter. The surface acoustic wave (SAW) delay line employed in this positive feedback loop establishes the bandwidth of the reference signal and, therefore, the bandwidth of the overall matched filter. Figure 2-14 shows the SAW device employed in the experimental DAR model and its amplitude-frequency characteristics is shown in Figure 3-21. Although the delay line itself has wide bandwidth, it has only a simple R-C bandpass characteristic. When the device is placed on a recirculating loop, the effective loop bandwidth is sharply reduced depending on the loop gain.

In the present DAR-IV, the loop gain of each channel varies between 0.93 and 0.95 and the 3 dB bandwidth of the loop, therefore, varies between 3.1 and 3.8 MHz. When the uncoded 1.75 Mbps pulse is passed through this filter, its 3 dB bandwidth is reduced nearly 20% from 1.8 MHz to 1.4 or 1.5 MHz. The coded pulse spectrum with 5.6 MHz bandwidth is essentially reduced to the bandwidth of the filter or 3.1 to 3.8 MHz. Hence, an effective 3 dB bandwidth of W = 1.4 MHz is obtained for the uncoded 1.75 Mbps waveform and W = 3.1 MHz is obtained for the spread-spectrum coded waveform.

The bandwidth problem of the present SAW delay line can be completely avoided by employing a new delay line design for future equipment. Figure 3-22 shows the bandpass of the old delay line design (dashed lines) and also the new design (solid line). Basically,

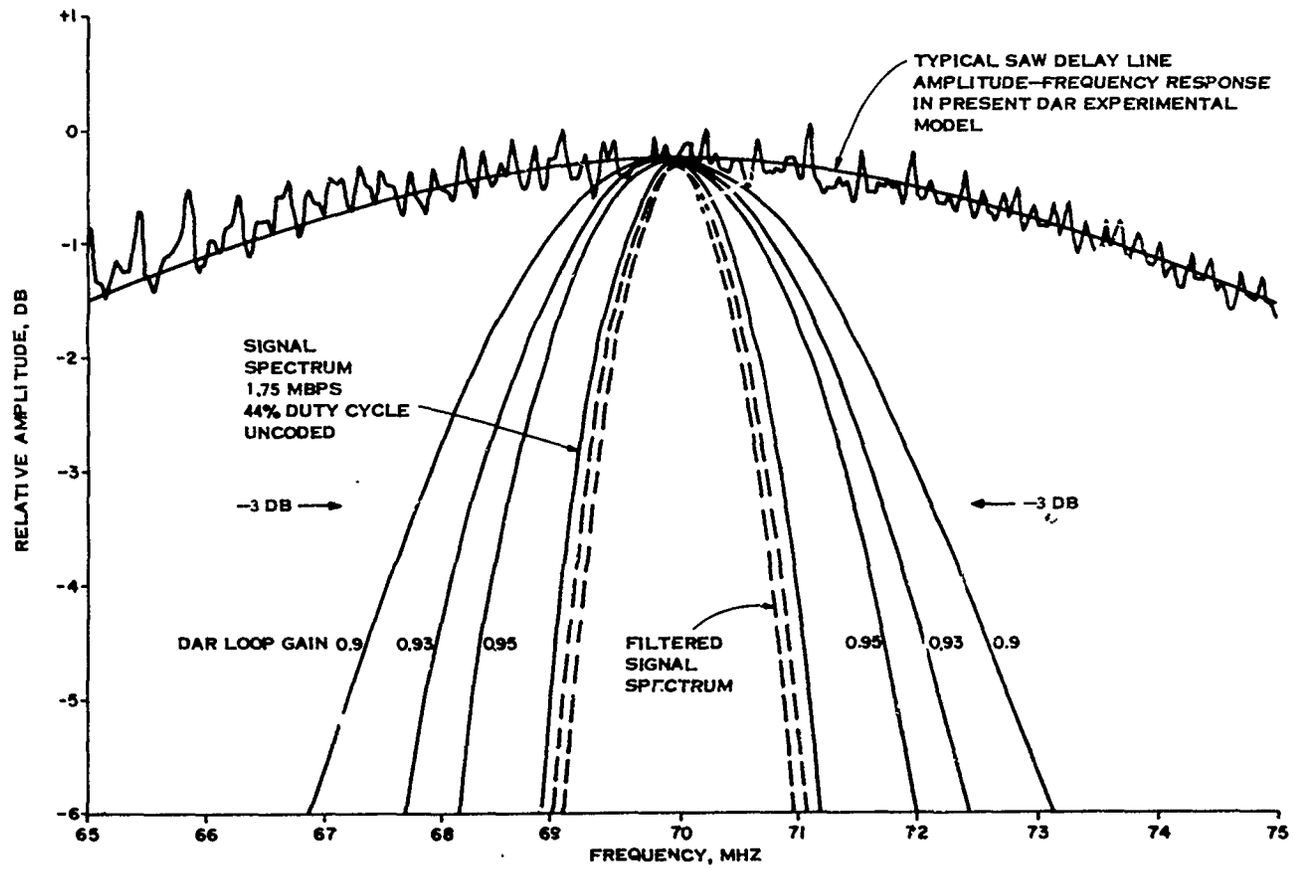

FIGURE 3-21 REFERENCE SIGNAL BAND LIMITING PHENOMENON IN DAR EXPERIMENTAL MODEL

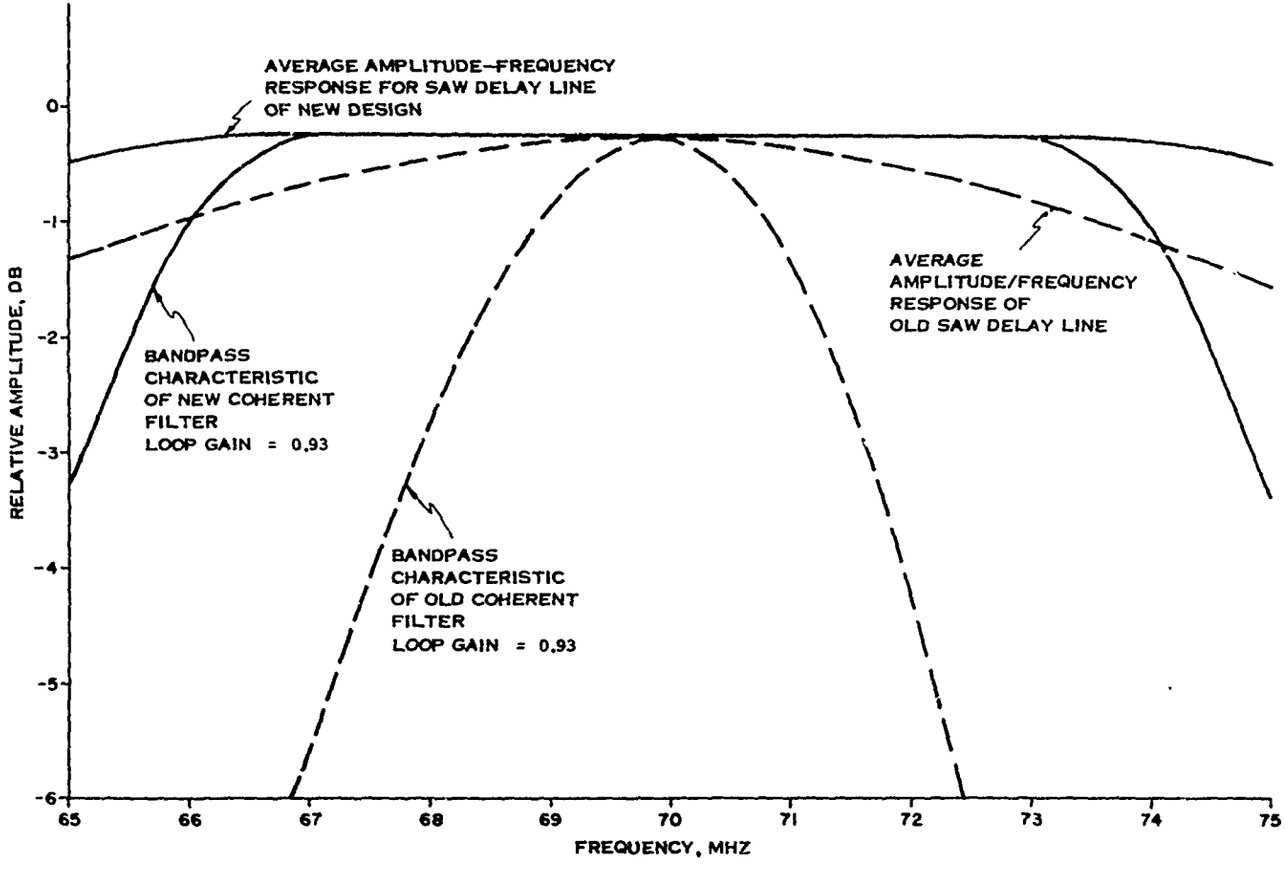

FIGURE 3-22 ILLUSTRATION OF IMPROVED COHERENT FILTER CHARACTERISTIC COMPARED TO CHARACTERISTIC OF PRESENT EXPERIMENTAL MODEL

the new device will employ a Butterworth type of passband characteristic instead of a simple RC roll-off. Delay lines of this type and meeting similar overall requirements have already been designed, built, and incorporated in exacting military systems. Even after filtering, the reference signal bandlimiting will then be relatively insignificant in the reference circuit on the DAR-IV. The use of this wider band reference circuit would enhance the intrinsic performance of Figure 3-20 still further. For example, for profile #3, the implementation loss would be reduced by nearly 3 dB while the diversity gain would increase by more than 2 dB. Hence, the required E_b/N_o for 10^{-5} BER would then be less than 9 dB. For larger multipath spread under these conditions, the required E_b/N_o would then approach the limiting value of 7 dB for a non-fading channel.

3.2.3.5 3.5 Mbps Performance

During the tactical test program, a limited amount of data was also taken at the 3.5 Mbps bit rate of the experimental DAR-IV modem. The DAR-IV model delivered to RADC provided data rates of 1.75, 3.5, or 7 Mbps with switch selection. No adjustments or modifications to the DAR-IV are required or were performed during this data rate transition since the DAR-IV incorporates design features which greatly simplify multiple data rate operation.

The 3.5 Mbps tests were performed using the "unscaled" multipath delay power spectra defined by Table 3-1. Thus, while the previous tests used scaled multipath profiles to represent 2.3 Mbps transmission on the AN/TRC-97 derived profiles, the 3.5 Mbps tests represent direct 3.5 Mbps transmission of the AN/TRC-97 profiles. The resultant test information is useful in indicating the potential future bit rate growth capabilities of the DAR-IV in the tactical environment.

The majority of tests performed at 3.5 Mbps employed a spread spectrum coded pulse with 7 MHz bandlimiting. This type of transmission pulse was previously shown to provide wider "illumination" of the RF bandwidth and thus provide improved performance. Figure 3-23 shows the spectrum of the 011 (or 100) phase code used for the 50% duty cycle pulse of the 3.5 Mbps transmission. This simple code is actually a Barker code which has the well known two level autocorrelation function and a corresponding spectrum which is very flat across the transmission band.

Figure 3-24 shows the actual filtered 3.5 Mbps QPSK waveform. Note that the waveform somewhat resembles the previous 1.75 Mbps coded waveform of Figure 3-18 except that the time sidelobe on one side of the pulse is absent.

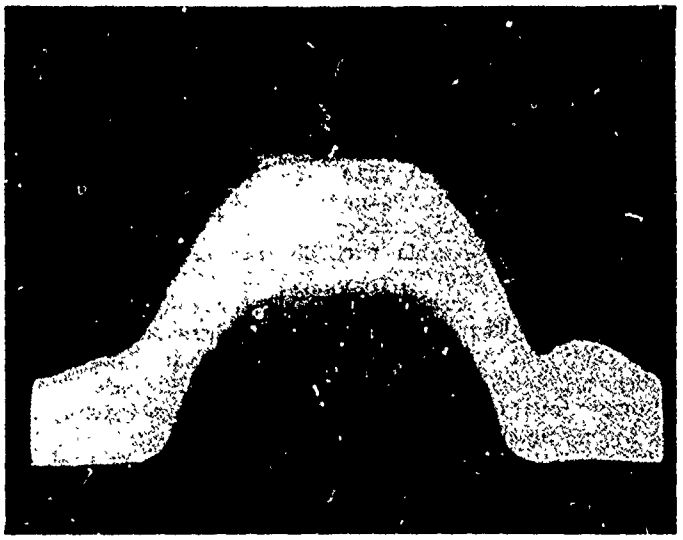

FIGURE 3-23

DAR-IV TRANSMISSION SPECTRUM

50% DUTY CYCLE
SPREAD SPECTRUM CODING
011 PHASE CODE
7 MHz 3 DB BANDWIDTH

10 db/DIV x 2 MHz/DIV

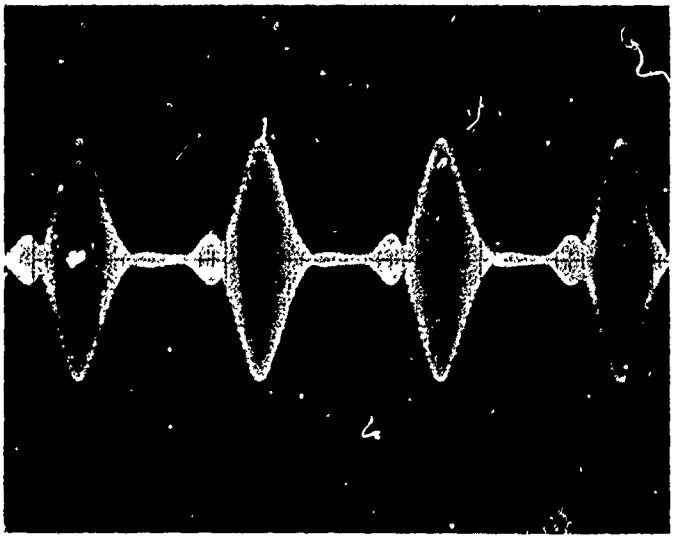

FIGURE 3-24

DAR-IV TRANSMISSION WAVEFORM

50 % DUTY CYCLE
011 PHASE CODE
7 MHz 3 DB BANDWIDTH

200 nSEC/DIV

Figure 3-25 summarizes the 3.5 Mbps performance for dual diversity under the various conditions of selective fading represented by multipath profiles 1 through 6 of Table 2-1 as well as flat fading. The results shown are only for the Barker phase-coded transmission pulse with 7 MHz bandwidth. Note the performance is nearly comparable to the "equivalent 2.3 Mbps performance" shown in Figure 3-8. The major difference is that the "tailing-off" phenomenon of the DAR-IV occurs at multipath profile #4 (2×10^{-6} BER) instead of profile #5 for the previous lower data rate results. It is evident that the DAR also provides significant performance capabilities at data rates of about twice the highest called for in the tactical tropo system.

3.2.4 Comparison with Predicted Results

The performance of the DAR-IV was estimated based on Monte Carlo computer simulation. This computer model is a direct, discrete time, sampled data simulation of all of the major circuit functions in the DAR-IV. Basically, a random data sequence of about 50 bit duration is processed in the DAR-IV simulation for each of a large number of instantaneous multipath "snapshots" which are members of the statistical multipath delay spread model of interest. The "eye opening" statistics of the DAR-IV for various orders of explicit diversity are then computed over the ensemble of multipath snapshots.

Figure 3-26 shows the computer simulation predictions for multipath profile #1 through #6. The predictions are shown for dual explicit diversity. The simulation conditions employ a DAR-IV loop gain of 0.93 (about 14 symbol reference memory) and a 99% spectral occupancy of 3.5 MHz approximately corresponding to the 1.75 Mbps test condition with 4 MHz bandwidth filtering.

Note from Figure 3-8 that the experimental results are significantly better than the computer prediction for error rates below 10^{-3} and the smaller profiles. This phenomenon is not a fault of the simulation programs, but rather a limitation in the interpretation of the computer results. To estimate the effective order of diversity (explicit times intrinsic) of the modem, n, it is assumed that the "eye opening" statistics of the DAR-IV can be modelled by Chi-square statistics with n degrees of freedom. This approach is very accurate when the individual contributors to the diversity mechanism (such as explicit channels and resolvable multipath contributions) are of equal strength. However, the intrinsic diversity action results from a number of "resolvable echos" whose strengths are generally unequal. In this case, the effective diversity action at low BER will be greater than that predicted by the Chi-square statistics.

FIGURE 3-25

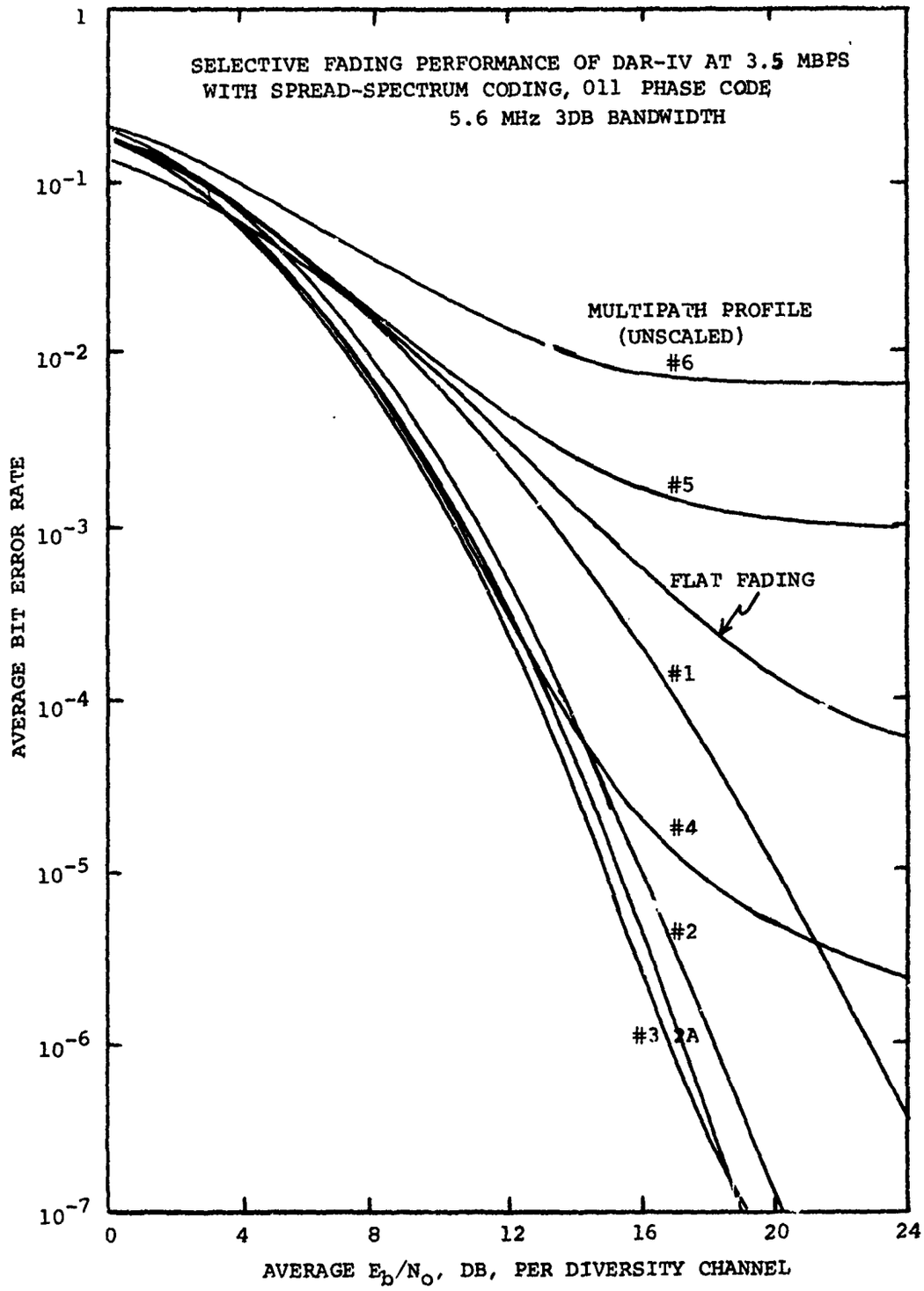
SELECTIVE FADING PERFORMANCE OF DAR-IV AT 3.5 MBPS
WITH SPREAD-SPECTRUM CODING, 011 PHASE CODE
5.6 MHz 3DB BANDWIDTH
MULTIPATH PROFILE
(UNSCALED)
#6
#5
FLAT FADING
#1
#4
#2
#3 2A
AVERAGE BIT ERROR RATE
1
10^{-1}
10^{-2}
10^{-3}
10^{-4}
10^{-5}
10^{-6}
10^{-7}
0
4
8
12
16
20
24
AVERAGE E_b/N_o, DB, PER DIVERSITY CHANNEL

FIGURE 3-26

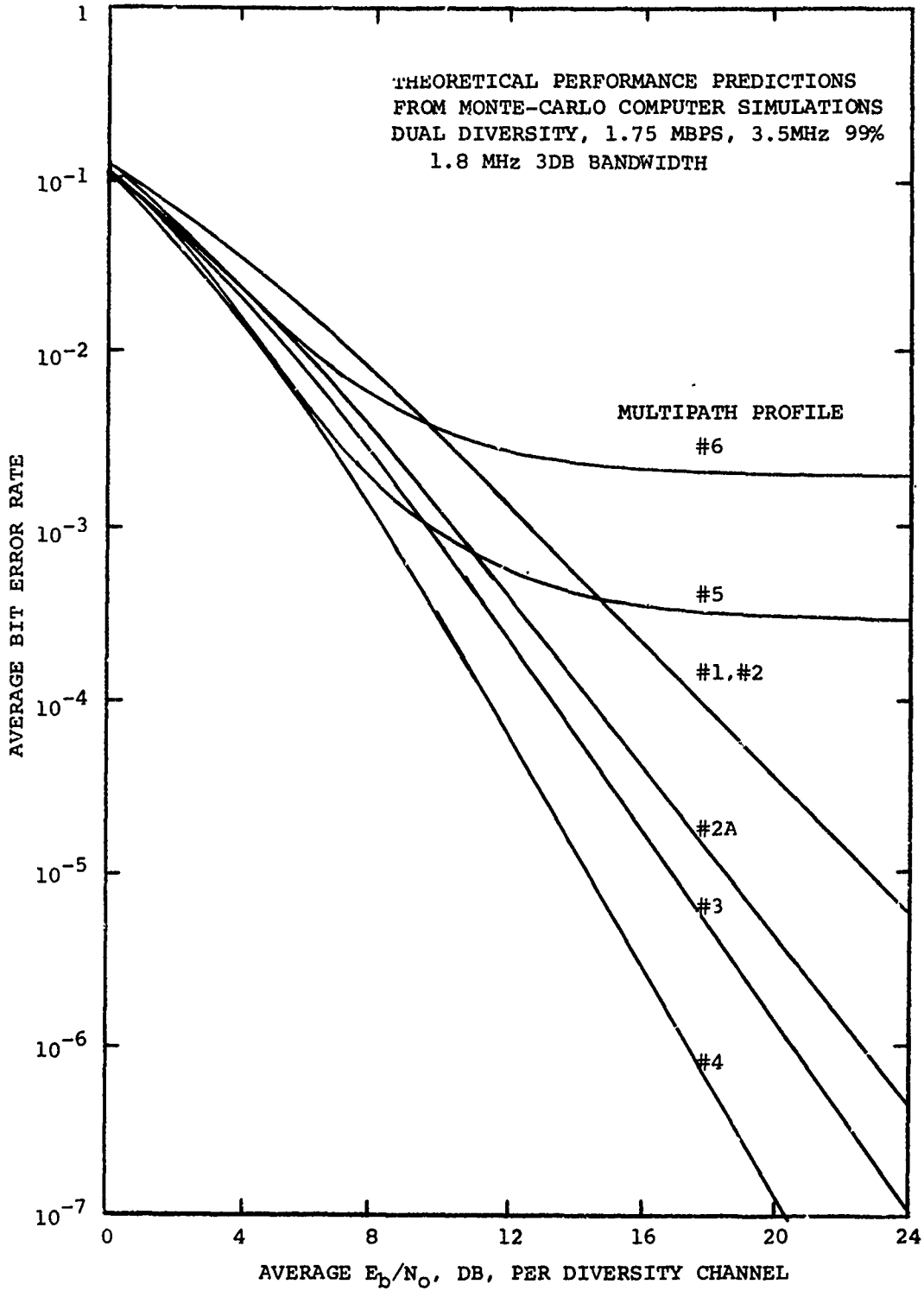
THEORETICAL PERFORMANCE PREDICTIONS
FROM MONTE-CARLO COMPUTER SIMULATIONS
DUAL DIVERSITY, 1.75 MBPS, 3.5MHz 99%
1.8 MHz 3DB BANDWIDTH
MULTIPATH PROFILE
#6
#5
#1,#2
#2A
#3
#4
AVERAGE BIT ERROR RATE
1
10^{-1}
10^{-2}
10^{-3}
10^{-4}
10^{-5}
10^{-6}
10^{-7}
0
4
8
12
16
20
24
AVERAGE E_b/N_o, DB, PER DIVERSITY CHANNEL

The interpretation of the computer simulation results is, therefore, pessimistic. If the simulation program could be run long enough, higher order statistics of the "eye opening" could be obtained which would more accurately describe the intrinsic diversity behavior. However, within the practical limits of simulation time, only the normalized rms eye opening can be accurately measured which can be then related to the Chi-square statistics.

For the larger multipath profiles, an irreducible error rate phenomenon is evident. However, non-diversity irreducible error rate is now low enough to permit a more accurate estimate from the result of the computer simulation. The irreducible error rate predictions of Figure 3-26 are within an order of magnitude of the measured results.

The computer simulation model can be used to predict nearly all of the performance trends observed in the experimental results of Figures 3-7 through 3-25. Examples of the performance variation versus pulse bandwidth, spread spectrum coding alternative, phase offset error, and timing offset error are included in the Math Model.

3.2.5 Summary and Conclusions on Tactical Simulator Results

Although not a part of the basic program, the test results which have been obtained for the operation of the DAR-IV modem on a simulated tactical troposcatter channel clearly indicate the benefit of a digital modem which is designed to use the effects of multipath propagation to advantage. Within certain broad bounds, the DAR-IV modem was shown to provide performance improvement as the channel's multipath dispersion increases. On most troposcatter links, the average received signal level tends to fall off as the average multipath dispersion increases. The adaptive matched filter action of the DAR-IV provides an intrinsic diversity performance gain which tends to offset this average signal level loss and thus may extend the time availability of the link.

From a system designers viewpoint, it is necessary to know what E_b/N_o is required to achieve a certain BER for a given condition of multipath spread and data rate. The bound on performance is the irreducible BER which establishes the maximum multipath spread allowable for a given data rate. Figure 3-27 summarizes all of the dual diversity irreducible error rate phenomena observed versus the normalized multipath spread. This multipath normalization consists of multiplying the rms multipath spread ($\Delta = 2\sigma$ of Table 3-1 or 3-2) times the transmission bit rate.

From Figure 3-27 it is evident that for a given normalized multipath spread, there is a dispersion of about three orders of magnitude in irreducible BER. The dashed line on the left represents an approximately upper bound on the irreducible BER for the simplest DAR-IV pulse shapes. In this case, a 50% duty cycle pulse with a spectral confinement of about 0.5

FIGURE 3-27
MEASURED IRREDUCIBLE ERROR RATE VERSUS
NORMALIZED MULTIPATH FOR DUAL DIVERSITY

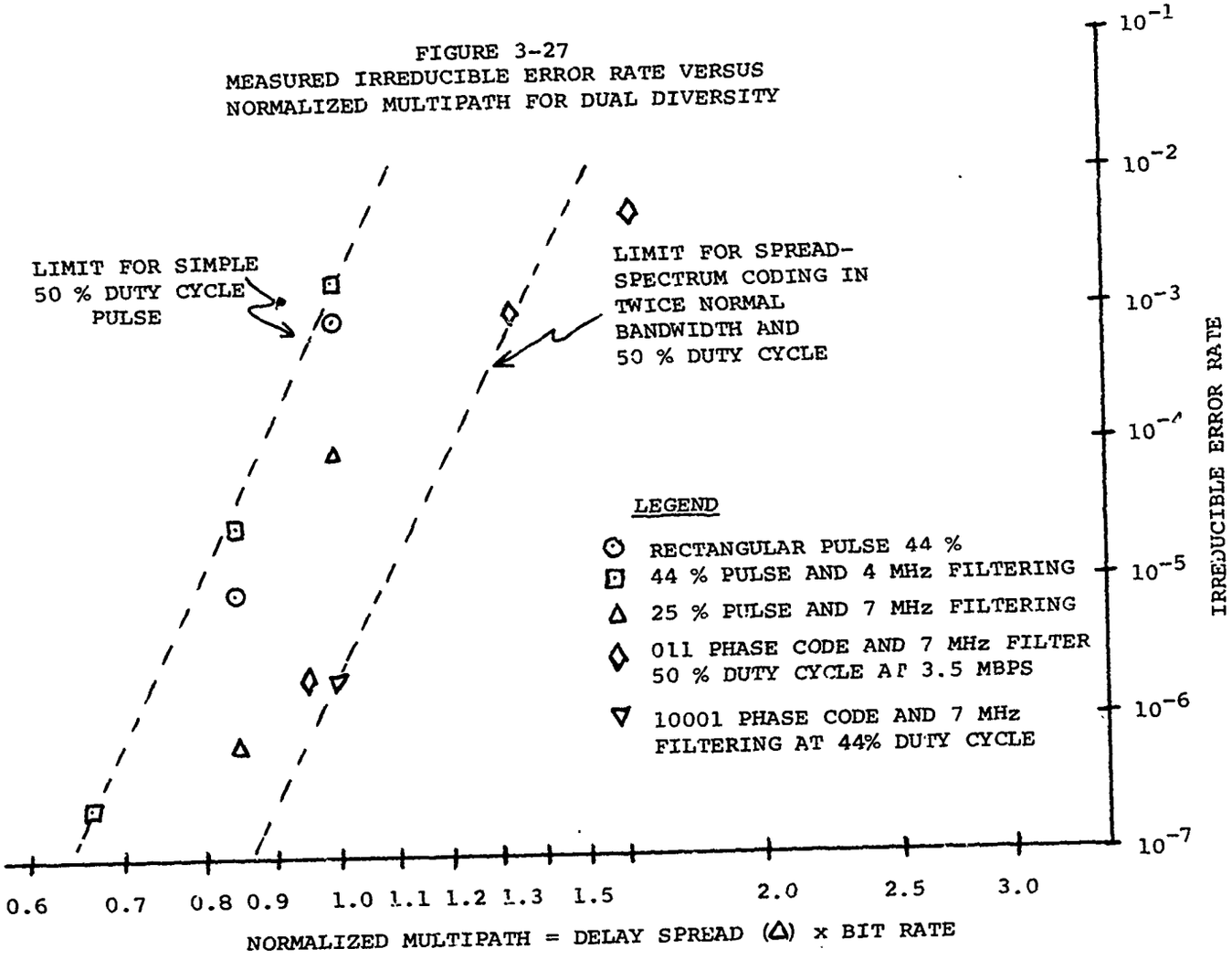

bit per Hertz is assumed. The dashed line to the right represents an approximately lower bound on BER for a spread-spectrum coded pulse (uniform bandwidth illumination) with a spectral confinement of about 0.25 bit/Hertz. Obviously, the results will be somewhat dependent on the shape of the multipath delay power spectrum as well as its rms value. However, since the multipath mechanism is similar in all tropo links, it is assumed that the variation in shape of the multipath delay spectrum can be neglected compared to its rms spread.

For a normalized multipath spread of unity, the dual diversity irreducible BER varies between 10^{-3} and 10^{-6} depending on the DAR-IV transmission bandwidth and choice of pulse shape. For non diversity operation, the corresponding irreducible BER would be about two orders of magnitude higher while for quad diversity, the BER would be about two orders of magnitude lower. The normalized multipath of unity for the QPSK DAR-IV signal with 50% duty cycle implies that the time gate duration (off time) is equal to the rms delay spread. Note that when the rms delay spread is equal to the time gate, the overlap of the adjacent pulses is quite large due to the "tails" of multipath spread. However, the DAR-IV provides serviceable irreducible BER values even under these conditions of intersymbol interference. Actually, it is the large intrinsic diversity gain of the DAR-IV which drastically reduces the onset of the irreducible rate phenomenon.

The average E_b/N_o per diversity channel necessary to maintain a specified BER can also be plotted as a function of normalized multipath spread. Figure 3-28 shows the experimental dual diversity data at 10^{-5} BER. As before, an approximate upper and lower limit on the E_b/N_o performance is indicated by the dashed lines for the various DAR-IV options on pulse shape and bandwidth. In the absence of multipath dispersion (negligible multipath spread), the DAR-IV requires about 25 dB average E_b/N_o for each diversity channel to achieve a dual diversity $\overline{BER}$ of 10^{-5}. As the multipath increases as shown in Figure 3-28, the performance rapidly improves due to the intrinsic mechanism of the adaptive matched filter receiver.

This improvement trend continues over a broad range of multipath spread up to normalized multipath spreads between 0.7 and 0.9, depending on the choice of DAR-IV pulse shape and bandwidth. At this point, the dual diversity operation of the DAR-IV requires only 13 to 15 dB E_b/N_o for 10^{-5} $\overline{BER}$. For a radio with 6 dB noise figure, this requirement translates to received levels of -92.5 to -90.5 dBm, respectively. Without the intrinsic diversity benefit of the DAR-IV, a 10 dB greater received signal level of -80.5 dBm would be needed to maintain 10^{-5} $\overline{BER}$.

To set the experimentally measured DAR-IV performance in proper perspective, it is instructive to compare its performance against a proper non adaptive, binary FSK modem which has been previously attempted for digital

FIGURE 3-28

REQUIRED E_b/N_o FOR 10^{-5} BER VERSUS
NORMALIZED MULTIPATH SPREAD FOR DUAL DIVERSITY

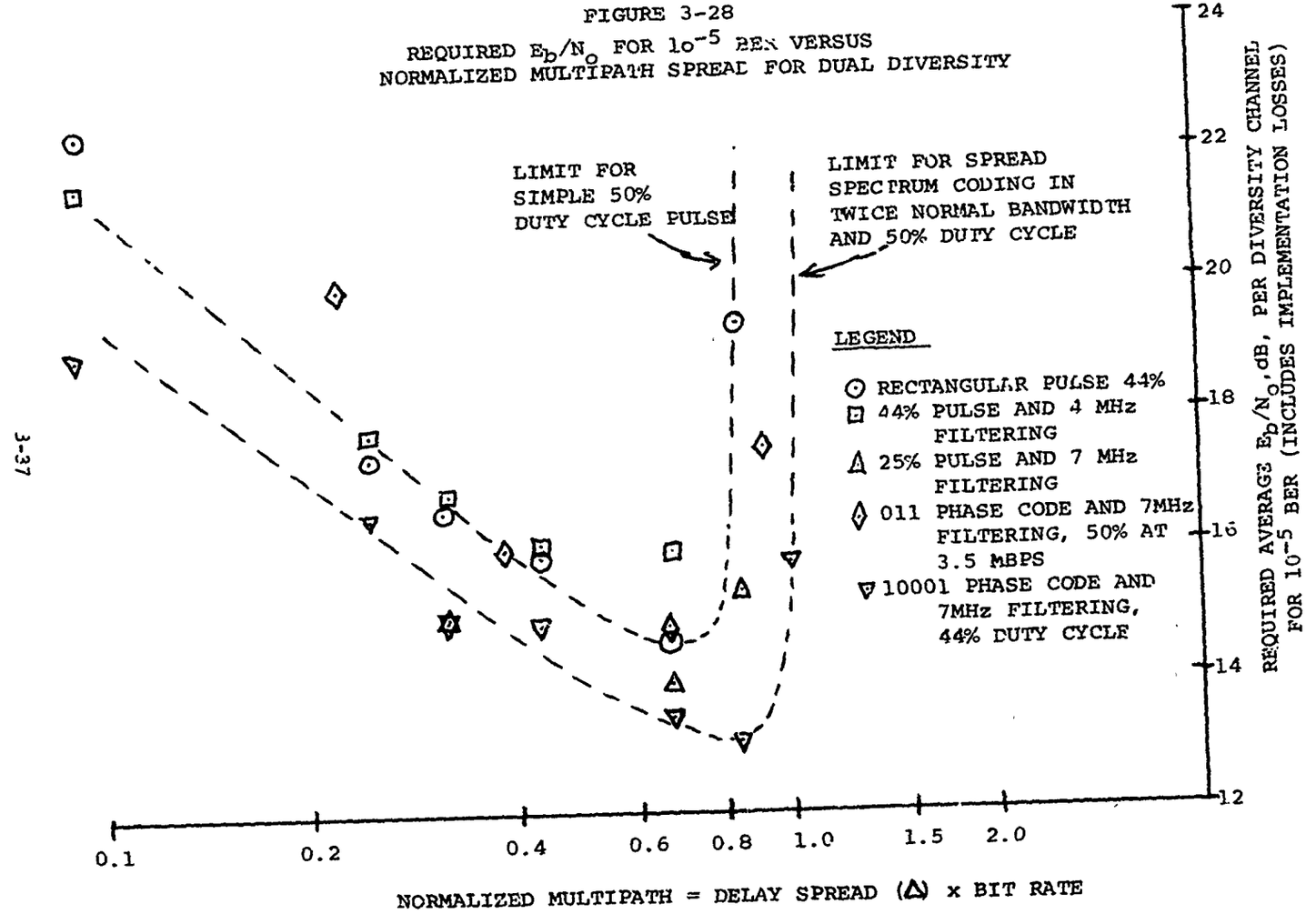

tropo. Since corresponding experimental results are not available for the FSK modem, it is necessary to employ theoretical predictions based on the work of Bello and Nelin and described in Chapter 11 of Communication Systems and Techniques by Schwartz, Bennett and Stein. Figure 11-3-6 of this reference shows the dual diversity SNR degradation of binary FSK with phase continuous transitions (best case) versus a normalized data rate, $d = 1/B_cT$, where B_c is the correlation bandwidth of the channel. For the corresponding theoretical calculation, the 2 σ multipath delay spread is given by $2\sigma = \sqrt{8}/\pi B_c$ and this expression may then be used to link the above results to the normalized multipath spread defined in Figures 3-27 and 3-28.

Figure 3-29 shows the resultant dual diversity FSK E_b/N_o required to maintain 10^{-5} $\overline{BER}$ versus normalized multipath spread with a 2 dB implementation loss added. For low multipath spread, the performance approaches the flat fading case with a required E_b/N_o of about 27 dB. As the multipath spread increases, the performance degrades since there is no intrinsic diversity mechanism to counteract the intersymbol interference. At a relatively low amount of multipath spread (for the 2.3 Mbps data rate) the FSK modem exhibits an irreducible $\overline{BER}$ worse than that of 10^{-5}.

Also shown in Figure 3-29 is the region of operation of the DAR based on the previous experimental results of Figure 3-28. (The shaded area represents the operational extremes of the present DAR-IV including differences in pulse shape and bandwidth over the range examined). Note the dramatic contrast between the performance of the two types of modems due to the intrinsic diversity advantage of the DAR-IV. This comparison is based on equal transmit power levels and, therefore, implies that the DAR-IV employs a peak-to-average power tradeoff in the Klystron HPA to provide equal average radiated power.

The dashed lines shown in Figure 3-29 indicate the approximate range of normalized multipath spread for an 87 mile AN/TRC-97 which is assumed to correspond to multipath profiles #2 through #4 of Table 3-1. Over this range, the simple binary FSK modem can not provide the required 10^{-5} BER while the DAR-IV requires only 15 to 18 dB or 13 to 16 dB E_b/N_o depending on choice of pulse shape.

Even if the simple FSK modem did not exhibit an irreducible BER (at much lower bit rates), the DAR-IV would still provide a significant performance advantage. Using spread spectrum phase coding, the DAR can maintain a nearly constant transmission bandwidth and intrinsic diversity benefit at all data rates. Figure 3-30 shows the resultant average improvement of the DAR-IV over the FSK modem as a function of required average BER. Note that this figure shows the minimum improvement of the DAR-IV relative to the FSK modem and is valid at lower data rates. At megabit

FIGURE 3-29
COMPARISON OF DAR-IV MODEM AND BINARY FSK MODEM FOR DUAL EXPLICIT DIVERSITY E_b/N_o, dB, FOR 10^{-5} BER VERSUS NORMALIZED MULTIPATH

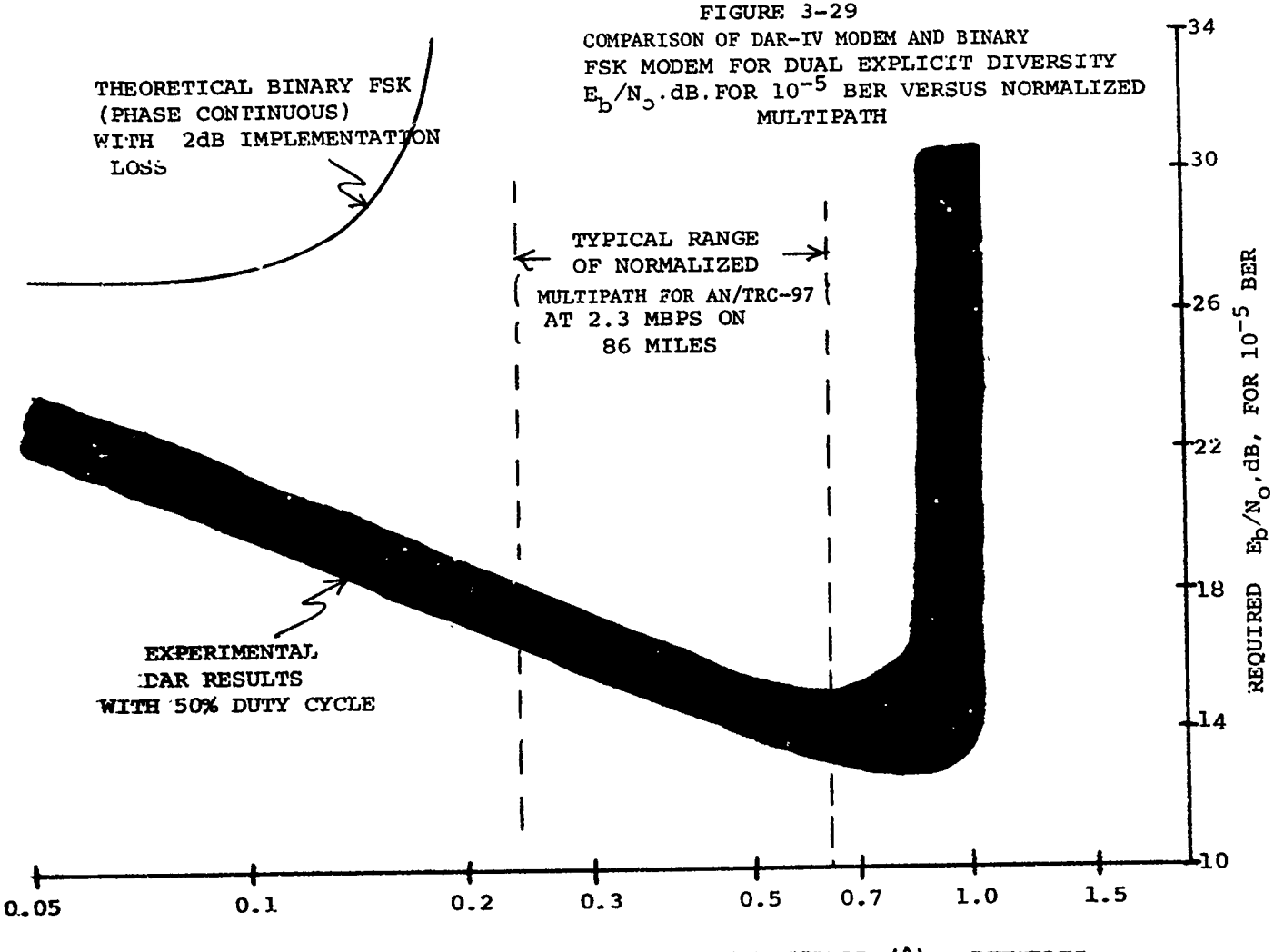

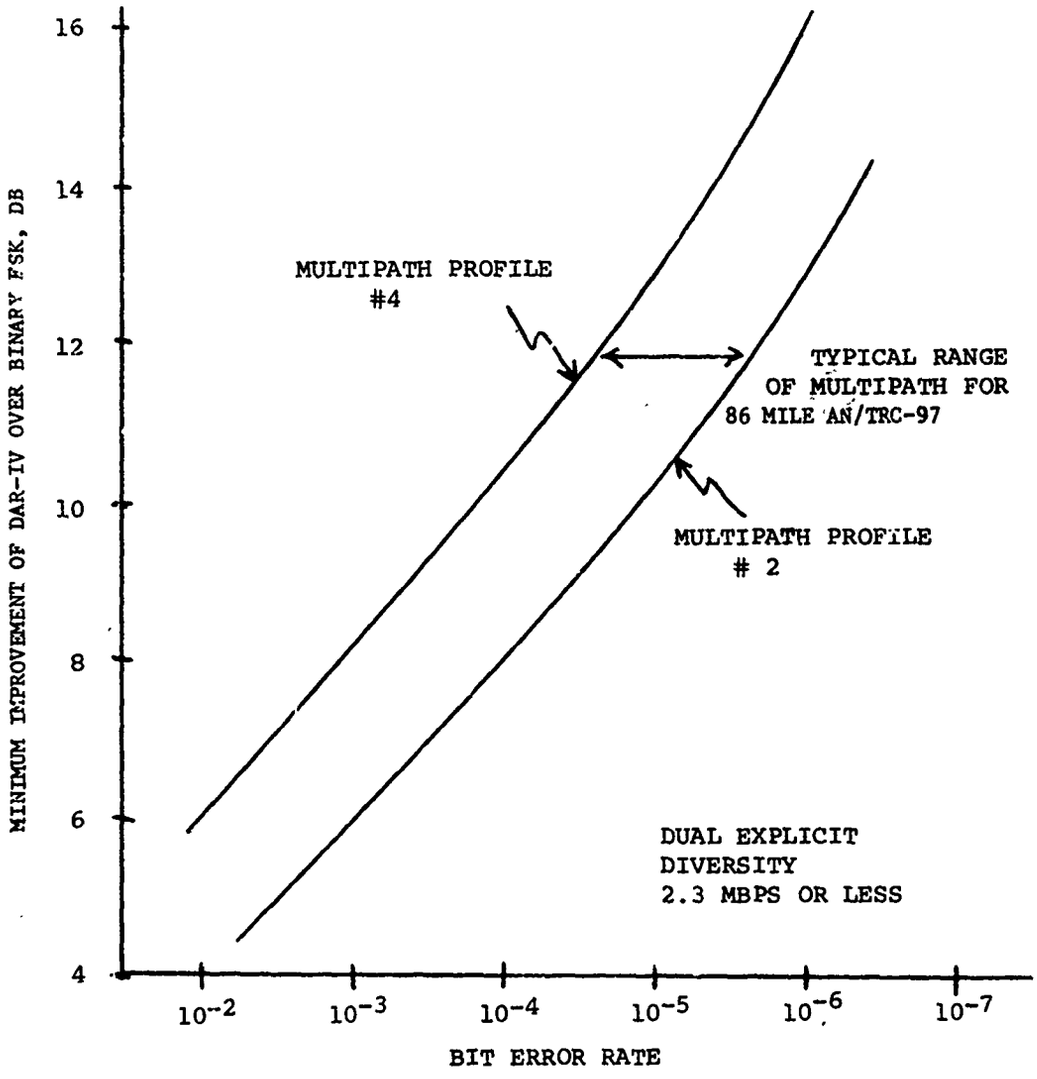

FIGURE 3-30

MINIMUM IMPROVEMENT OF QPSK DAR-IV OVER SIMPLE BINARY FSK MODEM WITH NO SENSITIVITY TO MULTIPATH. DAR-IV IMPROVEMENT IS DUE TO IMPLICIT DIVERSITY

rates, the non-adaptive FSK modem exhibits an irreducible BER which prevents it from ever reaching its BER objective. The advantage of using a modem specifically designed to operate in a multipath environment is evident in the results.

During the measurement of the results presented, no loss of bit count integrity (BCI) was observed at average error rates less than 0.1, which could be attributed to the DAR. This result was observed at both the 0.5 Hz and 5 Hz fading rates and for both non and dual diversity. Since the timing recovery loop and orderwire multiplex circuits in the present experimental model are far from optimum in both design and execution, but still yielded excellent BCI behavior, the DAR-IV can be said to have excellent BCI properties at the 2.3 Mbps data rate.

3.3 DCS Media Simulator Test Results

3.3.1 General

A series of tests were performed at the RADC laboratory channel simulator to evaluate the potential applicability of the DAR-IV modem technique to the future DCS troposcatter links. Tests were conducted at data rates of 1.75, 3.5, and 7 Mbps in non, dual and quad diversity with and without the benefit of a "tail cancelling" circuit. Channel multipath conditions representative of the "average" and "worst case" conditions (refractive indices of 1.33 and 0.75, respectively), were simulated for the 168 mile AN/MRC-98 tropo radio at 880 MHz and the 168 mile AN/TRC-132 tropo radio at C-band. Also simulated was the multipath conditions of a 250 mile path with 0.6° beamwidth antennas. The tests were concentrated on the higher orders of diversity and higher data rate modes consistent with possible future DCS applications.

The simulator test setup was the same as previously described for the tactical channel tests of Section 3.2. Most tests were performed with a nominal transmit pulse duty cycle of 50% although a coded pulse was employed in some examples.

Section 3.3.2 describes the multipath profiles simulated and their relation to the paths which were employed for over-the-air testing. Section 3.3.3 describes results of a series of tests which were used to establish a baseline for the long AN/MRC-98 tropo link. Section 3.3.4 describes the results of the tests for the long AN/TRC-132 tropo link as well as the model of a 250 mile link with 0.6° beamwidths.

3.3.2 Multipath Profiles for Simulator Testing

To employ the RADC tropo channel simulator, it is necessary

to specify a multipath delay power spectrum, $Q(\xi)$, and a two-sided rms doppler spread. The doppler spread is related to the fade rate of the channel and doppler spreads between 0.1 Hz and 10 Hz are selectable on the simulator. Based on preliminary simulator tests of the DAR-IV in the laboratory and theoretical considerations, it has been found that the DAR-IV performance is not very sensitive to the fade rates contained in this range. That is, the DAR-IV demodulator employs coherent reference and AGC time constants several orders of magnitude faster than the maximum anticipated fade rates. Only the bit timing recovery loop of the DAR-IV modem displays any sensitivity to fade rate with less than 1 dB of performance variation anticipated for the expected range of fading rates.

The major performance characteristics of the DAR-IV are thus determined by the average signal to noise ratio, the multipath delay power spectrum, and the diversity configuration assumed. Unfortunately, there is a scarcity of information, both theoretical and empirical on the multipath characteristics of troposcatter channels. A model for the multipath delay power spectrum has previously been proposed by Bello*. This model provides a reasonable description of the multipath profile for a simple, symmetrical, "smooth earth" troposcatter channel when the radio refractive index in known. A range of refractive index values can be used to represent both median and "worst case" propagation conditions.

In computing $Q(\xi)$, it is convenient to deal with a normalised delay variable

$$\delta = \frac{\xi - D/c}{D/c}$$

which is the percentage departure of the path delay ξ from the delay corresponding to line-of-sight transmission through a distance equal to the path length D. The quantity c is the speed of light.

Note that due to the shadowing effect of the earth, energy will be scattered for path delays exceeding some minimum path delay greater than D/c. If one assumes zero elevation angles for the antennas, the minimum value of ξ is readily computed to be

$$\delta_o = \frac{D^2}{8R^2}$$

where R is the earth's radius.

---

*P. A. Bello, "A Troposcatter Channel Model", IEEE Trans. on Comm. Tech., April 1969, pp. 130 - 138.

In terms of the normalized delay variable δ, the integral representation of the delay power spectrum for identical antennas at the same height pointing with maximum gain at 0-degree elevation (radio horizon) is found to be

$$Q(\xi) \equiv \hat{Q}(\delta) \frac{1}{\delta^{1+m/2}}$$

$$\cdot \int_{\sqrt{\delta_o/\delta}}^{\sqrt{\delta/\delta_o}} \frac{G(x\sqrt{2\delta} - \frac{D}{2R}) G(\frac{\sqrt{2\delta}}{x} - \frac{D}{2R})}{x(x + 1/x)^{m-2}} dx$$

where $G(\cdot)$ is the vertical antenna gain pattern.

This integral expression was evaluated by numerical integration on the digital computer. The antenna gain function was chosen as a symmetrical Gaussian shape which is typical of real antennas for small departures from boresight. The earth's radius must be modified to account for refractive bending of the radio rays. An equivalent earth radius, $R = Ka$, can be defined where a is the true radius and $K = 4/3$ for typical median propagation conditions in overland, temperate climate paths.

The resultant multipath profiles are shown in Figures 3-31, 3-32 and 3-33 for three paths of interest. Figure 3-31 shows the AN/MRC-98 long path, Figure 3-32 shows the AN/TRC-132 path, while Figure 3-33 shows a nominal 250 mile ("smooth earth") path with 28 foot antennas at C-band, or 60 foot antennas at 2 GHz, or 120 foot antennas at 1 GHz. The value $K = 1.33$ represents the median 4/3 earth's radius. The $K = 1$ value represents the approximate worst month median refractice index of an overland European path*. The $K = 0.75$ value is taken as the approximate "worst case" yearly refractive index.

The RADC channel simulator has a tapped delay model of the multipath structure. Up to 16 taps spaced by a 0.1 us can be used in the simulation. Table 3-3 provides the tap settings for the six multipath profiles to be simulated.

*P. F. Panter, Communication Systems Design, McGraw-Hill, New York, 1972, page 391.

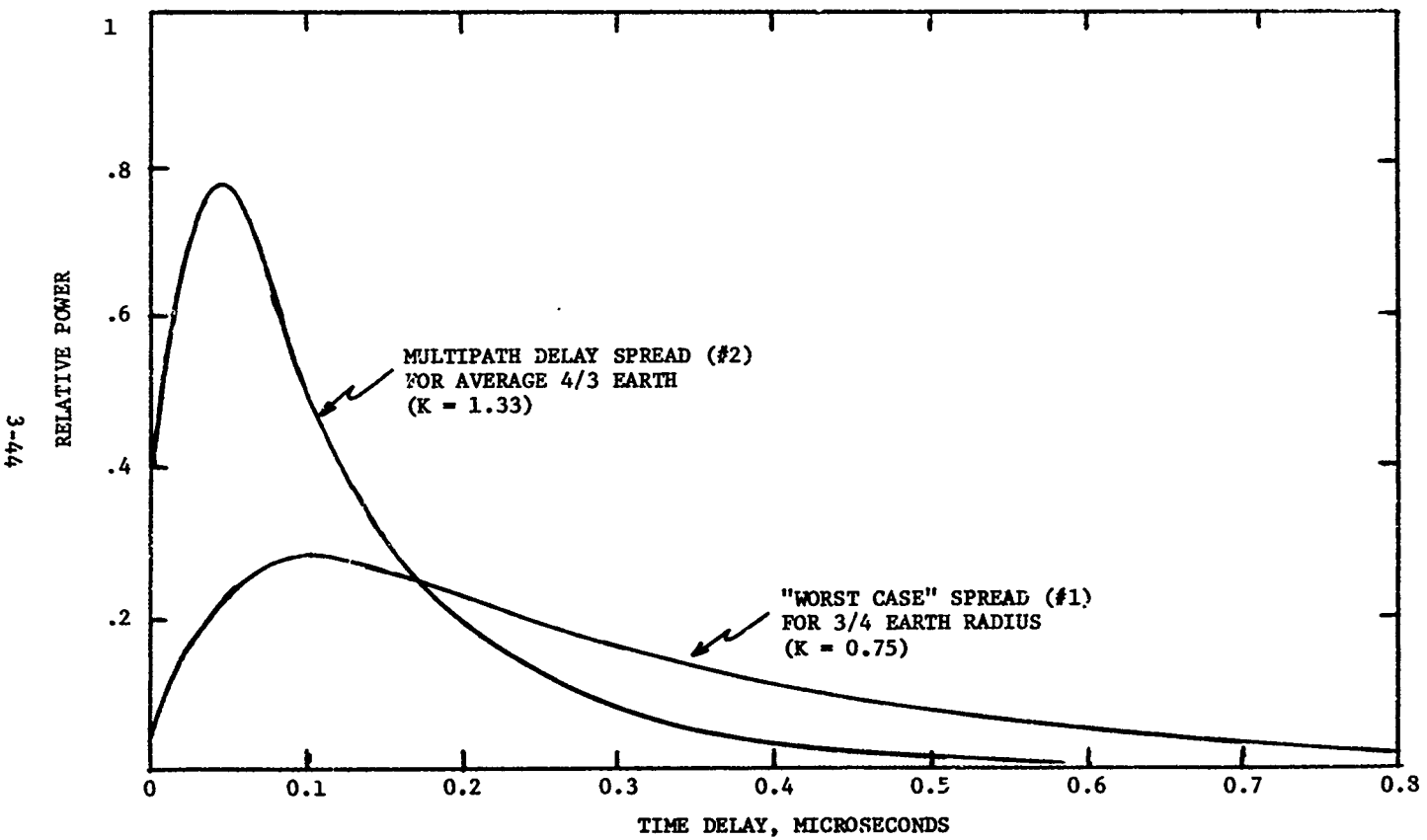

FIGURE 3-31 MULTIPATH DELAY SPREADS EMPLOYED FOR SIMULATION OF 168 MILE AN/MRC-98 TEST PATH (880 MHZ)

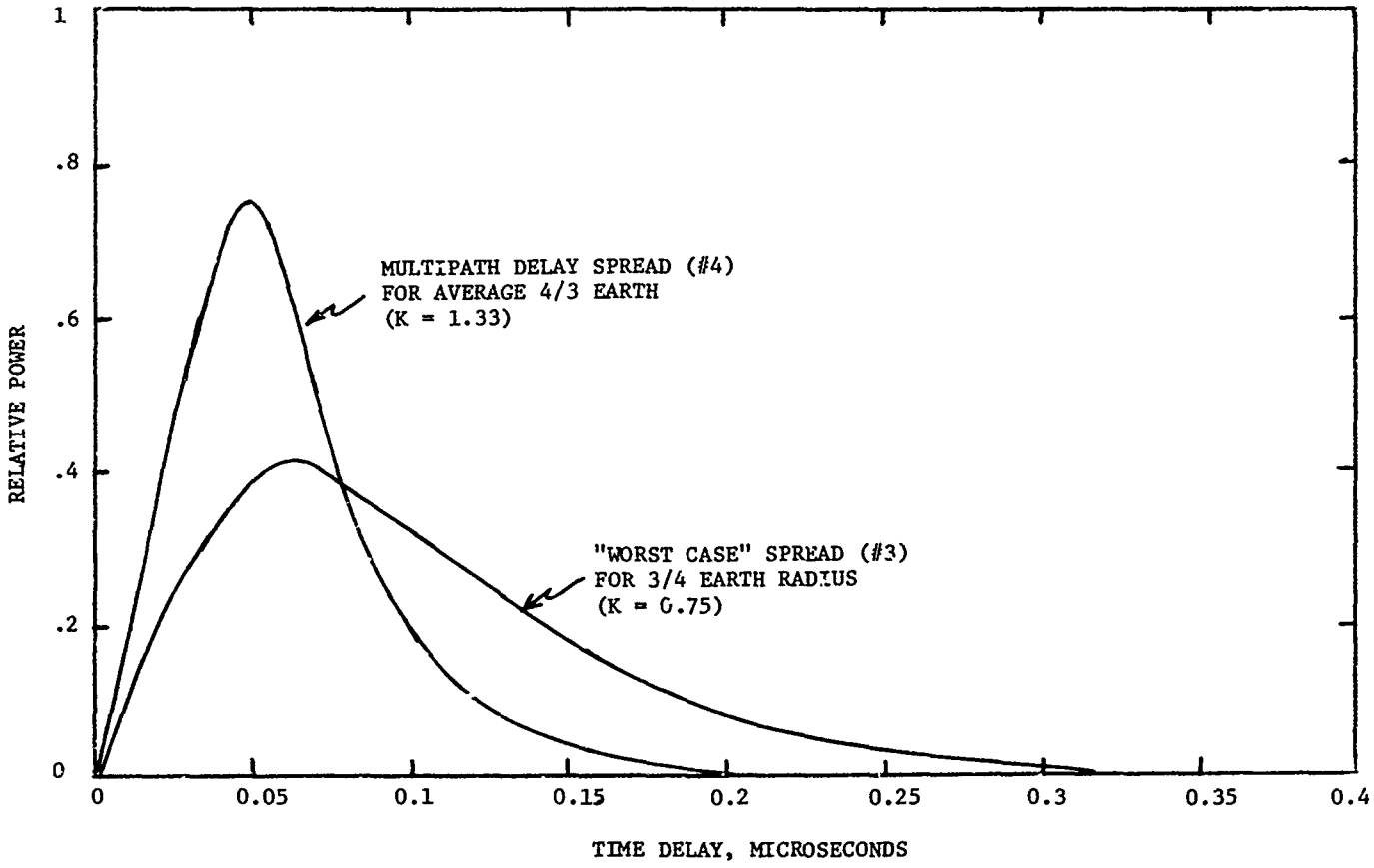

FIGURE 3-32. MULTIPATH DELAY SPREAD EMPLOYED FOR SIMULATION OF 168 MILE AN/TRC-132 TEST PATH (4.4 GHZ)

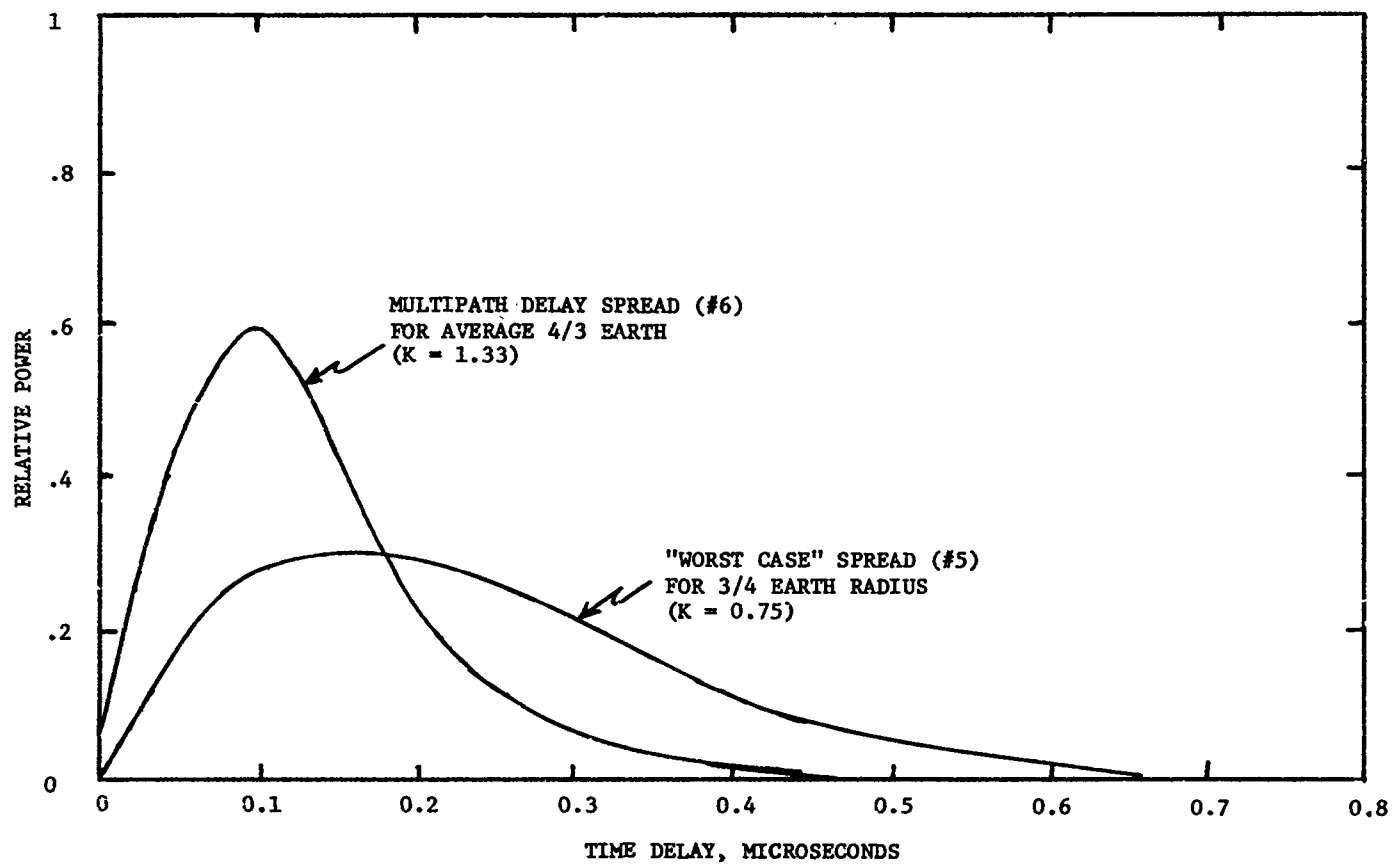

FIGURE 3-33. MULTIPATH DELAY SPREADS EMPLOYED FOR SIMULATION OF 250 MILE "SMOOTH EARTH" PATH WITH 0.6° BEAMWIDTH ANTENNAS

TABLE 3-3. SIMULATOR T . SETTINGS

	168 MILE AN/MRC-98 PATH		168 MILE AN/TRC-132 PATH		250 MILE 0.6° BEAMWIDTH	
	K=.75	K=1.33	K=.75	K=1.33	K=.75	K=1.33
TAP #	PROFILE #1	PROFILE #2	PROFILE #3	PROFILE #4	PROFILE #5	PROFILE #6
1	0	0	0	0	1	0
2	1	5	1	6	0	4
3	2	9	3	13	1	10
4	4	13	7	21	4	17
5	6	16	11	28	8	25
6	8	20	15	35	12	32
7	10	23	20	OFF	16	39
8	12	26	25	OFF	20	OFF
9	13	29	30	OFF	24	OFF
10	15	32	35	OFF	28	OFF
11	17	35	OFF	OFF	32	OFF
12	19	OFF	OFF	OFF	36	OFF
13	21	OFF	OFF	OFF	OFF	OFF
14	23	OFF	OFF	OFF	OFF	OFF
15	25	OFF	OFF	OFF	OFF	OFF
16	27	OFF	OFF	OFF	OFF	OFF
$\Delta=2\sigma=$	0.39 us	0.24 us	0.18 us	.062 us	.28 us	.14 us

3.3.3 AN/MRC-98 168 Mile Simulations

3.3.3.1 General

This series of tests is primarily intended to characterize the DAR-IV performance of the over-the-air tests between Youngstown and Verona, New York, using the AN/MRC-98 equipment.

The initial series of measurements were taken at data rates of 1.75 Mb/s, 3.5 Mb/s and 7 Mb/s, and included two path profiles - an expected and a "worst case" profile as described in Section 3.3.2. For all measurements, the DAR-IV time gate was set to approximately 50% and did not include any coding. Spectral occupancy was thus fixed at 1.5 Hz per bit.

This series of measurements together with the math model predictions provides the data base necessary for comparison of actual over-the-air results with expected or predicted performance.

The test configuration is depicted in Figure 3.1. The median value of E_b/N_o is varied by adjustment of the input signal level to the simulator from the DAR-IV transmitter via a variable attenuator.

Table 3-4 summarizes the series of measurements to be made. Results are plotted directly on Figures 3-34 through 3-37. Plotted profiles on these figures are the theoretical predicted performance for the DAR-IV using the math model and computer simulation. All profiles chosen are considered "representative" as described in Section 3.3.2.

3.3.3.2 Test Results

These initial simulator tests form the baseline for the DAR-IV performance on the 168 mile AN/MRC-98 link. Hence, both the "worst case" and median multipath profiles (profiles 1 and 2, respectively) were chosen for simulation as described in Section 3.3.2.

Tests 1 and 2 correspond to 1.75 Mbps DAR-IV performance in the quad diversity mode for the two multipath profiles mentioned above. Note from the computer simulated prediction of Figure 3-34 that there is relatively little performance difference in these cases. That is, at 1.75 Mbps, the multipath spread is very short in duration compared to a data symbol. The amount of in-band diversity available is small for the case of profile #2 (median) and only slightly greater for profile #1 (worst case). The approximately 2 dB implementation margin of the DAR-IV is not shown in these computer simulation results but the simulations do include the effect of the limited loop gain which has been measured to be K = 0.93. Figure 3-34 also shows the measured results for profiles #1 and #2. It will be noticed that the measured results compare

TABLE 3-4. 880 MHZ LONG PATH SIMULATOR MEASUREMENTS

TEST NO.	DATA RATE Mbps	DIVERSITY MODE	PROFILE	RECORDED ON FIG. NO.
1	1.75	Quad	#1	3-34
2	1.75	Quad	#2	3-34
3	3.5	Dual	#1	3-35
4	3.5	Dual	#2	3-36
5	3.5	Quad	#1	3-35
6	3.5	Quad	#2	3-36
7	7.0	Quad	#1	3-37
8	7.0	Quad	#2	3-37

FIGURE 3-34

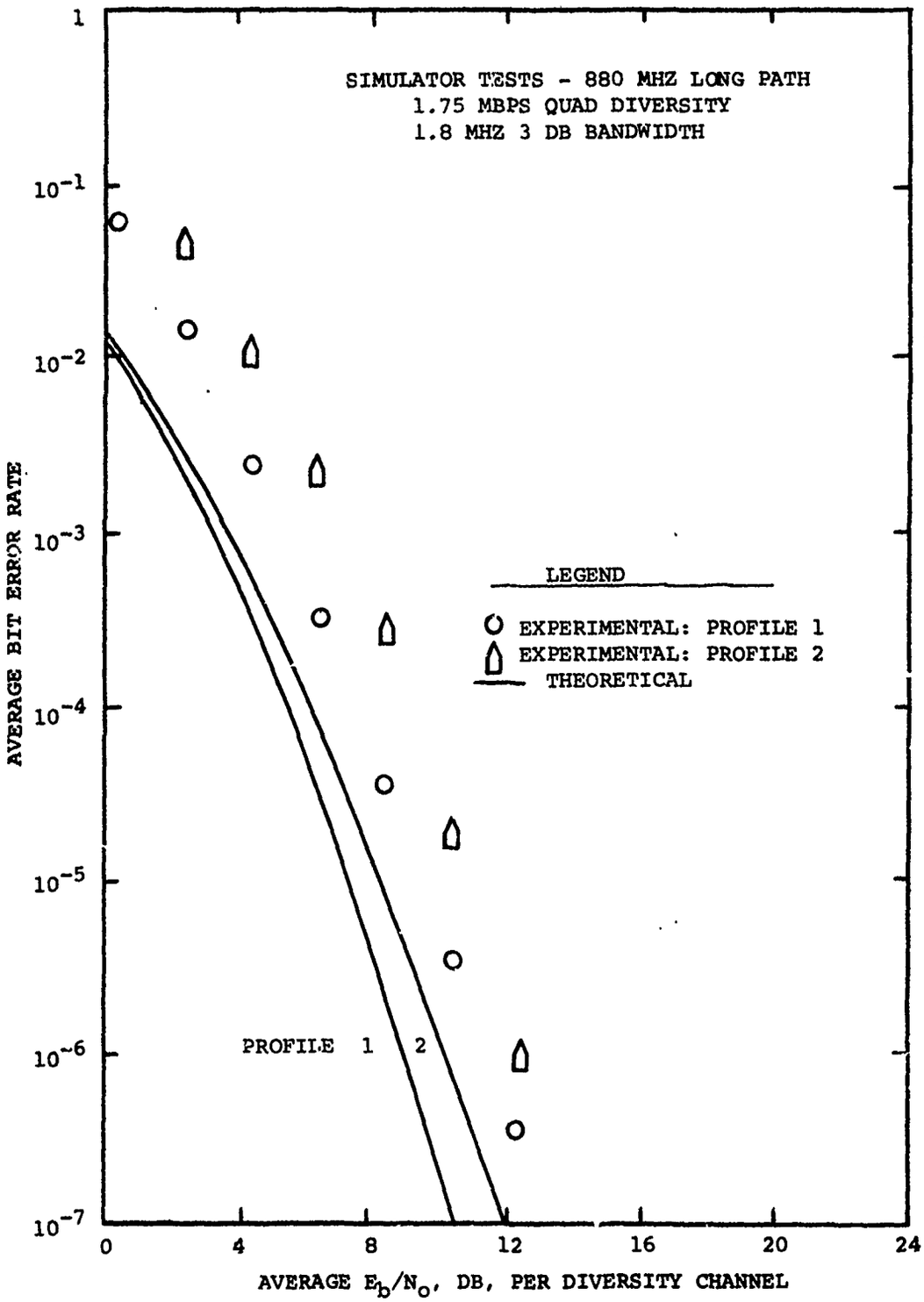
SIMULATOR TESTS - 880 MHZ LONG PATH
1.75 MBPS QUAD DIVERSITY
1.8 MHZ 3 DB BANDWIDTH
LEGEND
EXPERIMENTAL: PROFILE 1
EXPERIMENTAL: PROFILE 2
THEORETICAL
PROFILE 1 2
AVERAGE BIT ERROR RATE
1
10^{-1}
10^{-2}
10^{-3}
10^{-4}
10^{-5}
10^{-6}
10^{-7}
0
4
8
12
16
20
24
AVERAGE E_b/N_o, DB, PER DIVERSITY CHANNEL

quite favorably with the simulations. The slopes of the curves in both cases match the predictions quite closely and there is about a 2 dB offset which represents the implementation loss. Profile #1 shows a tendency to "tail off" around the 10^{-8} to 10^{-9} error rate. This tendency is not seen in the computer predictions primarily due to the fact that at such extremely low error rates, the computer model cannot look at enough profiles to see this tailing effect.

Tables 3-5 and 3-6 show the results of the error histogram measurements which were taken concurrently with the bit error rate runs. These tables show the distribution of the occurrence of the errors. The characteristics of the burst error channel may be seen by observing the distribution of the error clusters. On a LOS channel, the errors would all tend to occur in a single bin (one decade) for high E_b/N_o. Note that at high E_b/N_o on tropo, the errors tends to occur in "bursts" which dominate the average BER performance.

Tests 3 and 4 show the dual diversity performance at 3.5 Mbps for two previous multipath profiles, while tests 5 and 6 show the corresponding quad diversity performance. The results anticipated are shown in Figures 3-35 and 3-36 from the computer simulation. For multipath profile #2, the performance is similar to that previously described. For profile #1 which is more than twice as wide as profile #2, significant irreducible error rate phenomenon is observable in both dual and quad diversity. The "worst case" multipath irreducible BER is approximately 4×10^{-4} for quad diversity. The dual-plus-dual diversity mode operation of the DAR-IV at 7 Mbps can be inferred from these results.

In Figure 3-35 it can be seen that the measured irreducible error rate for dual diversity agreed quite closely with the computer predictions. At lower SNR's a 2 to 3 dB departure is observed. This higher error rate is probably due primarily to timing error in the timing recovery circuit. The present design will be pulled off correct timing by such prolonged periods of high error rates. This effect could be eliminated by choosing a more robust timing recovery scheme.

The quad diversity performance for profile #1 can also be seen on Figure 3-35. The measured results exhibit a uniform displacement from the predictions. This is due to the implementation loss in the modem and combiner circuitry.

Figure 3-36 shows the predicted and measured results for 3.5 Mb/s dual and quad diversity for profile #2. The measured results agree quite closely to the predicted with a 2 - 3 dB offset due to implementation loss in the modem. Both dual and quad diversity exhibit an irreducible error rate not seen in the predicted results. Once again, the failure of the prediction to show the flooring effect is due to the

TABLE 3-5

TEST #1

SIMULATOR TESTS

1.75 Mb/s 880 MHz Long Path

Profile 1 Fade Rate 10 Hz Sample Time 100 sec.

Quad Diversity

	ERROR BINS							
E_b/N_o	0	1-9	$10-10^2$	10^2-10^3	10^3-10^4	10^4-10^5	10^5-10^6	No. Samples
0.4	0	0	0	0	0	40	60	100
2.4	0	0	0	0	4	96	0	100
4.4	0	0	0	1	93	6	0	100
6.4	0	0	9	80	11	0	0	100
8.4	4	21	67	7	1	0	0	100
10.4	57	34	8	1	0	0	0	100
12.4	900	86	14	0	0	0	0	100
14.4	981	17	2	0	0	0	0	100

TABLE 3-6

TEST #2

SIMULATOR TESTS
1.75 Mb/s 800 MHz Long Path
Profile 2 Fade Rate 10 Hz Sample Time 100 sec.
Quad Diversity

	ERROR BINS							
E_b/N_o	0	1-9	$10-10^2$	10^2-10^3	10^3-10^4	10^4-10^5	10^5-10^6	No. Samples
0.5	0	0	0	0	0	0	100	100
2.5	0	0	0	0	0	72	25	100
4.5	0	0	0	0	16	84	0	100
6.5	0	0	0	11	81	8	0	100
8.5	0	2	24	56	18	0	0	100
10.5	19	37	32	12	0	0	0	100
12.5	74	23	3	0	0	0	0	100
14.5	982	18	0	0	0	0	0	1000

FIGURE 3-35

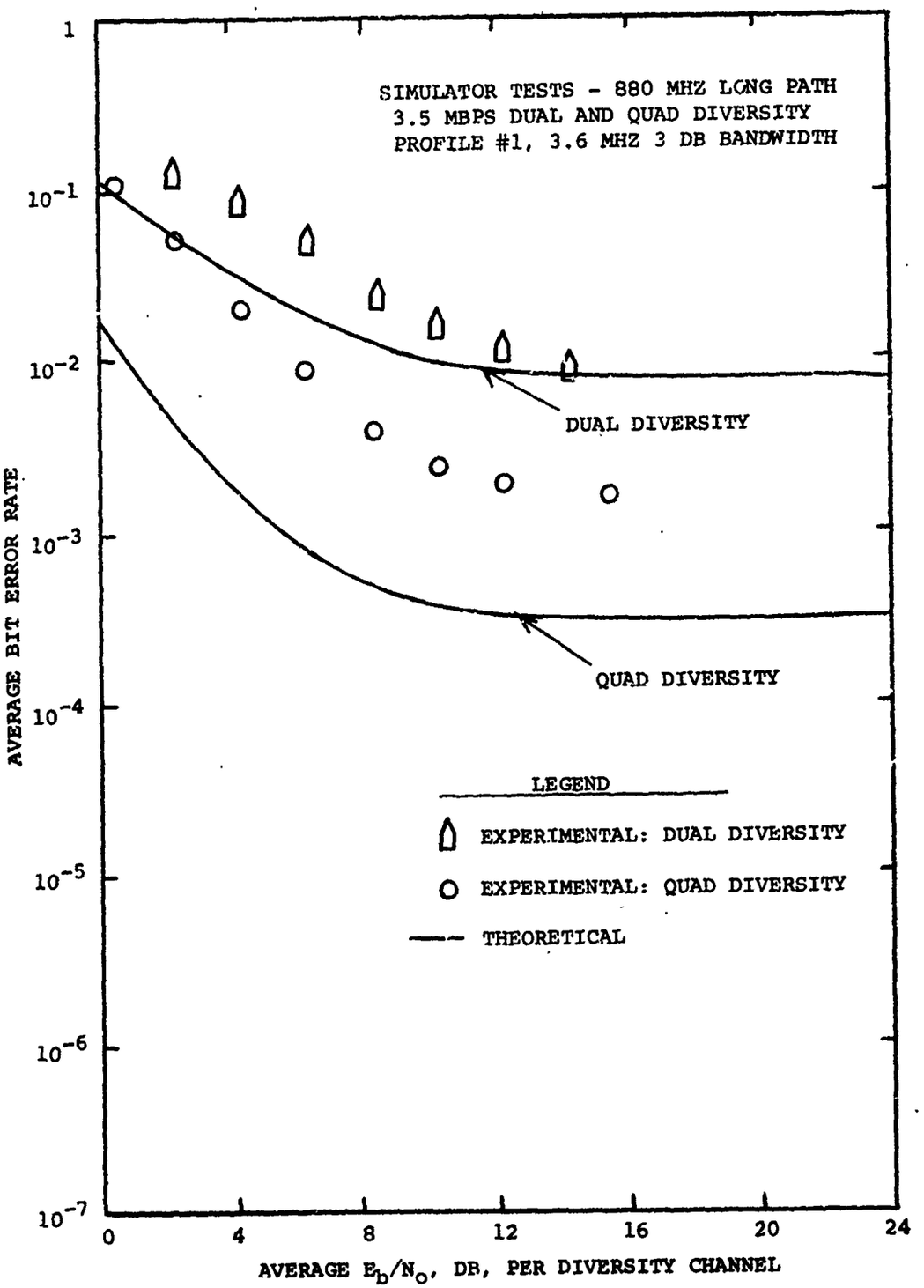
SIMULATOR TESTS - 880 MHZ LONG PATH
3.5 MBPS DUAL AND QUAD DIVERSITY
PROFILE #1, 3.6 MHZ 3 DB BANDWIDTH
DUAL DIVERSITY
QUAD DIVERSITY
LEGEND
EXPERIMENTAL: DUAL DIVERSITY
EXPERIMENTAL: QUAD DIVERSITY
THEORETICAL
AVERAGE BIT ERROR RATE
1
10^{-1}
10^{-2}
10^{-3}
10^{-4}
10^{-5}
10^{-6}
10^{-7}
0
4
8
12
16
20
24
AVERAGE E_b/N_o, DB, PER DIVERSITY CHANNEL

FIGURE 3-36

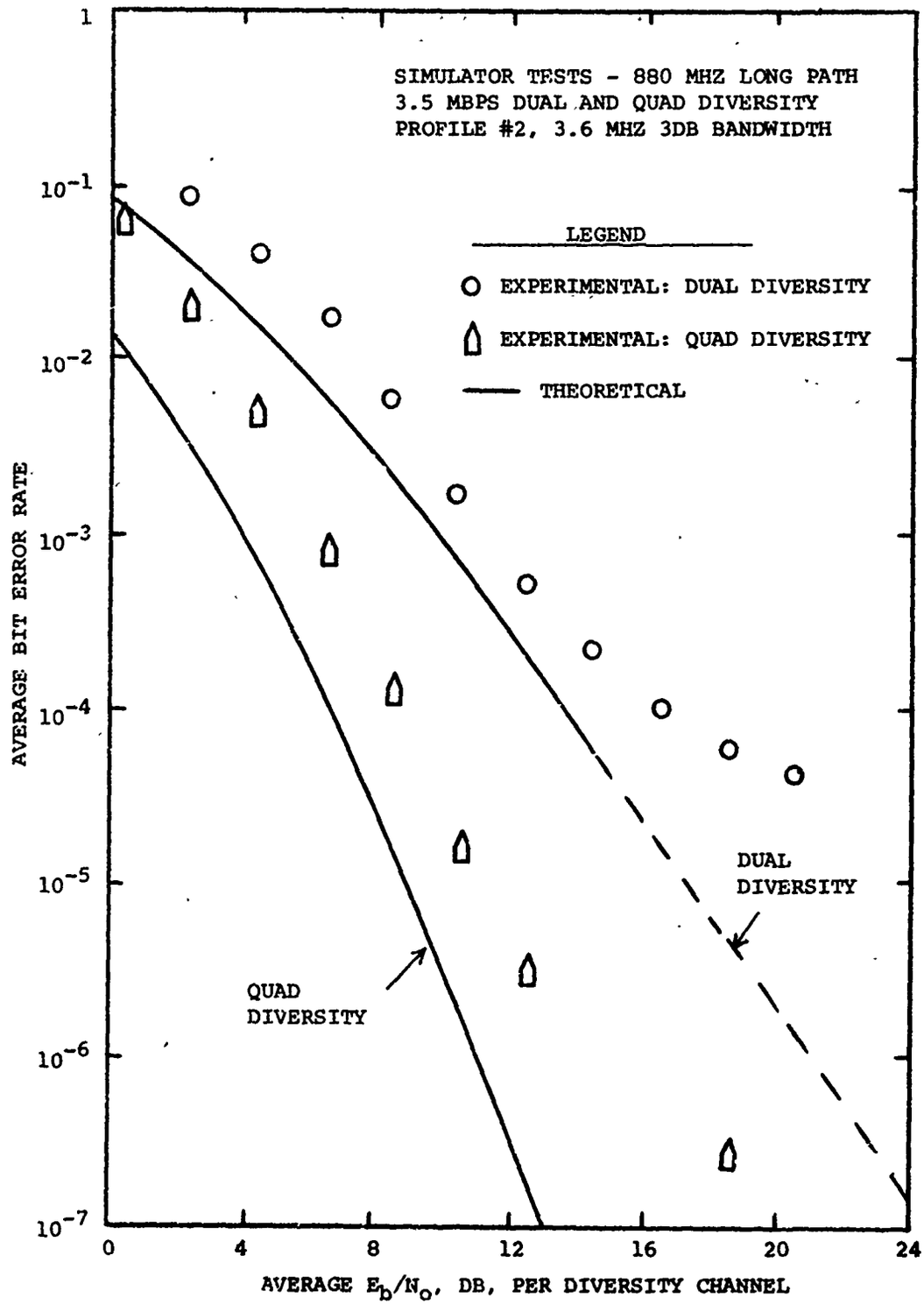
SIMULATOR TESTS - 880 MHZ LONG PATH
3.5 MBPS DUAL AND QUAD DIVERSITY
PROFILE #2, 3.6 MHZ 3DB BANDWIDTH
LEGEND
EXPERIMENTAL: DUAL DIVERSITY
EXPERIMENTAL: QUAD DIVERSITY
THEORETICAL
DUAL DIVERSITY
QUAD DIVERSITY
AVERAGE BIT ERROR RATE
1
10^{-1}
10^{-2}
10^{-3}
10^{-4}
10^{-5}
10^{-6}
10^{-7}
0
4
8
12
16
20
24
AVERAGE E_b/N_o, DB, PER DIVERSITY CHANNEL

computer time constraints that make it impractical to examine enough profiles at these low error rates to see the irreducible error rate come into play.

Tables 3-7 through 3-10 were included to show the results of the error histogram data taken along with the bit error rate data. Examination of these tables reveals the nature and distribution of the error bursts for tests 3 through 6. Note that when an irreducible BER phenomenon is obtained, the error histogram becomes independent of E_b/N_o.

Tests 7 and 8 represent quad diversity performance at 7 Mbps for profiles #1 and #2. Notice that in this case, both the median (profile #2) and "worst case" (profile #1) multipaths result in irreducible error rate of 4×10^{-6} and 10^{-3}, respectively. This irreducible error rate is due to overlap of adjacent distorted bits despite the use of a 50% transmitter time gate. The irreducible error rate floor can be substantially lowered by use of an adaptive "tail canceller" as described in the following sections.

Figure 3-37 shows the predicted and measured results for 7 Mb/s quad diversity for profiles #1 and #2. It can be seen that the computer predictions for profile #1 yield an extremely high irreducible error rate of about 3×10^{-1}. It was impossible to record data for this test because the continuous high error rate made it impossible for the timing recovery to maintain baud synchronization. As a result, a loss of bit count integrity was observed for each run. This performance could be improved by two to three orders of magnitude in error rate by going to a much longer memory in the matched filter or equivalently to a high loop gain, $K = 0.99$, for example.

Test 8 shows the performance of profile #2. The delay spread here is less severe than for profile #1 and no loss of bit count integrity was observed above 6 dB E_b/N_o. The measured performance is noticeably displaced from the predictions. There are two primary causes for this effect. The first is that the timing recovery loop at the 7 Mb/s rate is quite sensitive to error rate due to the reduced loop gain at the highest data rate. This can be overcome with a more robust clock recovery loop. The second effect here is the limited bandwidth of the surface wave devices in the coherent filter. At the highest data rate, a significant amount of energy in the received signal will be lost when passed through the surface wave devices. An alternate approach in the manufacture of these devices as described in Section 3.2 would result in much wider device bandwidth.

Table 3-11 shows the results of the error histogram data for test number 7.

FIGURE 3-37

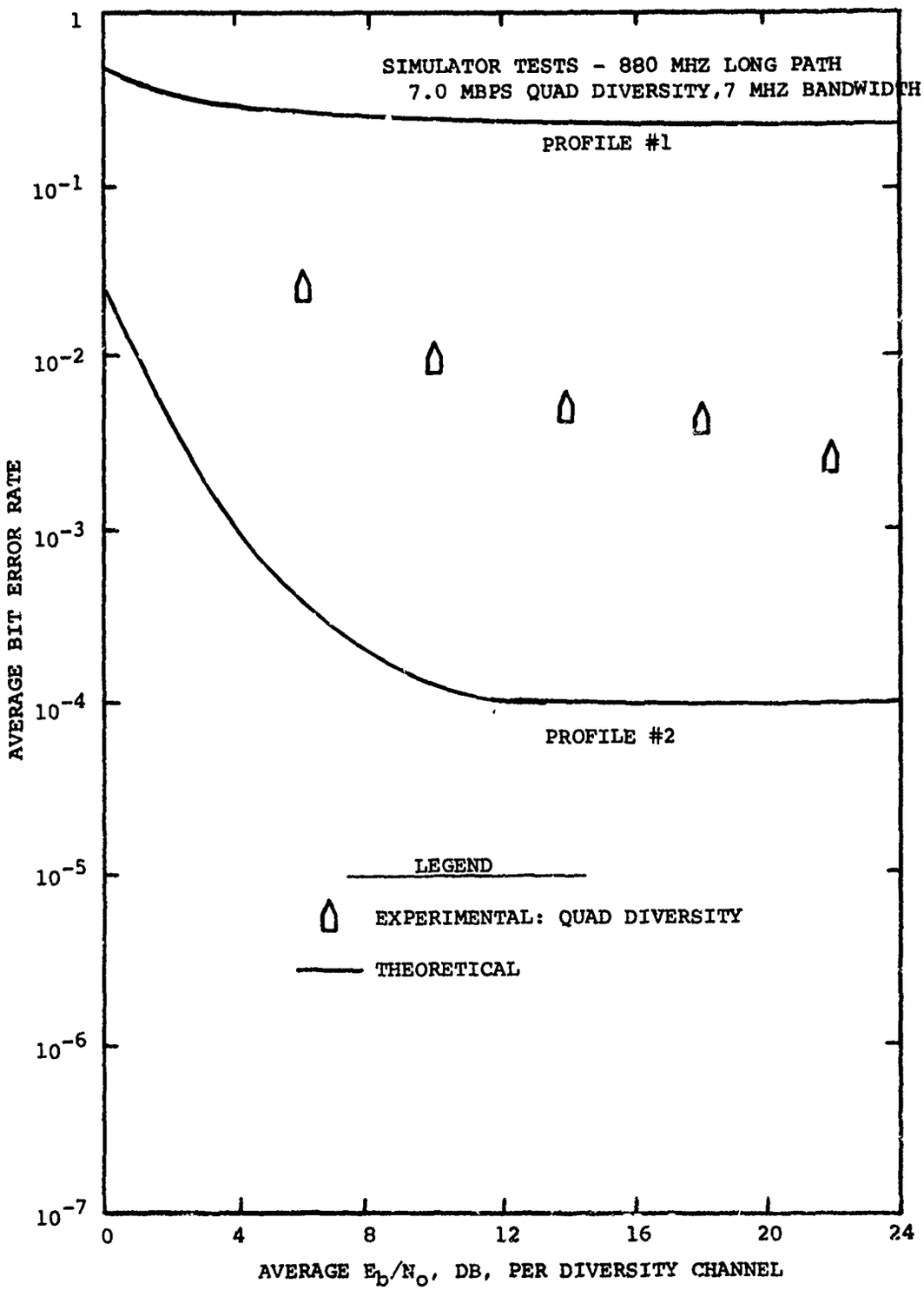
SIMULATOR TESTS - 880 MHZ LONG PATH
7.0 MBPS QUAD DIVERSITY,7 MHZ BANDWIDTH
PROFILE #1
PROFILE #2
LEGEND
EXPERIMENTAL: QUAD DIVERSITY
THEORETICAL
AVERAGE BIT ERROR RATE
1
10^{-1}
10^{-2}
10^{-3}
10^{-4}
10^{-5}
10^{-6}
10^{-7}
0
4
8
12
16
20
24
AVERAGE E_b/N_o, DB, PER DIVERSITY CHANNEL

TABLE 3-7

TEST #3

SIMULATOR TESTS

? 5 Mb/s 880 MHz Long Path

Profile 1 Fade Rate 10 Hz Sample Time 100 sec.

Dual Diversity

	ERROR BINS							
E_b/N_o	0	1-9	$10-10^2$	10^2-10^3	10^3-10^4	10^4-10^5	10^5-10^6	No. Samples
0.4	-	-	-	-	-	-	-	-
2.4	0	0	0	0	0	0	100	100
4.4	0	0	0	0	0	0	100	100
6.4	0	0	0	0	0	5	95	100
8.4	0	0	0	0	0	66	34	100
10.4	0	0	0	0	0	91	9	100
12.4	0	0	0	0	7	88	5	100
14.4	0	0	0	0	14	83	3	100
24.4	0	0	0	1	29	68	2	100

TABLE 3-8

TEST #4

SIMULATOR TESTS
3.5 Mb/s 880 MHz Long Path
Profile #2 Fade Rate 10 Hz Same Time 100 sec.
Dual Diversity

	ERROR BINS							
E_b/N_o	0	1-9	$10-10^2$	10^2-10^3	10^3-10^4	10^4-10^5	10^5-10^6	No. Samples
0.4	0	0	0	0	0	0	100	100
2.4	0	0	0	0	0	0	100	100
4.4	0	0	0	0	0	23	77	100
6.4	0	0	0	0	0	90	10	100
8.4	0	0	0	0	27	73	0	100
10.4	0	0	1	8	70	21	0	100
12.4	0	0	10	39	50	1	0	100
14.4	3	5	29	42	21	0	0	100
16.4	18	17	32	24	9	0	0	100
18.4	35	22	23	15	5	0	0	100
20.4	56	22	12	5	5	0	0	100
22.4	70	10	8	7	5	0	0	100

TABLE 3-9

TEST #5

SIMULATOR TESTS
3.5 Mb/s 880 MHz Long Path
Profile 1 Fade Rate 10 Hz Sample Time 100 sec.
Quad Diversity

	ERROR BINS							
E_b/N_o	0	1-9	$10-10^2$	10^2-10^3	10^3-10^4	10^4-10^5	10^5-10^6	No. Samples
0.4	0	0	0	0	20	978	2	1000
2.4	0	0	0	2	245	753	0	1000
4.4	0	0	3	74	692	231	0	1000
6.4	0	3	43	357	536	61	0	1000
8.4	13	43	19.6	449	274	25	0	1000
10.4	76	118	278	349	163	16	0	1000
12.4	190	185	252	231	124	18	0	1000
24.4	524	118	147	115	77	19	0	1000

TABLE 3-10
TEST #6

SIMULATOR TESTS
3.5 Mb/s 880 MHz Long Path
Profile 2 Fade Rate 10 Hz Sample Time 100 sec.
Quad Diversity

	ERROR BINS							
E_b/N_o	0	1-9	$10-10^2$	10^2-10^3	10^3-10^4	10^4-10^5	10^5-10^6	No. Samples
0.4	0	0	0	0	0	1	99	100
2.4	0	0	0	0	0	82	18	100
4.4	0	0	0	0	23	77	0	100
6.4	0	0	0	20	76	4	0	100
8.4	0	1	20	67	12	0	0	100
10.4	10	26	52	12	0	0	0	100
12.4	50	35	13	2	0	0	0	100
14.4	84	13	3	0	0	0	0	100
16.4	96	3	1	0	0	0	0	100
18.4	973	12	13	2	0	0	0	1000
24.4	989	10	0	1	0	0	0	1000

TABLE 3-11

TEST #7

SIMULATOR TESTS

7.0 Mb/s 880 MHz Long Path

Profile #1 Fade Rate 10 Hz Sample Time 100 sec.

Quad Diversity

	ERROR BINS							
E_b/N_o	0	1-9	$10-10^2$	10^2-10^3	10^3-10^4	10^4-10^5	10^5-10^6	No. Samples
6	0	0	0	0	0	15	85	100
10	0	0	0	0	3	75	22	100
14	0	0	0	0	18	76	6	100
18	0	0	0	0	20	77	3	100
22	0	0	0	3	35	58	4	100
24	0	0	0	19	57	23	1	100

3.3.4 AN/TRC-132 168 Mile Simulations

3.3.4.1 General

This series of tests is intended to characterize the DAR-IV performance for the over-the-air tests between Youngstown and Verona, New York, using the AN/TRC-132 equipment. As with the previous simulator tests described in paragraph 3.3.3, the equipment was configured per Figure 3.1 for the actual tests.

This series of simulator tests explored more fully the characteristics of the DAR-IV. In particular, the effects of varying the time gate duration, effects of coding and performance with and without the adaptive decision feedback equalizer (tail canceller) was addressed.

For selected test series, with emphasis again on quad diversity and higher bit rate modes of operation, data was taken for two different time gates and two different coding sequences. (Note that pulse phase coding is used for improved illumination of the available bandwidth.) Data was also taken for two links with two multipath profiles for each link - an "average"and "worst case". The effects of the adaptive decision feedback equalizer were evaluated for each.

Table 3-12 summarizes the series of measurements for this segment of the Final Acceptance Test. As with the preceding tests, the median value of E_b/N_o is varied by adjustment of the input signal level to the simulator from the DAR-IV transmitter via a variable attenuator. Results are plotted directly on Figures 3-38 through 3-46. Plotted profiles on these figures are the theoretical measured performance for the DAR-IV. See Section 3.3.2 for description of profiles selected.

3.3.4.2 Simulator Tests Without Tail Canceller

The tests described in Table 3-12 serve several purposes. Multipath profiles #3 and #4 are the "worst case" and median profiles for the 168 mile AN/TRC-132 test link. These profiles will serve to establish a baseline for the corresponding over-the-air performance. Multipath profiles #5 and #6 refer to a 250 mile "smooth earth" path which may be characteristic of long distance DCS paths. In this series of tests, a number of tests are repeated with and without the addition of a "tail canceller" circuit.

Tests 1, 2 and 3 show the non, dual and quad diversity performance of the DAR-IV at 1.75 Mbps without tail cancelling. All three tests are performed for the "worst case" multipath profile of the 168 mile AN/TRC-132 link. The large improvement due to diversity is

apparent as seen in Figure 3-38. There was no evidence of an irreducible error even at error rates of 10^{-8}. A 44% time gate was used for these measurements. The predicted quad diversity performance (dashed line) from a Monte-Carlo computer simulation is also shown. The predicted result is pessimistic at low BER as previously demonstrated in the tactical results of Section 3.2.

Tests 4, 5 and 6 show the effect of transmitter time gate variation as well as pulse phase coding also at 1.75 Mb/s, but for quad diversity without tail cancelling. These tests also used the "worst case" multipath profile of the 168 mile AN/TRC-132 link. These results are shown in Figure 3-39.

Test 4 reduces the time gate (on period) from 44% to approximately 30%. Due to the relatively low amount of multipath for this data rate, only a 1 to 2 dB improvement was observed over the results of test 3. Test 5 employed a spread spectrum phase coding of the transmitted pulses. The code used for this test was a 01110 code on each transmitted pulse which had a time gate of 44%. This code gives near optimum illumination of the transmit bandwidth. Once again, due to the relatively small amount of multipath, only a slight improvement over the 30% time gate was observed. Test 6 employed a spread spectrum code of 110011. It can be seen that this code was certainly less optimum than the previous code and shows a marked departure from the other curves at low error rates. This is because this particular code is effectively a square wave at more than twice the data rate. This type of coding tends to concentrate the transmit energy in a region where the bandlimited SAW recirculating delay line cannot effectively use it.

Tests 7, 8 and 9 are like the previously described tests 1, 2 and 3 except at the 3.5 Mb/s data rate. These tests show the non, dual and quad diversity performance for the "worst case" profile #3 using a 44% time gate. It can be seen here that the multipath relative to the data rate has become significant now producing irreducible error rates of approximately 6×10^{-3}, 1×10^{-4}, and 7×10^{-6} for non, dual and quad diversity respectively. The results of these tests are shown in Figure 3-40. The predicted quad diversity performance from Monte-Carlo computer analysis of the math model is also shown (dashed line). For BER > 10^{4}, the agreement is excellent differing only by the implementation loss. At lower BER, the predicted results do not show the irreducible BER phenomenon. The prediction is based on an ideal DAR-IV implementation with no bandlimiting in the SAW delay lines. The present band limiting reduces the useful bandwidths of the 3.5 Mbps signal and thereby restricts the available intrinsic diversity resulting in a higher irreducible BER.

Tests 10 and 11 show the effects of different time gate duration at 3.5 Mb/s corresponding to tests 3 and 4 at 1.75 Mb/s

FIGURE 3-38

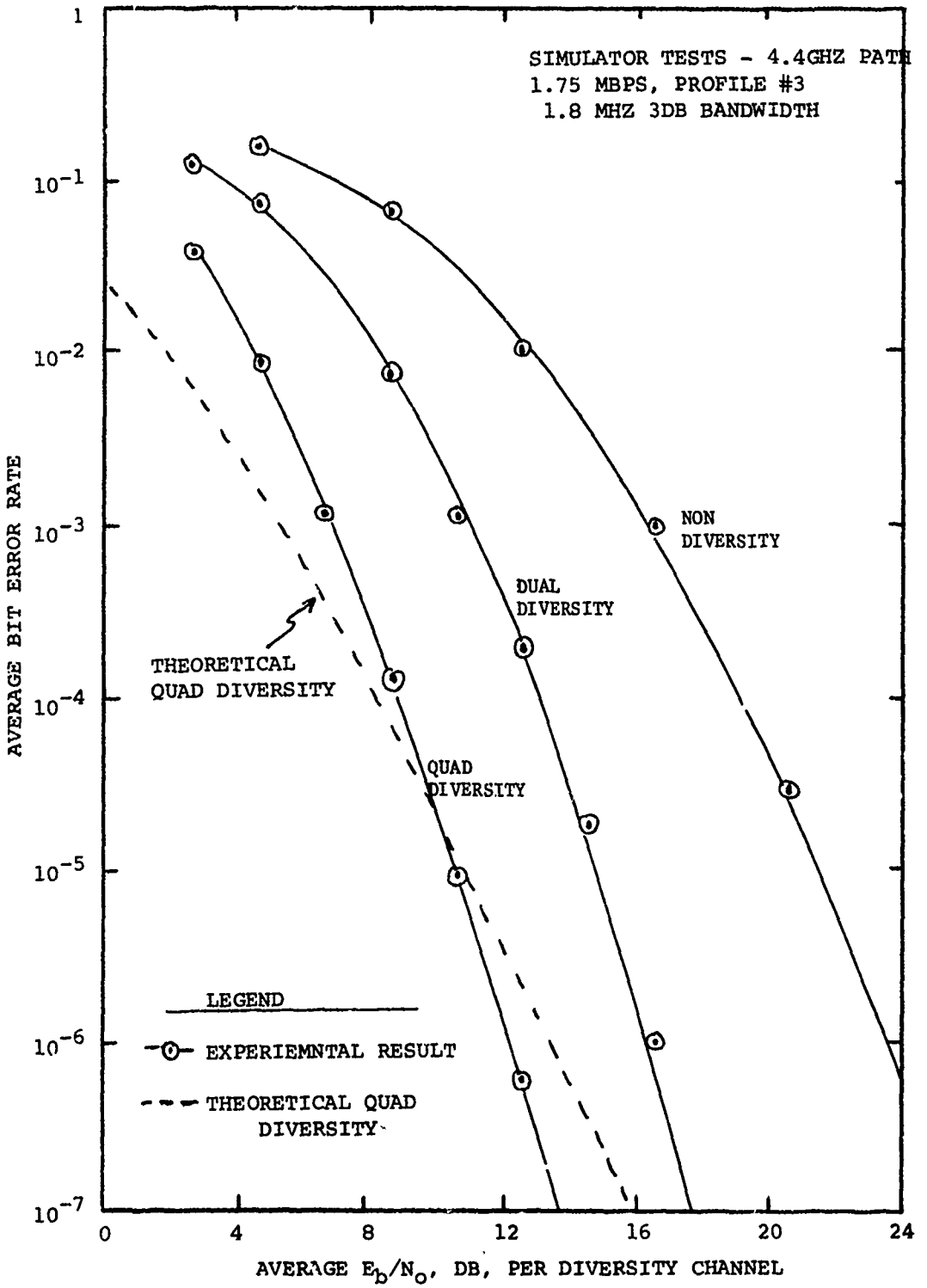
SIMULATOR TESTS - 4.4GHZ PATH
1.75 MBPS, PROFILE #3
1.8 MHZ 3DB BANDWIDTH
AVERAGE BIT ERROR RATE
1
10^{-1}
10^{-2}
10^{-3}
10^{-4}
10^{-5}
10^{-6}
10^{-7}
NON DIVERSITY
DUAL DIVERSITY
QUAD DIVERSITY
THEORETICAL QUAD DIVERSITY
LEGEND
EXPERIEMNTAL RESULT
THEORETICAL QUAD DIVERSITY
0
4
8
12
16
20
24
AVERAGE E_b/N_o, DB, PER DIVERSITY CHANNEL

FIGURE 3-39

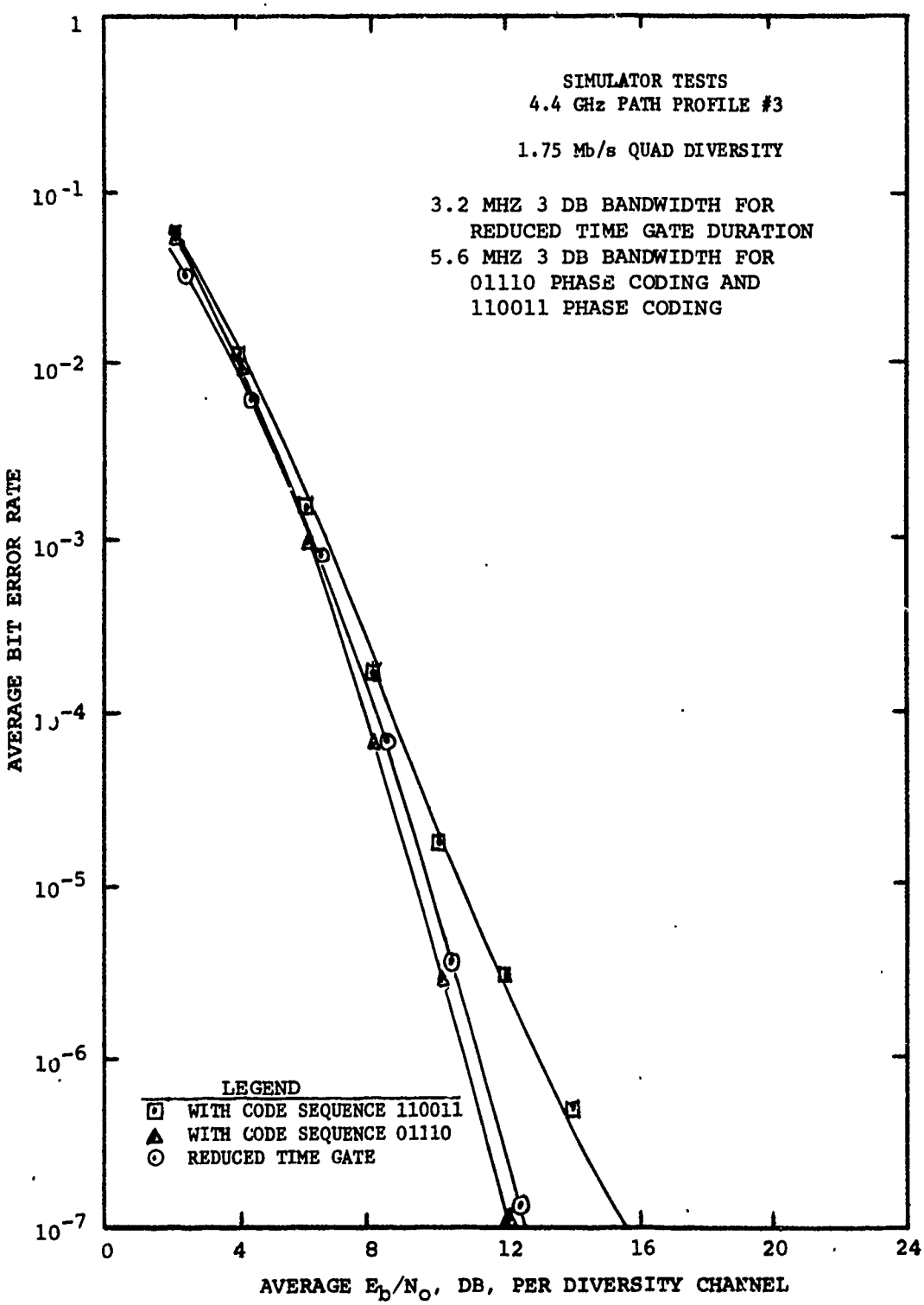
SIMULATOR TESTS
4.4 GHz PATH PROFILE #3
1.75 Mb/s QUAD DIVERSITY
3.2 MHZ 3 DB BANDWIDTH FOR
REDUCED TIME GATE DURATION
5.6 MHZ 3 DB BANDWIDTH FOR
01110 PHASE CODING AND
110011 PHASE CODING
AVERAGE BIT ERROR RATE
1
10^{-1}
10^{-2}
10^{-3}
10^{-4}
10^{-5}
10^{-6}
10^{-7}
LEGEND
WITH CODE SEQUENCE 110011
WITH CODE SEQUENCE 01110
REDUCED TIME GATE
0
4
8
12
16
20
24
AVERAGE E_b/N_o, DB, PER DIVERSITY CHANNEL

FIGURE 3-40

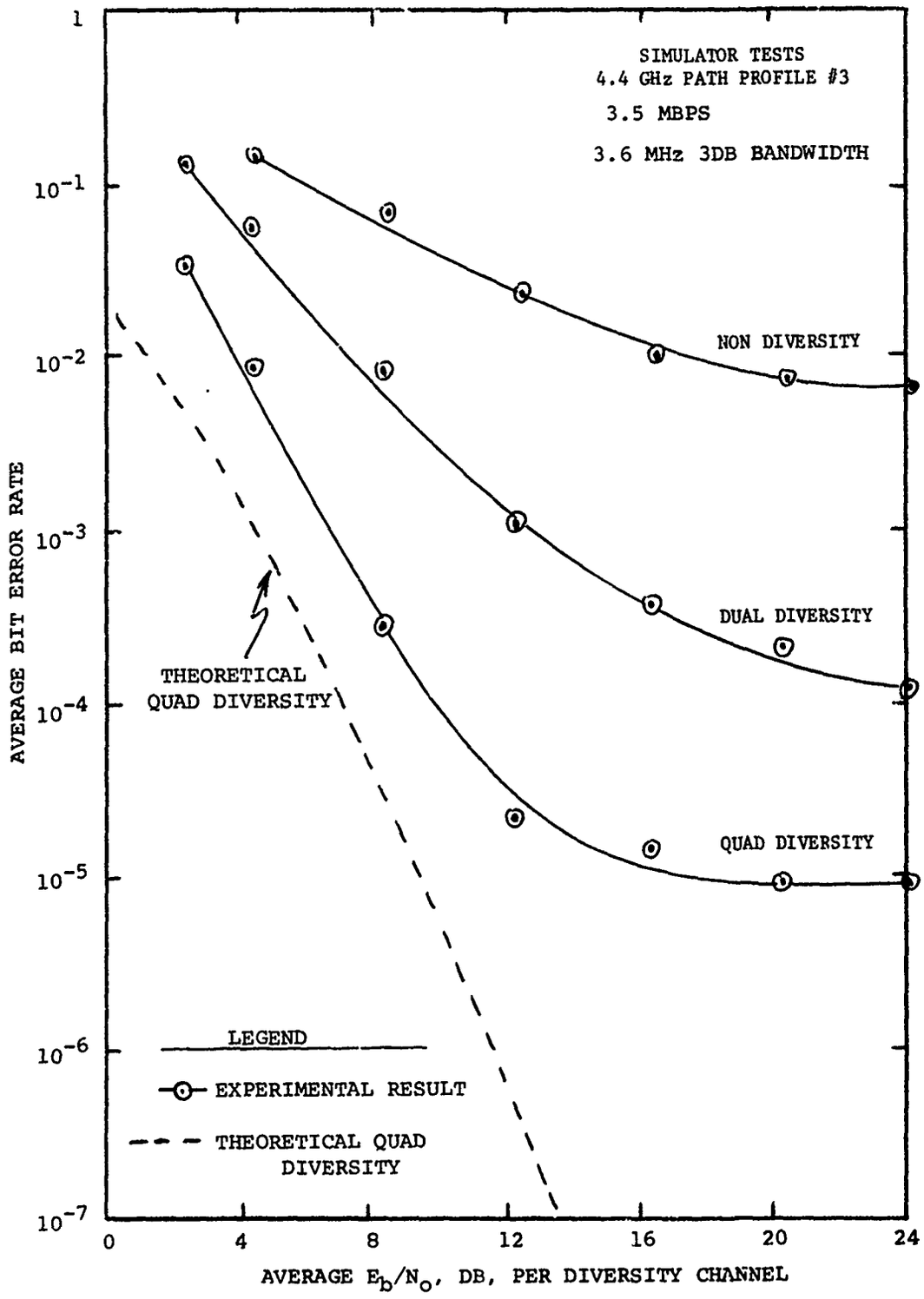
SIMULATOR TESTS
4.4 GHz PATH PROFILE #3
3.5 MBPS
3.6 MHz 3DB BANDWIDTH
NON DIVERSITY
DUAL DIVERSITY
QUAD DIVERSITY
THEORETICAL
QUAD DIVERSITY
LEGEND
EXPERIMENTAL RESULT
THEORETICAL QUAD
DIVERSITY
AVERAGE BIT ERROR RATE
1
10^{-1}
10^{-2}
10^{-3}
10^{-4}
10^{-5}
10^{-6}
10^{-7}
0
4
8
12
16
20
24
AVERAGE E_b/N_o, DB, PER DIVERSITY CHANNEL

TABLE 3-12

4.4 GHZ SIMULATOR MEASUREMENTS

TEST NO.	DATA RATE Mbps	DIVERSITY MODE	EQUALIZER	PROFILE NO.	TIME GATE	CODING	RECORDED ON FIG. NO.
1	1.75	Non	No	3	44%	None	3-38
2	1.75	Dual	No	3	44%	None	3-38
3	1.75	Quad	No	3	44%	None	3-38
4	1.75	Quad	No	3	30%	None	3-39
5	1.75	Quad	No	3	44%	Code #1	3-39
6	1.75	Quad	No	3	44%	Code #2	3-39
7	3.5	Non	No	3	44%	None	3-40
8	3.5	Dual	No	3	44%	None	3-40
9	3.5	Quad	No	3	44%	None	3-40
10	3.5	Quad	No	4	44%	None	3-41
11	3.5	Quad	No	4	30%	None	3-41
12	3.5	Quad	No	5	44%	None	3-41
13	3.5	Quad	No	6	44%	None	3-41
14	7.0	Non	No	3	44%	None	3-45
15	7.0	Dual	No	3	44%	None	3-45
16	7.0	Quad	No	3	44%	None	3-45
17	7.0	Quad	No	4	44%	None	3-46
18	7.0	Quad	No	5	44%	None	3-46
19	7.0	Quad	No	6	44%	None	3-46
20	1.75	Quad	Yes	3	44%	None	3-47
21	1.75	Quad	Yes	4	44%	None	3-47
22	1.75	Quad	Yes	5	44%	None	3-47
23	1.75	Quad	Yes	6	44%	None	3-47
24	3.5	Quad	Yes	3	44%	None	3-48
25	3.5	Quad	Yes	4	44%	None	3-48
26	3.5	Quad	Yes	5	44%	None	3-48
27	3.5	Quad	Yes	6	44%	None	3-48
28	7.0	Quad	Yes	3	44$	None	3-49
29	7.0	Quad	Yes	4	44%	None	3-49
30	7.0	Quad	Yes	5	44%	None	3-49
31	7.0	Quad	Yes	6	44%	None	3-49

previously described. In this case, however, the median multipath for the AN/TRC-132 test link is employed, that is profile #4. These tests were run for quad diversity. It can be seen on Figure 3-41 that only a small improvement was gained by using the reduced time gate since bandlimiting in the present DAR-IV experimental model limits the useful signal bandwidth. Test 12 and 13 show the results of 3.5 Mb/s data rate for the "worst case" and median profiles for a 250 mile link using antennas with a 0.6 degree beamwidth. This would be representative of an AN/TRC-132 "long path" link at 4.4 GHz. These results are also plotted in Figure 3-41. The "worst case" profile shows an irreducible error rate of 10^{-4} due to the severity of the multipath while test 13 using the median profile is very similar to tests 10 and 11.

Figure 3-42 shows the spectrum of the 7 Mb/s signal with rectangular pulse shape and 33% time gate (190 ns off-time). In the simulation, this signal was filtered by a 7 MHz 3 dB bandwidth filter with the amplitude versus frequency characteristic shown in Figure 3-43. The resultant transmission signal has the spectrum shown in Figure 3-44. The 3 dB bandwidth is approximately 7 MHz and the 99% power spectral confinement is approximately 13 MHz. The 7 Mb/s signal occupies a large 3 dB bandwidth which would normally lead to extra intrinsic diversity for a given multipath profile. However, as shown in Figure 3-21, the coherent reference recovery circuit of the present DAR-IV experimental model has only 3 to 4 MHz 3 dB bandwidth. Hence, the 7 Mbps signal will have less intrinsic diversity than predicted resulting in higher BER.

Tests 14, 15 and 16 again demonstrate non, dual and quad diversity operation for the "worst case" profile for the AN/TRC-132 link except at the 7 Mb/s data rate. These results may be seen on Figure 3-45. At this high data rate, using a 44% time gate, the multipath causes severe intersymbol interference. Irreducible error rates of 0.2, 5×10^{-2} and 3×10^{-2} were observed for non, dual and quad diversity respectively. Note that the predicted quad diversity performance for the worst case AN/TRC-132 multipath also displays an irreducible error rate but at 10^{-6} instead of 3×10^{-2} for the experimental results. The difference is largely due to the fact that the effective DAR-IV reference loop bandwidths are 3 to 4 MHz in the present experimental model. However, the signal has nearly 7 MHz bandwidth and half the potential intrinsic diversity gain of the modem is being lost because of this implementation problem. If a wider bandwidth SAW delay line was employed in the reference recovery circuit, the measured irreducible BER would drop dramatically to the predicted value. This performance could be improved still further by using a much longer memory in the adaptive matched filter in conjunction with the use of the adaptive decision feedback equalizer (or tail canceller).

Tests 17, 18 and 19 demonstrate the response of the DAR-IV to different multipath profiles for 7.0 Mb/s quad diversity.

FIGURE 3-41

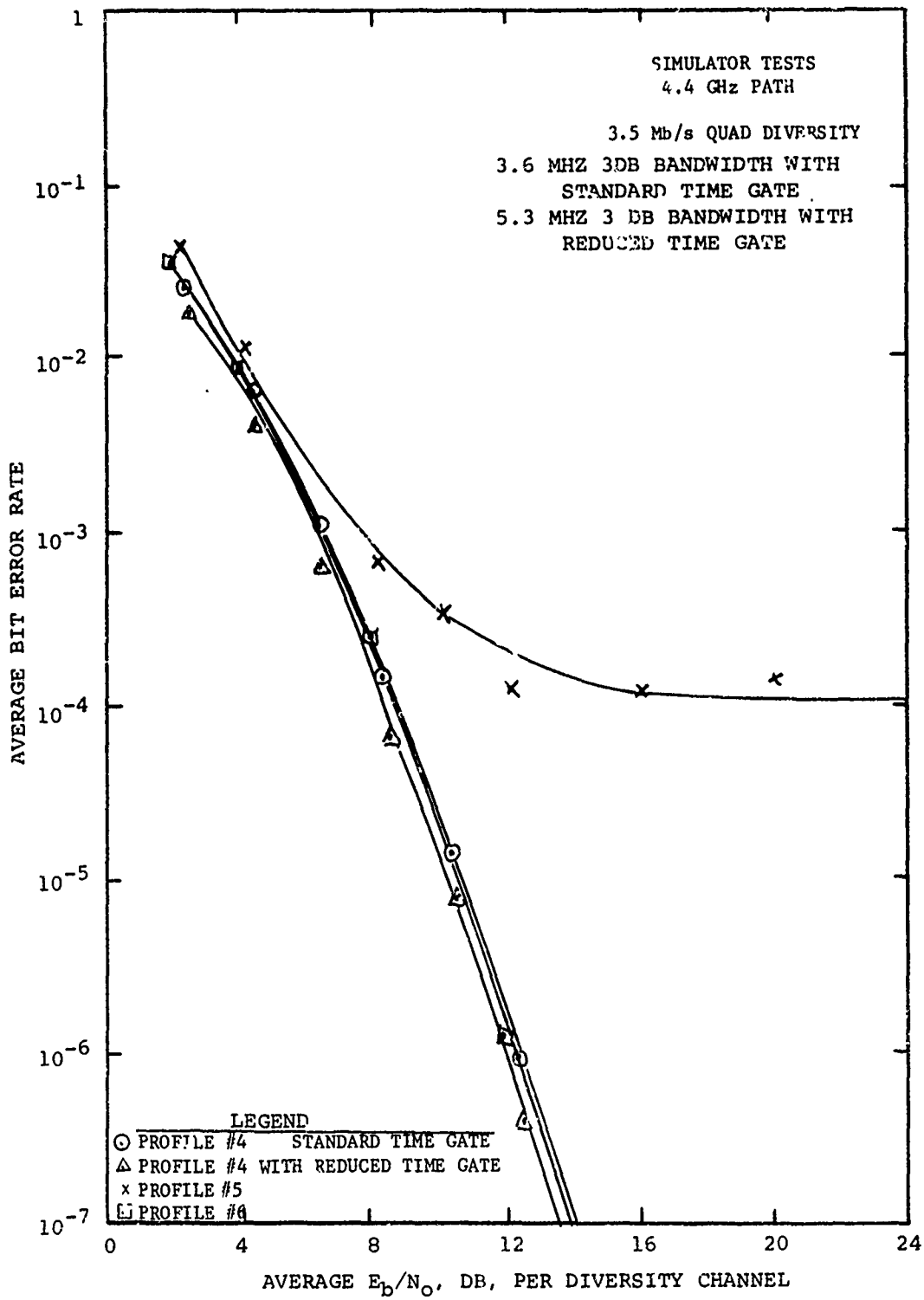
SIMULATOR TESTS
4.4 GHz PATH
3.5 Mb/s QUAD DIVERSITY
3.6 MHZ 3DB BANDWIDTH WITH STANDARD TIME GATE
5.3 MHZ 3 DB BANDWIDTH WITH REDUCED TIME GATE
AVERAGE BIT ERROR RATE
1
10^{-1}
10^{-2}
10^{-3}
10^{-4}
10^{-5}
10^{-6}
10^{-7}
0
4
8
12
16
20
24
AVERAGE E_b/N_o, DB, PER DIVERSITY CHANNEL
LEGEND
PROFILE #4 STANDARD TIME GATE
PROFILE #4 WITH REDUCED TIME GATE
PROFILE #5
PROFILE #6

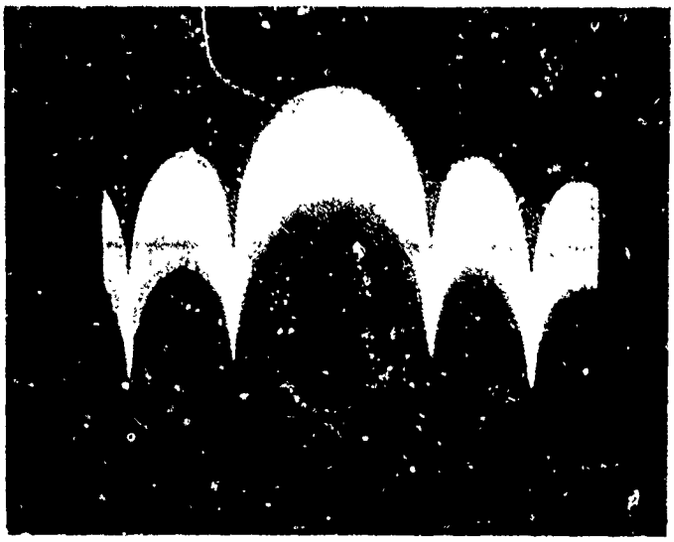

FIGURE 3-42

SPECTRUM OF 7.0 MBPS DAR WAVEFORM WITH RECTANGULAR PULSE SHAPE AND 33% TIME GATE

VERT: 10 DB/CM
HORZ: 5 MHz/CM

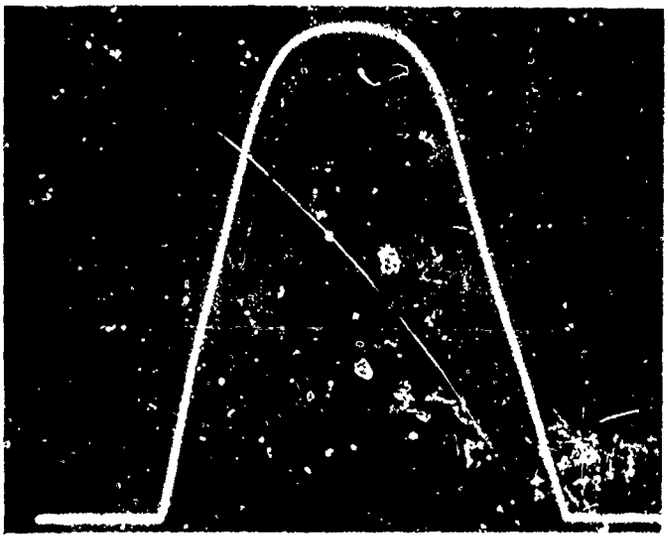

FIGURE 3-43

AMPLITUDE-FREQUENCY CHARACTERISTIC OF FILTER USED TO BAND-LIMIT 7 MBPS WAVEFORM

VERT: 2 DB/CM
HORZ: 2 MHz/CM

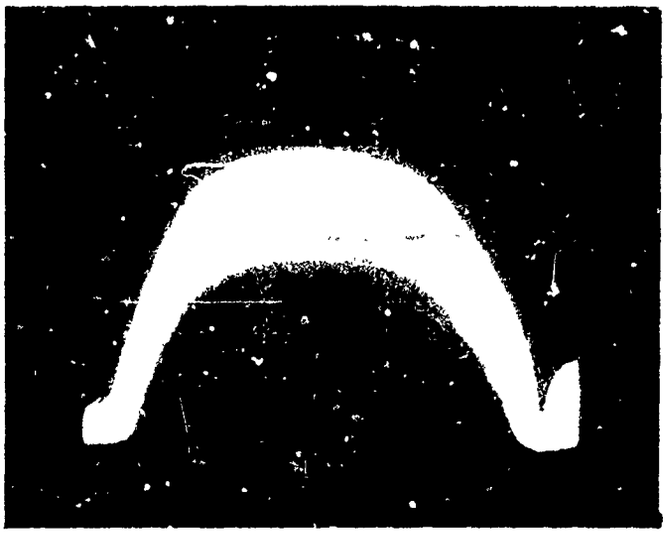

FIGURE 3-44

TRANSMISSION SPECTRUM OF 7 MBPS WAVEFORM AFTER FILTERING

VERT: 10 DB/CM
HORZ: 2 MHz/CM

FIGURE 3-45

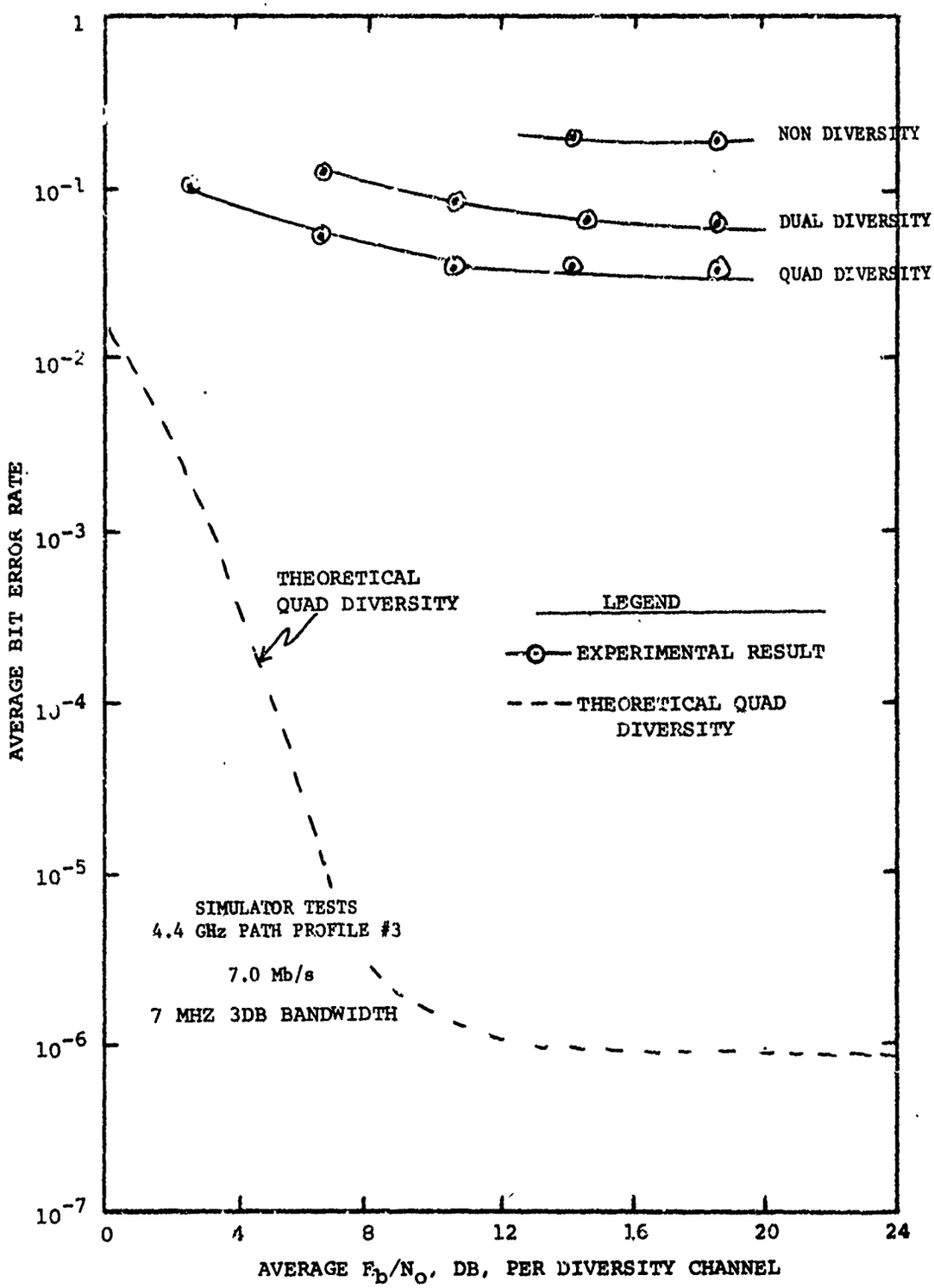
1
10^{-1}
10^{-2}
10^{-3}
10^{-4}
10^{-5}
10^{-6}
10^{-7}
AVERAGE BIT ERROR RATE
NON DIVERSITY
DUAL DIVERSITY
QUAD DIVERSITY
THEORETICAL
QUAD DIVERSITY
LEGEND
EXPERIMENTAL RESULT
THEORETICAL QUAD
DIVERSITY
SIMULATOR TESTS
4.4 GHz PATH PROFILE #3
7.0 Mb/s
7 MHZ 3DB BANDWIDTH
0
4
8
12
16
20
24
AVERAGE F_b/N_o, DB, PER DIVERSITY CHANNEL

The profiles selected were profiles #4, #5 and #6 which represent the median AN/TRC-132 performance over a 168 mile link, and the worst case and median 250 mile path for the AN/TRC-132 respectively.

The results of these tests are shown in Figure 3-46. Note that the results for profiles #4 and #6 which are both median multipath profiles show a significant improvement over the "worst case" profiles #5 and #3 (on Figure 3-42). Due to the reduced delay spread for the median profiles, the measured irreducible error rates are several orders of magnitude lower than for the "worst case" profiles. Once again, an increased bandwidth in the coherent filter would yield far better performance. The results for the worst case profiles #3 and #5 are further hampered by the fact that the present timing recovery loop is very sensitive at the high data rates to severe multipath distortion. This causes a significant timing offset which further degrades the performance. A more robust time recovery loop would yield significantly lower irreducible error rates.

3.3.4.3 Simulator Tests With Tail Canceller

All of the previously described tests were performed with the Decision Feedback Equalizer (DFE) or "tail canceller" disabled. Tests 20 through 31 were performed with the DFE activated. The results of these tests are found on Figures 3-47 through 3-49. These tests were all performed at quad diversity in order to emphasize the ability of the DFE to operate with different multipath profiles. As described in Section 2.2.2.4, the DFE was unable to show any real improvement in performance and was difficult to align properly due to the limited memory in the coherent filter which resulted in excessive data pattern sensitivity. Note that the DFE was an add-on feasibility model and not included in the original DAR-IV design. Provision for larger DAR-IV loop memory was not practical on the present model.

Tests 20 through 23 were all run at 1.75 Mb/s for profiles #3 and #4 (worst case and median for 168 miles AN/TRC-132) and profiles #5 and #6 (worst case and median for 250 mile AN/TRC-132). The results are shown in Figure 3-47. Since the relative multipath for the 1.75 Mb/s data rate is small enough not to create intersymbol interference, no real improvement would be expected from the DFE. The following observations may be made from examining Figure 3-47. In both instances, the worst case profile shows better performance than the median profiles due to efficient use of the added intrinsic diversity. Secondly, for profile #6, the most severe of the four profiles, the performance is best and exhibits no observable tendency to "tail off". Once again, this exhibits the DAR-IV's ability to utilize the available extra diversity.

FIGURE 3-46

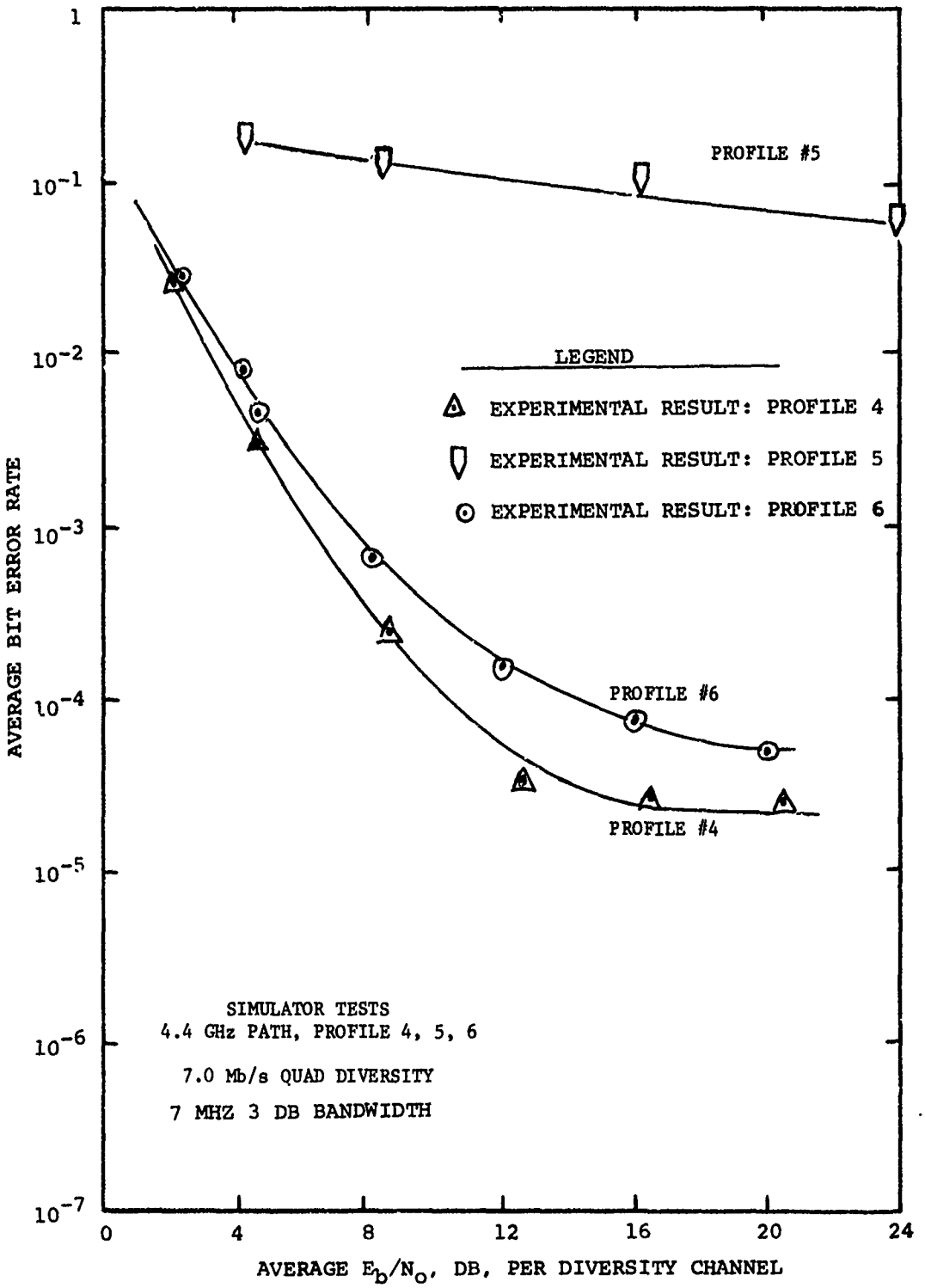
1
10^{-1}
10^{-2}
10^{-3}
10^{-4}
10^{-5}
10^{-6}
10^{-7}
AVERAGE BIT ERROR RATE
PROFILE #5
LEGEND
EXPERIMENTAL RESULT: PROFILE 4
EXPERIMENTAL RESULT: PROFILE 5
EXPERIMENTAL RESULT: PROFILE 6
PROFILE #6
PROFILE #4
SIMULATOR TESTS
4.4 GHz PATH, PROFILE 4, 5, 6
7.0 Mb/s QUAD DIVERSITY
7 MHZ 3 DB BANDWIDTH
0
4
8
12
16
20
24
AVERAGE E_b/N_o, DB, PER DIVERSITY CHANNEL

FIGURE 3-47

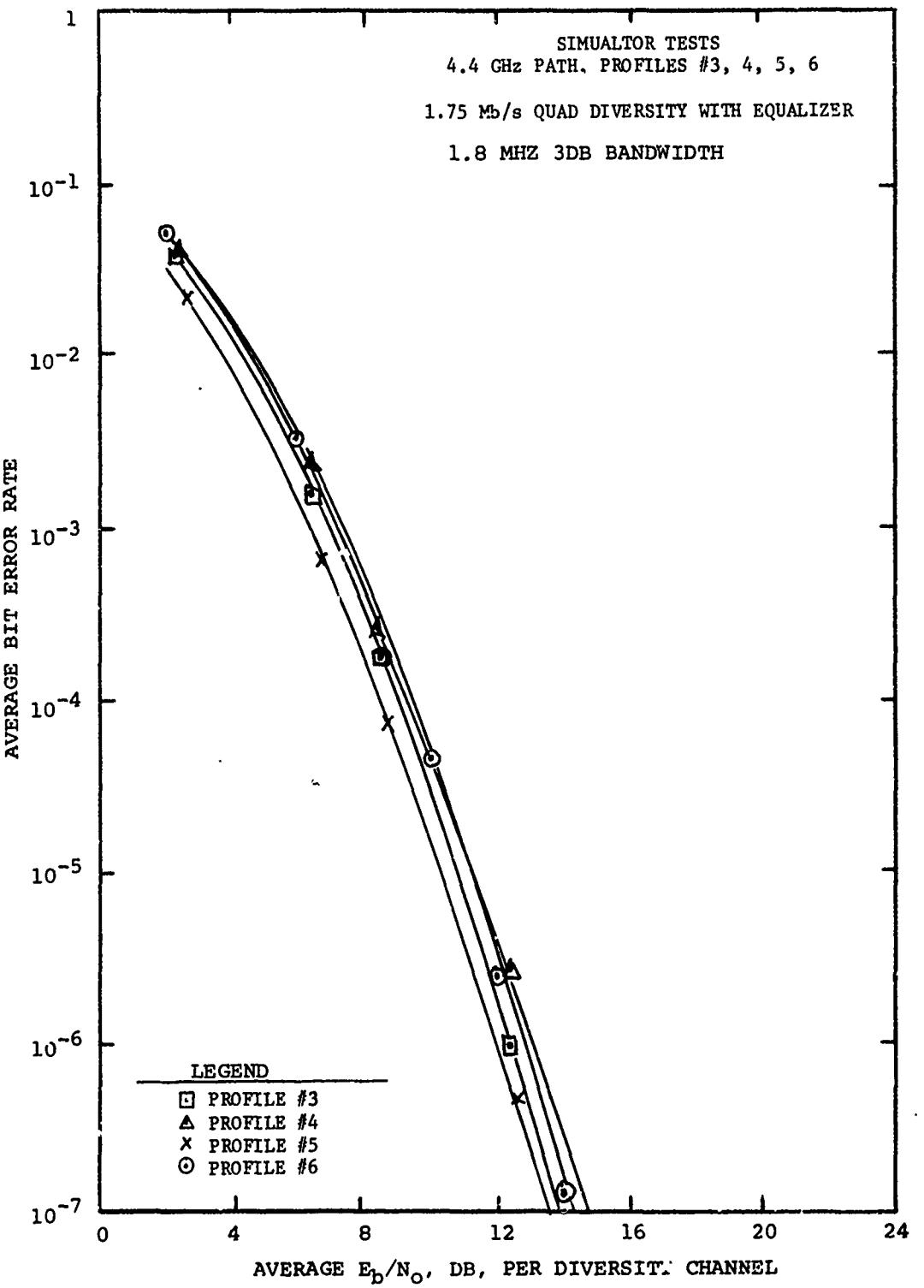
SIMUALTOR TESTS
4.4 GHz PATH, PROFILES #3, 4, 5, 6
1.75 Mb/s QUAD DIVERSITY WITH EQUALIZER
1.8 MHZ 3DB BANDWIDTH
AVERAGE BIT ERROR RATE
1
10^{-1}
10^{-2}
10^{-3}
10^{-4}
10^{-5}
10^{-6}
10^{-7}
LEGEND
PROFILE #3
PROFILE #4
PROFILE #5
PROFILE #6
0
4
8
12
16
20
24
AVERAGE E_b/N_o, DB, PER DIVERSITY CHANNEL

Tests 24, 25, 26 and 27 demonstrate the performance for 3.5 Mb/s quad diversity for profiles #3, #4, #5 and #6 with the DFE activated. These results are shown in Figure 3-48. For profiles #4 and #6 (the median profiles), there was no observable error rate floor, thus no improvement would be expected from the DFE. For profiles #3 and #5 (worst case paths), the DAR-IV exhibited error rate floors of 4×10^{-5} and 10^{-4} respectively. Here a significant improvement should have been obtained with the DFE activated but for the reasons outlined in Section 2 this was not the case.

Tests 28, 29, 30 and 31 in Figure 3-49 demonstrate the performance of the DAR-IV at 7 Mb/s for profiles #3, #4, #5 and #6 with the DFE activated. Profiles #3 and #5 (the two worst case profiles) exhibited relatively high error rate floors. The DFE operation here was further complicated by the timing errors due to the sensitivity of the highest error rate to severe intersymbol interference as described previously. The median profiles (profiles #4 and #6) yielded much lower irreducible error rates but once again the DFE provided little or no improvement in performance. As previously mentioned, improvement of the DAR-IV loop bandwidths is expected to lower the irreducible BER by about 2 to 4 orders of magnitude (doubling of the intrinsic diveristy as shown in the Math Model). Increasing the DAR-IV loop memory from its present 10 symbols to about 100 symbols and adding the DFE should lower the irreducible BER still another 2 to 3 orders of magnitude. With these improvements, the DAR-IV should provide no noticeable error floors above 10^{-7} even for the worst case multipath profiles of the AN/TRC-132 link at 7 Mb/s. A comprehensive set of performance predictions including the DFE are contained in the Math Model provided separately under this effort.

3.4 Conclusions on Simulator Testing

Both the tactical DAR-IV simulator test results of Section 3.2 and the DCS test results of Section 3.3 highlight the important benefit of intrinsic diversity in digital transmission on troposcatter channels. Intrinsic diversity was found to greatly lower the required signal strength to maintain a given average BER with even small amounts of multipath dispersion. The intrinsic diversity also plays an important part in preventing a high irreducible BER in the DAR-IV due to intersymbol interference caused by multipath propagation.

Figures 3-50 and 3-51 show some representative DAR-IV waveforms at 1.75 Mb/s for the median multipath (profile #2) of the AN/MRC-98 path (of Section 3.3.3). The upper trace is the received distorted signal and the lower trace is the DAR-IV integrate and dump filter output in non-diversity operation. Both figures are for the same multipath profile but represent different time "snap-shots". In Figure 3-50, the instantaneous multipath is such that the pulse is hardly distorted while in Figure 3-51, the received pulse is hardly recognizeable. The intrinsic

FIGURE 3-48

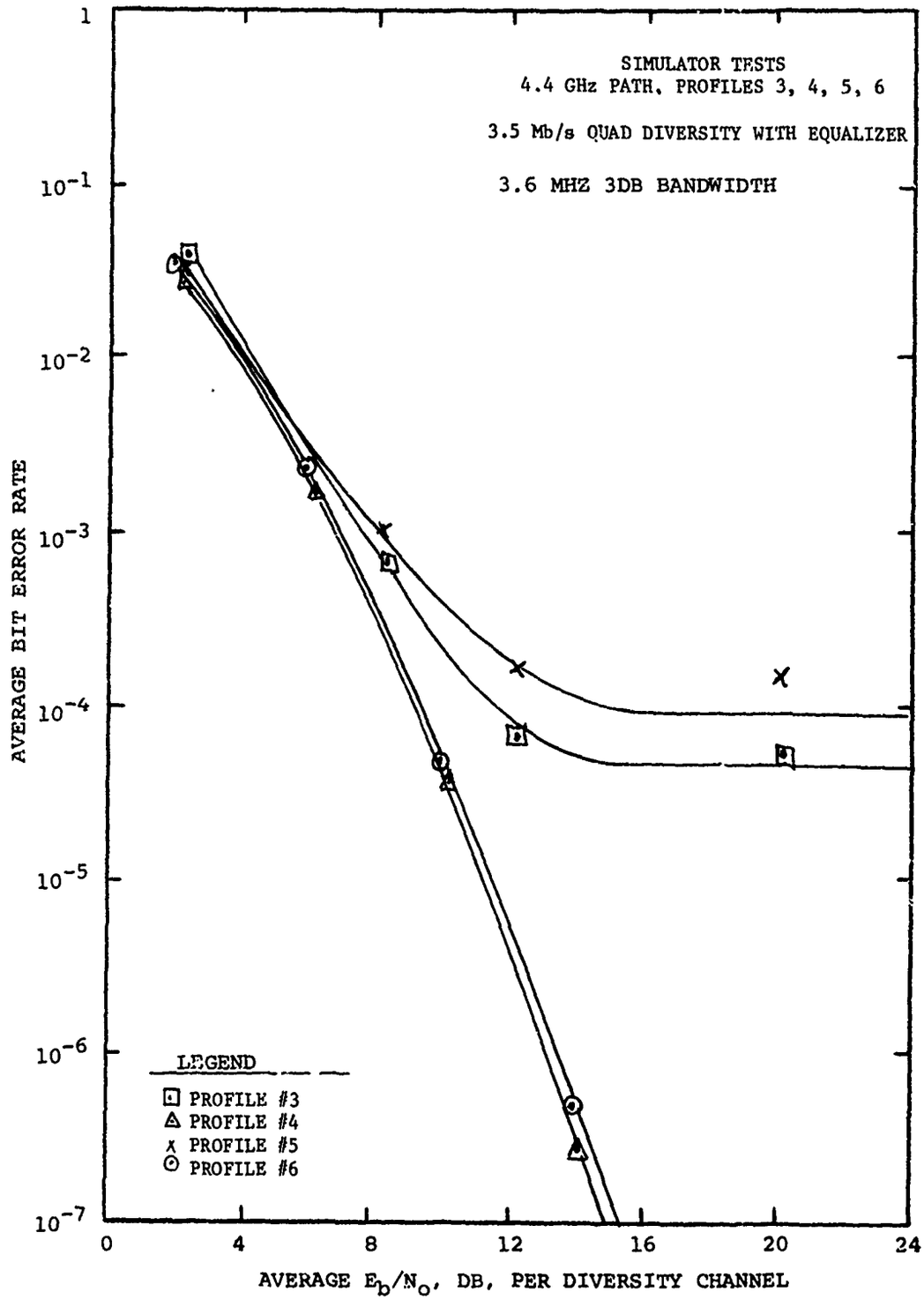
SIMULATOR TESTS
4.4 GHz PATH, PROFILES 3, 4, 5, 6
3.5 Mb/s QUAD DIVERSITY WITH EQUALIZER
3.6 MHZ 3DB BANDWIDTH
AVERAGE BIT ERROR RATE
1
10^{-1}
10^{-2}
10^{-3}
10^{-4}
10^{-5}
10^{-6}
10^{-7}
LEGEND
PROFILE #3
PROFILE #4
PROFILE #5
PROFILE #6
0
4
8
12
16
20
24
AVERAGE E_b/N_o, DB, PER DIVERSITY CHANNEL

FIGURE 3-49

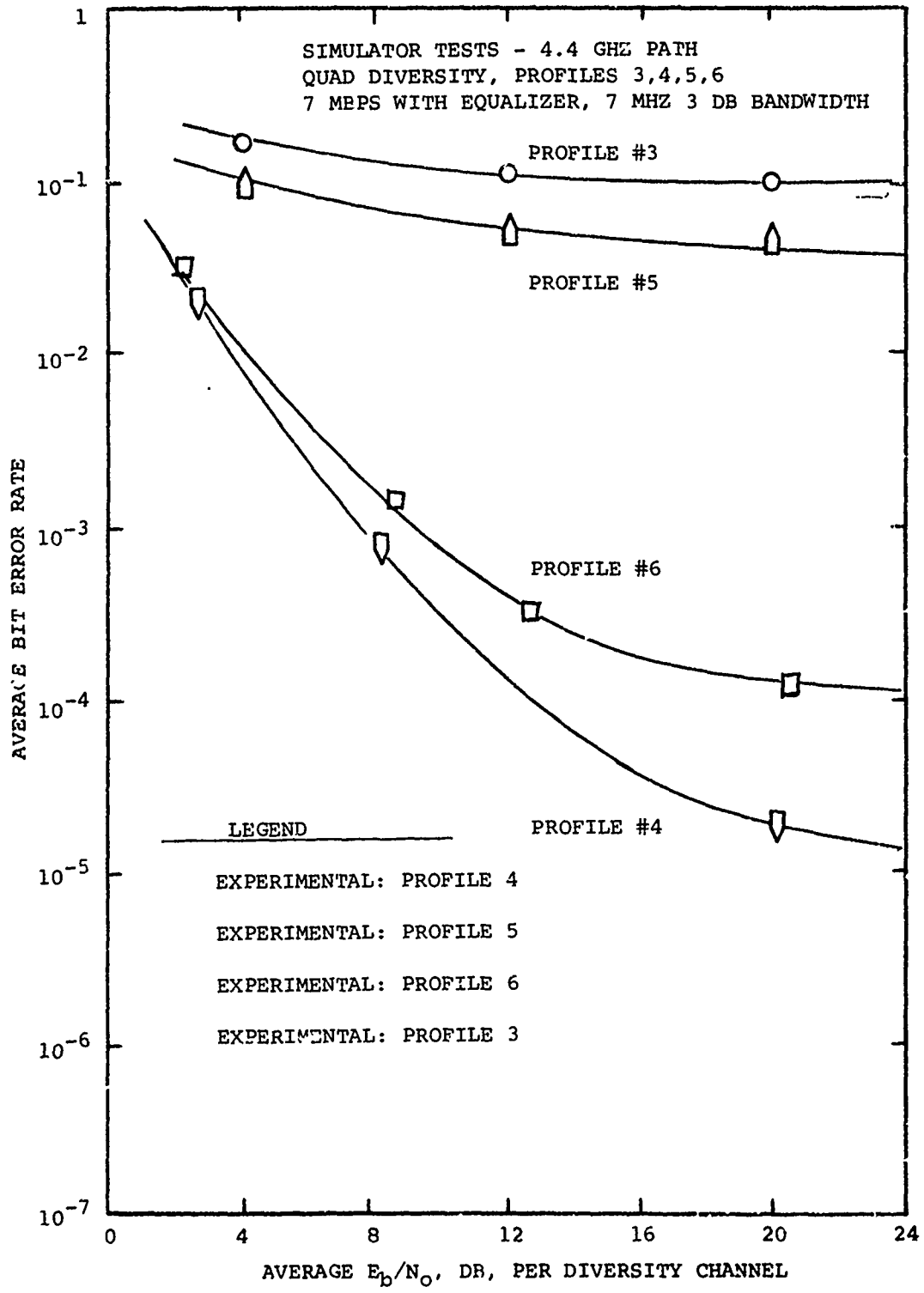
SIMULATOR TESTS - 4.4 GHZ PATH
QUAD DIVERSITY, PROFILES 3,4,5,6
7 MBPS WITH EQUALIZER, 7 MHZ 3 DB BANDWIDTH
PROFILE #3
PROFILE #5
PROFILE #6
PROFILE #4
LEGEND
EXPERIMENTAL: PROFILE 4
EXPERIMENTAL: PROFILE 5
EXPERIMENTAL: PROFILE 6
EXPERIMENTAL: PROFILE 3
AVERAGE BIT ERROR RATE
1
10^{-1}
10^{-2}
10^{-3}
10^{-4}
10^{-5}
10^{-6}
10^{-7}
0
4
8
12
16
20
24
AVERAGE E_b/N_o, DB, PER DIVERSITY CHANNEL

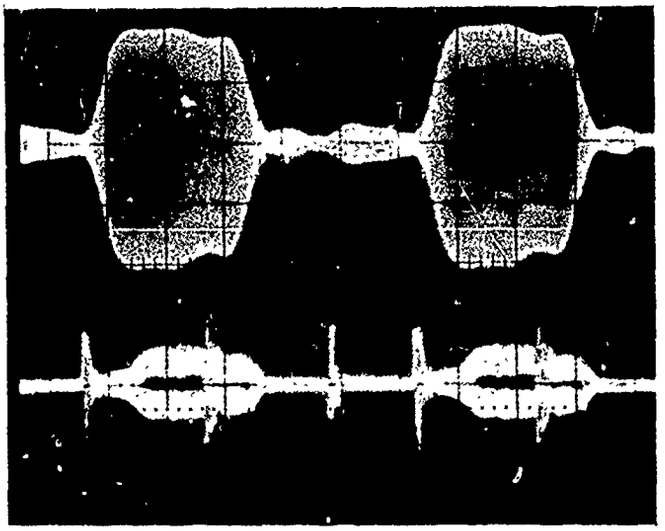

FIGURE 3-50

RECEIVED IF SIGNAL WITH
LOW DISTORTION AT 1.75 MBPS

PROFILE # 2

"EYE PATTERN" OF DAR

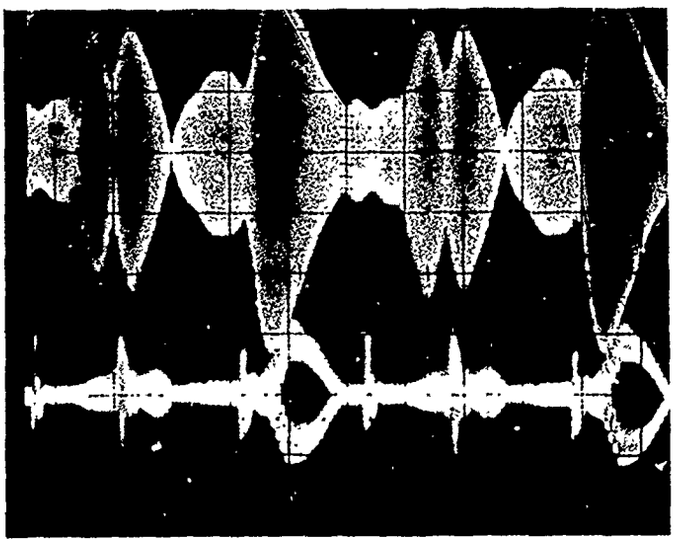

FIGURE 3-51

RECEIVED IF SIGNAL WITH
HIGH DISTORTION AT 1.75 MBP

PROFILE # 2

"EYE PATTERN" JF DAR

diversity mechanism is easily visualized from Figure 3-51 when it is realized that the various "sub-bursts" of the waveform are fading independently and must all fade simultaneously to produce a burst of errors.

Figures 3-52 and 3-53 show a similar set of snap-shots for 3.5 Mb/s operation with the same multipath profile as before. Again, Figure 3-52 shows a relatively undistorted pulse during an instant when the channel multipath structure resembled a single echo. Figure 3-53 shows the more common multipath condition for profile #2 with substantial overlap of adjacent pulses. The "double trace" effect shown in Figure 3-53 is the result of intersymbol interference which appears to be quite strong. To cause an irreducible BER, the intersymbol interference must be stronger than the main portion of the received pulse. Higher intrinsic diversity (more independently fading resolvable energy sub-bursts in the main segment of the received pulse) tends to counteract the effects of intersymbol interference in the same way it counteracts fading.

Figures 3-54 and 3-55 show the corresponding results for 7 Mb/s. In this case, a nearly non-distorted pulse was difficult to find, even for the moderate dispersion of multipath profile #2. Figure 3-55 shows the more common received signal which is subject to massive intersymbol interference. The fact that the DAR-IV can continue to function even with moderate 10^{-4} BER in the presence of such severe intersymbol interference indicates the power of an adaptive matched filter receiver and its intrinsic diversity benefits.

The DAR-IV experimental model displated excellent performance at 1.75 Mb/s and 3.5 Mb/s for most multipath profiles. At 7 Mb/s, the model tended to exhibit premature irreducible BER due to the suboptimum implementation as previously described. It is interesting to compare the performance outside of the irreducible BER region with theory to determine how well the DAR-IV acts as an adaptive matched filter.

Figure 3-56 shows the performance of an ideal CPSK modem for the orders of diversity indicated. In the DAR-IV, the diversity action is partially explicit as shown in Figure 3-56 and partly intrinsic. The effective order of diversity, N, for the DAR-IV can be described by the expression

$$N = M\ (1 + \alpha)$$

where M is the explicit order of diversity and α is a factor proportional to the intrinsic diversity (that is, proportional to the signal bandwidth times the multipath spread). The performance of an ideal DAR-IV with diversity N can be obtained from Figure 3-56 by using the curve for Nth order diversity with the E_b/N_o increased by the factor $(1 + \alpha)$.

FIGURE 3-52

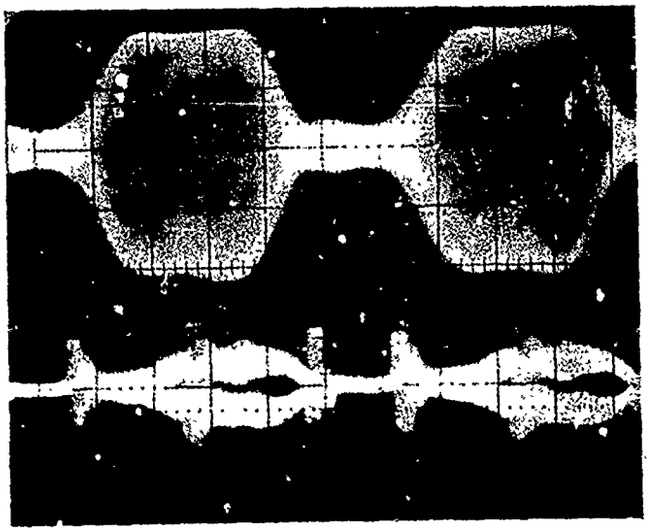

RECEIVED IF SIGNAL WITH
LOW DISTORTION AT 3.5 MBPS

PROFILE # 2

"EYE PATTERN" OF DAR

FIGURE 3-53

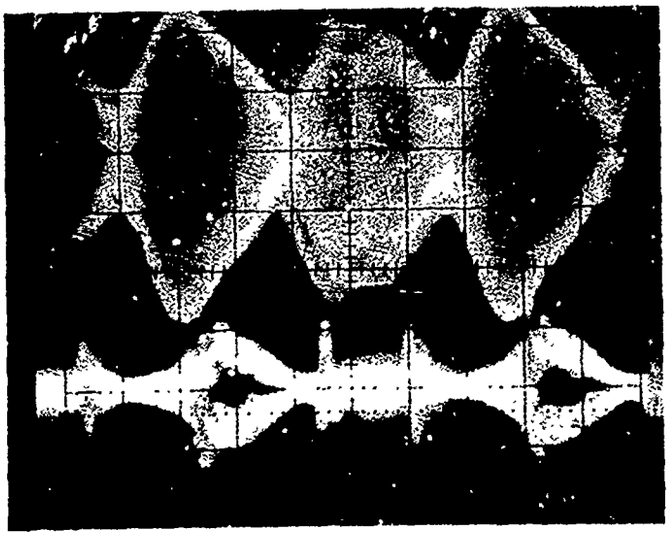

RECEIVED IF SIGNAL WITH
HIGH DISTORTION AT 3.5 MBPS

PROFILE # 2

"EYE PATTERN" OF DAR

FIGURE 3-54

RECEIVED IF SIGNAL WITH
LOW DISTORTION AT 7 MBPS

PROFILE # 2

"EYE PATTERN" OF DAR

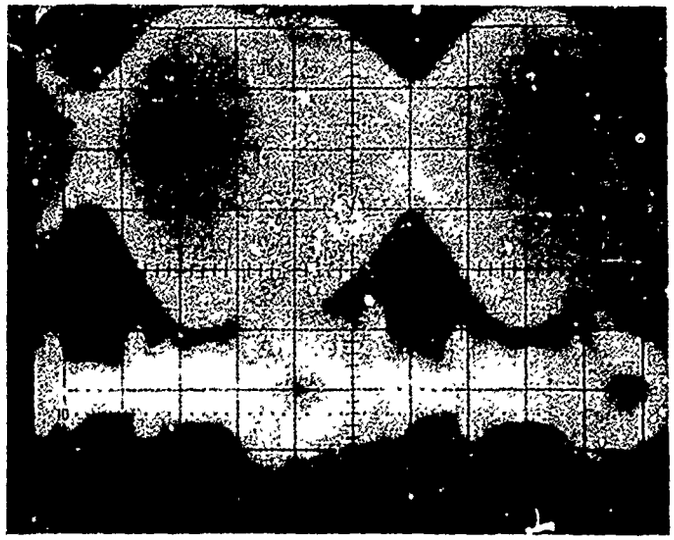

FIGURE 3-55

RECEIVED IF SIGNAL WITH
HIGH DISTORTION AT 7 MBPS

PROFILE # 2

"EYE PATTERN" OF DAR

FIGURE 3-56

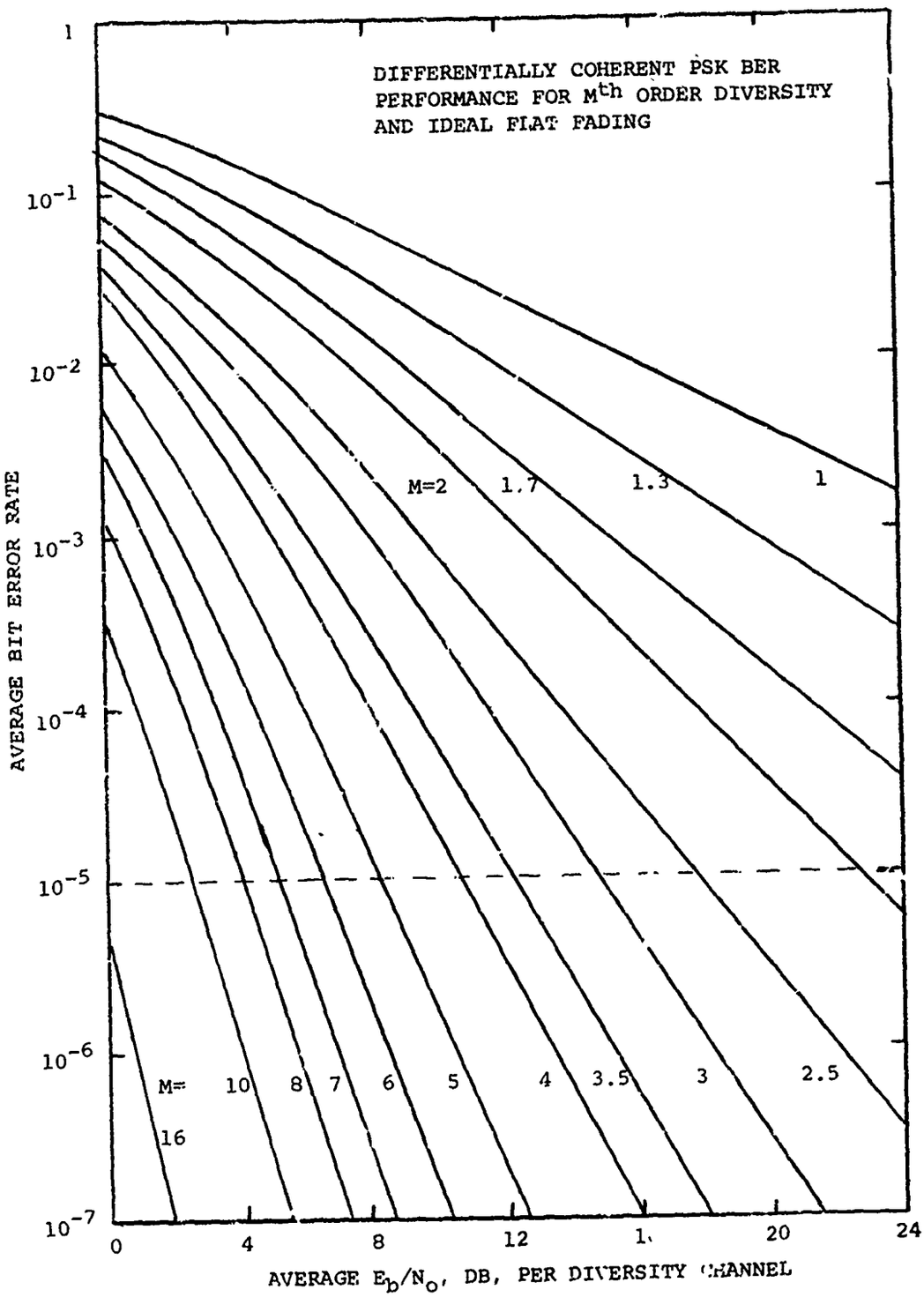
DIFFERENTIALLY COHERENT PSK BER
PERFORMANCE FOR Mth ORDER DIVERSITY
AND IDEAL FLAT FADING
AVERAGE BIT ERROR RATE
1
10-1
10-2
10-3
10-4
10-5
10-6
10-7
M=2
1.7
1.3
1
M=
16
10
8
7
6
5
4
3.5
3
2.5
0
4
8
12
1
20
24
AVERAGE Eb/No, DB, PER DIVERSITY CHANNEL

The results are shown in Figure 3-57 for both dual and quad explicit diversity. Here the E_b/N_o required for 10^{-5} BER is plotted against N (solid curves) and α (dashed curves). The curves show how the required E_b/N_o can be lowered at the effective order of diversity is increased (or as the multipath delay spread or signal bandwidths are increased).

An interesting phenomenon was observed if α is defined as $\alpha = 3.5\ \Delta W$ where Δ is the 2σ of the multipath spread and W is the 3 dB signal bandwidth. Figure 3-58 shows the dual diversity curve of Figure 3-57 plotted versus α. Also shown are the experimental dual diversity data points from Sections 3.2 and 3.3 with the implementation losses subtracted out. Note that with the above definition α, an almost perfect fit ($\pm$0.5 dB or less) between the experimental points and the theoretical curve results. A mathematic formula can be easily fitted to these results of the form:

$$E_b/N_o\ (10^{-5}) = \frac{16.8 + 7\ \alpha}{\alpha + 0.74}\ \text{dB}$$

to predict the required E_b/N_o required given a dual diversity channel, signal bandwidth W, and rms multipath dispersion, Δ.

Using the same definition of α, the quad diversity E_b/N_o requirements for 10^{-5} BER were also plotted versus α in Figure 3-59 and the theoretical curve of Figure 3-57 was also included. Again, excellent agreement between the measured results and the theoretical model is obtained. A simple mathematical expression can also be derived to predict the required E_b/N_o for 10^{-5} BER on a quad diversity channel of the form:

$$E_b/N_o\ (10^{-5}) = \frac{8.8 + 4\ \alpha}{\alpha + 0.83}\ \text{dB}$$

This expression and the previous one for dual diversity should greatly simplify the system designer's task in evaluating the performance of a digital adaptive matched filter modem on the troposcatter channel.

FIGURE 3-57

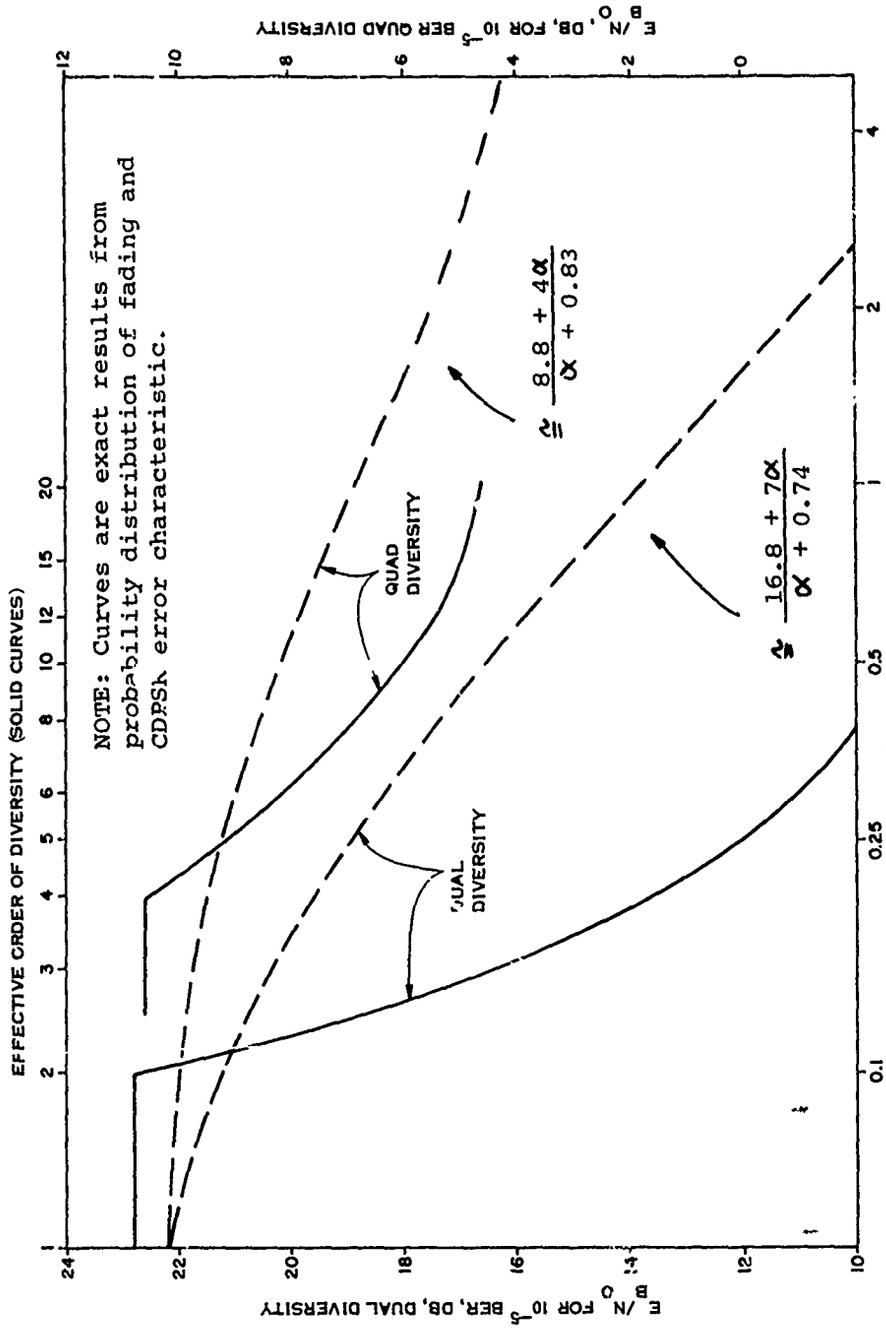

Figure 3-57 Theoretical Performance

FIGURE 3-58

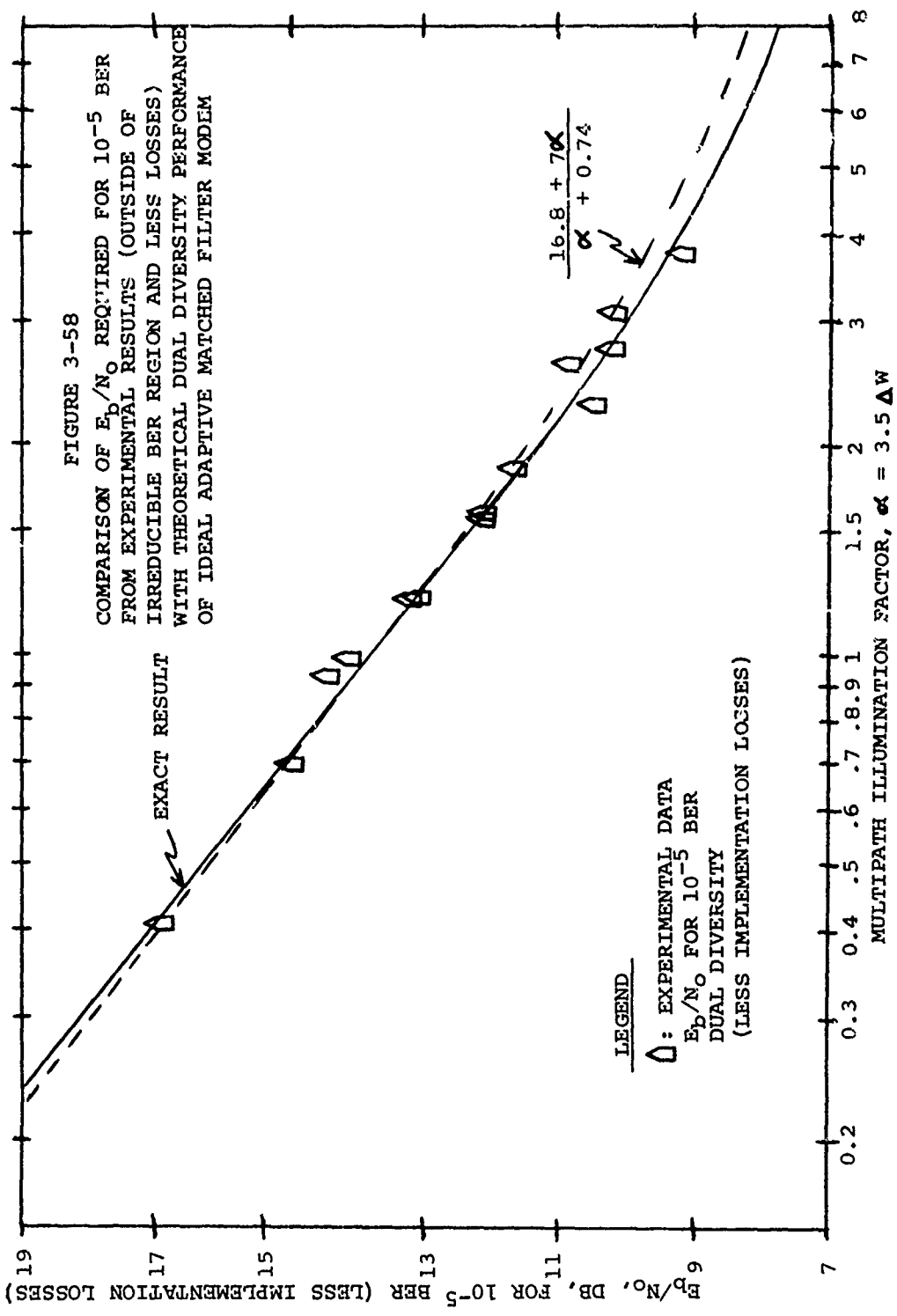
FIGURE 3-58
COMPARISON OF E_b/N_o REQUIRED FOR 10^{-5} BER FROM EXPERIMENTAL RESULTS (OUTSIDE OF IRREDUCIBLE BER REGION AND LESS LOSSES) WITH THEORETICAL DUAL DIVERSITY PERFORMANCE OF IDEAL ADAPTIVE MATCHED FILTER MODEM
EXACT RESULT
$\frac{16.8 + 7\alpha}{\alpha + 0.74}$
LEGEND
Δ: EXPERIMENTAL DATA
E_b/N_o FOR 10^{-5} BER
DUAL DIVERSITY
(LESS IMPLEMENTATION LOSSES)
E_b/N_o, DB, FOR 10^{-5} BER (LESS IMPLEMENTATION LOSSES)
MULTIPATH ILLUMINATION FACTOR, $\alpha = 3.5\Delta W$
7
9
11
13
15
17
19
0.2
0.3
0.4
.5
.6
.7
.8
.9
1
1.5
2
3
4
5
6
7
8

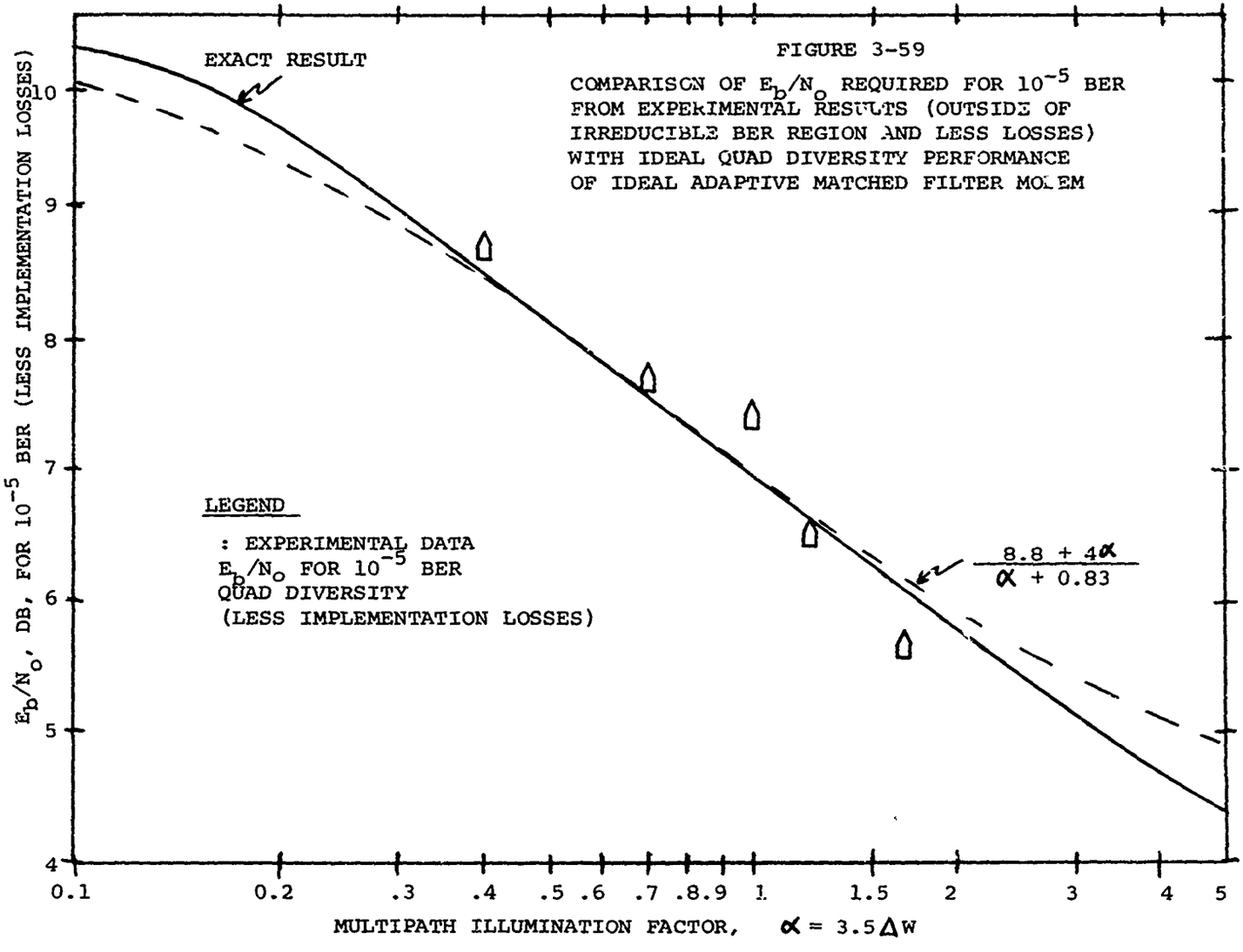

FIGURE 3-59

COMPARISON OF E_b/N_o REQUIRED FOR 10^{-5} BER FROM EXPERIMENTAL RESULTS (OUTSIDE OF IRREDUCIBLE BER REGION AND LESS LOSSES) WITH IDEAL QUAD DIVERSITY PERFORMANCE OF IDEAL ADAPTIVE MATCHED FILTER MODEM

4.0 OVER-THE-AIR TEST RESULTS

4.1 General

Over-the-air testing was conducted on the RADC Experimental Range. The DAR-IV was first interfaced with the AN/MRC-98, AN/TRC-132, and AN/TRC-97 at the Verona, New York, test site. Back-to-back testing was conducted at Verona to ensure proper operation of the deliverable equipment and also proper alignment of the receivers, filters and down-converter oscillators.

At the Youngstown site for the AN/MRC-98 and AN/MRC-132 or the Ontario Center Site for the AN/TRC-97, alignment of the transmitter chain was performed with special emphasis on the alignment of the filter characteristics of the up-converter, exciter, and power amplifier. The back-off of the power amplifier drive signal was also experimentally investigated to produce optimum operation as observed on an oscilloscope. The highest transmission level which yielded acceptable performance was then employed.

After system alignment, the modulator unit of the DAR-IV was then interfaced with the Youngstown or Ontario Center transmitter. The DAR-IV demodulator remained interfaced with the Verona receiver for the AN/MRC-98, AN/TRC-132 or AN/TRC-97 equipment. Various receiver configurations were tested including non, dual and quad path diversity.

Over-the-air tests were conducted on a daily basis for a period of approximately two weeks over each test path. Each consisted of a number of test runs of about five minutes duration. Each over-the-air test measured the following quantities for a set of system parameters:

Measurements/Test Interval

1.	Average BER	(Counter)*
2.	Error Histogram	(Raytheon Test Set/Printer)
3.	Average Orderwire TTNR	(Philco Test Set/Strip Chart)*
4.	RSL	(LEL/Strip Counter)*
5.	Average RSL	(Distribution Analyzer)*

* GFE

Tests on the 880 MHz AN/MRC-98 link included transmission at 1.75 and 3.5 Mb/s. For each data rate, the effect of non, dual and quad orders of explicit diversity were also examined.

Tests on the 4.4 GHz AN/TRC-132 link included all of the parameters tested on the 880 MHz link as described above. An additional objective of

the DAR-IV test program was inclusion of circuitry to demonstrate the feasibility of employing adaptive feedback equalization. This feedback equalization employs previous bit decisions to cancel intersymbol interference and thus extend the multipath range of the basic modem. Initial evaluation of this technique accomplished via the simulator tests described previously showed no significant improvement for the reasons outlined in Section 2, therefore, the decision feedback equalizer was not used during the over-the-air test period.

For these over-the-air tests, major emphasis was placed on the higher order diversity modes and higher data rates when signal levels permitted since these modes are more closely related to potential DCS system requirements. The sequence of testing and data accumulation was ordered accordingly to preclude any incomplete data for these modes in the event of unforeseen delays and/or problems, and to provide the capability to explore these modes more thoroughly.

Tests on the 4.4 to 5 GHz AN/TRC-97 link were performed at data rates of 1.75 and 3.5 Mb/s but concentrated on the lower data rate. In addition to the above measurements, five minute BER samples were interleaved with five minute intervals of RAKE multipath analysis. This RAKE data permits the comparison of over-the-air and simulator data on a 1 to 1 comparison.

Measured results for each system parameter of the over-the-air tests (i.e., data rate, order of diversity, etc.), is represented by a set of data curves. The major data curve plots average BER versus the median E_b/N_o of a single diversity channel. Based on the testing intervals allocated, each data curve represents 6 to 10 hours of performance accumulated over a one to two day period where possible. Individual BER measurements correspond to the average of five minute samples.

In addition to these average BER measurements, error histograms were also recorded for each nominal test run. The error histograms were measured automatically with test equipment constructed by Raytheon for this purpose. In a five minute test sample, the distribution of errors in approximately 100 ms intervals was recorded. This data may be used in developing system engineering criteria for the DCS application.

4.1.1 System Alignment and Calibration

The basic over-the-air system configuration is illustrated by Figures 4-1 and 4-2 for both the AN/MRC-98 or AN/TRC-132 equipments. For the AN/TRC-97, only half of the radio equipment shown in Figures 4-1 and 4-2 was employed (that is, one transmitter and two receivers) since this radio is capable of only dual space diversity operation.

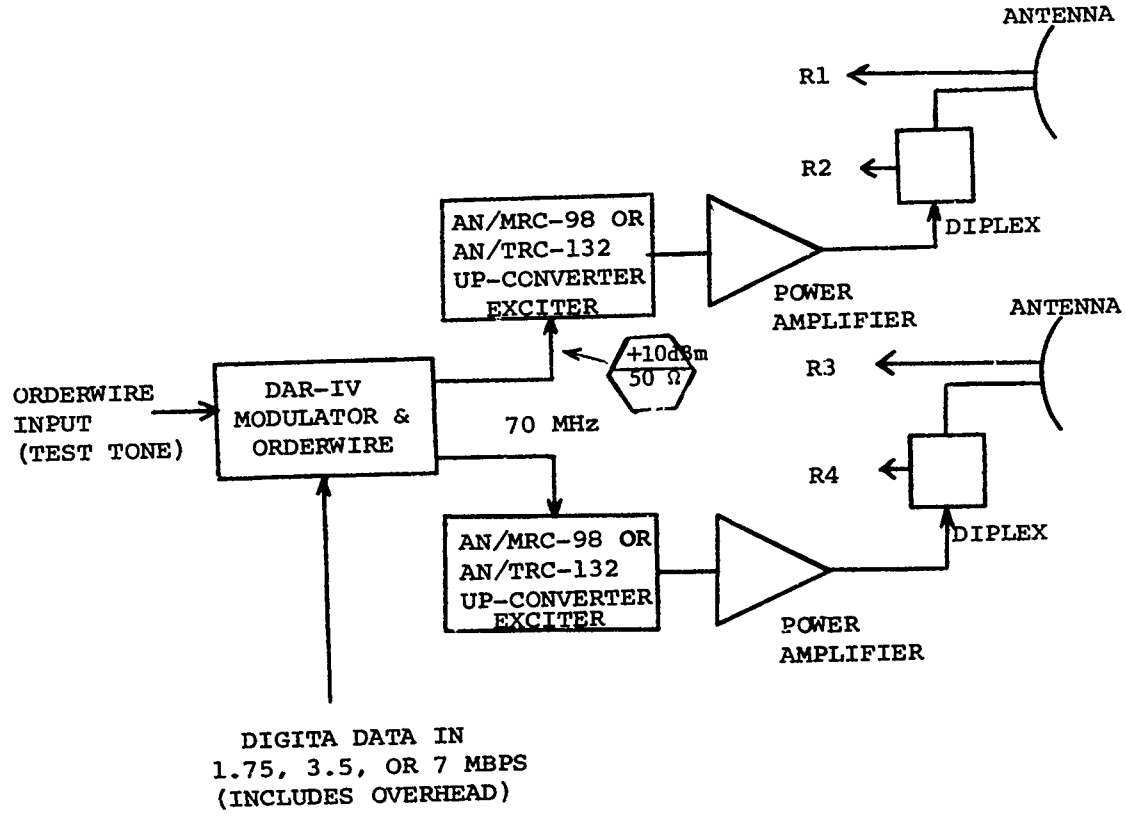

FIGURE 4-1 TYPICAL QUAD DIVERSITY TRANSMIT SITE CONFIGURATION (YOUNGSTOWN)

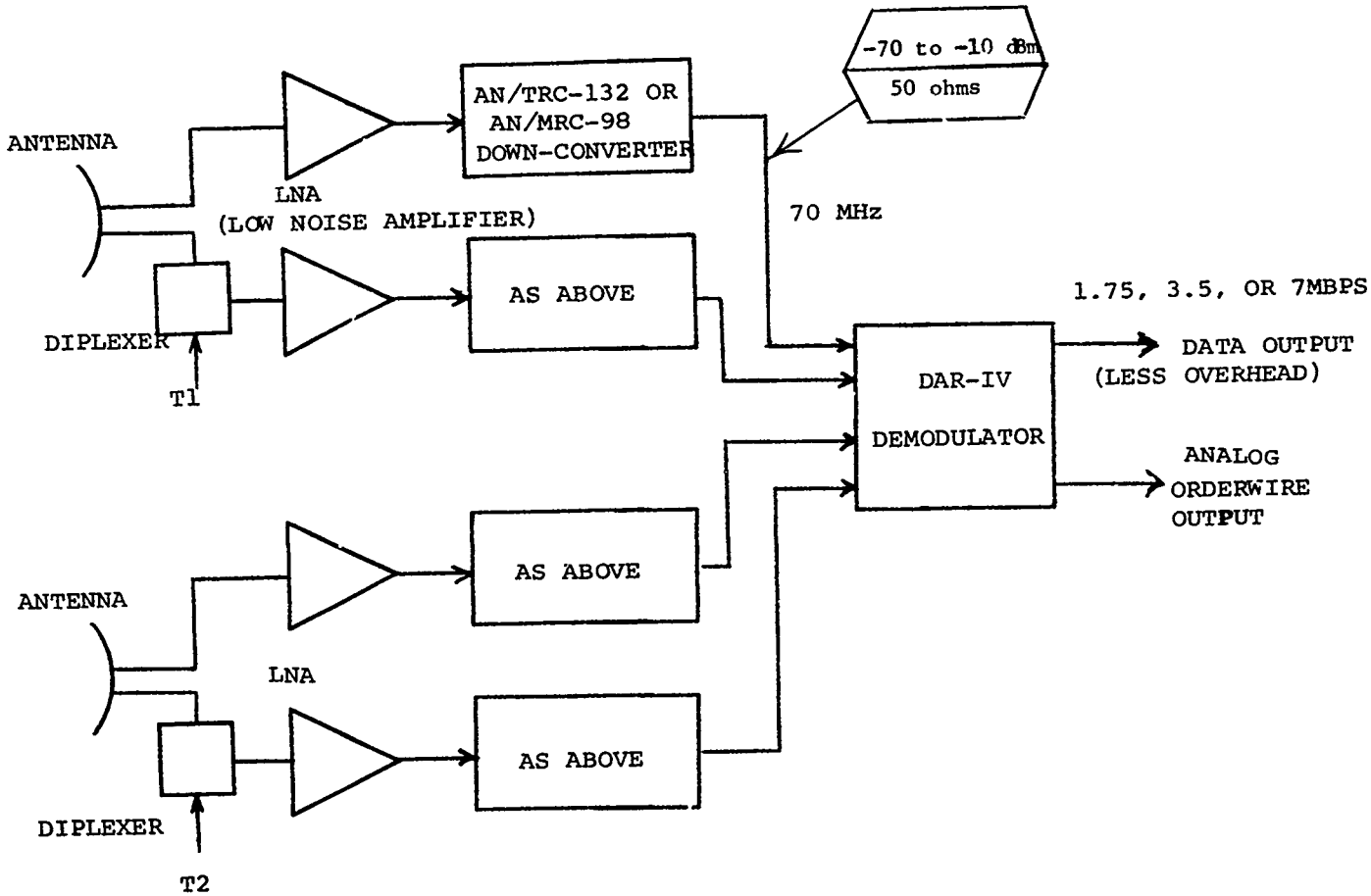

FIGURE 4-2 QUAD DIVERSITY RECEIVE SITE CONFIGURATION (VERONA)

As described in a preceding paragraph, system alignment and calibration consisted of alignment of the transmission chain and back-to-back functional validation at the receiving site.

At the Youngstown or Ontario Center transmitting site, with the assistance of RADC personnel, the transmitter chain was first aligned and special emphasis on the filter characteristics of the up-converter, exciter and power amplifier. The back-off of power amplifier drive signal was experimentally investigated to determine optimum performance by observation of the transmit waveform on an oscilloscope. The highest transmission level which yields acceptable performance was then employed.

Figures 4-3, 4-4 and 4-5 show the 1.75, 3.5 and 7 Mbps transmitter output waveforms, respectively, for the AN/MRC-98 transmitter at 880 MHz. The tuning procedure employed for all radios was to broad-band, stagger tune the radio to permit transmission at any of the three data rates without returning. This procedure greatly facilitated testing but resulted in some power inefficiency at the lower data rates. In the AN/MRC-98 klystron HPA, it was difficult to get a 7 MHz 3 dB bandwidth and some of the klystron gain was sacrificed. As a result, the respective average transmit powers were 2, 2, and 1 KW for 1.75, 3.5 and 7 Mbps, respectively. For the C-band radios, the 7 MHz bandwidth was more easily achieved and the average output power was about 5 dB below the klystron CW power level. Since the DAR-IV waveform has an inherent 3 dB loss with 50% duty cycle, the penalty paid for broadband tuning was approximately 2 dB. The output power loss can be reduced to nearly 3 dB at the lower data rates by reducing the tube bandwidth and increasing its drive. Since the peaks of the pulses can then saturate the amplifier.

At the Verona receiving site, the DAR-IV was first operated in a back-to-back configuration to verify proper functional performance. The DAR-IV receiving equipment was then interfaced with the appropriate receiver and the station test instrumentation per Figure 4-6. All test data was recorded on individual log sheets per Figure 4-7. Unfortunately, the log lin amplifiers used to measure Receiver Signal Level (RSL) had a simple envelope detector characteristic instead of a true square law or power meter characteristic. As a result, the RSL readings tend to fluctuate somewhat depending on the nature of the pulse distortion. Hence, individual point RSL readings are only accurate to within several dB but the average trend of the data points provides an accurate indication of performance.

Table 4.1 summarizes the test sequences which were performed over each link.

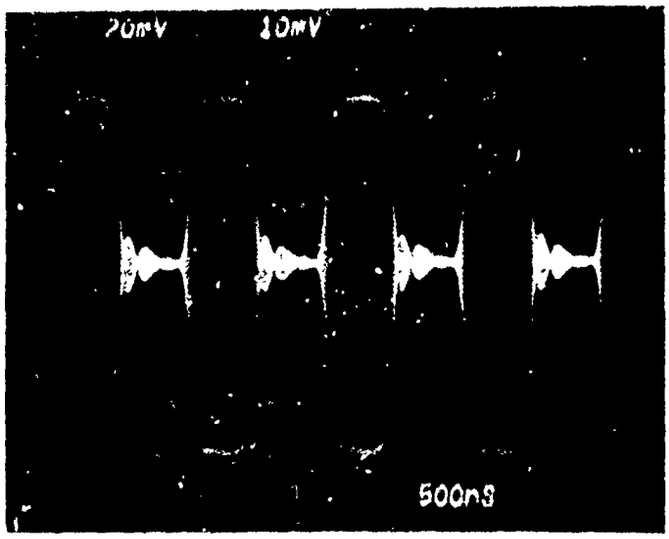

FIGURE 4-3

AN/MRC-98 TRANSMIT
WAVEFORM AT 1.75 MBPS

AVERAGE POWER= 2 KW

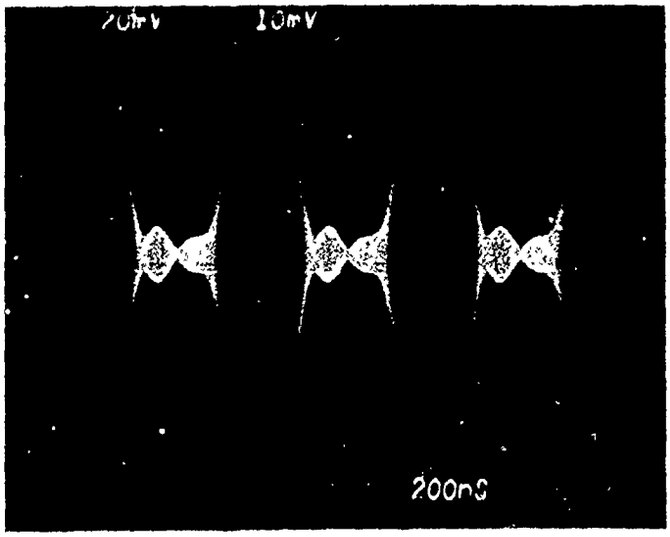

FIGURE 4-4

AN/MRC-98 TRANSMIT
WAVEFORM AT 3.5 MBPS

AVERAGE POWER = 2 KW

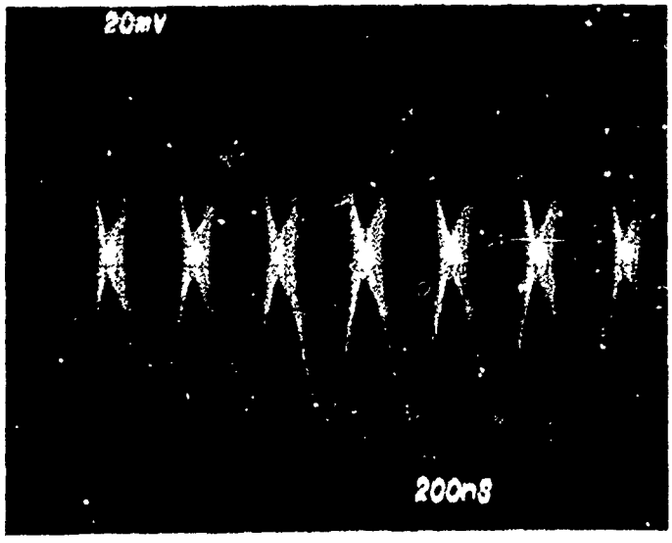

FIGURE 4-5

AN/MRC-98 TRANSMIT
WAVEFORM AT 7.0 MBPS

AVERAGE POWER = 1 KW

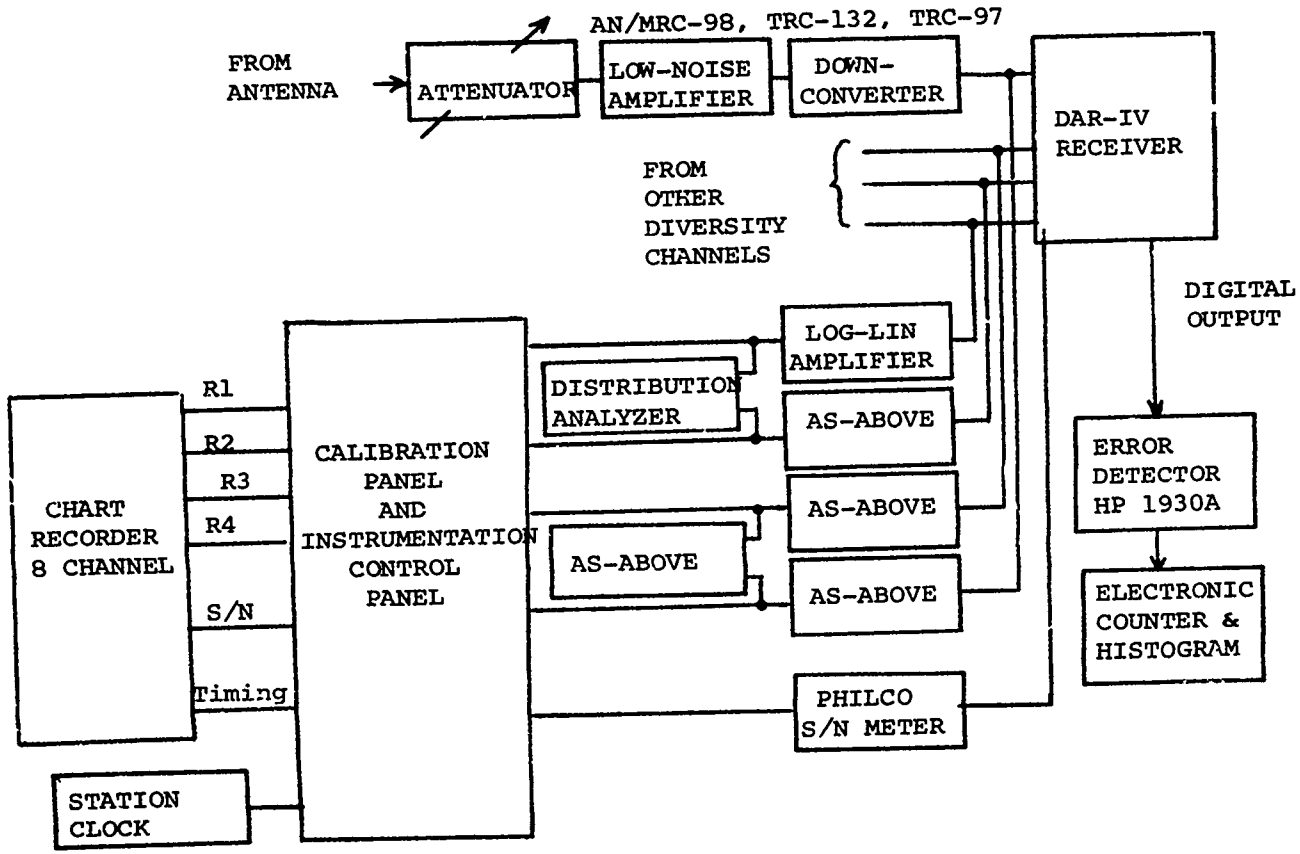

FIGURE 4-6 STATION TEST INSTRUMENTATION OVER-THE-AIR TEST BLOCK DIAGRAM

RADC TROPO DATA SHEET

DATE _____ RUN NO _____ TYPE TEST _____

PATH FROM _____ TO _____ OPERATOR _____

RUN TIME _____ LST TO _____ LST. TX PWR 882___ KW 907___ KW

ANT PADDING ALL RCVRS___ RX1 ___ RX2 ___ RX3 ___ RX4 ___

SLVT DATA _____ TOTAL COUNTS.

RX1	RX2	RX3	RX4

BIT ERROR RATE	TOTAL ERRORS	PE	S/N	MEDIAN
			1	RX 1
			2	RX 2
			3	RX 3
			4	RX 4
			AVE	AVE

COMMENTS

FIGURE 4-7

SAMPLE DATA SHEET FOR OVER THE AIR TESTS

TABLE 4.1

OVER-THE-AIR TEST CONFIGURATION

TEST NO.	DATA RATE Mb/s	DIVERSITY MODE
1	1.75	Non
2	1.75	Dual
3	1.75	Quad
4	3.5	Non
5	3.5	Dual
6	3.5	Quad
7	7.0	Non
8	7.0	Dual
9	7.0	Quad

4.2 AN/MRC-98 Over-the-Air Tests

4.2.1 General

This series of tests was performed over the Youngstown to Verona, New York, RADC test link during the month of February 1975. During this time frame allotted for the AN/MRC-98 over-the-air testing, the path conditions were such that during most of the operating time the received signal levels were extremely low and in many instances unusable. This, together with the large delay spreads encountered, prevented successful 7 Mb/s performance measurements. In addition to this, an unfortunate circumstance arose when, during a severe winter storm, one of the AN/MRC-98 antennas was upset by high winds. This required reguying the antenna as well as a major alignment of the all antennas. These circumstances resulted in a smaller amount of time for actual data recording that was originally planned.

4.2.2 AN/MRC-98 Performance at 1.75 Mb/s

The over-the-air results for 1.75 Mb/s non, dual and quad diversity are shown in Figures 4-8, 4-9 and 4-10 respectively. This data was taken for the digital transmission only, that is, no analog FM was being transmitted.

Although the data is sparse due to low signal levels, one can see the general outline of the performance curve for 1.75 Mb/s non diversity in Figure 4-8. Referring to Figure 4-9, the improvement gained by going to dual explicit diversity becomes readily apparent. Also shown on Figure 4-8 is the ideal DAR-IV performance (with 3 dB implementation loss)

FIGURE 4-8

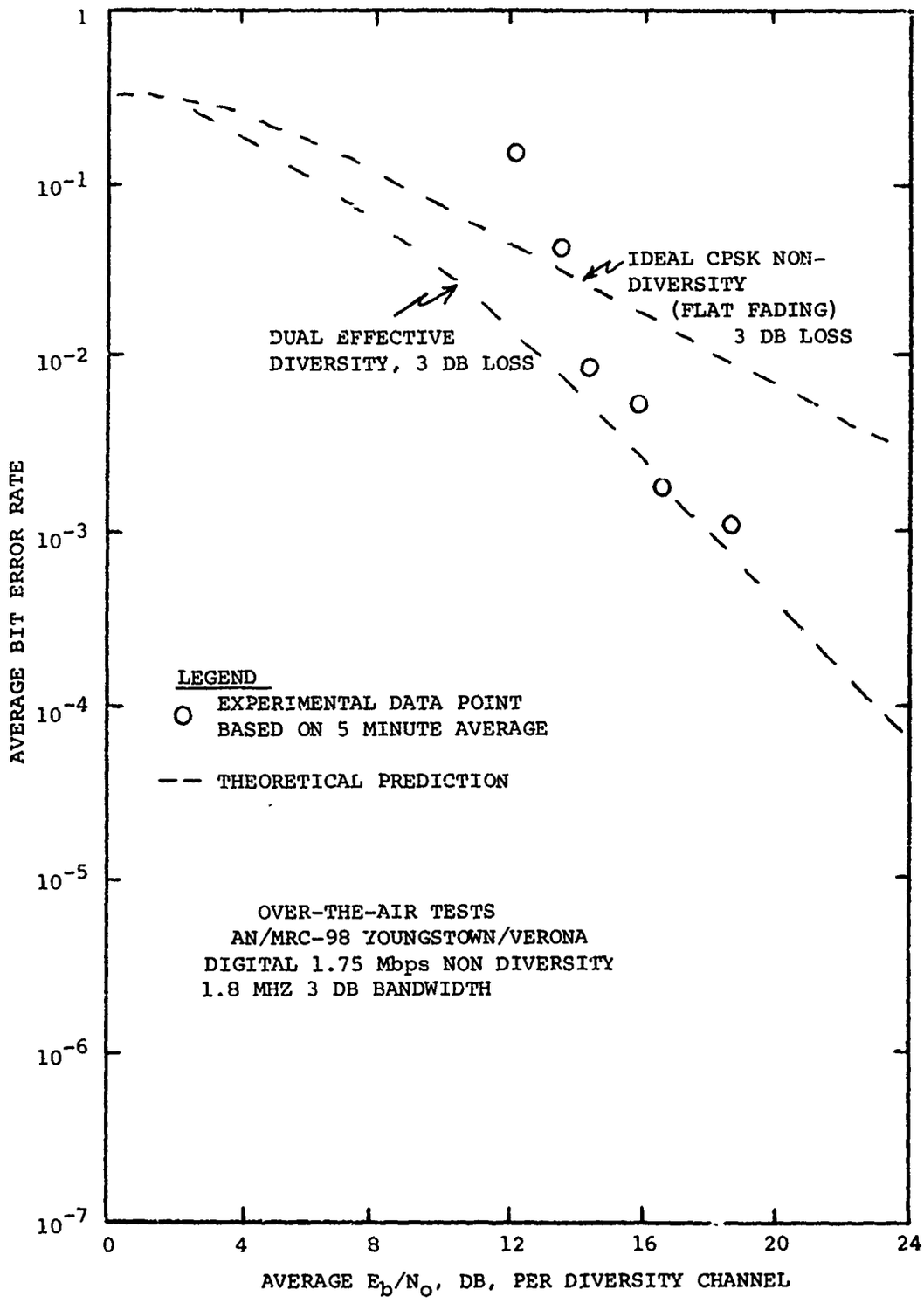
1
10^{-1}
10^{-2}
10^{-3}
10^{-4}
10^{-5}
10^{-6}
10^{-7}
AVERAGE BIT ERROR RATE
IDEAL CPSK NON-DIVERSITY (FLAT FADING) 3 DB LOSS
DUAL EFFECTIVE DIVERSITY, 3 DB LOSS
LEGEND
EXPERIMENTAL DATA POINT BASED ON 5 MINUTE AVERAGE
THEORETICAL PREDICTION
OVER-THE-AIR TESTS
AN/MRC-98 YOUNGSTOWN/VERONA
DIGITAL 1.75 Mbps NON DIVERSITY
1.8 MHZ 3 DB BANDWIDTH
0
4
8
12
16
20
24
AVERAGE E_b/N_o, DB, PER DIVERSITY CHANNEL

FIGURE 4-9

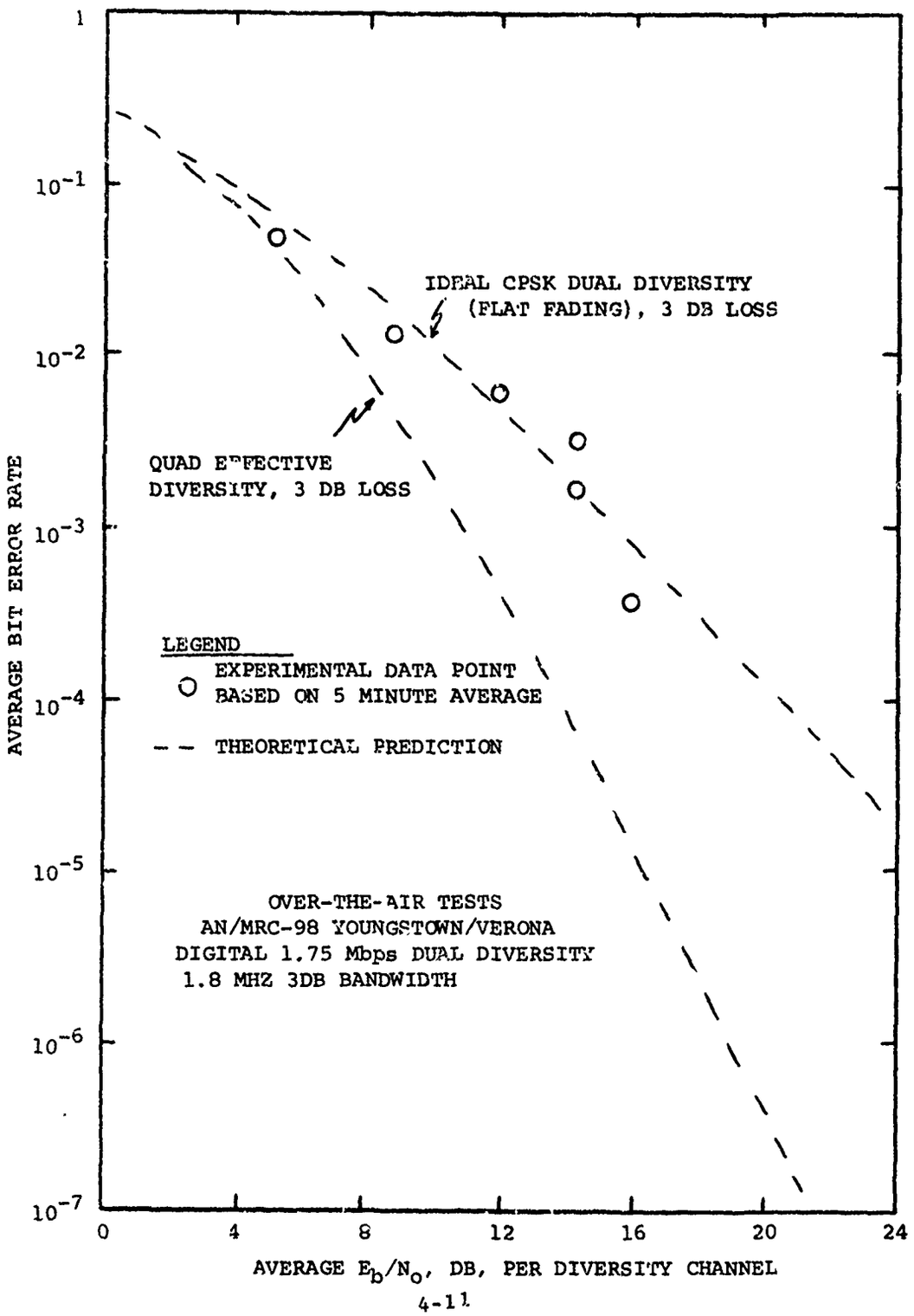
1
10^{-1}
10^{-2}
10^{-3}
10^{-4}
10^{-5}
10^{-6}
10^{-7}
AVERAGE BIT ERROR RATE
IDEAL CPSK DUAL DIVERSITY
(FLAT FADING), 3 DB LOSS
QUAD EFFECTIVE
DIVERSITY, 3 DB LOSS
LEGEND
EXPERIMENTAL DATA POINT
BASED ON 5 MINUTE AVERAGE
THEORETICAL PREDICTION
OVER-THE-AIR TESTS
AN/MRC-98 YOUNGSTOWN/VERONA
DIGITAL 1.75 Mbps DUAL DIVERSITY
1.8 MHZ 3DB BANDWIDTH
0
4
8
12
16
20
24
AVERAGE E_b/N_o, DB, PER DIVERSITY CHANNEL

FIGURE 4-10

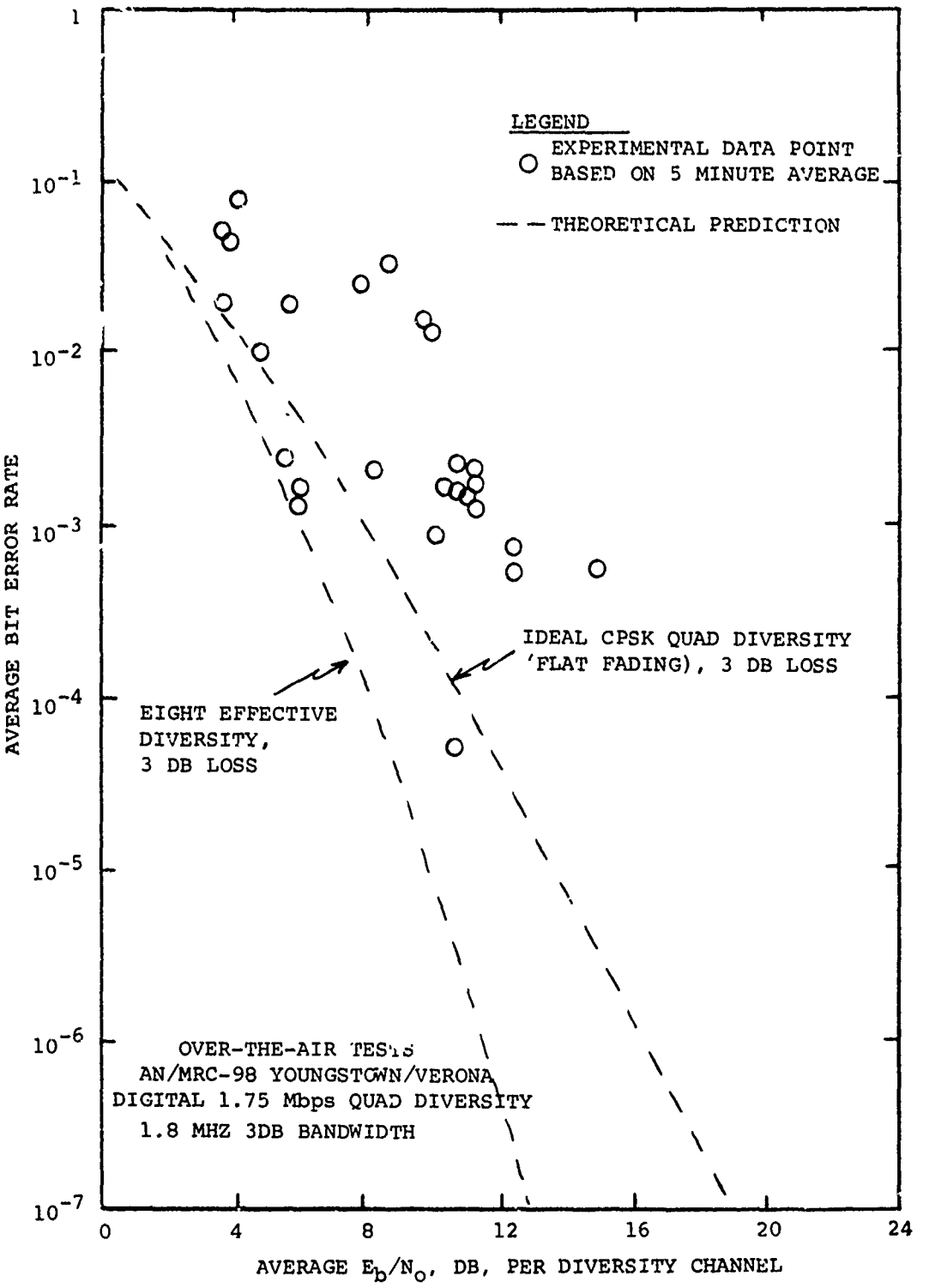
LEGEND
EXPERIMENTAL DATA POINT BASED ON 5 MINUTE AVERAGE
THEORETICAL PREDICTION
IDEAL CPSK QUAD DIVERSITY 'FLAT FADING), 3 DB LOSS
EIGHT EFFECTIVE DIVERSITY, 3 DB LOSS
OVER-THE-AIR TESTS
AN/MRC-98 YOUNGSTOWN/VERONA
DIGITAL 1.75 Mbps QUAD DIVERSITY
1.8 MHZ 3DB BANDWIDTH
AVERAGE BIT ERROR RATE
1
10^{-1}
10^{-2}
10^{-3}
10^{-4}
10^{-5}
10^{-6}
10^{-7}
0
4
8
12
16
20
24
AVERAGE E_b/N_o, DB, PER DIVERSITY CHANNEL

for non explicit diversity and also for dual effective diversity (non explicit with dual intrinsic). The data points are generally in good agreement with theory and show some implicit diversity gain. An exact comparison with the channel simulator results is not meaningful since the multipath spread corresponding to each measured point is not known. Similar conclusions can also be drawn for the dual diversity results of Figure 4-9.

Figure 4-10 shows a good scatter plot of the quad diversity performance of the DAR-IV for 1.75 Mb/s. Once again, the improvement due to the higher order of diversity becomes apparent when these results are compared with the preceding figures. The scattering of the data indicates the effects of different delay spreads for the same received signal level yielding various amounts of implicit diversity. Note that the data points tend to lie several dB to the right of the ideal dual diversity curve. The reason for this apparent extra implementation loss is probably due to the wide difference in per channel median RSL values for the AN/MRC-98. This effect results in some loss of diversity gain as described in the following section.

4.2.3 AN/MRC-98 Performance at 3.5 Mb/s

The DAR-IV performance at 3.5 Mb/s for non, dual and quad diversity is shown in Figures 4-11, 4-12 and 4-13 respectively. These results are also for the digital transmission mode only as described previously.

Figure 4-11 shows the non-diversity 3.5 Mb/s performance of the DAR-IV. The scatter of the points shows the results of large variations in the delay spread in terms of the amount of intrinsic diversity gain. Comparing Figure 4-12 to Figure 4-11, one can see the significant improvement gained by the added order of explicit diversity. The data points show a general outline of the performance curve for 3.5 Mb/s dual diversity covering the range of almost 10^{-1} to 10^{-6}.

Figure 4-13 shows the quad diversity performance of the DAR-IV. Comparing this with Figure 4-12 the improvement due to the higher order of diversity may be readily seen. These points give a good indication of the quad diversity performance curve. Data points cover error rates ranging from 10^{-1} to 10^{-7}. Note the large spread of the data points at the lower signal to noise ratios. This scattering is due to variations in the delay spread (the variations are larger at higher path losses) and also due to the fact that the four receivers had appreciably different received signal levels. At very low signal levels, the weaker two receivers would be below threshold of the DAR-IV frequently, hence, reducing the real explicit order of diversity. This accounts for the cluster of points at low SNR that appear to be above the nominal performance curve.

FIGURE 4-11

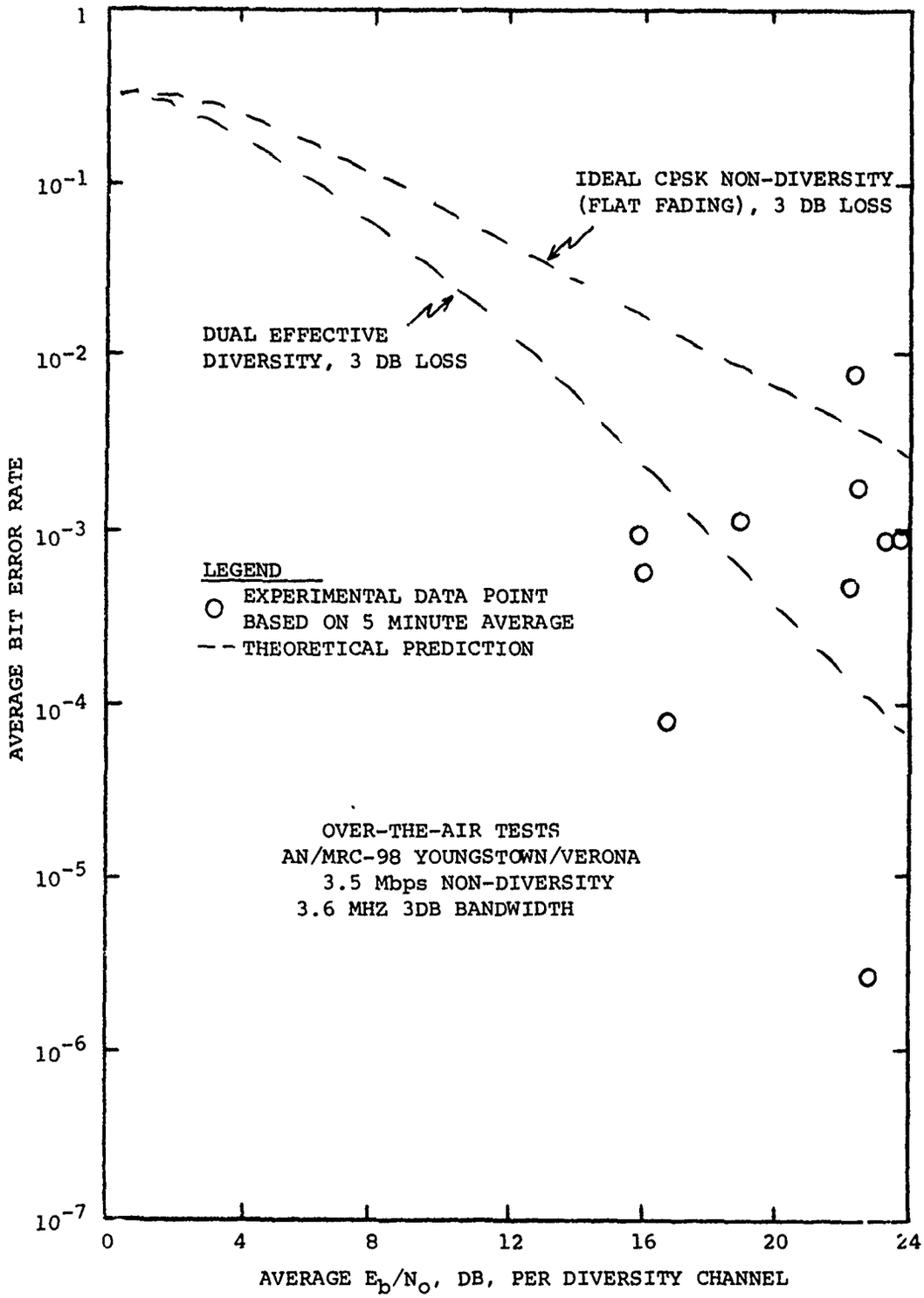
1
10^{-1}
10^{-2}
10^{-3}
10^{-4}
10^{-5}
10^{-6}
10^{-7}
AVERAGE BIT ERROR RATE
IDEAL CPSK NON-DIVERSITY
(FLAT FADING), 3 DB LOSS
DUAL EFFECTIVE
DIVERSITY, 3 DB LOSS
LEGEND
EXPERIMENTAL DATA POINT
BASED ON 5 MINUTE AVERAGE
THEORETICAL PREDICTION
OVER-THE-AIR TESTS
AN/MRC-98 YOUNGSTOWN/VERONA
3.5 Mbps NON-DIVERSITY
3.6 MHZ 3DB BANDWIDTH
0
4
8
12
16
20
24
AVERAGE E_b/N_o, DB, PER DIVERSITY CHANNEL

FIGURE 4-12

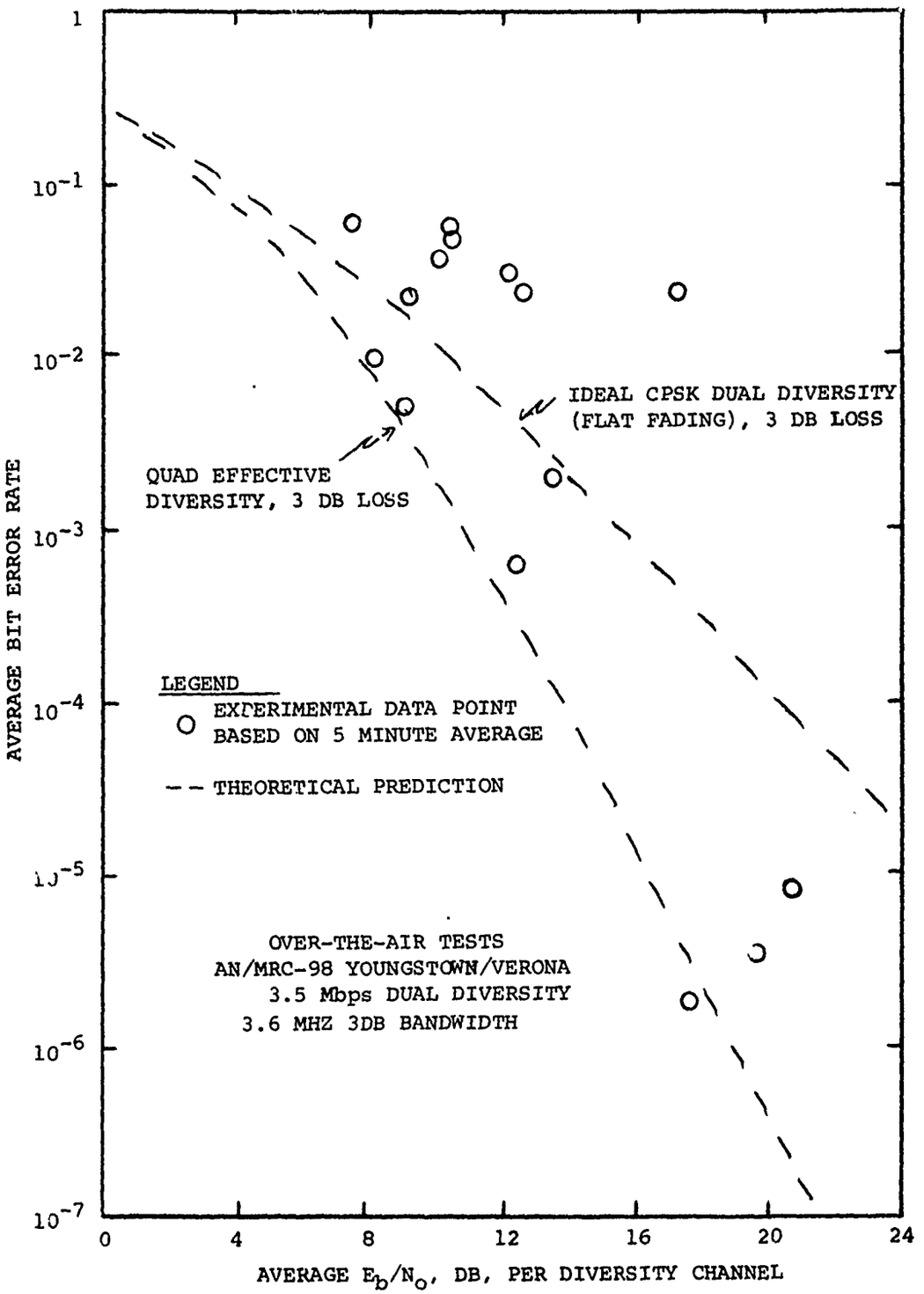
1
10^{-1}
10^{-2}
10^{-3}
10^{-4}
10^{-5}
10^{-6}
10^{-7}
AVERAGE BIT ERROR RATE
0
4
8
12
16
20
24
AVERAGE E_b/N_o, DB, PER DIVERSITY CHANNEL
IDEAL CPSK DUAL DIVERSITY (FLAT FADING), 3 DB LOSS
QUAD EFFECTIVE DIVERSITY, 3 DB LOSS
LEGEND
EXPERIMENTAL DATA POINT BASED ON 5 MINUTE AVERAGE
THEORETICAL PREDICTION
OVER-THE-AIR TESTS
AN/MRC-98 YOUNGSTOWN/VERONA
3.5 Mbps DUAL DIVERSITY
3.6 MHZ 3DB BANDWIDTH

FIGURE 4-13

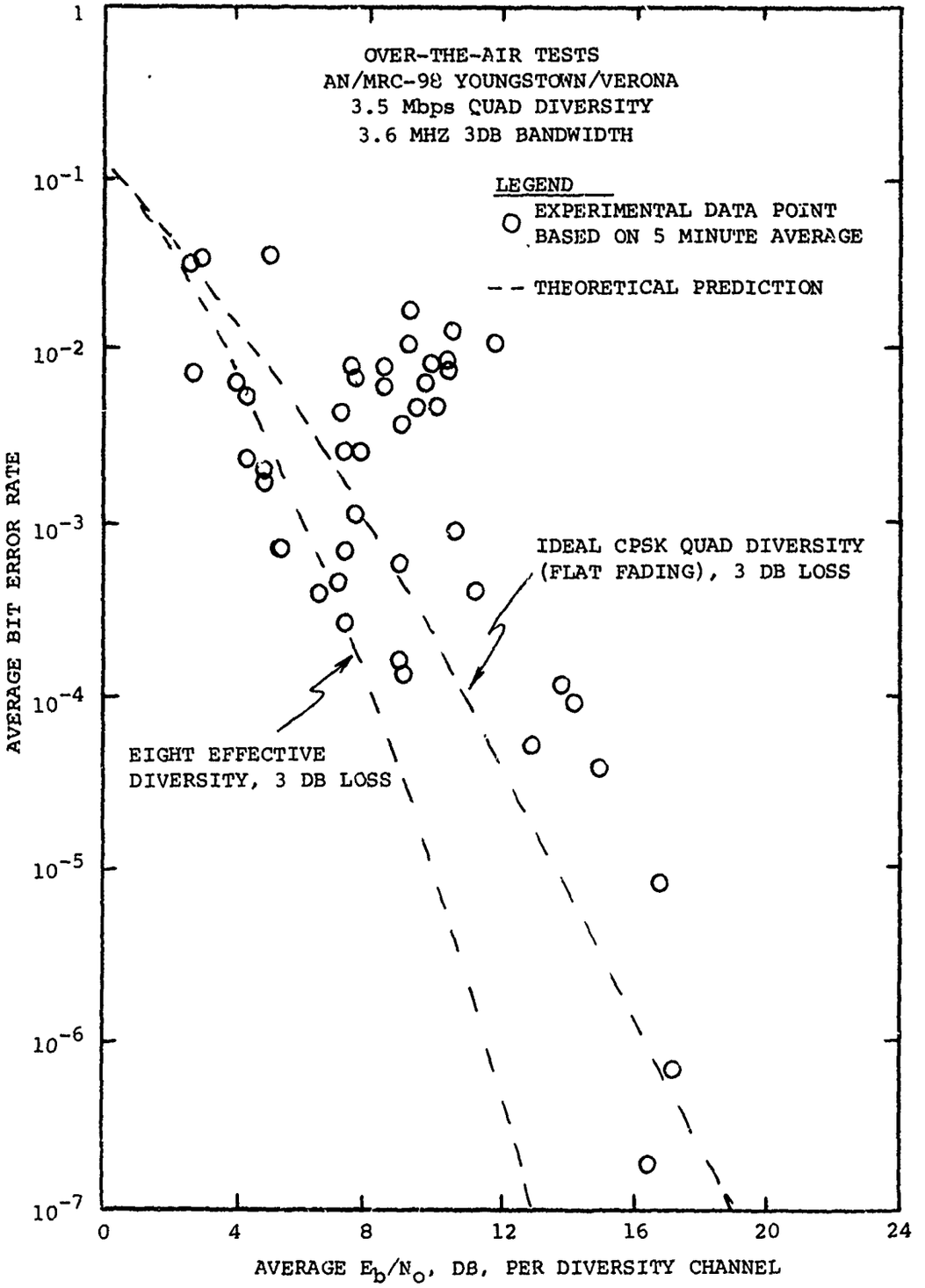
OVER-THE-AIR TESTS
AN/MRC-98 YOUNGSTOWN/VERONA
3.5 Mbps QUAD DIVERSITY
3.6 MHZ 3DB BANDWIDTH
LEGEND
EXPERIMENTAL DATA POINT
BASED ON 5 MINUTE AVERAGE
THEORETICAL PREDICTION
IDEAL CPSK QUAD DIVERSITY
(FLAT FADING), 3 DB LOSS
EIGHT EFFECTIVE
DIVERSITY, 3 DB LOSS
AVERAGE BIT ERROR RATE
1
10^{-1}
10^{-2}
10^{-3}
10^{-4}
10^{-5}
10^{-6}
10^{-7}
0
4
8
12
16
20
24
AVERAGE E_b/N_o, DB, PER DIVERSITY CHANNEL

As mentioned previously, due to the low average received signal levels and the large delay spread of the multipath, a successful measure of the 7 Mb/s data performance was not possible. This can be seen in Figures 4-14 and 4-15. Figure 4-14 is a bar graph of the percentage of time the received signal was equal to a given level. This data was compiled during the actual over-the-air testing concurrent with each data point shown in Figures 4-8 through 4-13. Examination of Figure 4-14 shows that the statistical mean for each channel in received level is

Channel 1 -96 dBm
Channel 2 -100 dBm
Channel 3 -98 dBm
Channel 4 -94 dBm

It is clear that Channels 2 and 3 are considerably weaker than Channels 1 and 4 with Channel 4 being the best channel over all. It can also be seen that the percentages of time that the RSL exceeded the mean were quite small. This can be seen more clearly by referring to Figure 4-15 which shows the probability that the received signal exceeded various signal to noise ratios for each of the four receivers. Here, it is evident that Channels 2 and 3 are weaker than Channels 1 and 4. In fact, Channel 2 had only an 80% probability of exceeding 0.5 dB E_b/N_o. The result of these variations in signal levels is that the full benefit of the higher orders of diversity is not realized and consequently the full potential of the DAR-IV was not utilized. It is believed that these differences in level were equipment related such as due to antenna misalignment or feed misalignment. However, the severe weather and high winds during the test period made verification of this factor difficult.

4.3 AN/TRC-132 Over-the-Air Results

4.3.1 General

This series of tests was performed over the Youngstown to Verona RADC Experimental Tropo path. The power amplifiers were adjusted for optimum performance at all data rates. This configuration yielded about 1.5 KW average power output or 3 KW peak power output. The tubes were broadbanded to provide a 10 MHz 3 dB bandwidth. The AN/TRC-132 receivers had a very narrow IF bandwidth of approximately 3 or 4 MHz. These were subsequently broadbanded to provide a 20 MHz 1 dB IF bandwidth at 70 MHz. About midway through the test period it was discovered that one of the oscillators in the frequency synthesizer portion of the AN/TRC-132 was randomly breaking lock. This would cause large error bursts independent of the channel characteristics and even for strong received signal level. Since the DAR-IV and receiving equipment were in a physically remote location relative to the recording instrumentation, it was not always

FIGURE 4-14

RECEIVED SIGNAL LEVEL HISTOGRAM
3.5 Mbps QUAD DIVERSITY OVER-THE-AIR
FEBRUARY 1975

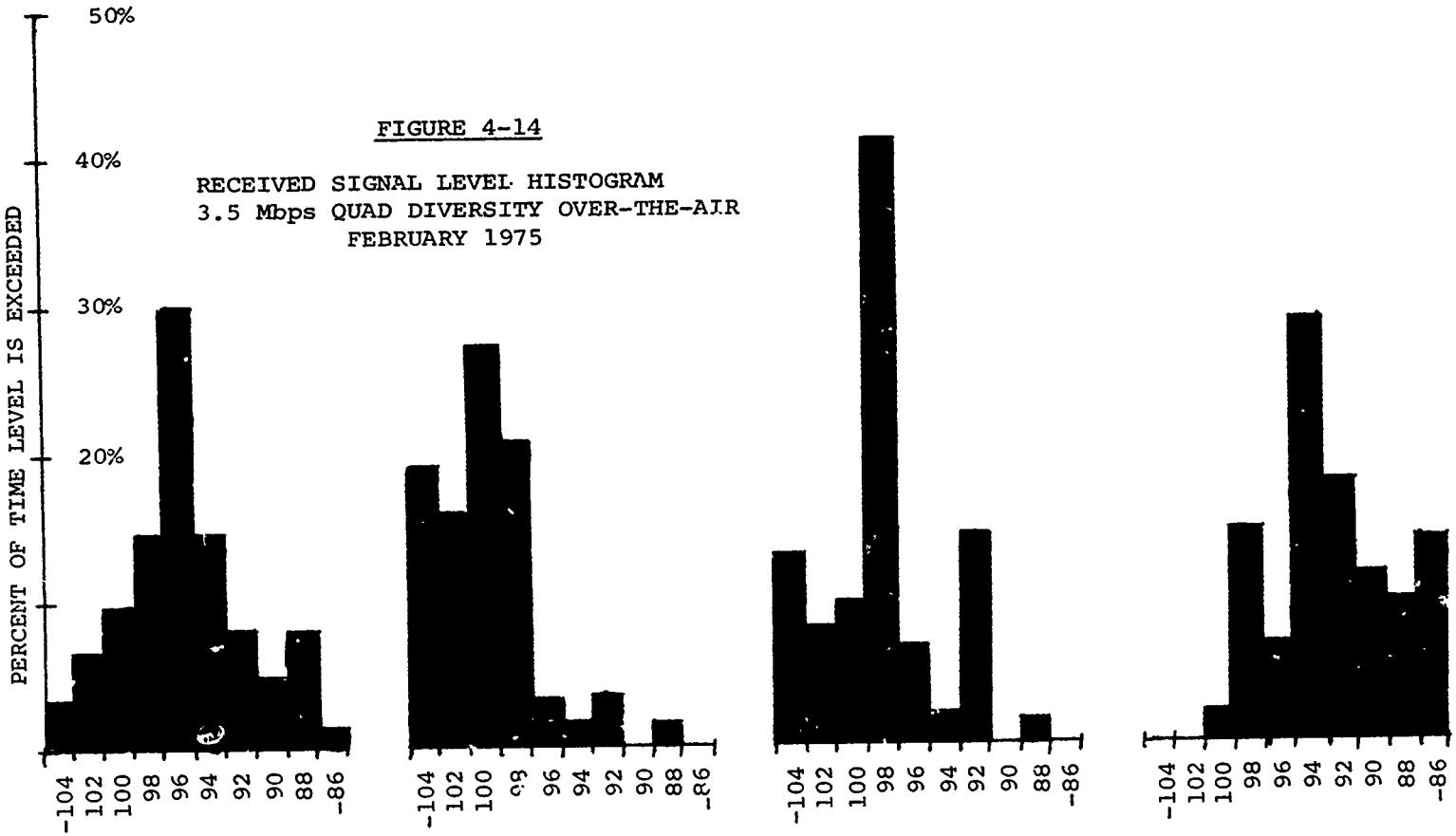

FIGURE 4-15 SIGNAL LEVEL DISTRIBUTION FOR 3.5 MBPS QUAD DIVERSITY OVER-THE-AIR FEBRUARY 1975

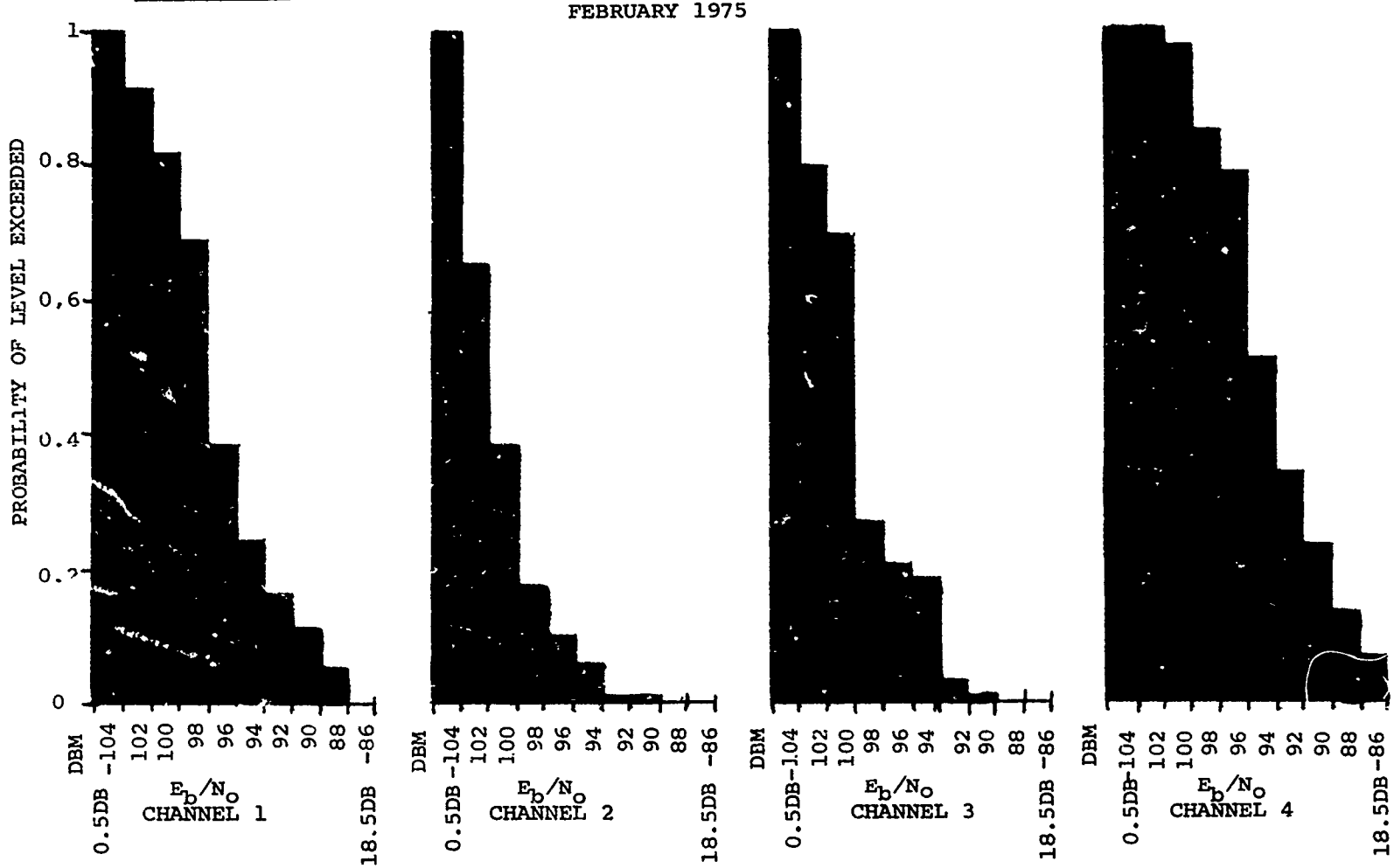

possible to isolate which runs suffered from the loss of lock condition, hence, all recorded data is included for completeness.

The AN/TRC-132 operates at C-Band and has considerably lower multipath spreads that the previous UHF link. This, coupled with significantly higher average RSL permitted data to be taken at all data rates and all diversities with the exception of 7 Mb/s non-diversity. These tests were run during the months of April and May 1975 and significant variation in median RSL from channel to channel was not encountered with this equipment. During the data recording, emphasis was placed on the higher data rates and higher orders of diversity as these are of the most interest to the DCS system.

4.3.2 Over-the-Air Test Results for the AN/TRC-132 at 1.75 Mb/s

Figure 4-16 shows the recorded data for 1.75 Mb/s non diversity. Not shown is a data point at 10^{-8} for E_b/N_o equal to 16.5 dB. Although there is not much data, the performance is demonstrated by the fact that 10^{-8} error rate is achievable over the air. A high level of intrinsic diversity was achieved in these tests. The higher error rate points are due to normal variations in multipath delay spread and possibly also the local oscillator loss-of-lock problem. Also shown in Figure 4-16 is the theoretical non-diversity and dual effective diversity curves with 3 dB implementation loss. The point above the theoretical curve is most likely caused by oscillator loss of lock.

Figure 4-17 shows the DAR-IV performance for 1.75 Mb/s dual diversity. The one point which is far above the theoretical dual diversity curve is most likely due to loss of lock in the local oscillator. The remaining points are a good representation of the dual diversity performance with varying levels of intrinsic diversity. Not shown are three data points between 10^{-7} and 10^{-8}. The spread in error rate performance shows the significant improvement in the DAR-IV's performance for increased delay spread. The implicit diversity varies between none to about fourth order. Figure 4-18 shows the error probability density for 1.75 Mb/s dual diversity. This data was extracted for the error histogram data taken concurrently with the over-the-air error rate data. The probability density is based on a histogram of 20,000 error samples each 100 msec in duration. What is shown here is the probability of getting various grouping of errors. Note, for example, that there is an 80% probability of receiving an error free segment of data in a 100 msec sample. Note also that the errors, when they occur, tend to occur in large bursts.

Figure 4-19 demonstrates the quad diversity performance of the DAR-IV for 1.75 Mb/s. The measured error rates ranged from 10^{-2} to better than 10^{-8} (not shown in curve). The higher error rates (greater than the upper theoretical curve) are primarily due to loss of lock in the local oscillator. Figure 4-20 shows the corresponding error statistics.

FIGURE 4-16

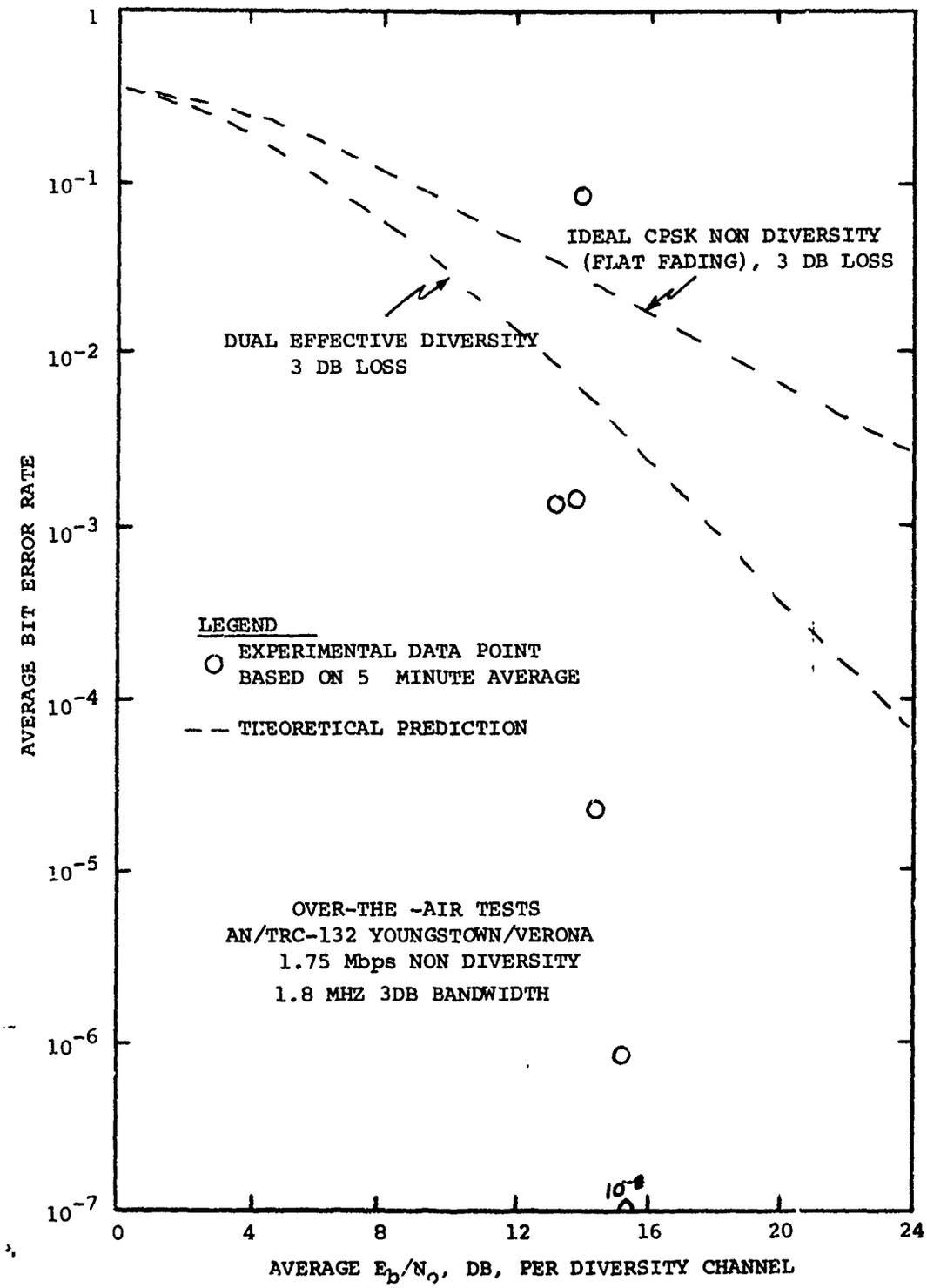
1
10^{-1}
10^{-2}
10^{-3}
10^{-4}
10^{-5}
10^{-6}
10^{-7}
AVERAGE BIT ERROR RATE
IDEAL CPSK NON DIVERSITY
(FLAT FADING), 3 DB LOSS
DUAL EFFECTIVE DIVERSITY
3 DB LOSS
LEGEND
EXPERIMENTAL DATA POINT
BASED ON 5 MINUTE AVERAGE
THEORETICAL PREDICTION
OVER-THE -AIR TESTS
AN/TRC-132 YOUNGSTOWN/VERONA
1.75 Mbps NON DIVERSITY
1.8 MHZ 3DB BANDWIDTH
10^{-6}
0
4
8
12
16
20
24
AVERAGE E_b/N_o, DB, PER DIVERSITY CHANNEL

FIGURE 4-17

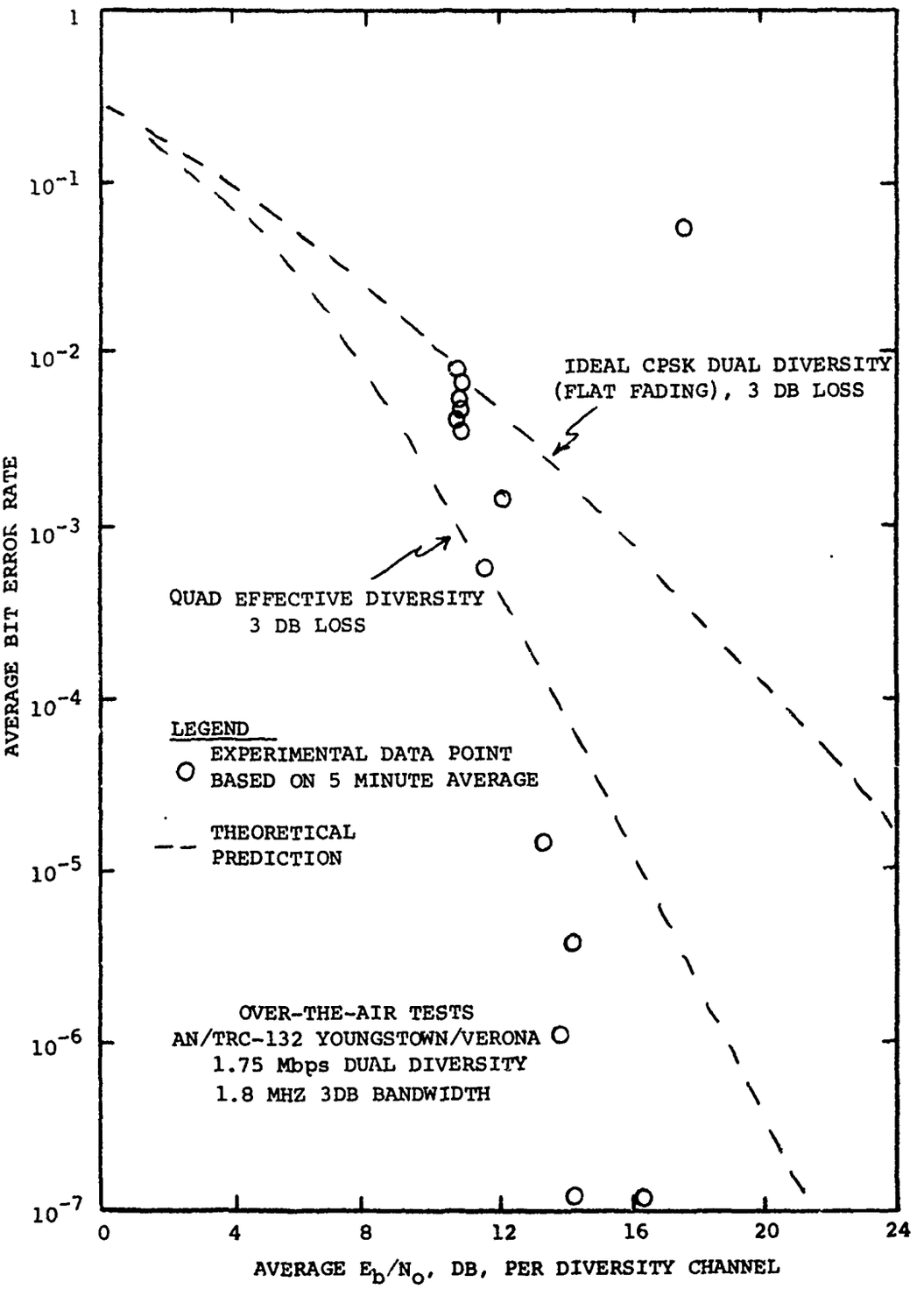
AVERAGE BIT ERROR RATE
1
10^{-1}
10^{-2}
10^{-3}
10^{-4}
10^{-5}
10^{-6}
10^{-7}
0
4
8
12
16
20
24
AVERAGE E_b/N_o, DB, PER DIVERSITY CHANNEL
IDEAL CPSK DUAL DIVERSITY
(FLAT FADING), 3 DB LOSS
QUAD EFFECTIVE DIVERSITY
3 DB LOSS
LEGEND
EXPERIMENTAL DATA POINT
BASED ON 5 MINUTE AVERAGE
THEORETICAL
PREDICTION
OVER-THE-AIR TESTS
AN/TRC-132 YOUNGSTOWN/VERONA
1.75 Mbps DUAL DIVERSITY
1.8 MHZ 3DB BANDWIDTH

FIGURE 4-18

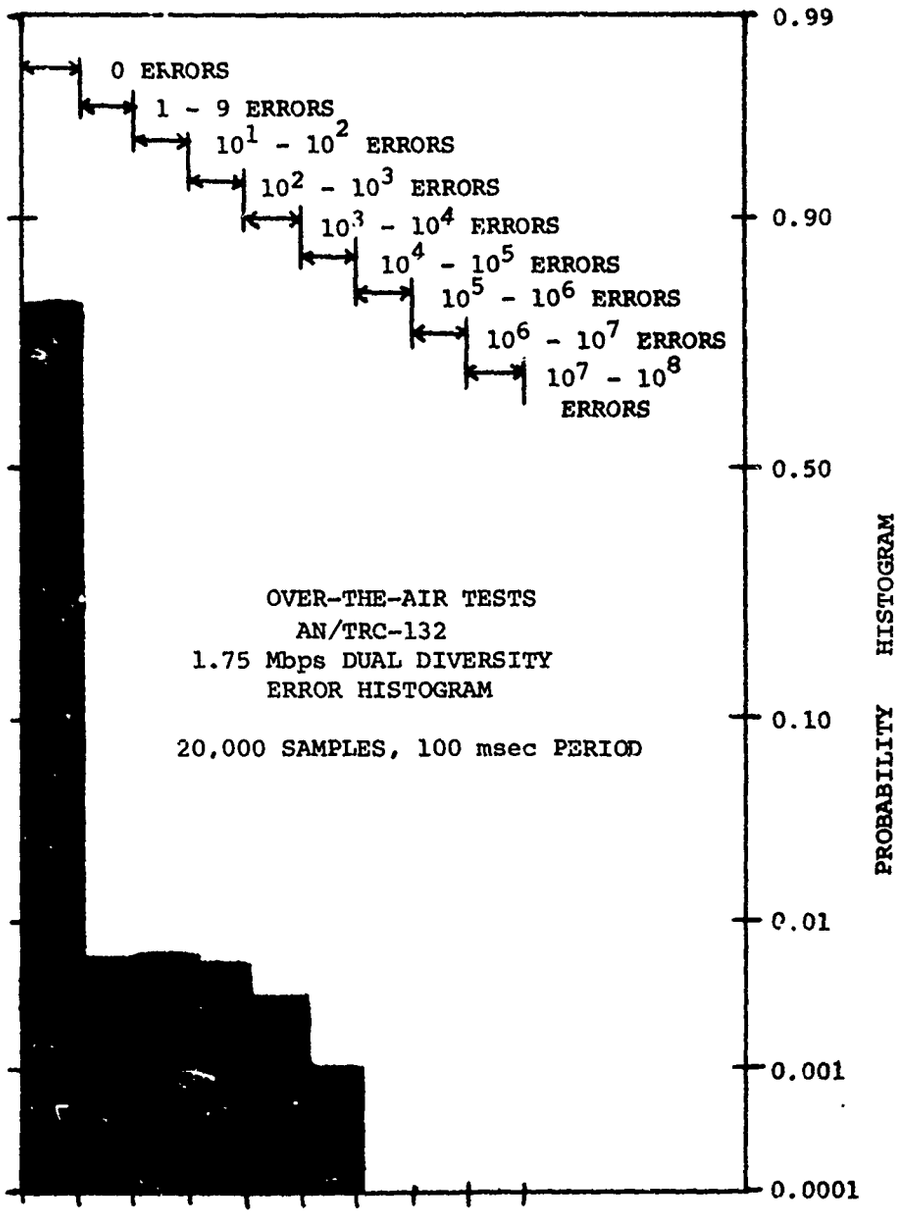
0 ERRORS
1 - 9 ERRORS
10^1 - 10^2 ERRORS
10^2 - 10^3 ERRORS
10^3 - 10^4 ERRORS
10^4 - 10^5 ERRORS
10^5 - 10^6 ERRORS
10^6 - 10^7 ERRORS
10^7 - 10^8 ERRORS
OVER-THE-AIR TESTS
AN/TRC-132
1.75 Mbps DUAL DIVERSITY
ERROR HISTOGRAM
20,000 SAMPLES, 100 msec PERIOD
0.99
0.90
0.50
0.10
0.01
0.001
0.0001
PROBABILITY HISTOGRAM

FIGURE 4-19

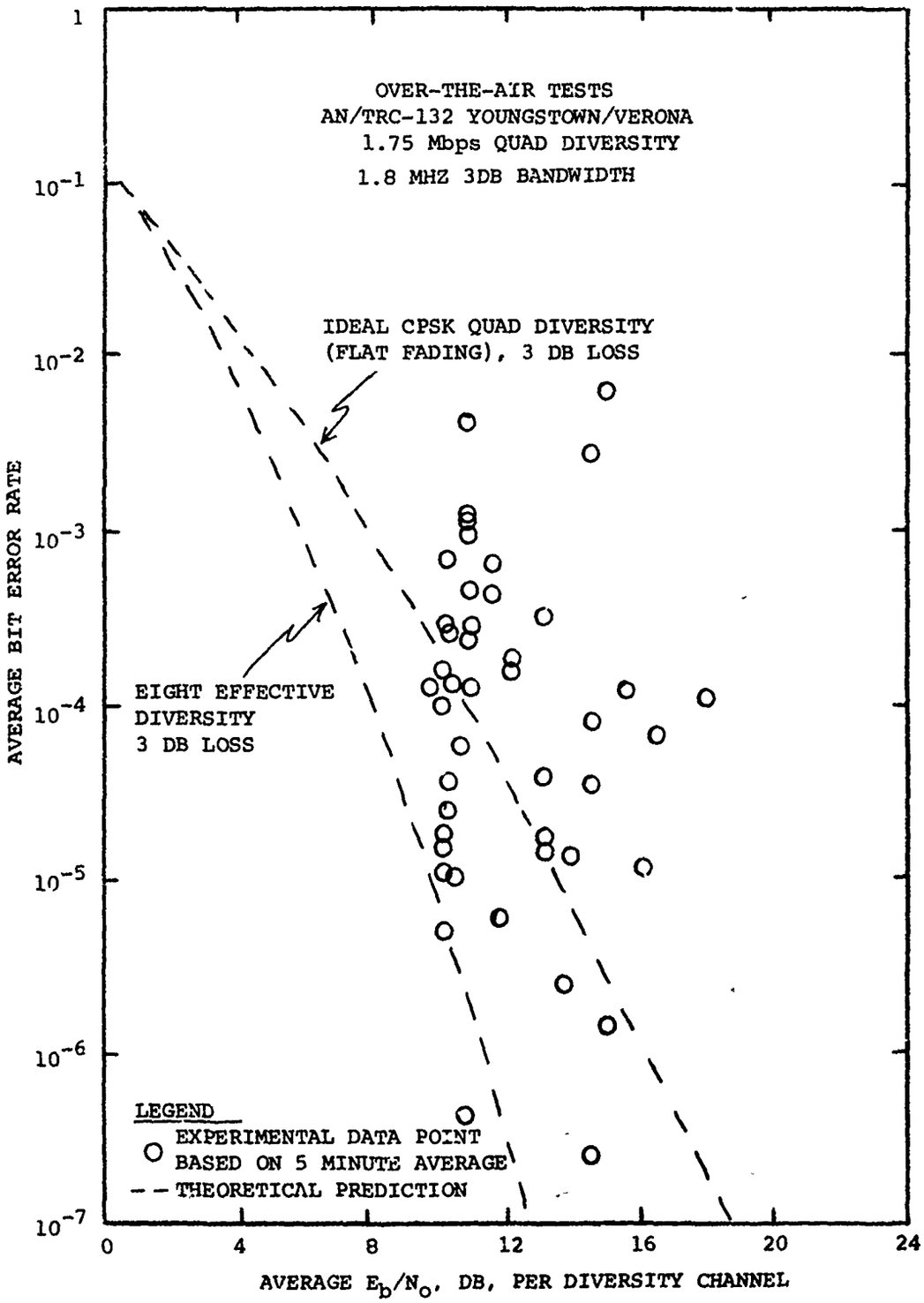
OVER-THE-AIR TESTS
AN/TRC-132 YOUNGSTOWN/VERONA
1.75 Mbps QUAD DIVERSITY
1.8 MHZ 3DB BANDWIDTH
IDEAL CPSK QUAD DIVERSITY
(FLAT FADING), 3 DB LOSS
EIGHT EFFECTIVE
DIVERSITY
3 DB LOSS
AVERAGE BIT ERROR RATE
1
10^{-1}
10^{-2}
10^{-3}
10^{-4}
10^{-5}
10^{-6}
10^{-7}
LEGEND
EXPERIMENTAL DATA POINT
BASED ON 5 MINUTE AVERAGE
THEORETICAL PREDICTION
0
4
8
12
16
20
24
AVERAGE E_b/N_o, DB, PER DIVERSITY CHANNEL

FIGURE 4-20

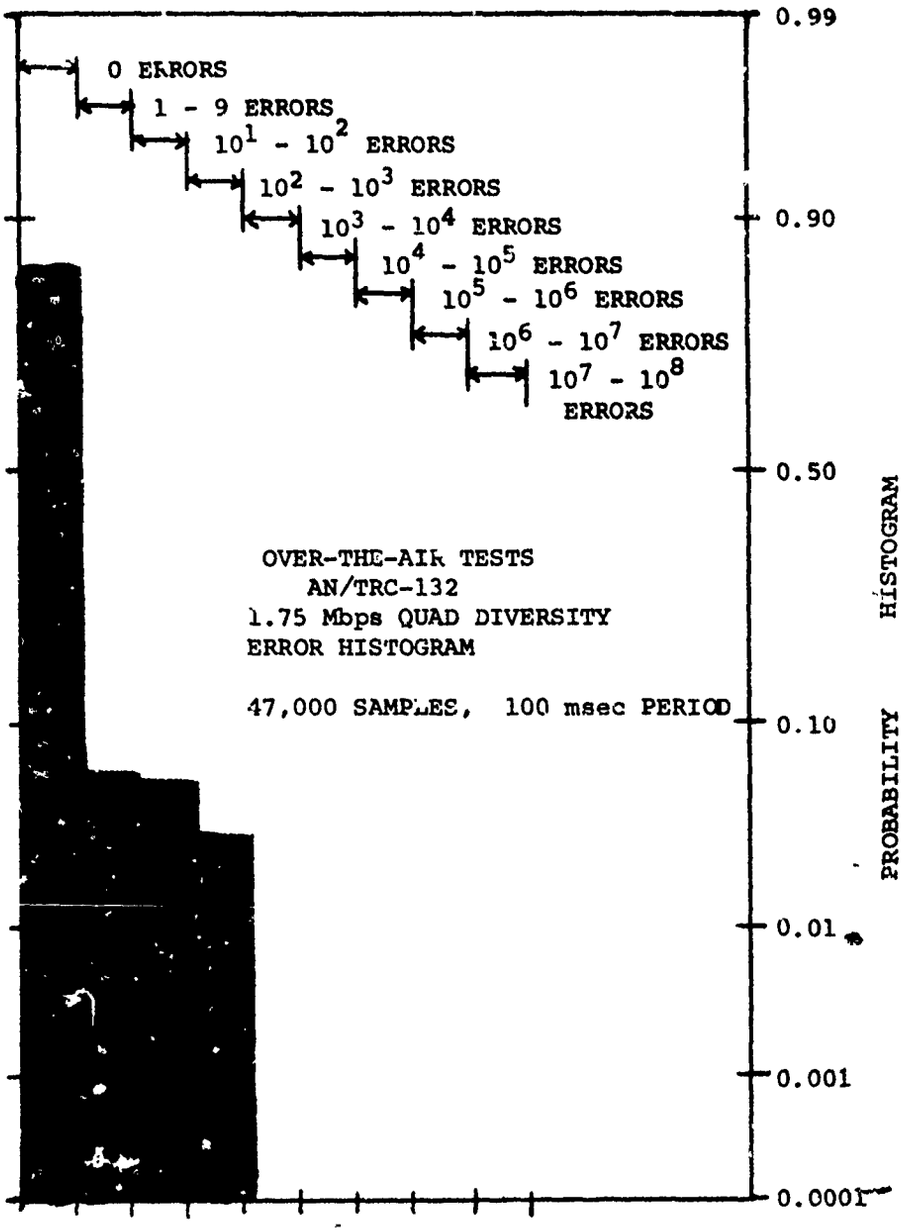
0 ERRORS
1 - 9 ERRORS
10^1 - 10^2 ERRORS
10^2 - 10^3 ERRORS
10^3 - 10^4 ERRORS
10^4 - 10^5 ERRORS
10^5 - 10^6 ERRORS
10^6 - 10^7 ERRORS
10^7 - 10^8 ERRORS
OVER-THE-AIR TESTS
AN/TRC-132
1.75 Mbps QUAD DIVERSITY
ERROR HISTOGRAM
47,000 SAMPLES, 100 msec PERIOD
0.99
0.90
0.50
0.10
0.01
0.001
0.0001
PROBABILITY
HISTOGRAM

It is interesting to note that of 47,000 samples, nearly 40,000 were error free, that is there is a 85% probability that a 100 msec segment of data will be error free. Of the remaining errors, a large majority of them occurred in groupings between 1 and 100 error block sizes per 100 msec. This result is very impressive because it demonstrates that even for what appears to be relatively high error rates, this composition of the errors consists of relatively few segments with a very high error rate and a large percentage of the segments are error free. Note that this error distribution verifies that the points above the theoretical curve are not due to intersymbol interference since then some 100 msec readings of 10^5 to 10^6 errors would have resulted.

4.3.3 Over-the-Air Test Results for 3.5 Mb/s

This series of tests demonstrates the performance of the DAR-IV at 3.5 Mb/s for non, dual and quad orders of explicit diversity.

Figure 4-21 shows the error rates for the non-diversity configuration. Very few loss of lock occurrences were present during this set of data. The error rates ranged from 10^{-3} to almost 10^{-5} for an input SNR range of 14 to 21 dB. It can be seen that the data is in a relatively tight cluster. The effects of the intrinsic diversity action can be seen by observing that for a given SNR, the error rates exhibit a large improvement over the theoretical flat fading curve and in most cases are better than the theoretical effective dual diversity. Figure 4-22 shows the error distribution characteristics. These results are extremely impressive. From Figure 4-22, it can be seen that of 29,000 samples, approximately 27,000 or 96% were error free. Of the remaining 2000 samples, 1000 of them had blocks of 100 or less errors. However, even with the benefit of large intrinsic diversity gain, the errors still tend to occur in bursts.

Figure 4-23 shows the results of the 3.5 Mb/s dual diversity tests. There is a good spread of data here ranging from almost 10^{-1} to better than 10^{-8}. Not shown are about a dozen points between 10^{-7} and 7×10^{-9}. These points together with the error distribution histogram verify that the over-the-air tests exhibit no irreducible error rates above at least 10^{-9}. The points above the theoretical flat fading curve are due to unlocking of the receiver local oscillator as described previously. The greatly improved path conditions may be seen by the large number of samples taken at high signal to noise ratios. This condition permits examining the DAR-IV performance at very low error rates. Figure 4-24 shows the error burst probability density statistics for the dual diversity case. Once again, the high probability of receiving error free segments is demonstrated, in this instance better than 90% of the 49,000 sample points were error free. The high number of error bursts of 10^3 through 10^4 length are due primarily to the unstable local oscillator condition.

FIGURE 4-21

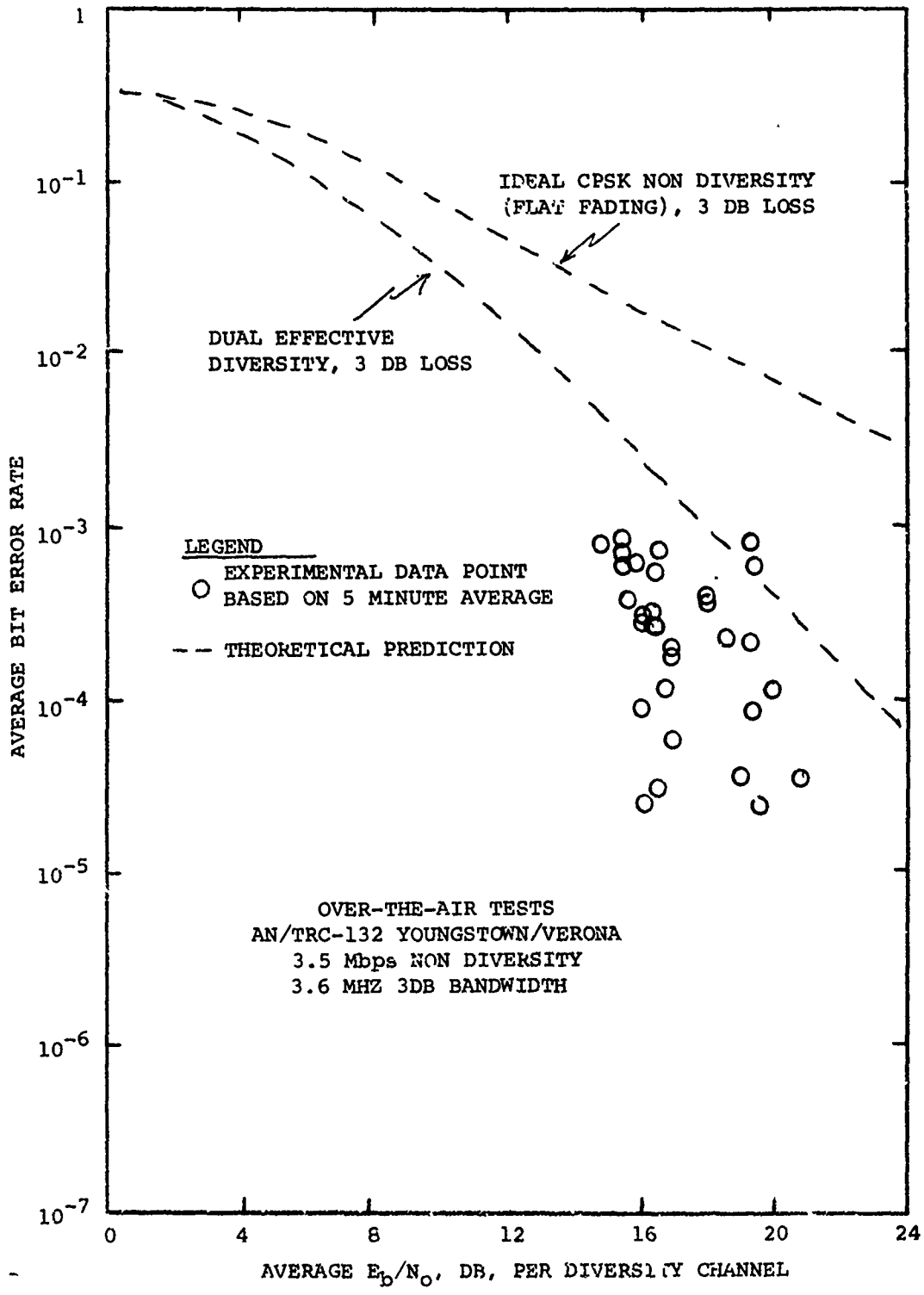
1
10^{-1}
10^{-2}
10^{-3}
10^{-4}
10^{-5}
10^{-6}
10^{-7}
AVERAGE BIT ERROR RATE
IDEAL CPSK NON DIVERSITY
(FLAT FADING), 3 DB LOSS
DUAL EFFECTIVE
DIVERSITY, 3 DB LOSS
LEGEND
EXPERIMENTAL DATA POINT
BASED ON 5 MINUTE AVERAGE
THEORETICAL PREDICTION
OVER-THE-AIR TESTS
AN/TRC-132 YOUNGSTOWN/VERONA
3.5 Mbps NON DIVERSITY
3.6 MHZ 3DB BANDWIDTH
0
4
8
12
16
20
24
AVERAGE E_b/N_o, DB, PER DIVERSITY CHANNEL

FIGURE 4-22

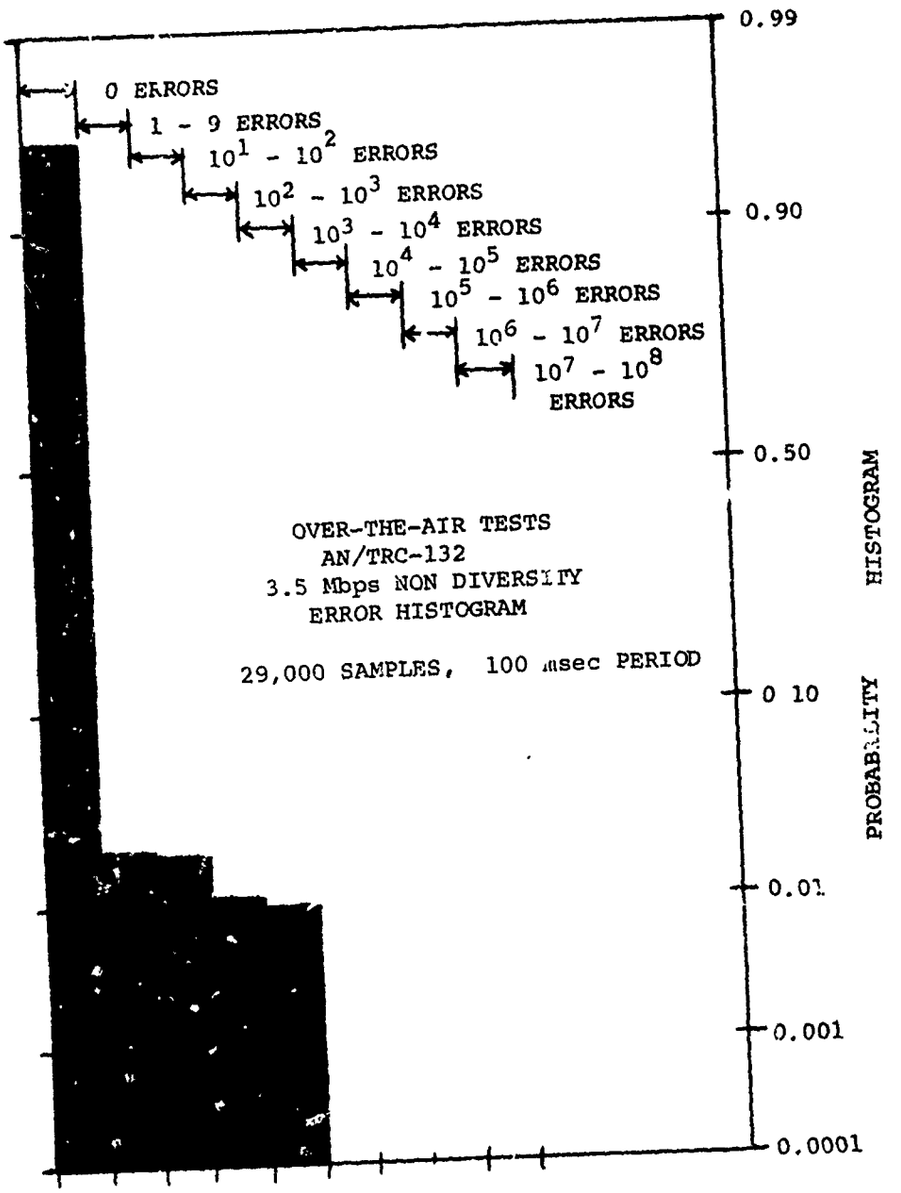
0 ERRORS
1 - 9 ERRORS
10^1 - 10^2 ERRORS
10^2 - 10^3 ERRORS
10^3 - 10^4 ERRORS
10^4 - 10^5 ERRORS
10^5 - 10^6 ERRORS
10^6 - 10^7 ERRORS
10^7 - 10^8 ERRORS
0.99
0.90
0.50
0 10
0.01
0.001
0.0001
PROBABILITY HISTOGRAM
OVER-THE-AIR TESTS
AN/TRC-132
3.5 Mbps NON DIVERSITY
ERROR HISTOGRAM
29,000 SAMPLES, 100 msec PERIOD

FIGURE 4-23

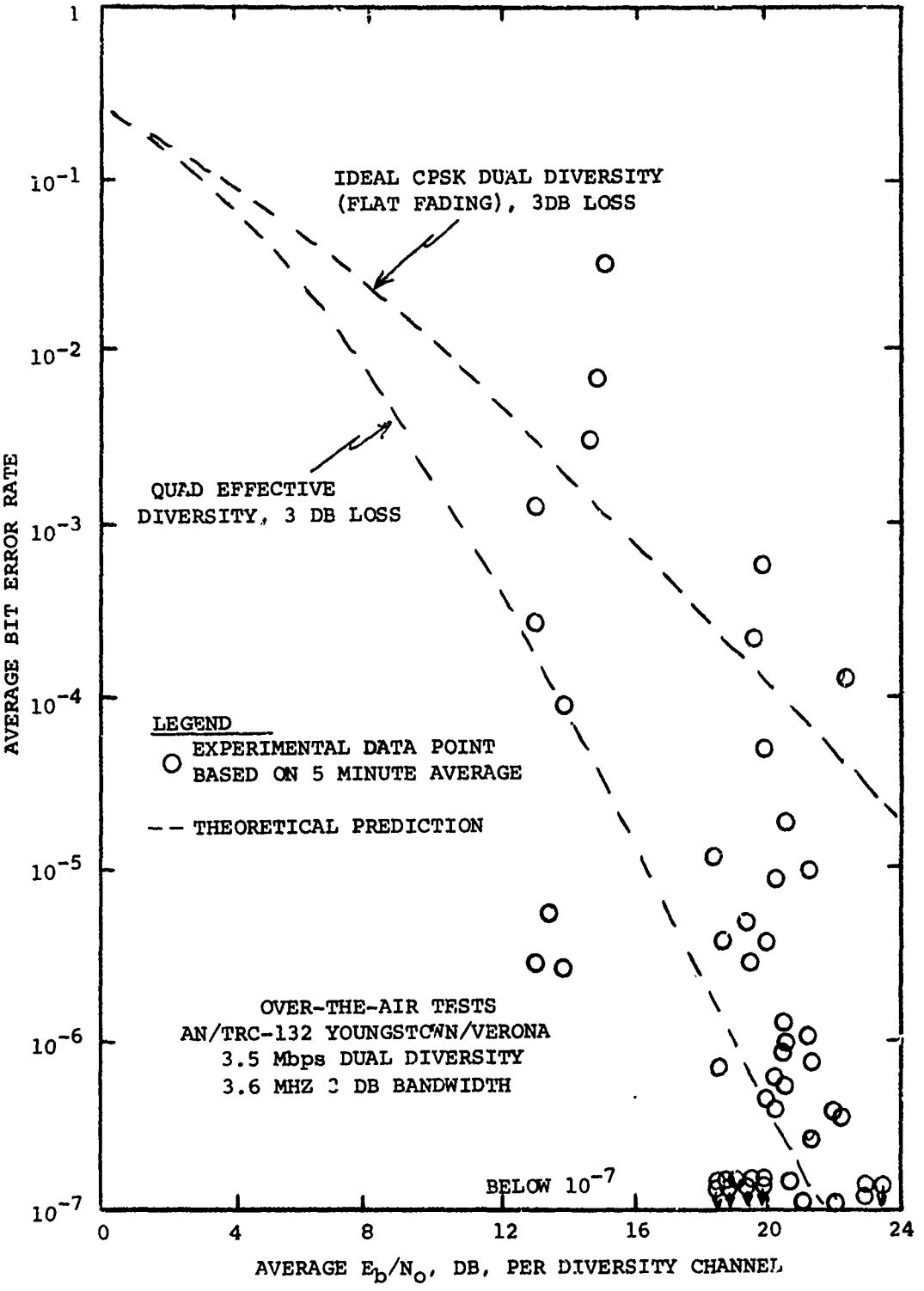
1
10^{-1}
10^{-2}
10^{-3}
10^{-4}
10^{-5}
10^{-6}
10^{-7}
AVERAGE BIT ERROR RATE
IDEAL CPSK DUAL DIVERSITY
(FLAT FADING), 3DB LOSS
QUAD EFFECTIVE
DIVERSITY, 3 DB LOSS
LEGEND
EXPERIMENTAL DATA POINT
BASED ON 5 MINUTE AVERAGE
THEORETICAL PREDICTION
OVER-THE-AIR TESTS
AN/TRC-132 YOUNGSTOWN/VERONA
3.5 Mbps DUAL DIVERSITY
3.6 MHZ 3 DB BANDWIDTH
BELOW 10^{-7}
0
4
8
12
16
20
24
AVERAGE E_b/N_o, DB, PER DIVERSITY CHANNEL

FIGURE 4-24

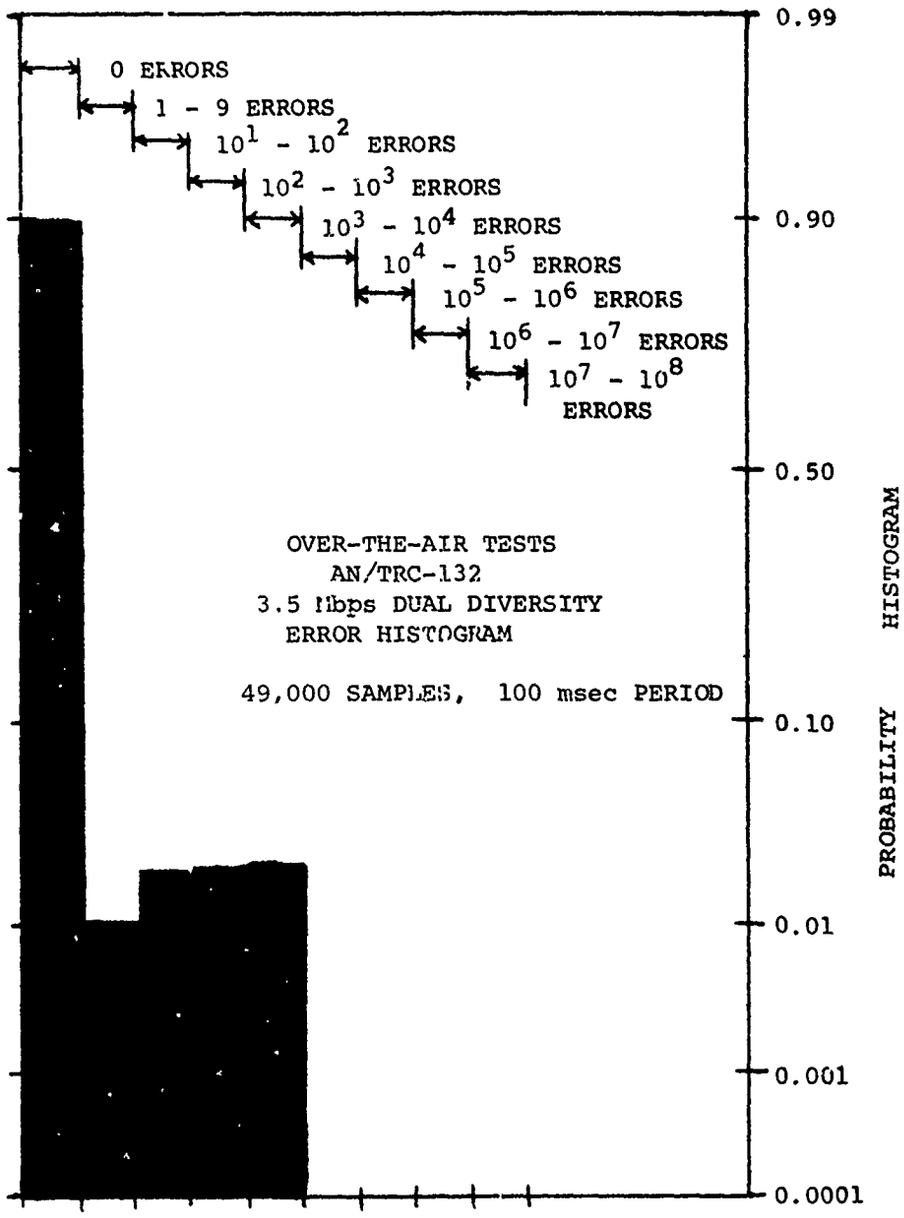
0 ERRORS
1 - 9 ERRORS
10^1 - 10^2 ERRORS
10^2 - 10^3 ERRORS
10^3 - 10^4 ERRORS
10^4 - 10^5 ERRORS
10^5 - 10^6 ERRORS
10^6 - 10^7 ERRORS
10^7 - 10^8 ERRORS
OVER-THE-AIR TESTS
AN/TRC-132
3.5 Mbps DUAL DIVERSITY
ERROR HISTOGRAM
49,000 SAMPLES, 100 msec PERIOD
0.99
0.90
0.50
0.10
0.01
0.001
0.0001
PROBABILITY HISTOGRAM

The results for 3.5 Mb/s quad diversity are illustrated in Figure 4-25. There were three data points that fell between 10^{-7} and 10^{-8} at a E_b/N_o of 12 dB. Once again, this demonstrates the ability of the DAR-IV to achieve very low error rates over a practical link. The remainder of the points ranged from error rates of 10^{-3} to 10^{-7}. During this series of tests the local oscillator unlocking became quite frequent, thus yielding a number of high error rate data points on high signal to noise ratios. The major emphasis should be placed on the data points below 10^{-4} as these points were not effected by the loss of lock. Figure 4-26 shows the error statistics. Once again, note the high percentage of error free segments.

4.3.4 Over-the-Air Test Results for 7.0 Mb/s

The last series of tests run were for 7.0 Mb/s dual and quad diversities. Due to time limitations as well as the desired emphasis on higher order diversities, no data was obtained for 7 Mb/s non-diversity. These tests are probably the most interesting in that they demonstrate the capacity of the DAR-IV to operate at a high data rate over a practical tropo link.

Figure 4-27 shows the 7 Mb/s dual diversity performance. A good distribution of data points is evident as the recorded measurements cover a range of approximately 10^{-1} through 10^{-5}. Figure 4-28 shows the error distribution characteristics. It can be seen that for dual diversity out of 28,000 sample points, 80% of these were error free. It is interesting to note the almost uniform distribution of the errors in block sizes of 1 to 10^4. This corresponds with the near uniform distribution of the data points in Figure 4-27 in the error rate ranges of 10^{-2} to 10^{-5}. As with the previous results, the large performance benefits of intrinsic diversity provided by the DAR-IV are clearly evident. A performance gain of nearly 12 dB over a flat fading channel is indicated.

The quad diversity performance is illustrated in Figure 4-29. Since the primary interest was in the high data rates and higher order of diversity, it may be seen in Figure 4-29 that a large number of data points were recorded for the 7 Mb/s quad diversity case. The results shown here are very gratifying as the error rates measured ranged from 10^{-1} through 10^{-8} covering signal to noise ratios of 0 to 18 dB. The data points give a very good outline of the general performance curve of the DAR-IV for this mode. Not shown are about a dozen points in the 10^{-7} to 10^{-8} range. A 10^{-8} error rate was achieved at signal to noise ratios as low as 10 dB. Figure 4-30 shows the error distribution characteristics corresponding to the measured bit error rates in Figure 4-29. These characteristics are composed of 61,000 measurements of which 70% are error free. Again, note that the error occurrences are quite uniformly distributed which is representative of the fact that the error tends to occur in bursts and the nearly uniform distribution of samples between 10^{-1} and 10^{-7} BER.

FIGURE 4-25

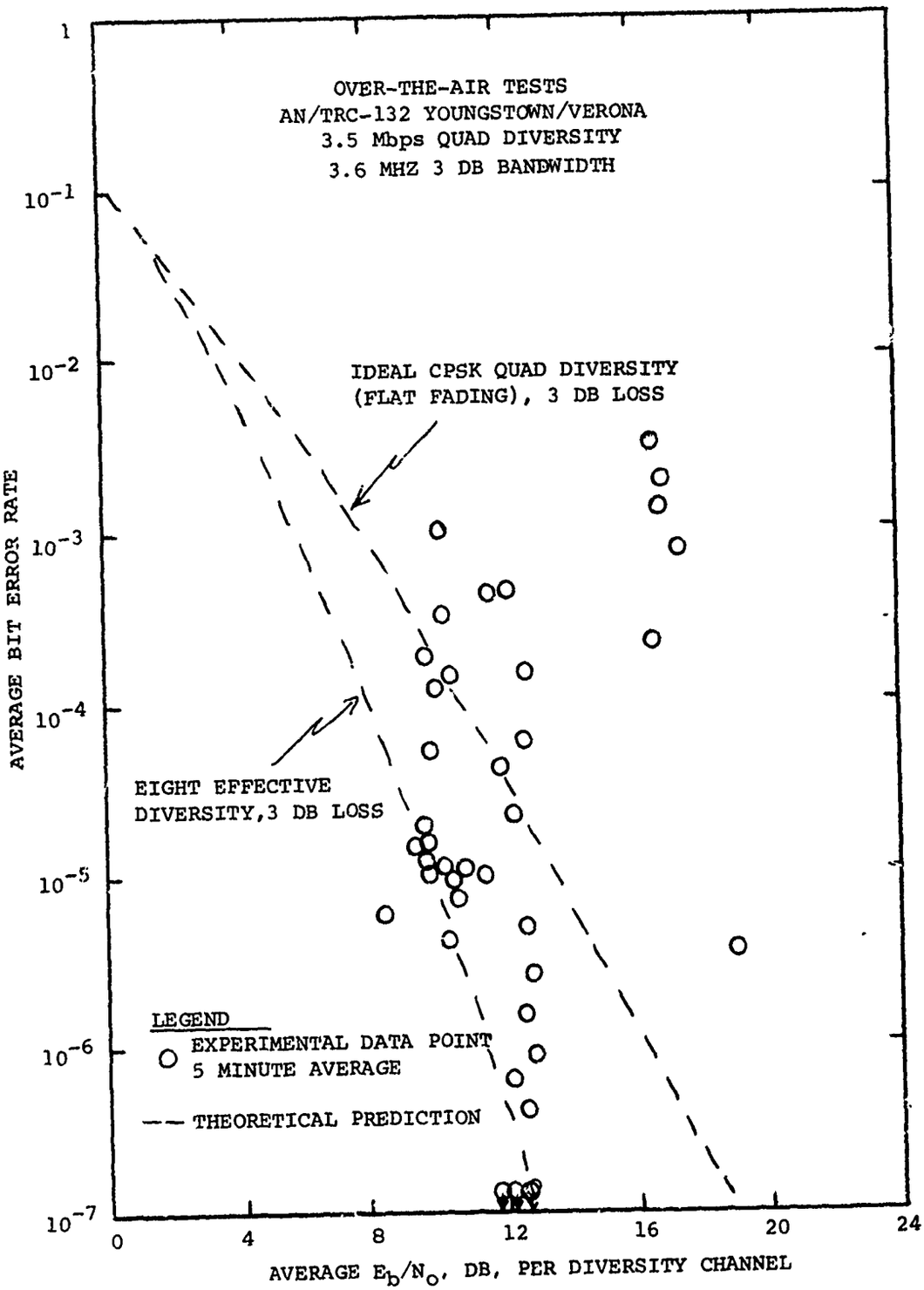
OVER-THE-AIR TESTS
AN/TRC-132 YOUNGSTOWN/VERONA
3.5 Mbps QUAD DIVERSITY
3.6 MHZ 3 DB BANDWIDTH
IDEAL CPSK QUAD DIVERSITY
(FLAT FADING), 3 DB LOSS
EIGHT EFFECTIVE
DIVERSITY,3 DB LOSS
LEGEND
EXPERIMENTAL DATA POINT
5 MINUTE AVERAGE
THEORETICAL PREDICTION
AVERAGE BIT ERROR RATE
1
10^{-1}
10^{-2}
10^{-3}
10^{-4}
10^{-5}
10^{-6}
10^{-7}
0
4
8
12
16
20
24
AVERAGE E_b/N_o, DB, PER DIVERSITY CHANNEL

FIGURE 4-26

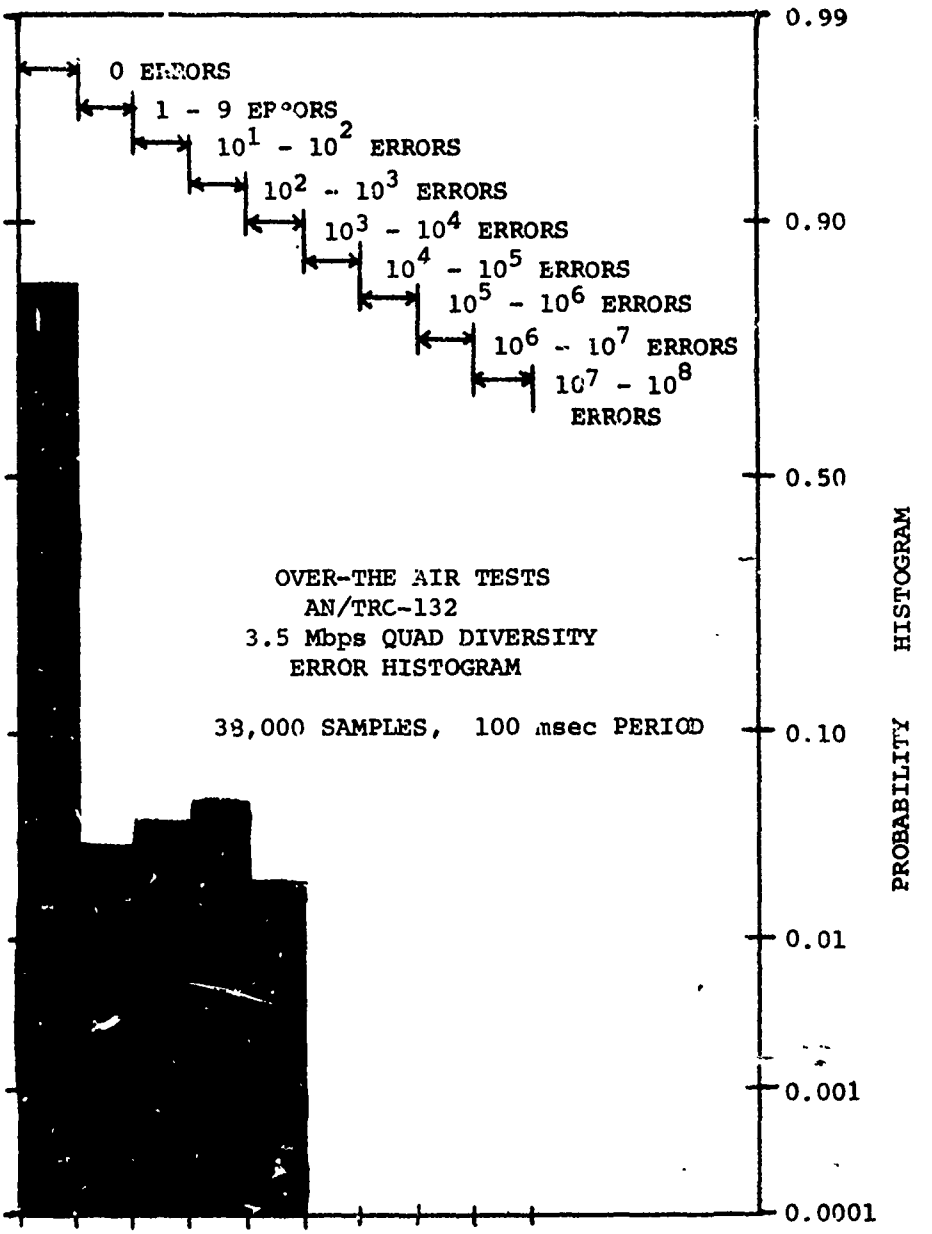
0 ERRORS
1 - 9 ERRORS
10^1 - 10^2 ERRORS
10^2 - 10^3 ERRORS
10^3 - 10^4 ERRORS
10^4 - 10^5 ERRORS
10^5 - 10^6 ERRORS
10^6 - 10^7 ERRORS
10^7 - 10^8 ERRORS
OVER-THE AIR TESTS
AN/TRC-132
3.5 Mbps QUAD DIVERSITY
ERROR HISTOGRAM
38,000 SAMPLES, 100 msec PERIOD
0.99
0.90
0.50
0.10
0.01
0.001
0.0001
PROBABILITY HISTOGRAM

FICURE 4-27

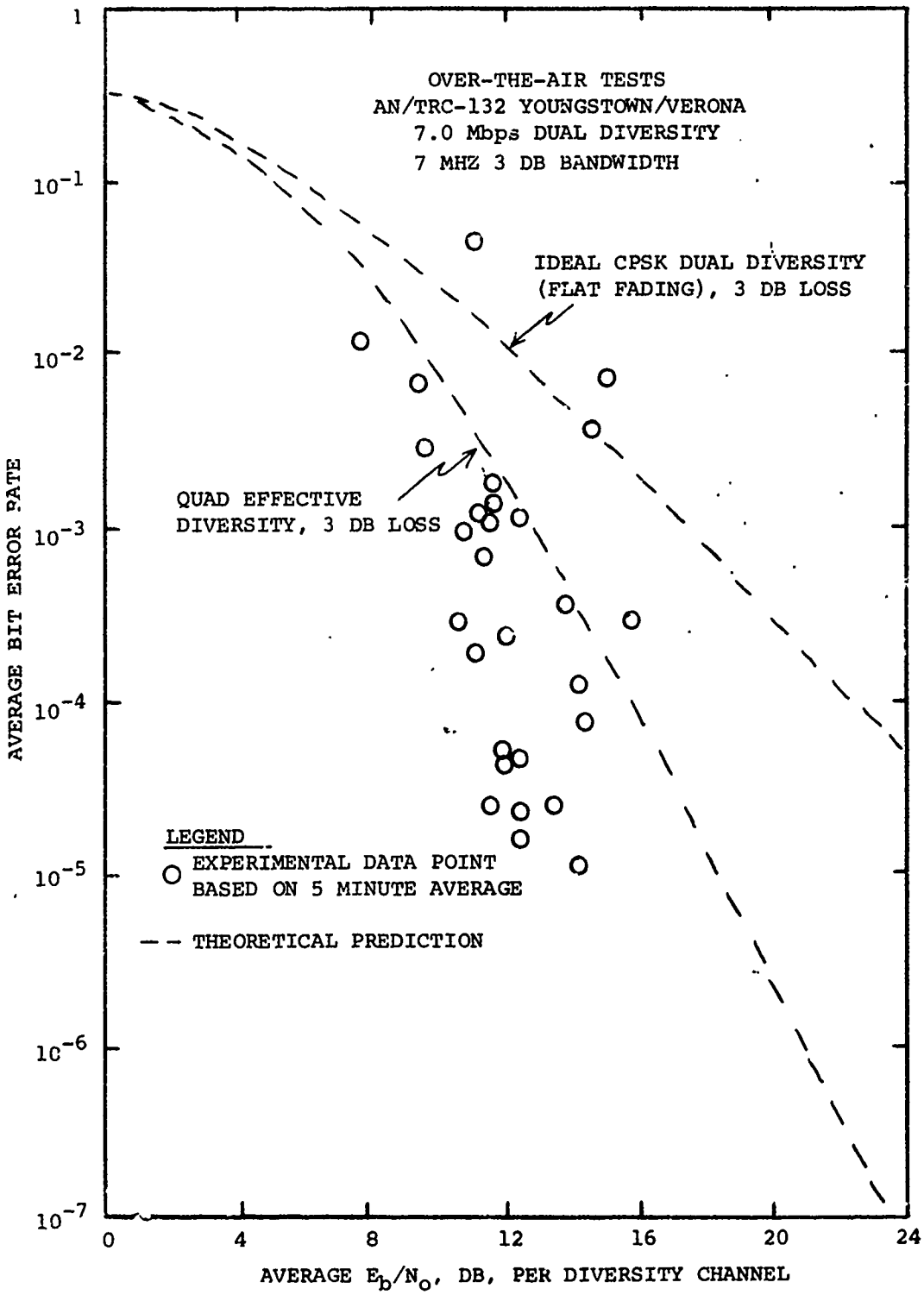
OVER-THE-AIR TESTS
AN/TRC-132 YOUNGSTOWN/VERONA
7.0 Mbps DUAL DIVERSITY
7 MHZ 3 DB BANDWIDTH
IDEAL CPSK DUAL DIVERSITY
(FLAT FADING), 3 DB LOSS
QUAD EFFECTIVE
DIVERSITY, 3 DB LOSS
LEGEND
EXPERIMENTAL DATA POINT
BASED ON 5 MINUTE AVERAGE
THEORETICAL PREDICTION
AVERAGE BIT ERROR RATE
1
10^{-1}
10^{-2}
10^{-3}
10^{-4}
10^{-5}
10^{-6}
10^{-7}
0
4
8
12
16
20
24
AVERAGE E_b/N_o, DB, PER DIVERSITY CHANNEL

FIGURE 4-28

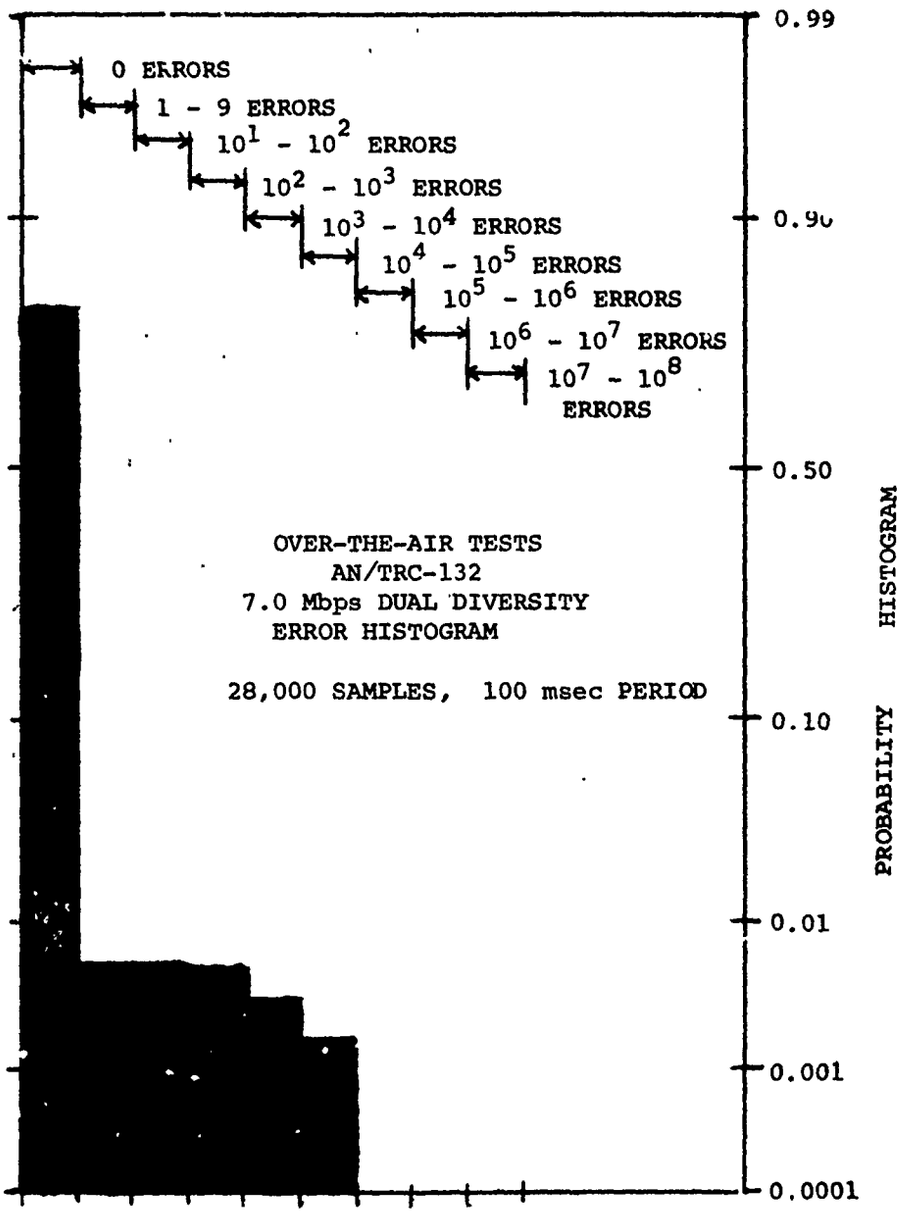
0 ERRORS
1 - 9 ERRORS
10^1 - 10^2 ERRORS
10^2 - 10^3 ERRORS
10^3 - 10^4 ERRORS
10^4 - 10^5 ERRORS
10^5 - 10^6 ERRORS
10^6 - 10^7 ERRORS
10^7 - 10^8 ERRORS
OVER-THE-AIR TESTS
AN/TRC-132
7.0 Mbps DUAL DIVERSITY
ERROR HISTOGRAM
28,000 SAMPLES, 100 msec PERIOD
0.99
0.90
0.50
0.10
0.01
0.001
0.0001
PROBABILITY HISTOGRAM

FIGURE 4-29

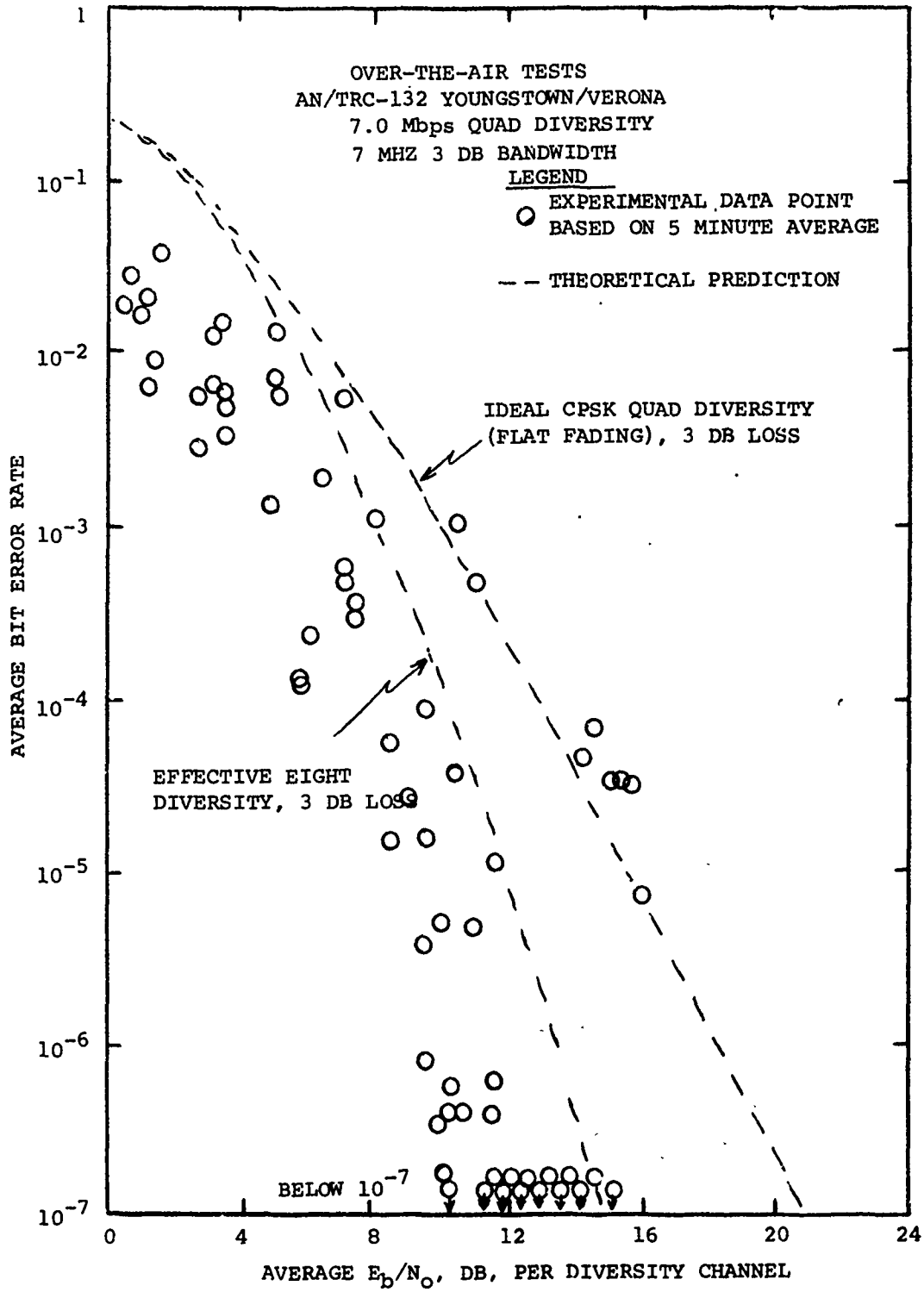
OVER-THE-AIR TESTS
AN/TRC-132 YOUNGSTOWN/VERONA
7.0 Mbps QUAD DIVERSITY
7 MHZ 3 DB BANDWIDTH
LEGEND
EXPERIMENTAL DATA POINT BASED ON 5 MINUTE AVERAGE
THEORETICAL PREDICTION
IDEAL CPSK QUAD DIVERSITY (FLAT FADING), 3 DB LOSS
EFFECTIVE EIGHT DIVERSITY, 3 DB LOSS
BELOW 10^{-7}
AVERAGE BIT ERROR RATE
1
10^{-1}
10^{-2}
10^{-3}
10^{-4}
10^{-5}
10^{-6}
10^{-7}
0
4
8
12
16
20
24
AVERAGE E_b/N_o, DB, PER DIVERSITY CHANNEL

FIGURE 4-30

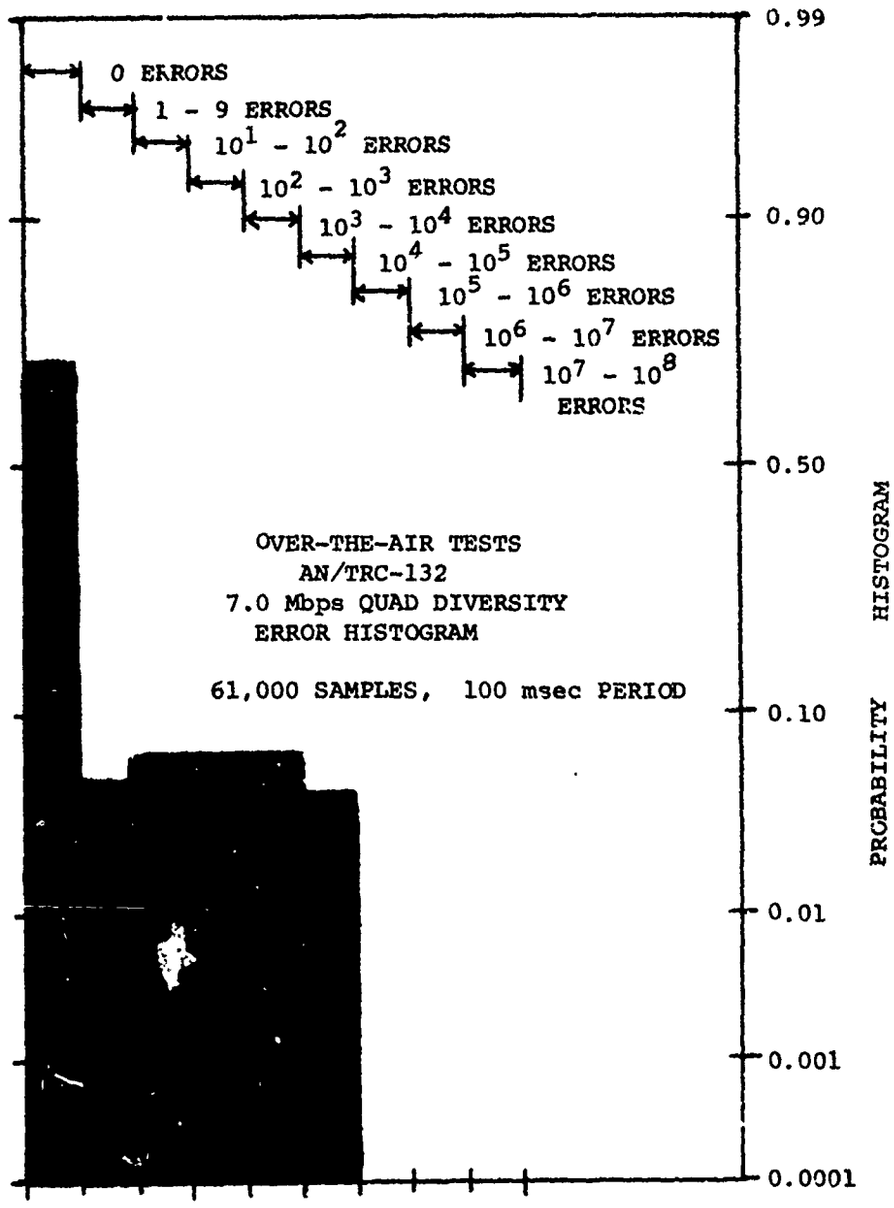
0 ERRORS
1 - 9 ERRORS
10^1 - 10^2 ERRORS
10^2 - 10^3 ERRORS
10^3 - 10^4 ERRORS
10^4 - 10^5 ERRORS
10^5 - 10^6 ERRORS
10^6 - 10^7 ERRORS
10^7 - 10^8 ERRORS
OVER-THE-AIR TESTS
AN/TRC-132
7.0 Mbps QUAD DIVERSITY
ERROR HISTOGRAM
61,000 SAMPLES, 100 msec PERIOD
0.99
0.90
0.50
0.10
0.01
0.001
0.0001
PROBABILITY HISTOGRAM

The improvement due to the added orders of explicit diversity can be readily seen by comparing the results shown in Figure 4-29 for quad diversity with those in Figure 4-27 for dual diversity.

4.4 AN/TRC-97 Over-the-Air Tests

4.4.1 General

This series of tests was performed under TRI-TAC/ESD/RADC sponsorship (as previously referenced) to evaluate the DAR-IV for tactical application. A second goal of the test program was to relate the over-the-tests to the channel simulator tests to verify that the simulator provides a realistic estimate of actual performance.

The interface and modifications to the AN/TRC-97 were similar to those performed on the AN/MRC-98 and AN/TRC-132 radios. Tests were run during the months of May and June on the dual diversity radio with one significant different in the test procedure. That is, after every one or two five minute average BER versus RSL measurements, five minutes of RAKE multipath analysis was performed using the RADC multipath analyzer. The RAKE data was reduced off-line to provide a measure of the rms multipath delay spread associated with each BER point. These three pieces of information, BER, RSL, and multipath spread, allow the over-the-air and simulator results to be compared directly.

4.4.2 AN/TRC-97 Performance at 1.75 Mbps

Tests were conducted at 1.75 Mbps and 3.5 Mbps on the AN/TRC-97. Also, some tests were run using 8' receive antennas while others were run using 15' antennas. Problems in calibrating the RSL indicators lead to the negation of the first few weeks of data since the RSL accuracy was only $\pm$ several dB which was not adequate for the over-the-air versus channel simulator comparison. After careful calibration of the RSL detectors, the results shown in Figures 4-31 through 4-37 was obtained.

Figure 4-31 shows a composite of the dual diversity test results for all multipath spreads. Also shown is the ideal dual diversity flat fading performance of a CPSK modem with 3 dB implementation loss (upper dashed line). The lower dashed lines show the same theoretical modem with quad and eight order effective diversity (due to intrinsic diversity) respectively. Note that because of the intrinsic diversity provided by the DAR-IV, the performance was typically between quad and 8 order effective diversity. The gain over a flat fading modem is 8 to 12 dB.

Figures 4-32 through 4-37 show the same data points but segregated according to the rms multipath spread that existed when the data point was obtained. Figure 4-32 shows all data points whose multipath

FIGURE 4-31 AN/TRC-97 DUAL DIVERSITY PERFORMANCE AT 1.75 MBPS (COMPOSITE OF RESULTS)

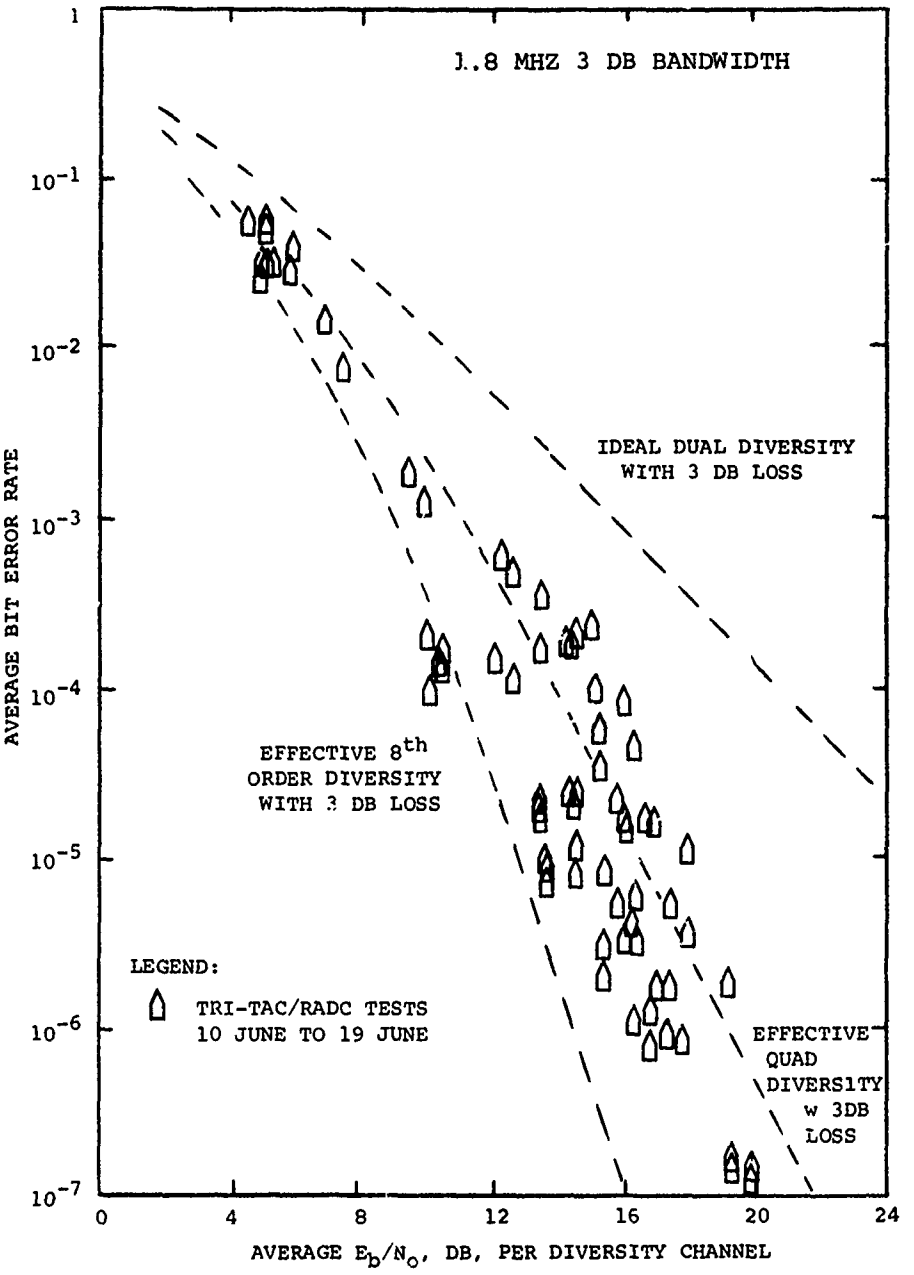

FIGURE 4-32 AN/TRC-97 DUAL DIVERSITY PERFORMANCE AT 1.75 MBPS

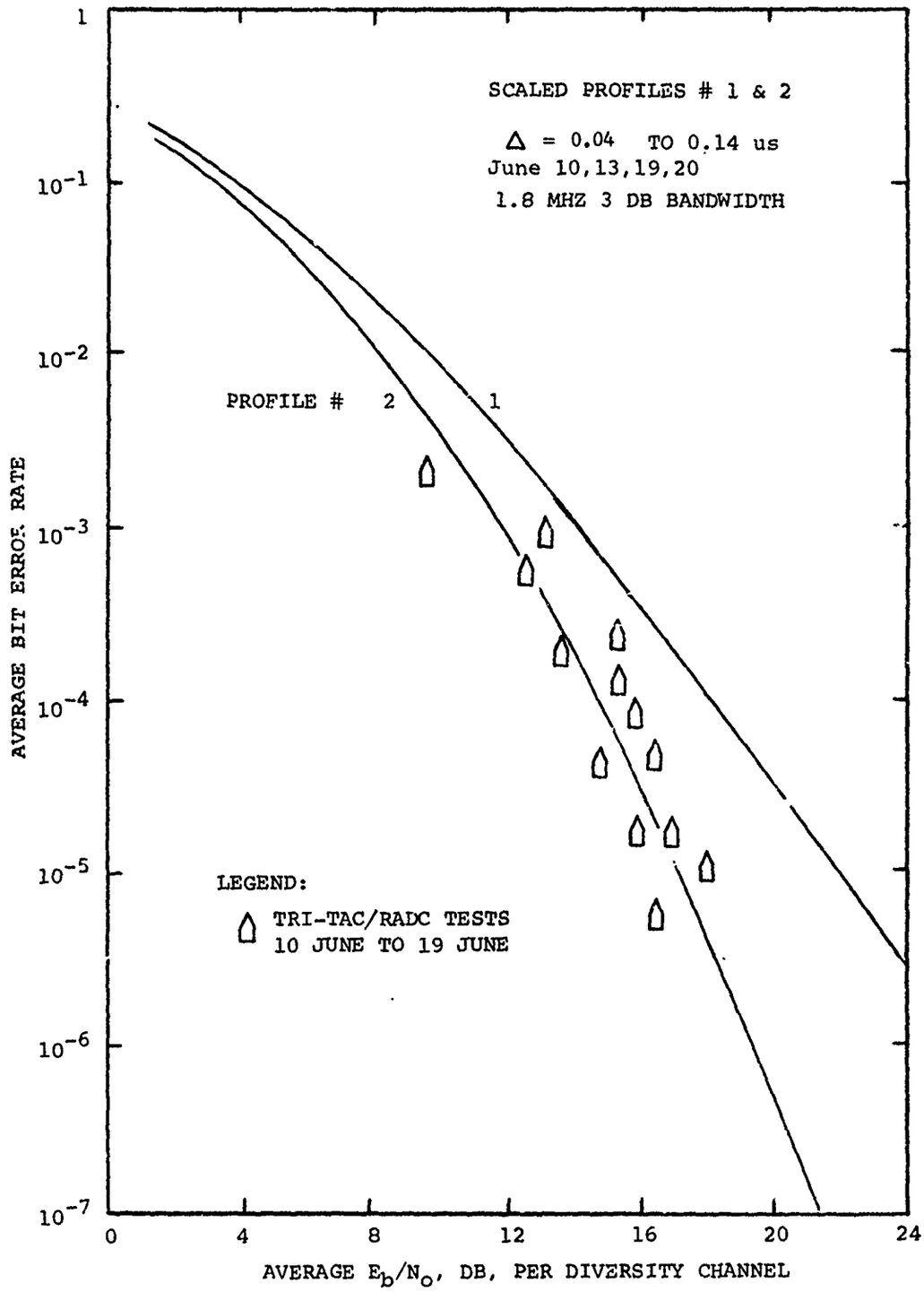

spreads varied between 0.04 and 0.14 us. Also shown on the figure is the channel simulator results for the corresponding multipath profiles described in Section 3.2 with rms spreads of 0.04 and 0.14 us, respectively. Note that agreement between the over-the-air data and the channel results is excellent.

Figures 4-33 through 4-37 show similarly good agreement between the over-the-air test data and the channel simulator results. The tests show conclusively that the DAR-IV simulator results are an accurate prediction of over-the-air performance. Anomalous propagation effects such as "aircraft fading" were found to actually enhance performance rather than degrade it. In the first series of tests, approximately 365 data points were taken of five minute duration. About 15% of these points included aircraft fades with no loss of bit count integrity and with apparent performance improvement in each case.

4.5 Summary of Over-the-Air Test Results

The DAR-IV Modem was tested on three troposcatter tests links of 168, 168, and 86 mile lengths using the AN/MRC-98, AN/TRC-132 and AN/TRC-97 tropo radios, respectively. Digital transmission tests were performed at 1.75, 3.5, and 7 Mb/s where permitted by path conditions and radio system parameters. The test results showed that the over-the-air performance of the DAR-IV agreed well with the performance measured on the laboratory channel simulator. Where signal strengths were adquate (representing threshold or better propagation conditions), the DAR-IV generally provided reliable digital transmission and significant performance benefits due to efficient utilization of intrinsic diversity.

Tests on the AN/MRC-98 at 880 MHz were somewhat limited to prevailing high average path loss and significantly different median signal levels on the four diversity receivers. Even so, reliable operation at 1.75 and 3.5 Mb/s was demonstrated without disruption by normal path anomalies such as aircraft fading and ducting. In fact, the modem performance tends to improve during such periods. Out of 178 five-minute test points, 27 contained aircraft fading and only one such record showed a loss of BCI. However, this loss of BCI was at a time of very low signal level and was probably only marginally influenced by the aircraft presence.

Tests at 7 Mb/s on the AN/MRC-98 were hampered by low signal level. To transmit at a 7 MHz rate on the AN/MRC-98, it was necessary to "broad-band" tune the AN/MRC-98 klystron power amplifier resulting in a loss of tube gain and a lowered output power level. At the lower power level and high path loss, the received signal was too low to maintain BCI over the five minute sample intervals. The problem is compounded by the fact that the present DAR-IV experimental model has limited bandwidth in the coherent reference signal recovery loop and can only use half the available

FIGURE 4-33 AN/TRC-97 DUAL DIVERSITY PERFORMANCE AT 1.75 MBPS

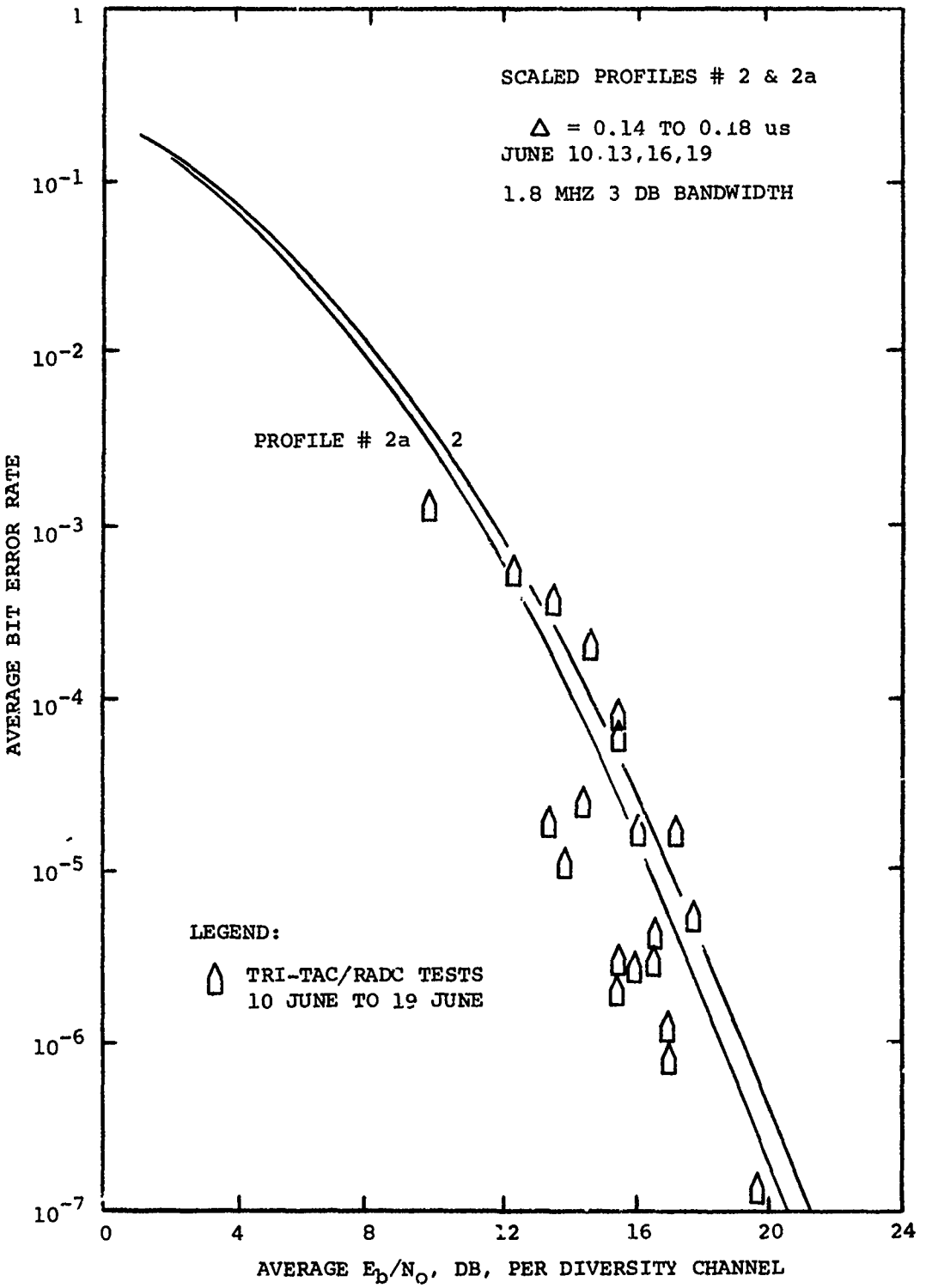

FIGURE 4-34 AN/TRC-97 DUAL DIVERSITY PERFORMANCE AT 1.75 MBPS

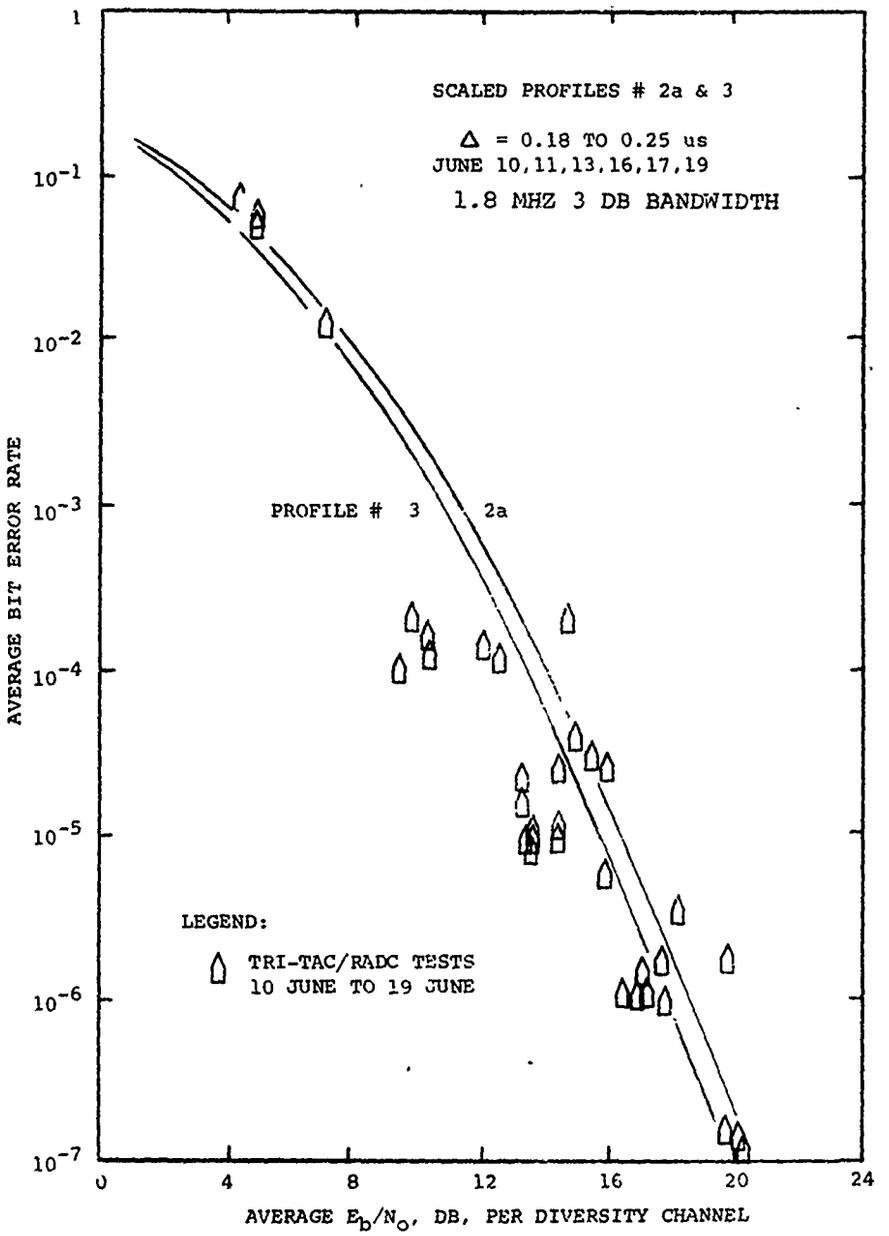

FIGURE 4-35 AN/TRC-97 DUAL DIVERSITY PERFORMANCE AT 1.75 MBPS

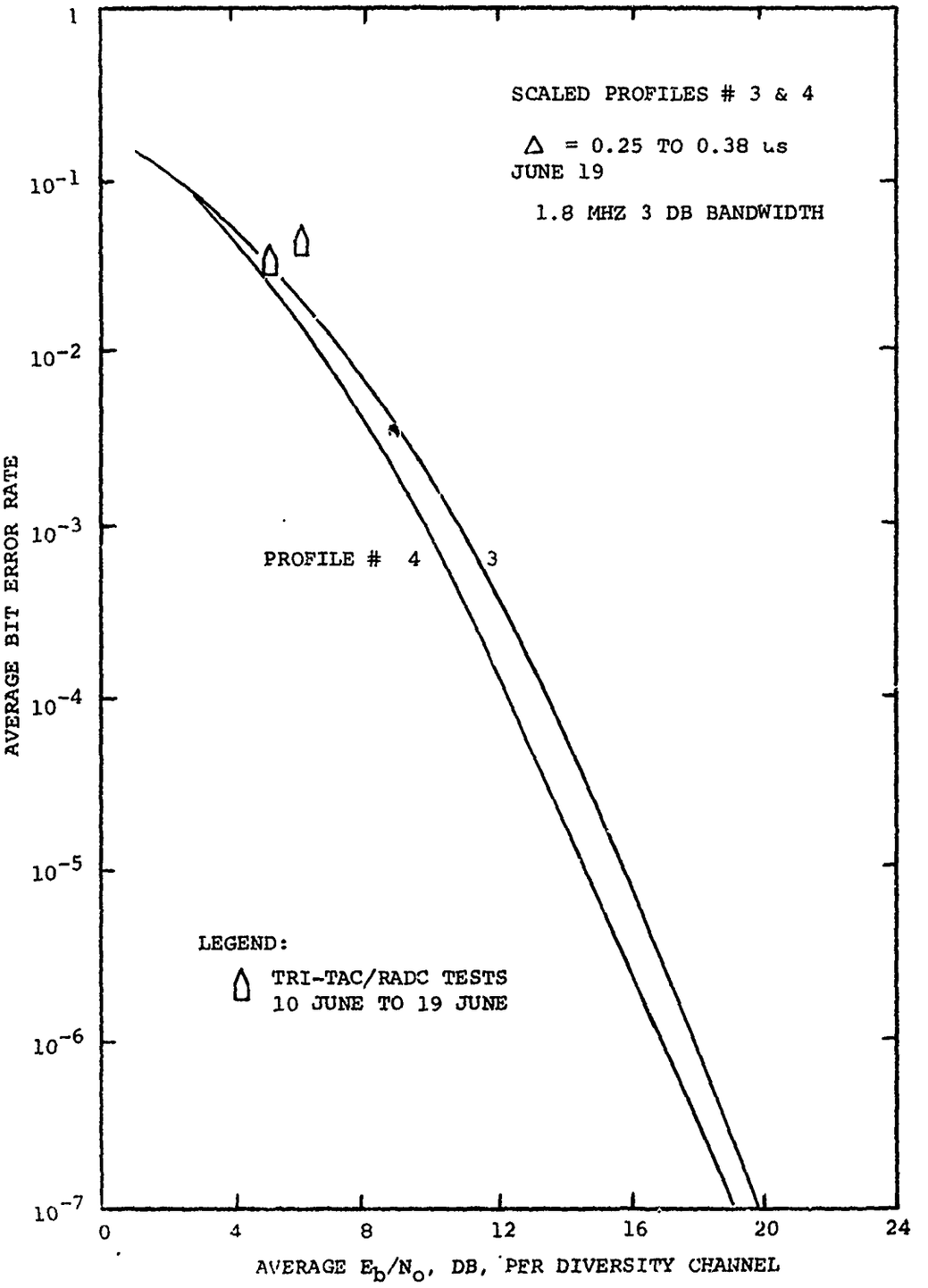

FIGURE 4-36 AN/TRC-97 DUAL DIVERSITY PERFORMANCE AT 1.75 MBPS

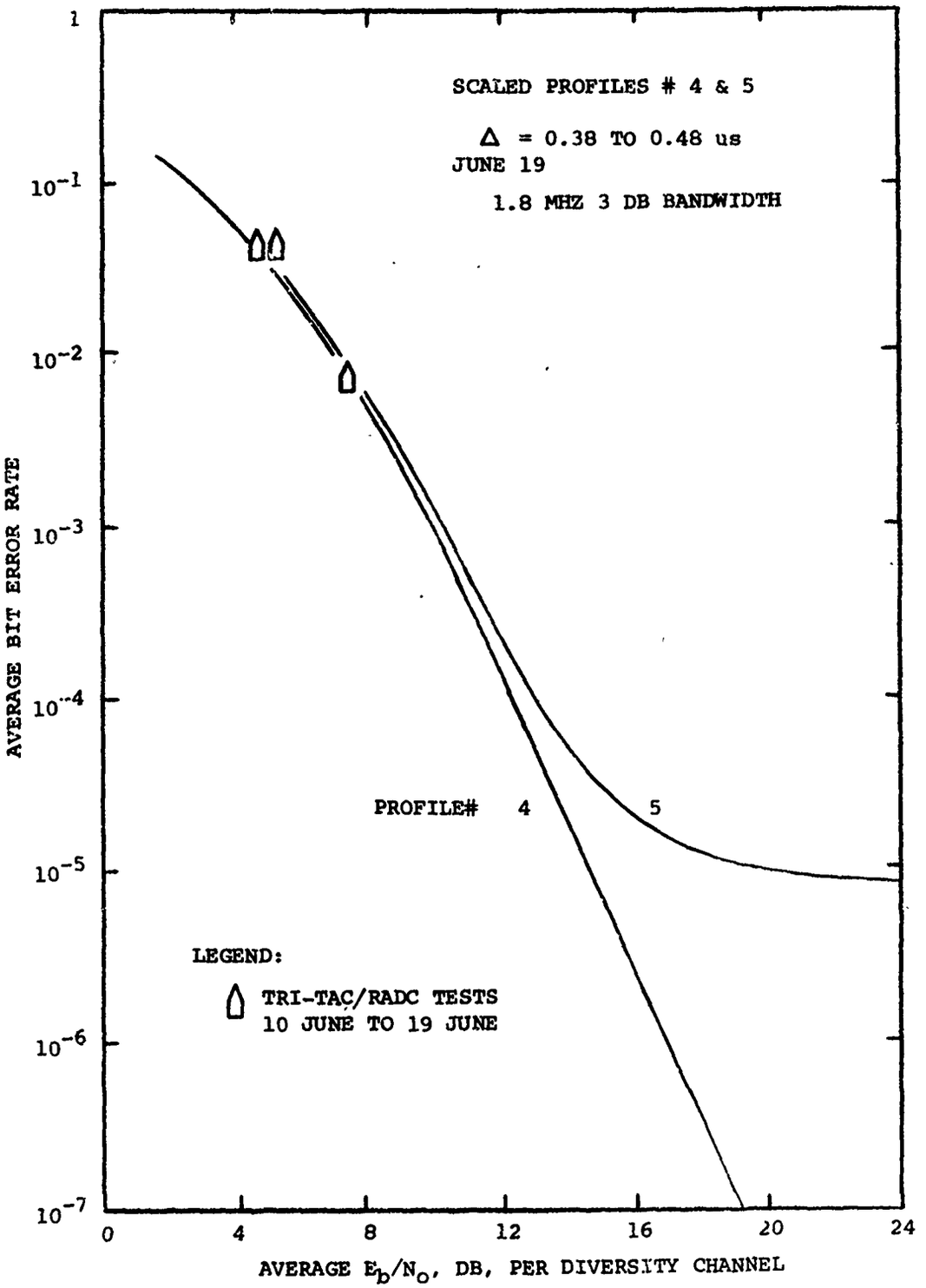

FIGURE 4-37 AN/TRC-97 DUAL DIVERSITY PERFORMANCE AT 1.75 MBPS

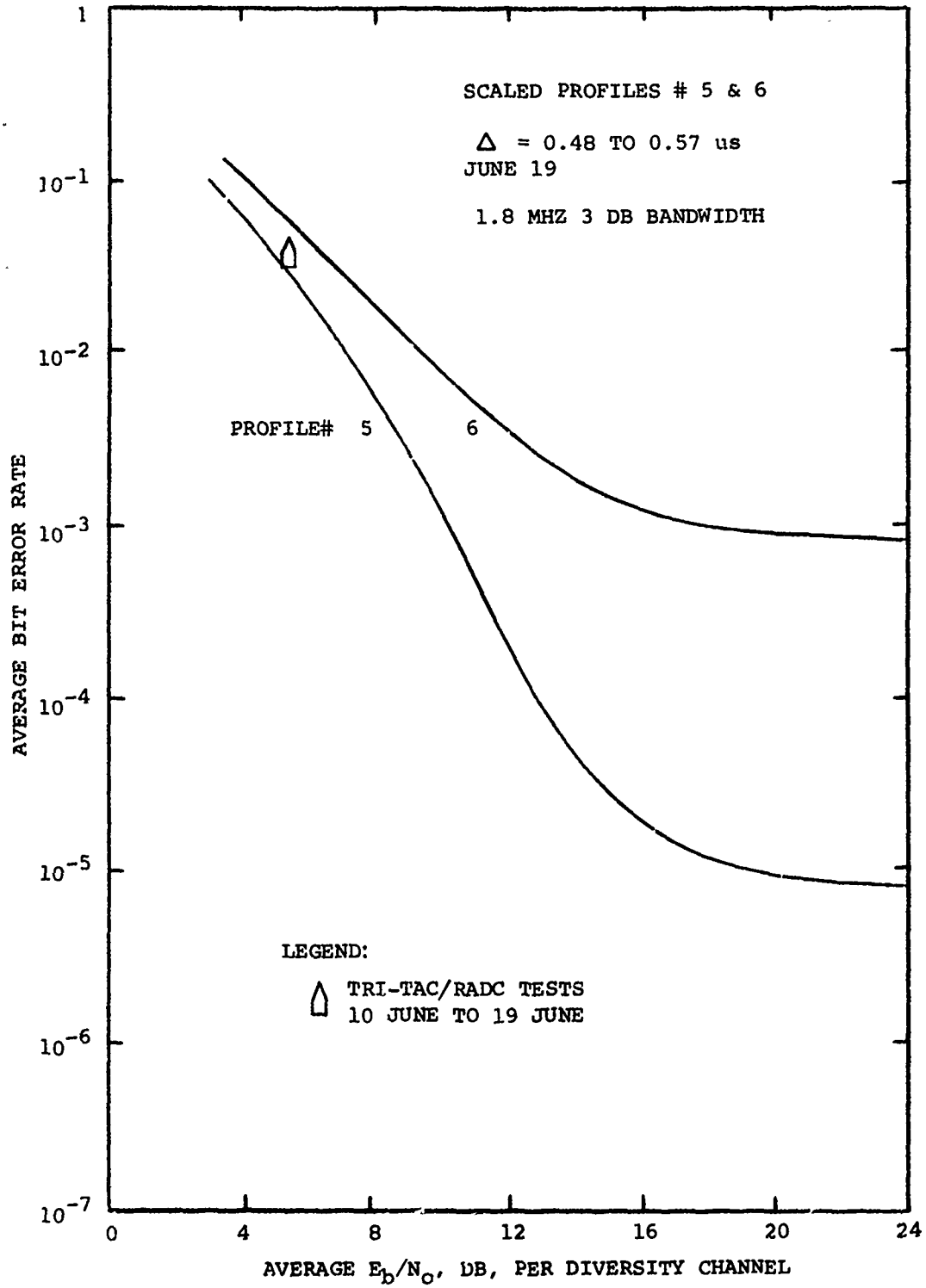

signal bandwidths. If this reference circuit were redesigned, the gain in signal energy and intrinsic diversity should lead to successful 7.0 Mb/s testing on the AN/MRC-98.

Math Model predictions and NBS-101 path loss statistics were combined to generate an availability prediction for the AN/MRC-98 as shown in Figure 4-38 (solid lines). This figures shows the cumulative probability that a given BER level will be available at 1.75, 3.5, and 7 Mb/s using the transmit power backoff experimentally determined and the DAR-IV predicted performance from the Math Model. The availability predictions are shown only for quad diversity since this is the normal operating mode of the equipment. The experimental data points are also shown from the over-the-air tests. Note that the availability experimentally obtained is substantially poorer than predicted. This difference is mainly due to the fact that the tests were performed during the worst propagation conditions for the 168 mile path when signal medians are 15 to 20 dB below the yearly average. The unequal median of the diversity channels also resulted in less diversity gain than anticipated.

The tests on the C-band AN/TRC-132 were conducted at 1.75, 3.5 and 7 Mb/s. Although there was a local oscillator spurious oscillation (break lock phenomenon) problem that occurred in many of the test runs, the tests clearly showed that 1.75, 3.5 and 7 Mb/s could be achieved with low BER by the DAR-IV on a properly functioning radio equipment. Five minute BER samples which were free of the oscillator instability showed very low BER values indicating high levels of intrinsic diversity gain.

An availability prediction was also prepared for the 168 mile AN/TRC-132 link as shown in Figure 4-39. Agreement here between theory and experiment is much better than for the AN/MRC-98 link of Figure 4-38. However, the results are still significantly to the left of the yearly availability. Part of this discrepancy is due to the local oscillator "break-lock" phenomenon and oscillator jitter. A "jittery" local oscillator can lead to the modem degradation indicated.

Tests performed on the AN/TRC-97 were relatively free of radio equipment malfunctions. A large number of test points were obtained at 1.75 Mb/s and some data was also taken at 3.5 Mb/s. The BER samples were interleaved with multipath spread measurements and excellent agreement between the over-the-air results and previous channel simulator tests was observed. As with the other paths, no problems due to anomalous propagation were observed.

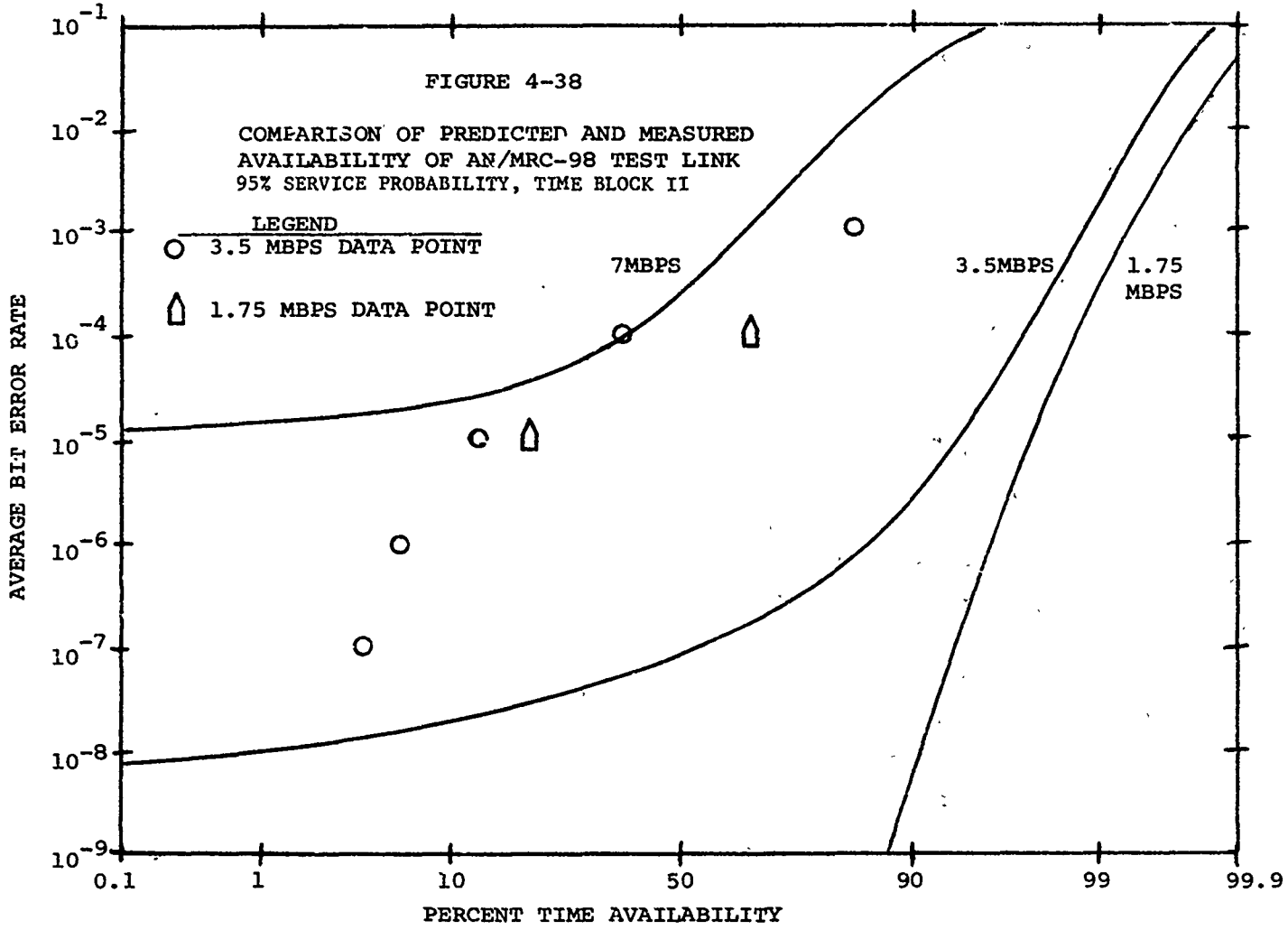
FIGURE 4-38
COMPARISON OF PREDICTED AND MEASURED AVAILABILITY OF AN/MRC-98 TEST LINK 95% SERVICE PROBABILITY, TIME BLOCK II
LEGEND
3.5 MBPS DATA POINT
1.75 MBPS DATA POINT
7MBPS
3.5MBPS
1.75 MBPS
AVERAGE BIT ERROR RATE
10^{-1}
10^{-2}
10^{-3}
10^{-4}
10^{-5}
10^{-6}
10^{-7}
10^{-8}
10^{-9}
0.1
1
10
50
90
99
99.9
PERCENT TIME AVAILABILITY

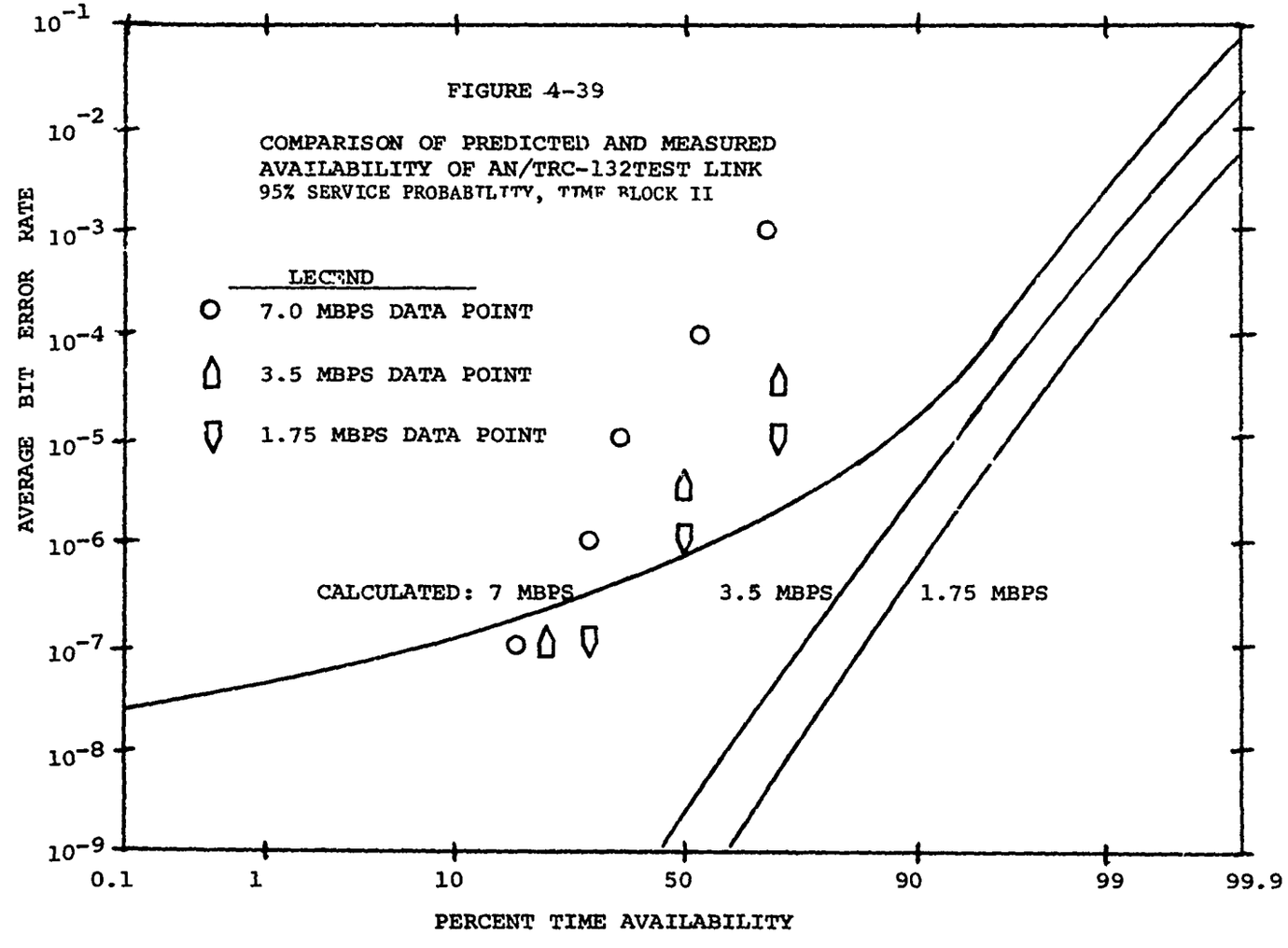

FIGURE 4-39

COMPARISON OF PREDICTED AND MEASURED AVAILABILITY OF AN/TRC-132TEST LINK 95% SERVICE PROBABILITY, TIME BLOCK II

5.0 HYBRID TEST RESULTS

5.1 Introduction

One of the operational configurations of the DAR-IV is a hybrid mode consisting of analog FDM/FM data and digital data. This operational mode is achieved by using two subcarriers centered around the 70 MHz IF frequency. The upper subcarrier contains the 1.75 Mb/s digital data stream whereas the lower subcarrier contains 24, 48 or 60 channels of FM traffic. The DAR-IV transmit unit contains a single Hybrid Translator plug-in module that provides the necessary frequency translations to permit simultaneous transmission of the digital and analog data. The digital portion of the DAR-IV transmit unit operates the same as in the all digital mode generating a pair of 70 MHz QPSK carriers. The analog FM data is supplied to the DAR-IV as a 70 MHz FM carrier. The hybrid translator then translates these two 70 MHz carriers above and below the center frequency by 1.75 MHz. This is the composite signal to be supplied to the tropo radio equipment.

The DAR-IV receive unit contains a pair of Hybrid Translator plug-in modules that accept the composite signals from up to four tropo radio receivers. These translators essentially undo the operation performed by the DAR-IV transmit translator and provide 70 MHz FM signals for predetection combining and FM demodulation as well as 70 MHz QPSK signals to be used by the DAR-IV for digital demodulation.

5.2 Theory of Operation

Figure 5-1 shows a block diagram of the dual carrier transmit system, while Figure 5-2 illustrates the corresponding diversity receiver. The system interface between hybrid digital and analog modulation is at the nominal 70 MHz IF. The DAR-IV QPSK modulator is designed so that it can be optimized for all analog loading from 24 to 60 channels. Table 5-1 lists the FM IF subcarrier frequencies and the DAR-IV subcarrier frequency at the up-converter input to achieve the desired nominal composite hybrid signal bandwidth. Both the digital IF waveform and the FDM/FM IF waveform are strictly bandlimited in sharp cut-off filters to prevent interference and crosstalk. Adequate filtering can be employed to insure that a back-to-back analog NPR of at least 55 dB is achievable together with a digital BER of less than 10^{-7}.

Note that the addition to the AN/MRC-98 transmitter is very simple. A relatively simple translation oscillator and sharp cut-off filter are added to the output of the AN/MRC-98 FM modulator to shift the FDM/FM signal slightly in frequency and also strictly bandlimit it. To the resultant signal is added the output of the DAR-IV modulator which contains its own internal frequency control and bandlimiting. The resultant hybrid signal is finally passed to the AN/MRC-98 dual frequency diversity transmit chain

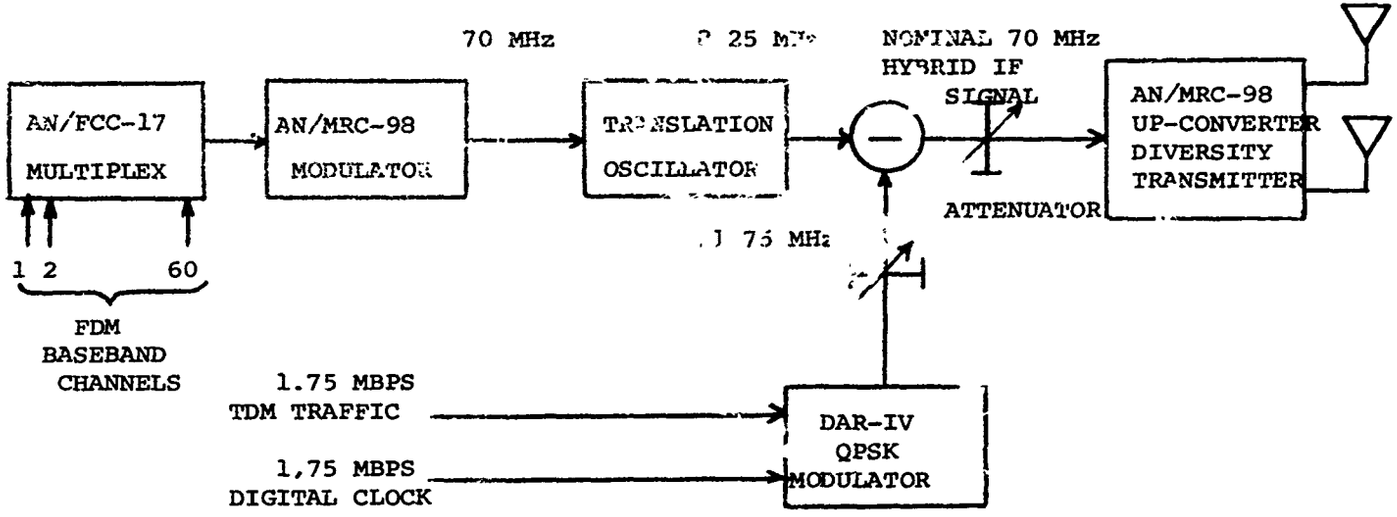

FIGURE 5-1 HYBRID MODULATOR BLOCK DIAGRAM
1.75 MBPS DIGITAL DATA - 24, 48, OR 60 CHANNEL ANALOG

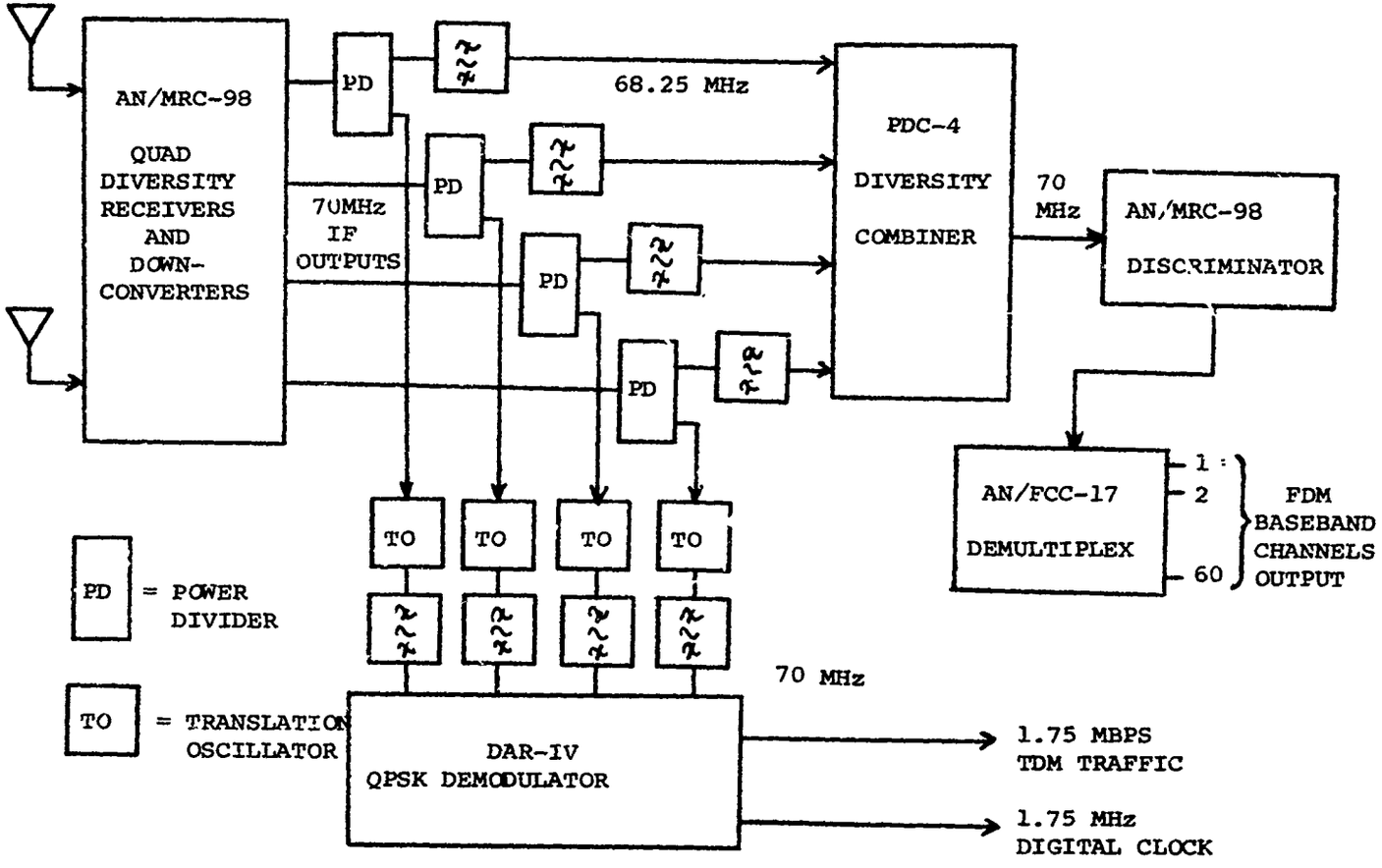

FIGURE 5-2 HYBRID DEMODULATOR BLOCK DIAGRAM FOR
1.75 MBPS DIGITAL LOADING AND UP TO 60 CHANNELS ANALOG

TABLE 5-1

DUAL SUBCARRIER CHARACTERISTICS FOR 1.75 Mbps OPERATION

NO. OF FDM CHANNELS	FM BANDWIDTH (MHZ) MODULATION INDEX = 3	FM SUBCARRIER MHz	DAR 1.75 Mbps QPSK DIGITAL BANDWIDTH, MHz	SUBCARRIER MHz	HYBRID 3 dB BANDWIDTH MHz
24	1.5	68.25	3.5	71.75	5.0
48	2.5	68.25	3.5	71.75	5.5
60	3.0	68.25	3.5	71.75	6.0

through a precision attenuator for amplitude control.

The corresponding hybrid receiver is shown in Figure 5-2. Each diversity output of the AN/MRC-98 at the nominal 70 MHz IF is split two ways. One path is filtered by a bandpass filter centered at the IF frequency of the FDM/FM subcarrier (68.25 MHz) and then translated to 70 MHz IF. This signal then contains only the FDM/FM modulation and it is passed on to the usual PDC-4 diversity combiner input with the three other corresponding diversity signals.

The other output of the power splitter is also passed to a frequency translator which translates the 71.75 MHz digital subcarrier to 70 MHz. This translation allows the use of the same DAR-IV demodulator for both the 1.75 and 3.5 MHz operation with only a few plug-in module circuit alterations. The translation oscillator output is also filtered by an appropriate bandpass filter centered at the 70 MHz second IF. This filter isolates the digital signal from the FDM/FM carrier and eliminates intercarrier interference. The DAR-IV demodulator accepts the four diversity channels of multipath corrupted QPSK pulses and provides adaptive matched filter detection (of each individual diversity channel) together with maximal ratio combining all received frequency and space signal energy. Output signals consisting of the demodulated 1.75 Mb/s digital data as well as the recovered digital clock are provided by the DAR-IV. A clock recovery Phase Locked Loop (PLL) time constant of several seconds insures data synchronization maintenance even during deep fades.

The anticipated analog performance for the proposed hybrid modulation technique with up to 60 channel loading will be essentially unchanged from normal FDM/FM only transmission. The only change to the FDM/FM carrier is to shift it to one side of the channel bandwidth and reduce its transmission level. Shifting the FDM/FM carrier to one side of the channel bandwidth may result in some additional group delay distortion due to the bandpass characteristics of the klystron power amplifier. If excess group delay distortion is encountered, a phase equalization filter will be inserted into the FDM/FM carrier path to reduce it to an insignificant level.

To maintain a 55 dB NPR in the analog system under back-to-back operation, the carrier to interference (C/I) must be greater than 28 dB for a deviation index of 3. An $n = 5$, 0.1 dB ripple, Chebyshev filter with bandwidth consistent with Table 5-1 can be used to confine the digital signal and prevent C/I lower than 28 dB in the FM signal.

Measurements on a typical klystron power amplifier reveal that for two carrier operation, a backoff of 6 dB from saturated carrier operation results in a carrier to interference ratio of about 30 dB. For 8 dB backoff, this number reduces to 40 dB. The required backoff varies slightly from one klystron to another, but a 6 dB backoff should yield a reasonable

compromise between efficiency and intermodulation noise. For the Youngstown-Verona link with 24 channel FDM loading, the path induced intermodulation noise (due to frequency selectivity) results in a median NPR of only about 46 dB. For 60 channel operation, this IM induced NPR is only about 38 dB. Hence, the klystron PA backoff can be reduced to only 4 to 5 dB and still provide over-the-air analog performance which is degraded less than 3 dB by the presence of digital loading.

5.3 Over-the-Air Test Program

5.3.1 General

A series of over-the-air tests were conducted to evaluate the performance of the DAR-TT operating in the hybrid configuration. The purpose of these tests was to investigate the mutual interference effects of the digital and analog signals as well as evaluating the level of performance of the transmission mode relative to an all digital or all FM system.

Over-the-air testing was conducted on the RADC Tropo Experimental Range. The Hybrid Tropo Transmission System (HTTS) was first interfaced with the AN/MRC-98 at the Verona, New York, test site. Back-to-back testing was then conducted at Verona to ensure proper operation of the deliverable equipment and also proper alignment of the receivers, filters and down converter oscillators. These tests also verified the alignment of the FDM/FM mulitplex equipment and voice channel signal to noise ratio recording equipment.

These back-to-back tests were also repeated at the Youngstown, New York, transmitting site. At the Youngstown site, special emphasis was placed on the alignment of the filter characteristics of the up-converter, exciter, and power amplifier of the transmission chain. Using a Network Analyzer, the best tuning of the power amplifier was experimentally established for maximum amplitude and group delay "flatness". The backoff of the power amplifier drive signal was experimentally investigated to produce acceptable analog digital mutual interference levels in back-to-back operation. The highest transmission level which yielded acceptable back-to-back performance was then employed.

After system alignment, the modulator unit of the HTTS remainded interfaced with the Youngstown transmitter. the HTTS demodulator was again interfaced with the Verona receivers for the nominal 200 mile link. Various receiver configurations were tested including non, dual and quad path diversity operation of the HTTS.

Over-the-air tests were conducted on a daily basis for a period of approximately two weeks. The data consists of a number of test runs of about 10 minutes duration. In each run, the Received Signal Level (RSL) for each diversity receiver, the analog signal to noise ratio (using a test tone), and the bit error occurrences were recorded. At the end of each run, the median RSL, average voice signal to noise ratio, and average bit error rate were computed and recorded in a test log. The tests were repeated for the various receiver diversity configurations of the HTTS. Also, any losses of bit count integrity in the digital performance such as loss of receiver synchronization were recorded in the test log.

5.3.2 System Calibration

The basic over-the-air system configuration is illustrated by Figure 5-3 and 5-4 in the hybrid transmission mode. Calibration procedures were performed by RADC and AFCS personnel for measurement of deviation index (by carrier drop-out), adjustment of oscillator frequencies and interface levels. To employ the PDC-4 combiner and hybrid demodulator, it is desirable to ensure that all diversity IF frequencies are within 500 Hz of the 70 MHz center frequency. An unmodulated carrier was transmitted from Youngstown and all down-converter local oscillators were adjusted to meet this condition. The oscillator stability was found to be adquate to maintain this condition with only periodic readjustment.

Variable attenuators were also placed in each IF input line to the PDC-4 predetection combiner and DAR-IV demodulator. These attenuators were then adjusted so that the level of front-end thermal noise is equal on all diversity IF signals. This procedure results in optimum operation of the PDC-4 for maximal ratio carrier to noise weighting.

5.3.3 Back-to-Back Testing

To establish a performance baseline and verify proper equipment operation, back-to-back tests will be first performed at the Verona (receiving) site. Figure 5-5 shows a block diagram of the test configuration to measure both analog NPR and digital BER performance. Unlike the laboratory tests which used a simple Marconi FDM noise loading test set for NPR measurements, the on-site back-to-back tests employ the AN/FCC-17 frequency multiplex and individual channel noise loading.

Noise loading of the AN/FCC-17 multiplex to simulate the FDM traffic was accomplished with an RADC multiple channel noise generator. Initially, 24, 48 or 60 channels of the multiplex were all equally noise loaded so that the composite baseband deviation index of 3 was achieved. The multiplex output was then connected directly to the demultiplex input for back-to-back NPR testing of the AN/FCC-17 alone. An RADC NPR test set was used to measure analog performance in several of the baseband channels.

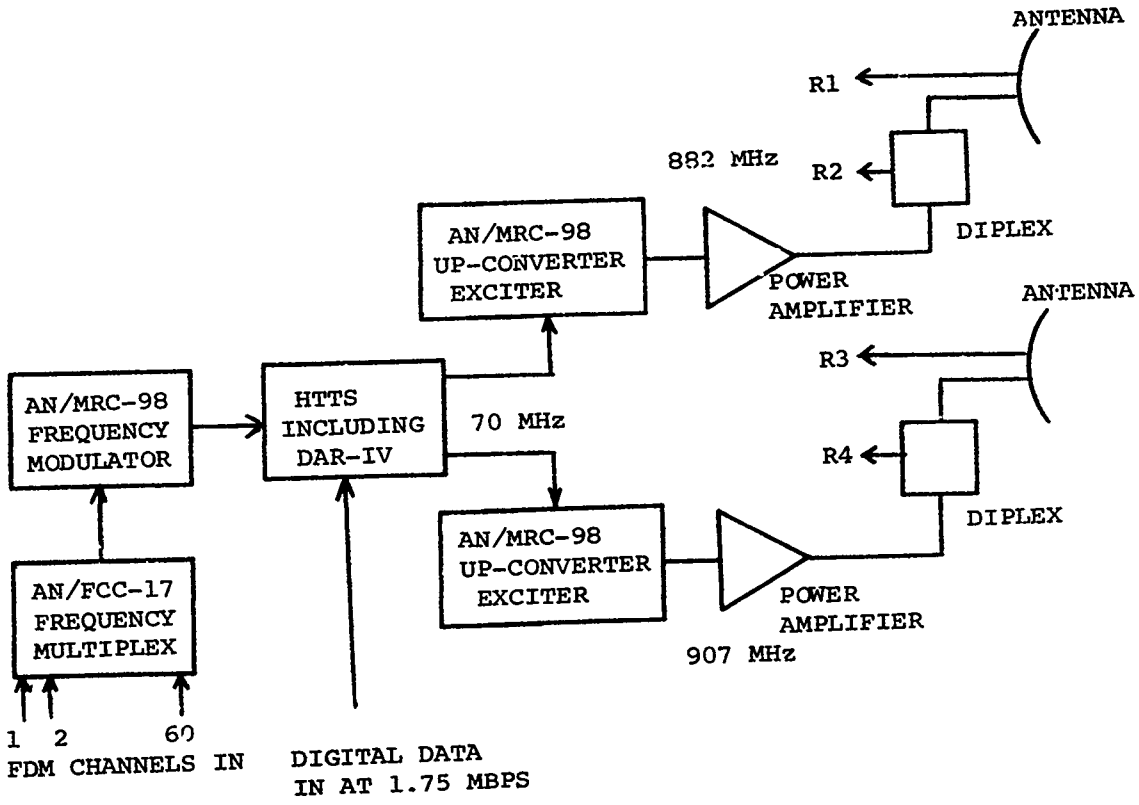

FIGURE 5-3 QUAD DIVERSITY TRANSMIT SITE CONFIGURATION (YOUNGSTOWN)

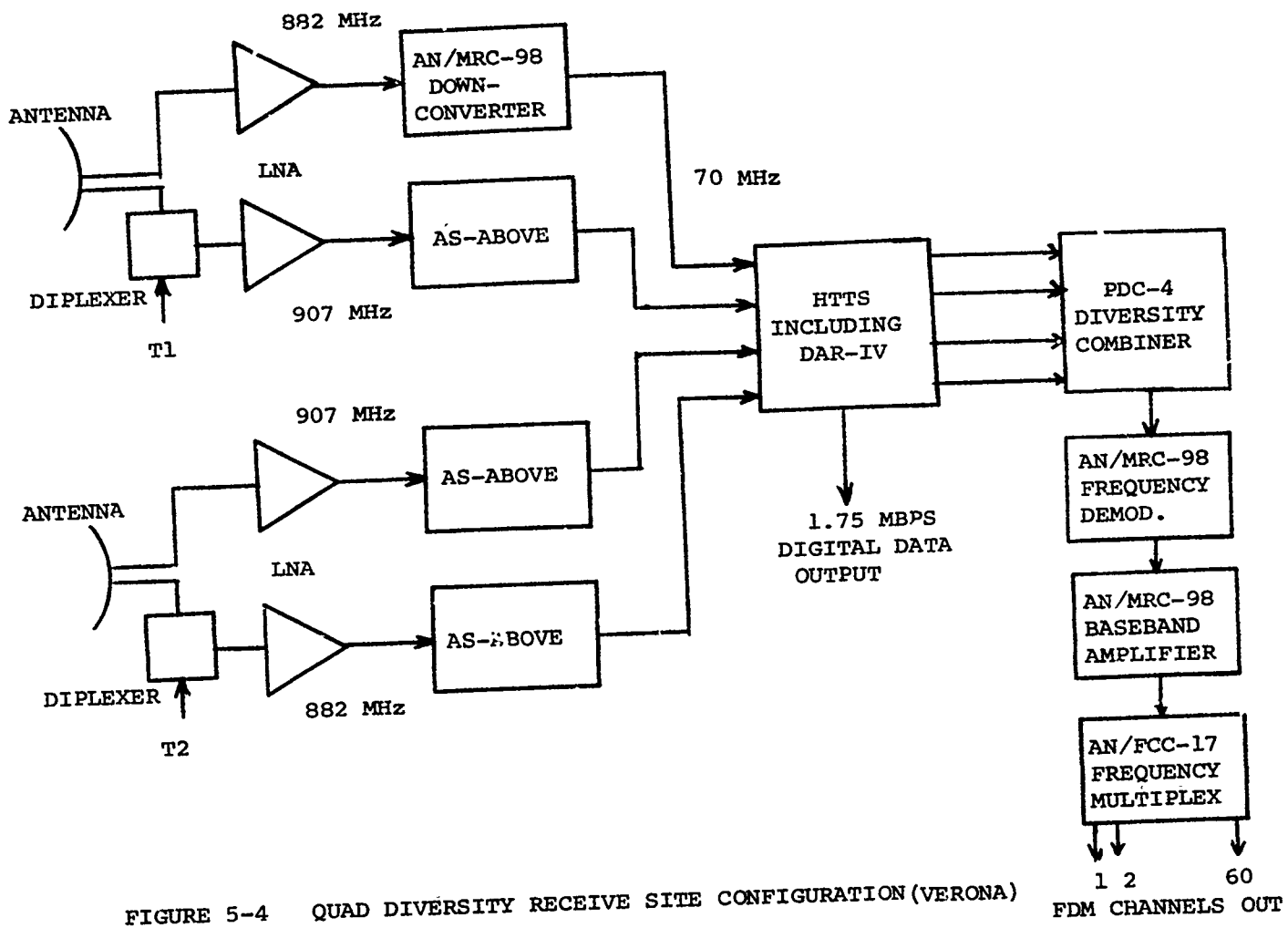

FIGURE 5-4 QUAD DIVERSITY RECEIVE SITE CONFIGURATION (VERONA)

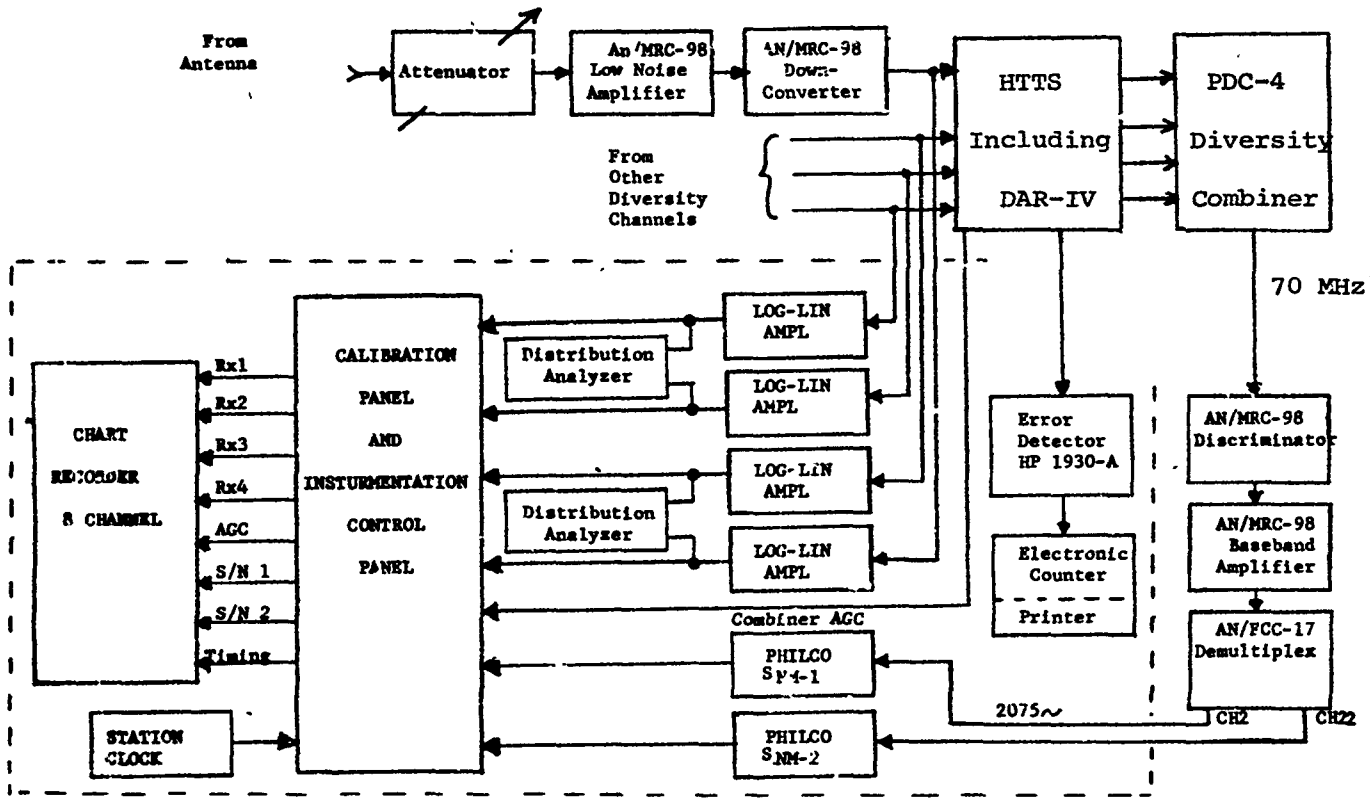

FIGURE 5-5 STATION TEST INSTRUMENTATION FOR OVER-THE-AIR TESTING

Previous back-to-back testing of the AN/FCC-17 with all 24 channels loaded showed a maximum NPR of only 28 to 32 dB across the entire baseband. Examination of the schematic diagram of the AN/FCC-17 revealed that a common frequency translation sub-carrier was shared by two symmetrically located baseband channels. It was subsequently determined that noise loading of one channel of a pair will cause crosstalk into the other, unoccupied channel which is down by only about 30 dB. This multiplex performance would make it impossible to measure NPR or voice channel SNR above about 30 dB. Hence, to overcome this problem only the even numbered channels of the baseband were noise loaded (the odd numbered channels left inactive). In this mode of operation, crosstalk was eliminated and NPR on the order of 50 dB was measured in the even numbered channels. The composite levels of the individual noise signals were increased so that the overall FM deviation index was equal to 3. Since the simulated baseband signal is still spread across the appropriate baseband range and provided the correct deviation index very little loss in test usefulness or effectiveness results.

During the process of making back-to-back measurements, the Philco baseband SNR test sets were also calibrated against the RADC NPR test set. Both methods of measuring analog performance showed good agreement. The Philco SNR test sets were later used to measure analog performance in the over-the-air tests as described in the following section.

5.3.4 Over-the-Air Testing

To conduct over-the-air tropo testing, the HTTS Modulator was installed at the Youngstown, New York, transmitter site. This installation was an exact duplicate of that employed for back-to-back testing at Verona. The simulated traffic set up at the transmit site was for 24, 48 or 60 channel FDM loading and 1.75 Mbps TDM loading.

The simulated FDM channel loading consisted of individual noise loading of all even numbered channels except for a channel which is loaded by a test tone as explained below. The composite deviation (channel amplitude) was then adjusted to provide an FM deviation of three as in the back-to-back testing. The simulated digital traffic was obtained by use of a Hewlett-Packard Digital Test Set (HP1930A).

After testing and transmitter alignment had been successfully completed at Youngstown, over-the-air testing was started and for each test conducted, the median received signal plus noise level was recorded together with the analog signal to noise ratio and the average digital Bit Error Rate (BER). The analog signal to noise ratio was measured by inserting a 2075 Hz tone in one of the voice channels and measuring the received test tone signal to noise ratio on the Philco test set. The average digital BER was measured by accumulating error counts over the test period.

The RADC receiving site test instrumentation was employed to record on strip charts the IF signal plus noise level of each diversity carrier, the PDC-4 combiner AGC level and the Philco signal to noise ratio meter reading in an AN/FCC-17 voice channel slot near the upper end of the baseband. Cumulative digital errors were recorded using the HP counter/paper tape printer combination. Each test period of approximately 10 minute duration was keyed by and under control of the RADC test instrumentation and calibration control console.

On-line, RADC distribution analyzers were employed to determine the median carrier plus noise level of each diversity signal and this information was also entered in the test data log. A data log was jointly maintained by the RADC site engineer and Raytheon personnel. This log contains the pertinent statistics of each test run including time-of-day, type of run (order of diversity, type of loading, equipment mode), distribution analyzer readings, and average BER.

Each test consisted of taking a number of data points of analog and/or digital performance versus median received signal level. Ideally, at the low fade rates of the test link, each data point should represent an average over a several hundred minute test run. However, due to short term fading of the median signal level, it is not practical to accumulate data points of more than 10 to 20 minute duration. As a result, each test run must be repeated a larger number of times (5 to 10 times), in order to obtain a statistically meaningful "scatter plot" of the performance.

Because of the large amount of time required to obtain statistically meaningful data (8 to 16 hours per test), the number of different test conditions which could be accommodated during the duration of the over-the-air program was limited. In testing, primary emphasis was placed on normal quad diversity operation of 24 or 48 channel analog loading together with 1.75 Mbps digital loading. The case of 48 channel analog loading with 1.75 Mbps digital loading was examined more thoroughly in terms of non, dual, and quad diversity operation as well as no digital or no analog loading.

5.4 Hybrid Test Results (Digital)

Test data was taken for 24 and 48 channel analog and 1.75 Mb/s digital data for non, dual and quad orders of diversity. This digital error rate performance for the hybrid transmission mode is illustrated in Figures 5-6 through 5-11. Due to a combination of low received signal levels, time limitations, and test equipment failures, no data was taken at 60 channel FM loading and not as much data was recorded as was desired.

Figure 5-6 shows the test results for 24 channel FM loading in the non-diversity configuration. Measured error rates of from 10^{-1} to 10^{-3} were obtained during this sequence of tests with received signal levels ranging from about 19 to 23 dB E_b/N_o. Also shown by the dashed lines is the theoretical performance for a CPSK modem with non-diversity (flat fading) and dual effective diversity. The theoretical modem is assigned a 3 dB loss due to power sharing (at the receiver) between digital and analog carriers and a 3 dB modem implementation loss. Note that the data points are clustered about the non-diversity curve (within the measurement accuracy) and show somewhat less intrinsic diversity gain than the non-hybrid case previously described. Actually, the amount of intrinsic diversity gain achieveable is not that much different than for the digital only case since the pulse 3 dB bandwidths are similar.

The dual diversity performance with 24 channel loading is illustrated in Figure 5-7. A reasonably large number of data points was obtained for this configuration. Here error rates from greater than 10^{-1} to almost 10^{-4} were recorded. The combining efficiency of the DAR-IV can be seen by comparing these results with those for non-diversity in Figure 5-6. The results are generally clustered about the anticipated dual diversity flat-fading performance with occasional improvements due to intrinsic diversity and occasional degradations due to unequal channel median levels as previously described in Section 4.2.

Figure 5-8 shows the results for 24 channel loading in a quad diversity configuration. Receiver signal levels during these tests were lower than during the previous tests. This coupled with some antenna problems precluded taking very many data points. It can be seen, however, that there is improvement in error rate due to the added orders of diversity. Note, however, that the data points are somewhat above the flat fading prediction. This effect is due to unequal median channel levels (as previously described for the AN/MRC-98) which produced some loss in effective diversity gain.

The next series of tests were run for 48 channel FM loading in non, dual and quad diversity configurations. Figure 5-9 illustrates the digital error performance for the non-diversity configuration. Comparison of Figures 5-9 and 5-6 reveals that similar digital error rate performance was obtained for both 24 and 48 channel loading.

In similar fashion Figure 5-10 demonstrates the performance for dual diversity. Comparing these results with those of Figure 5-7 for channel loading again shows the minimal effect on the digital performance with increased channel loading.

Lastly, the quad diversity results may be seen in Figure 5-11. Here it can be seen that a good range of received signal levels was obtained

FIGURE 5-6

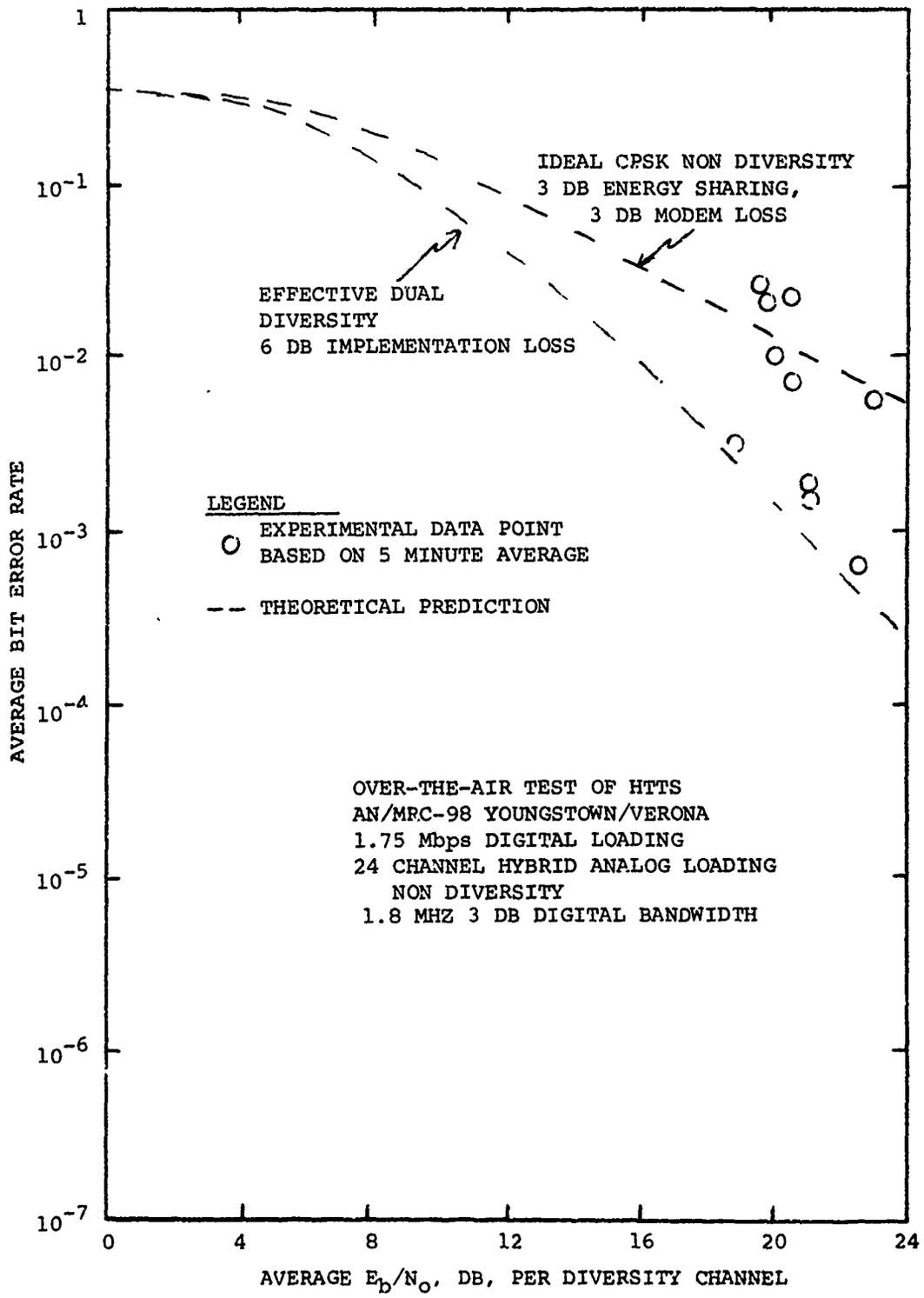
1
10^{-1}
10^{-2}
10^{-3}
10^{-4}
10^{-5}
10^{-6}
10^{-7}
AVERAGE BIT ERROR RATE
IDEAL CPSK NON DIVERSITY
3 DB ENERGY SHARING,
3 DB MODEM LOSS
EFFECTIVE DUAL
DIVERSITY
6 DB IMPLEMENTATION LOSS
LEGEND
EXPERIMENTAL DATA POINT
BASED ON 5 MINUTE AVERAGE
THEORETICAL PREDICTION
OVER-THE-AIR TEST OF HTTS
AN/MRC-98 YOUNGSTOWN/VERONA
1.75 Mbps DIGITAL LOADING
24 CHANNEL HYBRID ANALOG LOADING
NON DIVERSITY
1.8 MHZ 3 DB DIGITAL BANDWIDTH
0
4
8
12
16
20
24
AVERAGE E_b/N_o, DB, PER DIVERSITY CHANNEL

FIGURE 5-7

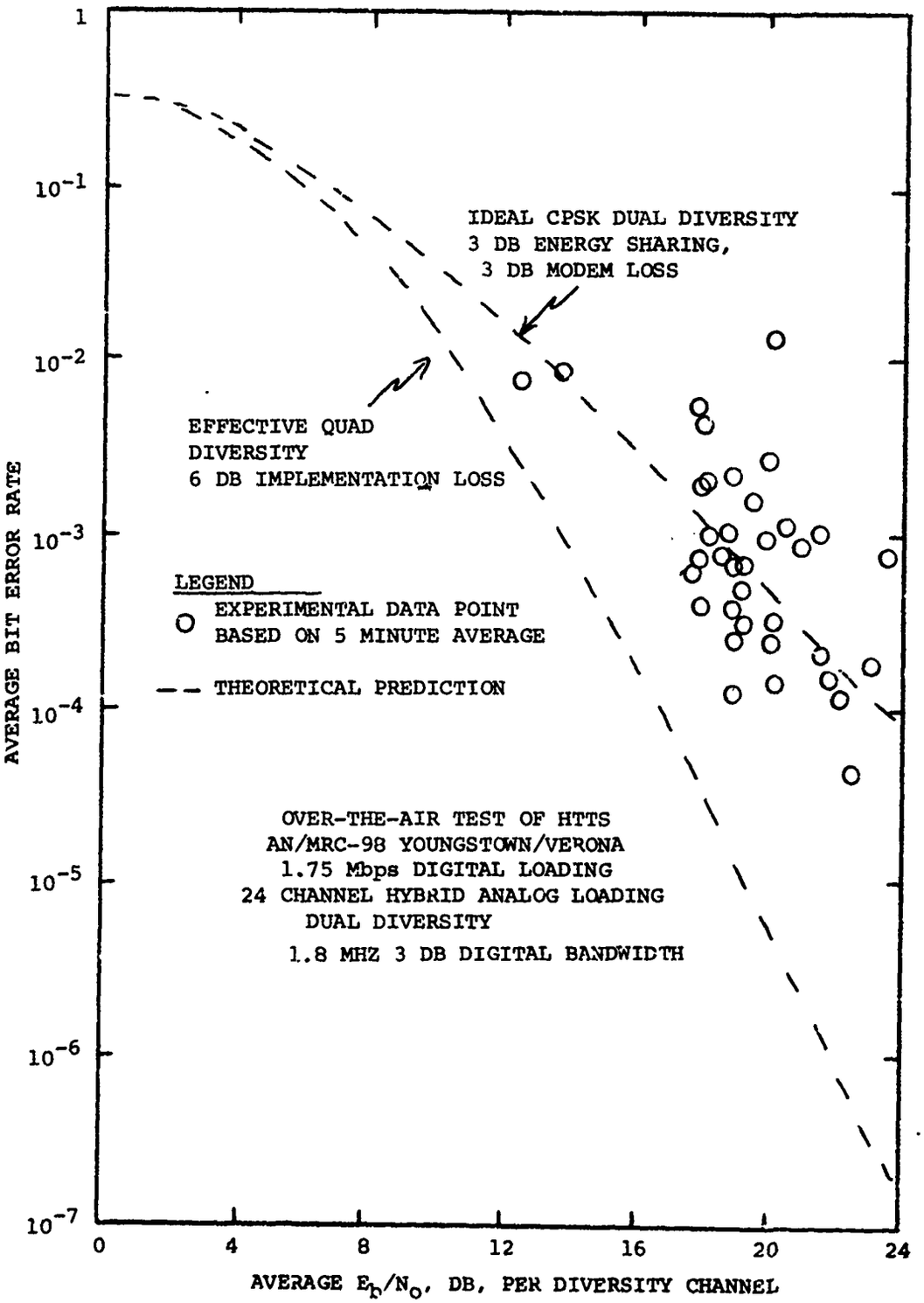
1
10^{-1}
10^{-2}
10^{-3}
10^{-4}
10^{-5}
10^{-6}
10^{-7}
AVERAGE BIT ERROR RATE
IDEAL CPSK DUAL DIVERSITY
3 DB ENERGY SHARING,
3 DB MODEM LOSS
EFFECTIVE QUAD
DIVERSITY
6 DB IMPLEMENTATION LOSS
LEGEND
EXPERIMENTAL DATA POINT
BASED ON 5 MINUTE AVERAGE
THEORETICAL PREDICTION
OVER-THE-AIR TEST OF HTTS
AN/MRC-98 YOUNGSTOWN/VERONA
1.75 Mbps DIGITAL LOADING
24 CHANNEL HYBRID ANALOG LOADING
DUAL DIVERSITY
1.8 MHZ 3 DB DIGITAL BANDWIDTH
0
4
8
12
16
20
24
AVERAGE E_b/N_o, DB, PER DIVERSITY CHANNEL

FIGURE 5-9

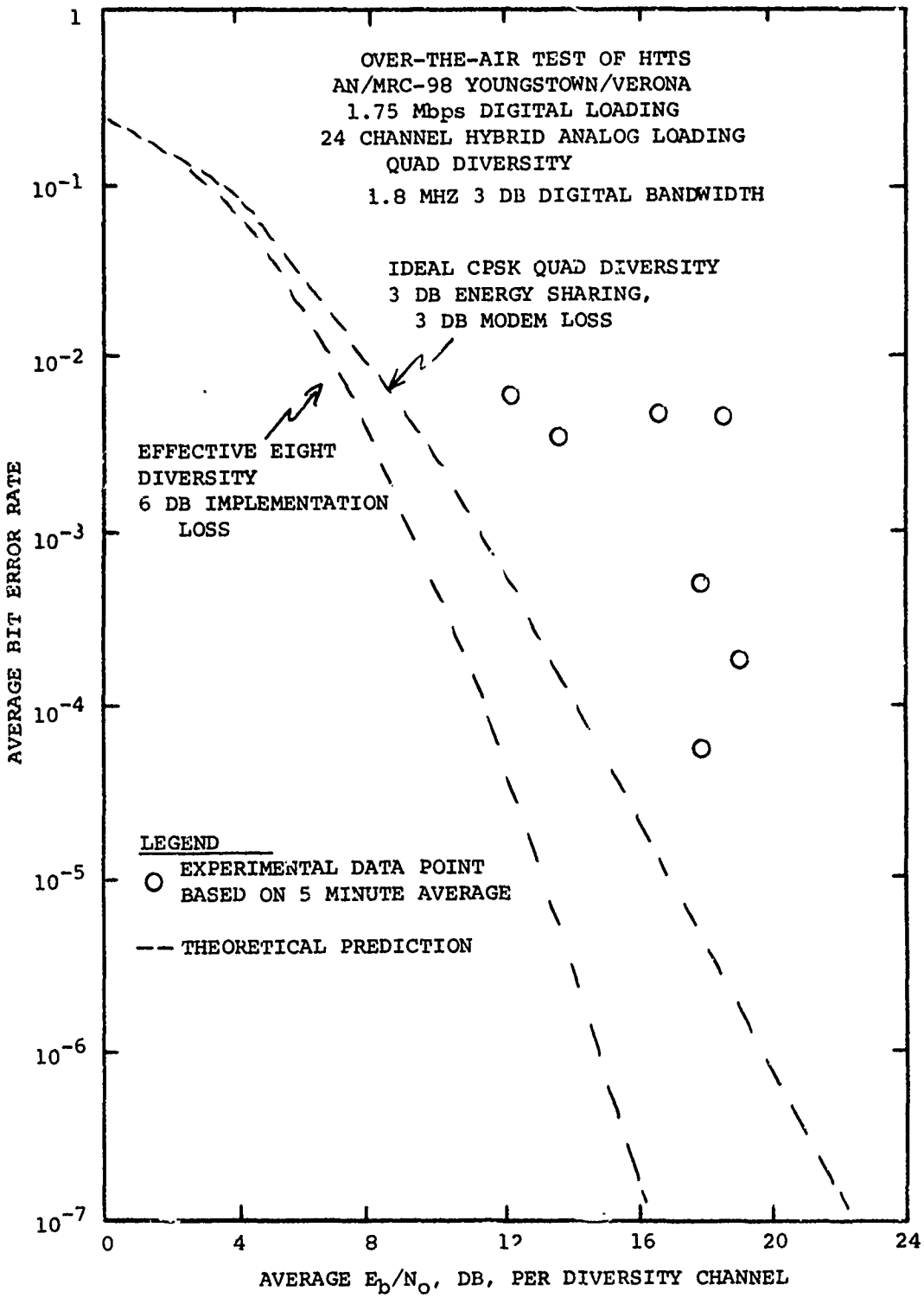
OVER-THE-AIR TEST OF HTTS
AN/MRC-98 YOUNGSTOWN/VERONA
1.75 Mbps DIGITAL LOADING
24 CHANNEL HYBRID ANALOG LOADING
QUAD DIVERSITY
1.8 MHZ 3 DB DIGITAL BANDWIDTH
IDEAL CPSK QUAD DIVERSITY
3 DB ENERGY SHARING,
3 DB MODEM LOSS
EFFECTIVE EIGHT
DIVERSITY
6 DB IMPLEMENTATION
LOSS
LEGEND
EXPERIMENTAL DATA POINT
BASED ON 5 MINUTE AVERAGE
THEORETICAL PREDICTION
AVERAGE BIT ERROR RATE
1
10^{-1}
10^{-2}
10^{-3}
10^{-4}
10^{-5}
10^{-6}
10^{-7}
0
4
8
12
16
20
24
AVERAGE E_b/N_o, DB, PER DIVERSITY CHANNEL

FIGURE 5-9

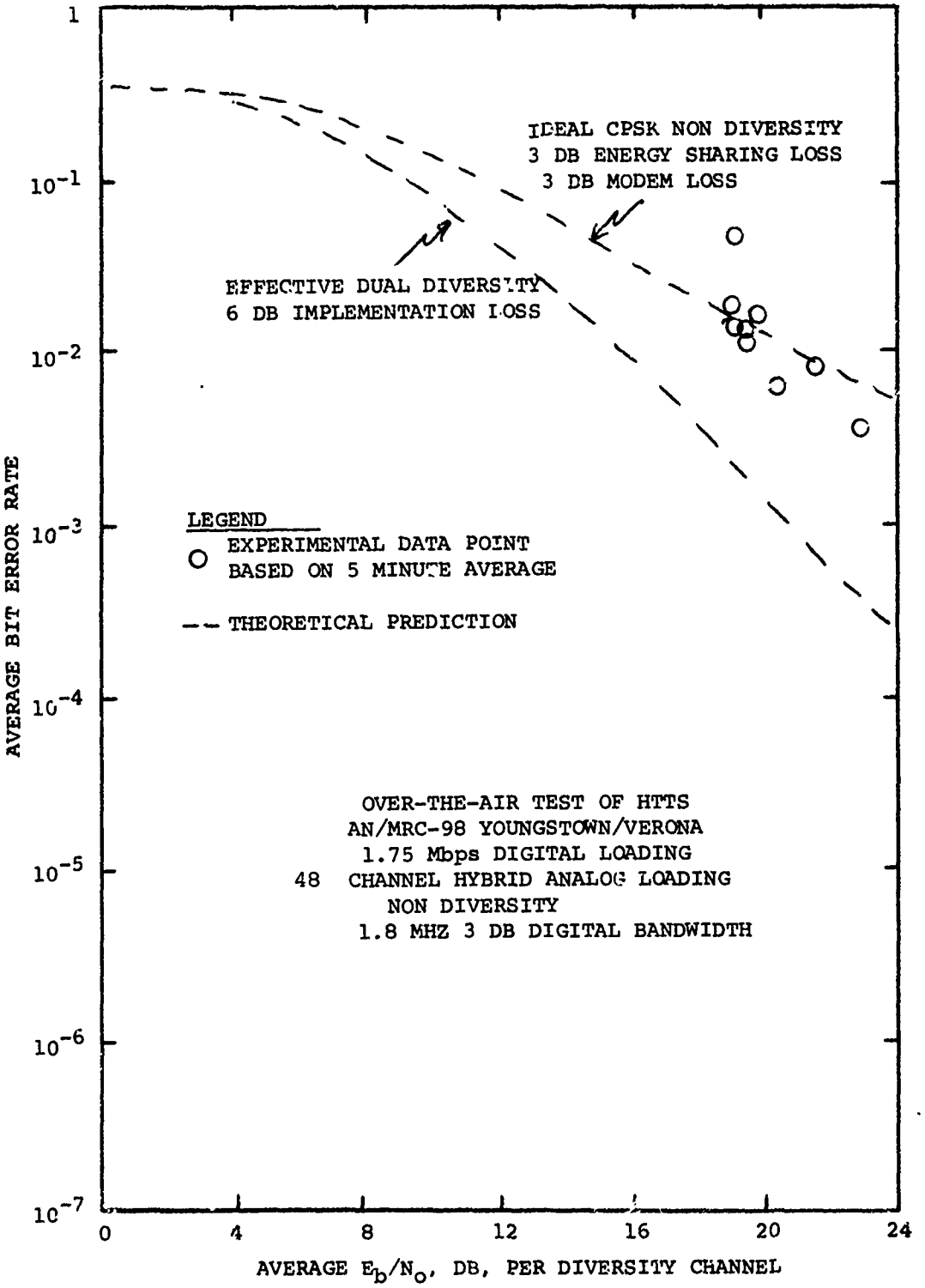
1
10^{-1}
10^{-2}
10^{-3}
10^{-4}
10^{-5}
10^{-6}
10^{-7}
AVERAGE BIT ERROR RATE
IDEAL CPSK NON DIVERSITY
3 DB ENERGY SHARING LOSS
3 DB MODEM LOSS
EFFECTIVE DUAL DIVERSITY
6 DB IMPLEMENTATION LOSS
LEGEND
EXPERIMENTAL DATA POINT
BASED ON 5 MINUTE AVERAGE
THEORETICAL PREDICTION
OVER-THE-AIR TEST OF HTTS
AN/MRC-98 YOUNGSTOWN/VERONA
1.75 Mbps DIGITAL LOADING
48 CHANNEL HYBRID ANALOG LOADING
NON DIVERSITY
1.8 MHZ 3 DB DIGITAL BANDWIDTH
0
4
8
12
16
20
24
AVERAGE E_b/N_o, DB, PER DIVERSITY CHANNEL

FIGURE 5-10

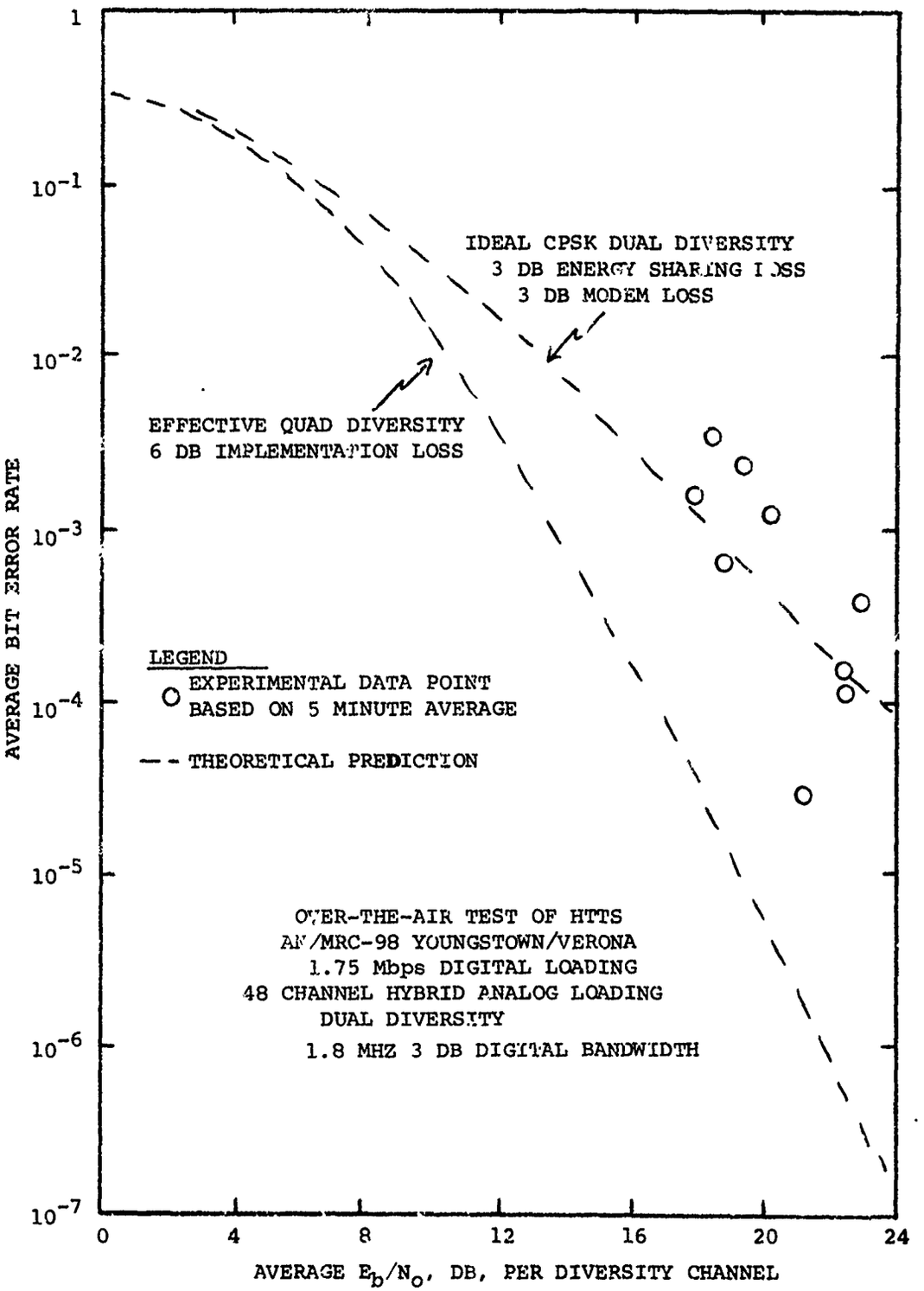
1
10^{-1}
10^{-2}
10^{-3}
10^{-4}
10^{-5}
10^{-6}
10^{-7}
AVERAGE BIT ERROR RATE
IDEAL CPSK DUAL DIVERSITY
3 DB ENERGY SHARING LOSS
3 DB MODEM LOSS
EFFECTIVE QUAD DIVERSITY
6 DB IMPLEMENTATION LOSS
LEGEND
EXPERIMENTAL DATA POINT
BASED ON 5 MINUTE AVERAGE
THEORETICAL PREDICTION
OVER-THE-AIR TEST OF HTTS
AF/MRC-98 YOUNGSTOWN/VERONA
1.75 Mbps DIGITAL LOADING
48 CHANNEL HYBRID ANALOG LOADING
DUAL DIVERSITY
1.8 MHZ 3 DB DIGITAL BANDWIDTH
0
4
8
12
16
20
24
AVERAGE E_b/N_o, DB, PER DIVERSITY CHANNEL

FIGURE 5-11

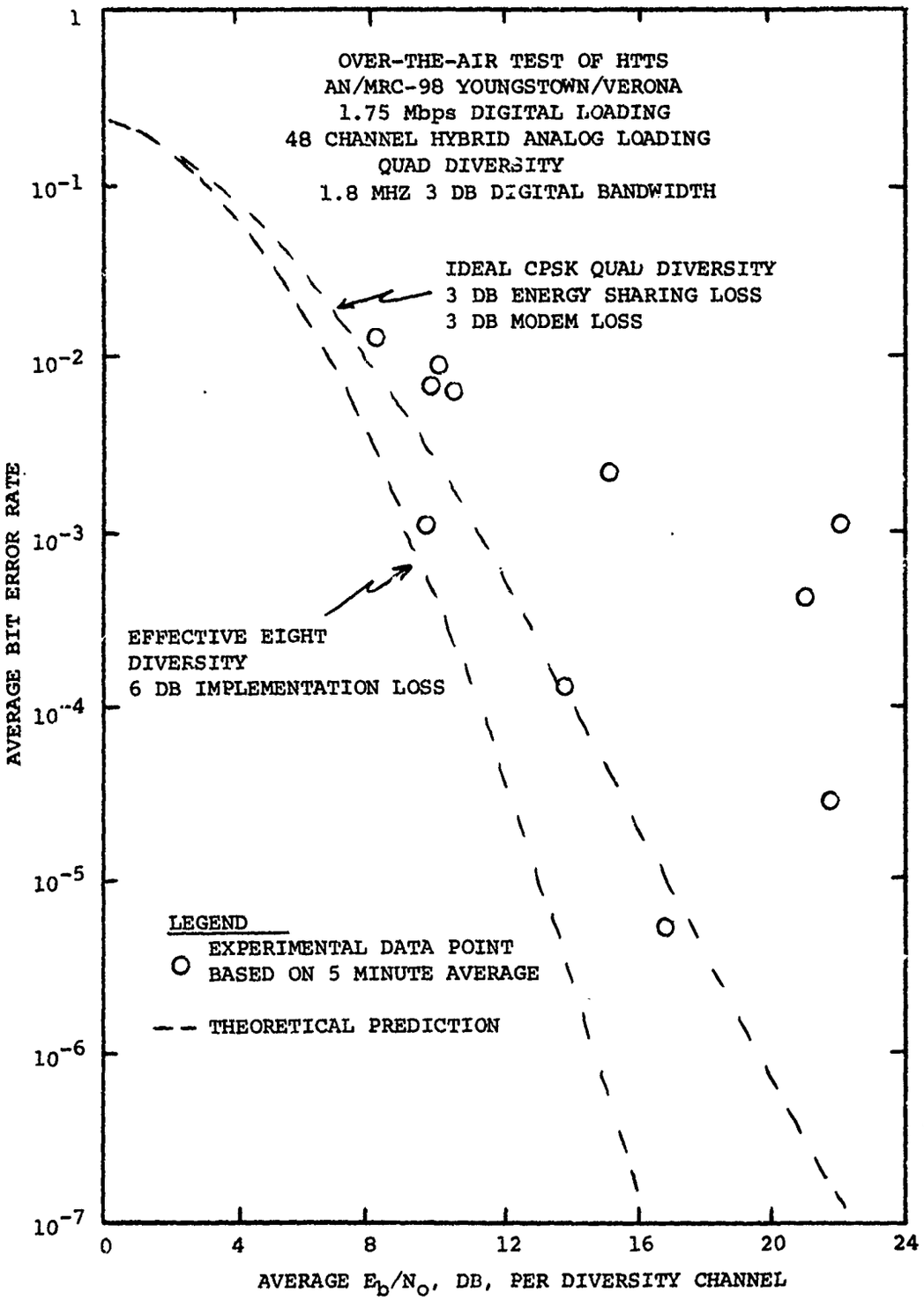
OVER-THE-AIR TEST OF HTTS
AN/MRC-98 YOUNGSTOWN/VERONA
1.75 Mbps DIGITAL LOADING
48 CHANNEL HYBRID ANALOG LOADING
QUAD DIVERSITY
1.8 MHZ 3 DB DIGITAL BANDWIDTH
IDEAL CPSK QUAD DIVERSITY
3 DB ENERGY SHARING LOSS
3 DB MODEM LOSS
EFFECTIVE EIGHT
DIVERSITY
6 DB IMPLEMENTATION LOSS
LEGEND
EXPERIMENTAL DATA POINT
BASED ON 5 MINUTE AVERAGE
THEORETICAL PREDICTION
AVERAGE BIT ERROR RATE
1
10^{-1}
10^{-2}
10^{-3}
10^{-4}
10^{-5}
10^{-6}
10^{-7}
0
4
8
12
16
20
24
AVERAGE E_b/N_o, DB, PER DIVERSITY CHANNEL

during this series of test runs. Measured error rates ranged from greater than 10^{-2} to almost 10^{-5}. The improvement gained from the added orders of diversity may be seen by comparing these results with those for dual diversity in Figure 5-16. Again, a minimal effect may be seen due to the increase in channel loading when comparing these results to those for 24 channel loading in Figure 5-8. Some intrinsic diversity improvement is observable but the major performance factor stems from degraded diversity performance due to the unequal signal levels.

5.5 Hybrid Test Results (Analog)

The AN/FCC-17 Frequency Multiplex equipment was configured for white noise loading for 24 or 48 channels. As described previously, only the even numbered channels were loaded while the odd numbered channels were left vacant to permit voice channel SNR's of greater than 30 dB to be measured. The FM outputs of the DAR-IV receiver unit Hybrid Translator were connected to a PDC-4 telemetry predetection combiner. The combiner output was applied to the AN/MRC-98 FM discriminator and baseband amplifier. The baseband information was subsequently demultiplexed by the AN/FCC-17 demultiplex unit and the top channel supplied to the Philco SNM-2 signal to noise ratio meter. For each test run, the output of the Philco signal to noise ratio meter was recorded on the RADC strip chart recorder along with the received signal level for each of the AN/MRC-98 receivers being used.

Test data was recorded for 24 and 48 channel loading in non, dual and quad diversity configurations. Figures 5-12 through 5-19 illustrate some typical data for each test configuration. Prior to each test sequence, the RADC control console performs a calibration run to establish reference input signal levels. These calibration marks may be seen and the left hand side of each data run in Figures 5-12 through 5-19 and serve as a guide in interpreting the strip chart data.

In all instances, the upper most strip of each group represents the top channel baseband signal to noise ratio as a function of time whereas the remaining strips in each grouping represent the received signal level for each receiver being employed during that particular data run over the exact same time period. Thus, direct relationships between the received signal level characteristics and the baseband signal to noise ratio may be obtained by drawing a vertical line through all the strips in a particular group.

Figure 5-12 illustrates some representative data for 24 channel loading in a non diversity configuration. These three groups illustrated the performance for relatively high, median and low average received signal levels respectively.

Figure 5-13 shows the performance for 24 channel loading in a dual diversity configuration. The lower most group demonstrates the DAR-IV performance during a period of extremely rapid fading during a period of apparent ducting. By noting the higher baseband SNR during this period, it can be seen that the DAR-IV is capable of following these rapid fades accurately.

Figure 5-14 and 5-15 represent 24 channel loading in a quad diversity configuration. Of particular interest in these runs is the performance again during a rapid fading period as seen in the upper group in Figure 5-14 and the performance during a period of scintillation due to an aircraft in the common volume as seen in the lower group of Figure 5-14. The aircraft's presence may be clearly seen on the RSL tracks by observing the pronounced peak in the signal level accompanied by very rapid fading.

In similar fashion, Figures 5-16 through 5-19 show the performance of the DAR-IV for 48 channel loading in non, dual, and quad diversity configurations. Again, these figures were selected to represent a variety of received signal levels as well as to illustrate performance during extreme channel conditions such as ducting and aircraft produced scintillations. As previously mentioned, by direct vertical comparisons with each group, the effect of the RSL characteristics may be seen in the baseband signal to noise ratio.

5.6 Summary of Hybrid Testing

The tests performed on the HTTS indicate that the dual subcarrier approach can be employed to provide simultaneous analog and digital transmission on troposcatter links. However, there is a penalty paid for this mode of operation due to energy sharing and the need to employ power backoff (6 to 8 db) at the transmitter. On many DCS troposcatter links, a loss of several dB in system gain will result in substantially reduced link availability. Hence, the hybrid approach to digital/analog troposcatter transmission would only be applied to links with excess average received signal strength from the viewpoint of path availability (percentage of time above threshold). A major feature of the HTTS is its low cross-talk between analog and digital subcarriers even in the presence of multipath which would not result in a conventional data under/over voice FDM-FM hybrid approach.

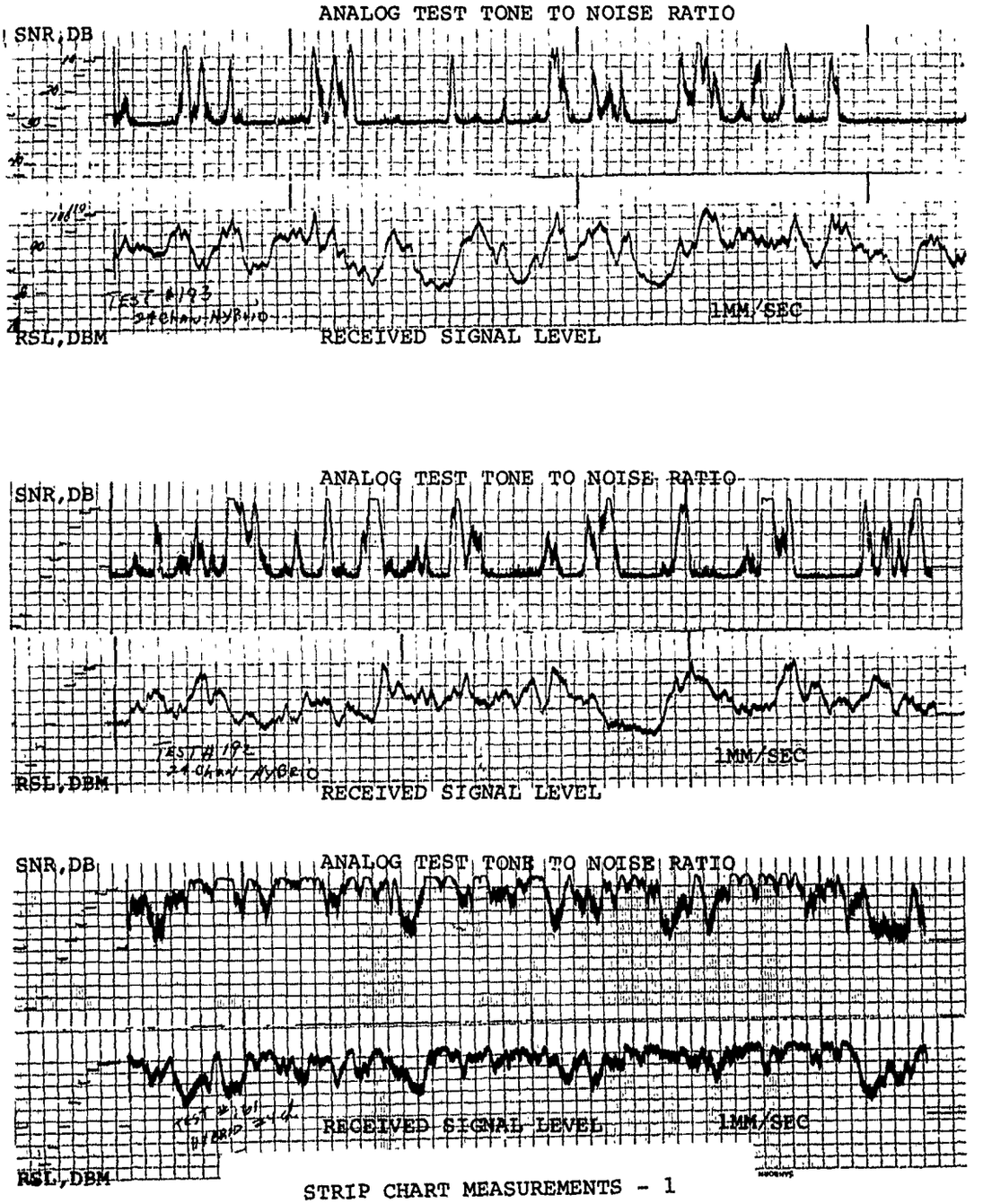

STRIP CHART MEASUREMENTS - 1

FIGURE 5-12

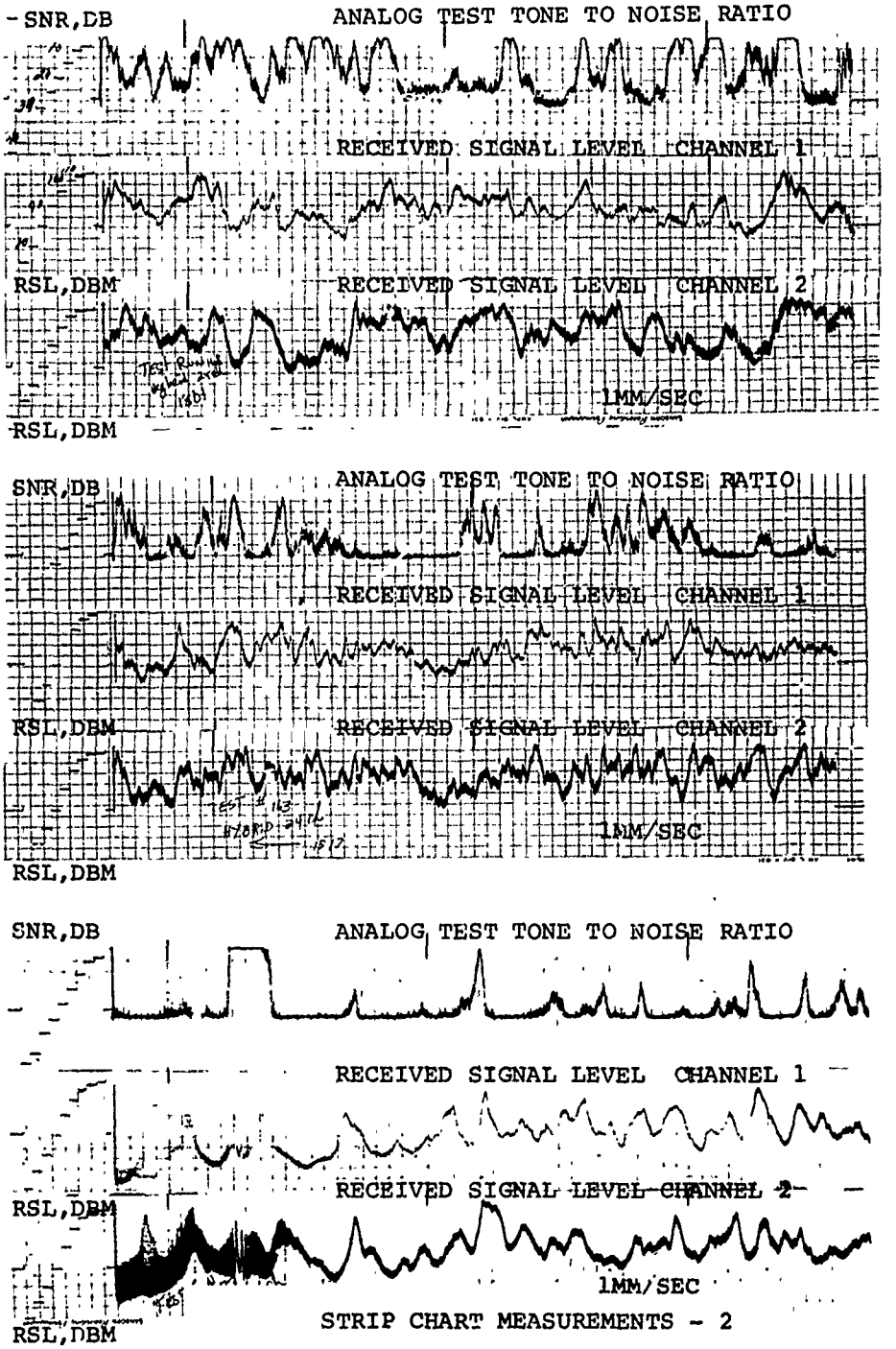

STRIP CHART MEASUREMENTS - 2

FIGURE 5-13

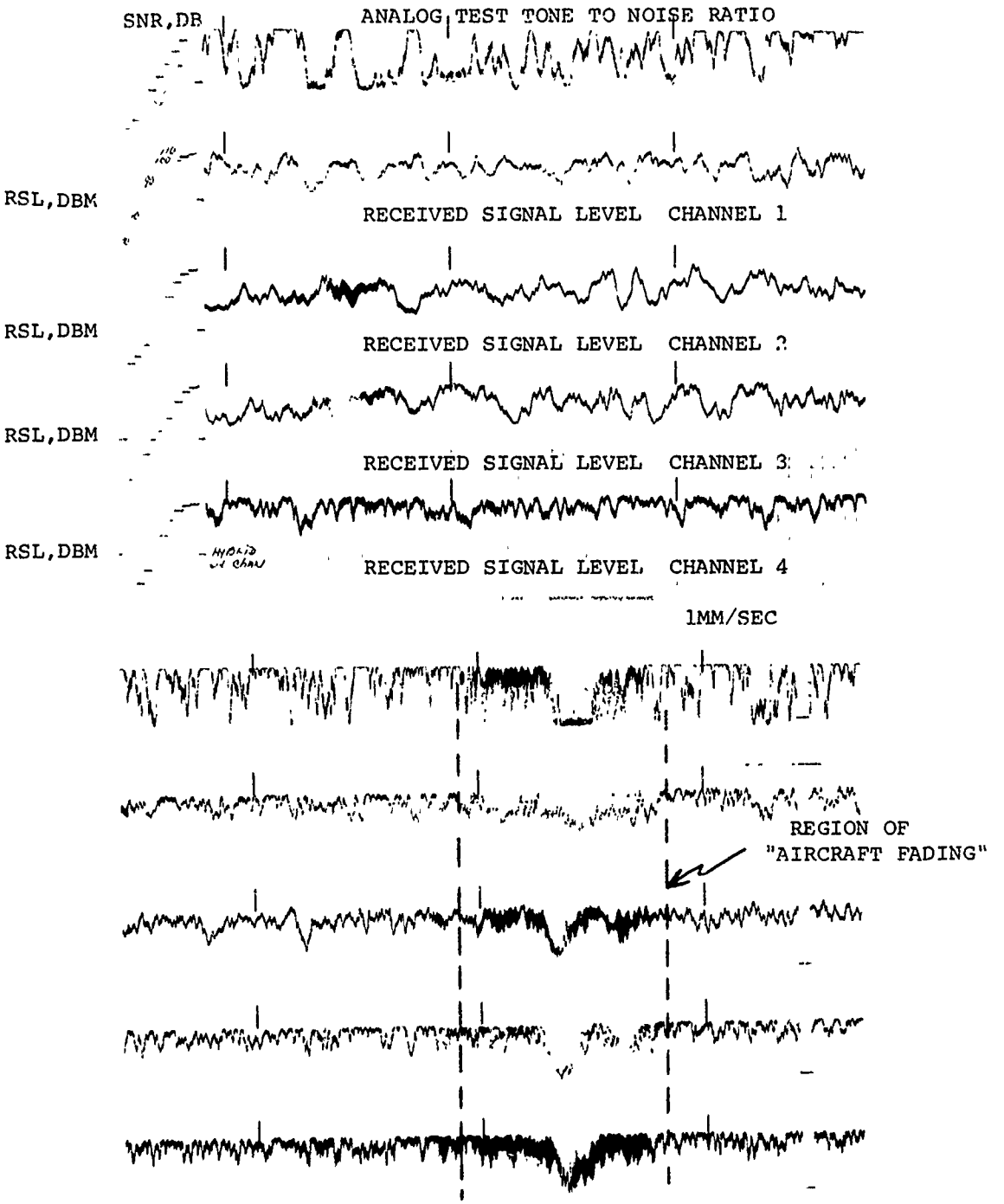

STRIP CHART MEASUREMENTS - 3
FIGURE 5-14

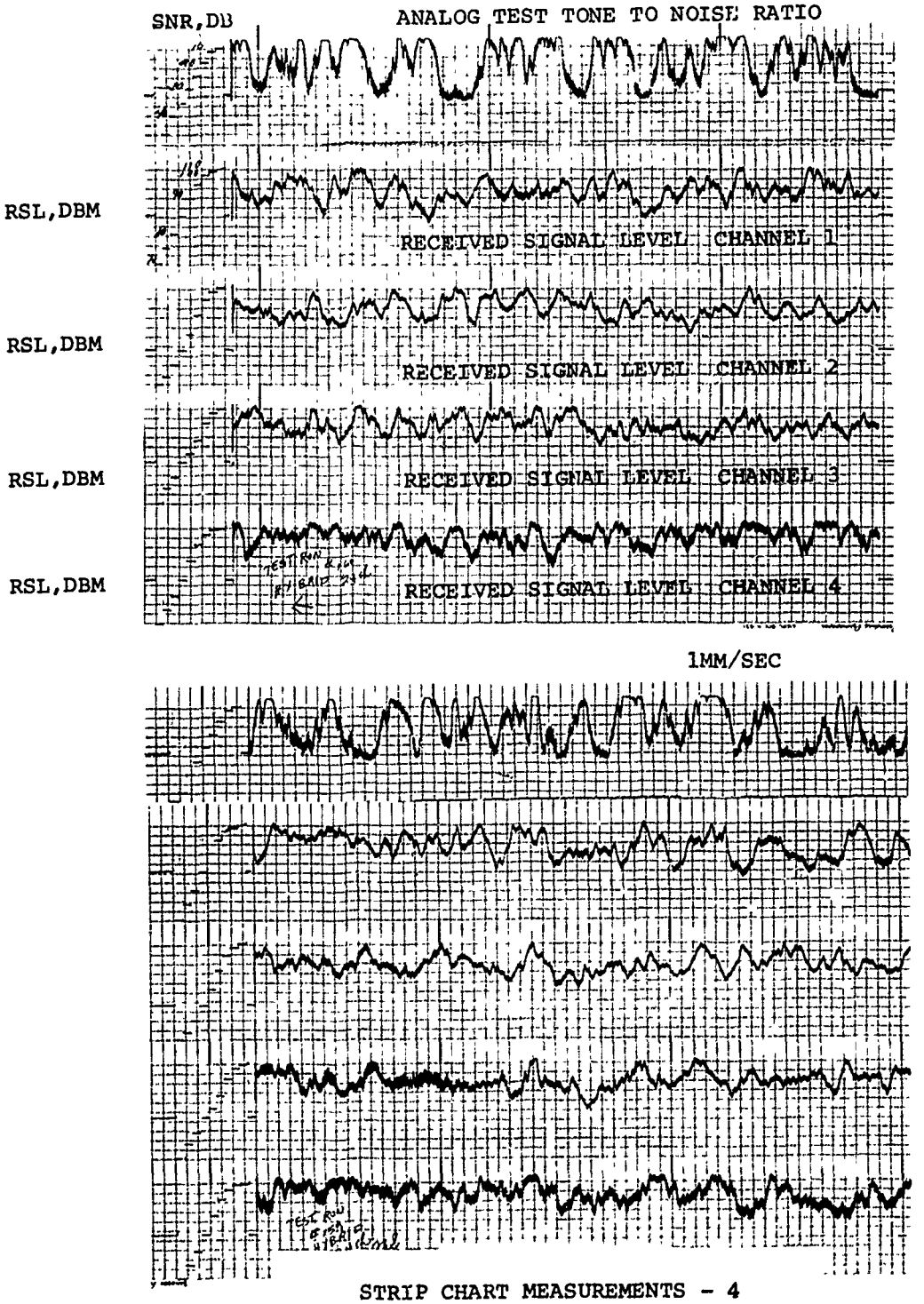

STRIP CHART MEASUREMENTS - 4
FIGURE 5-15

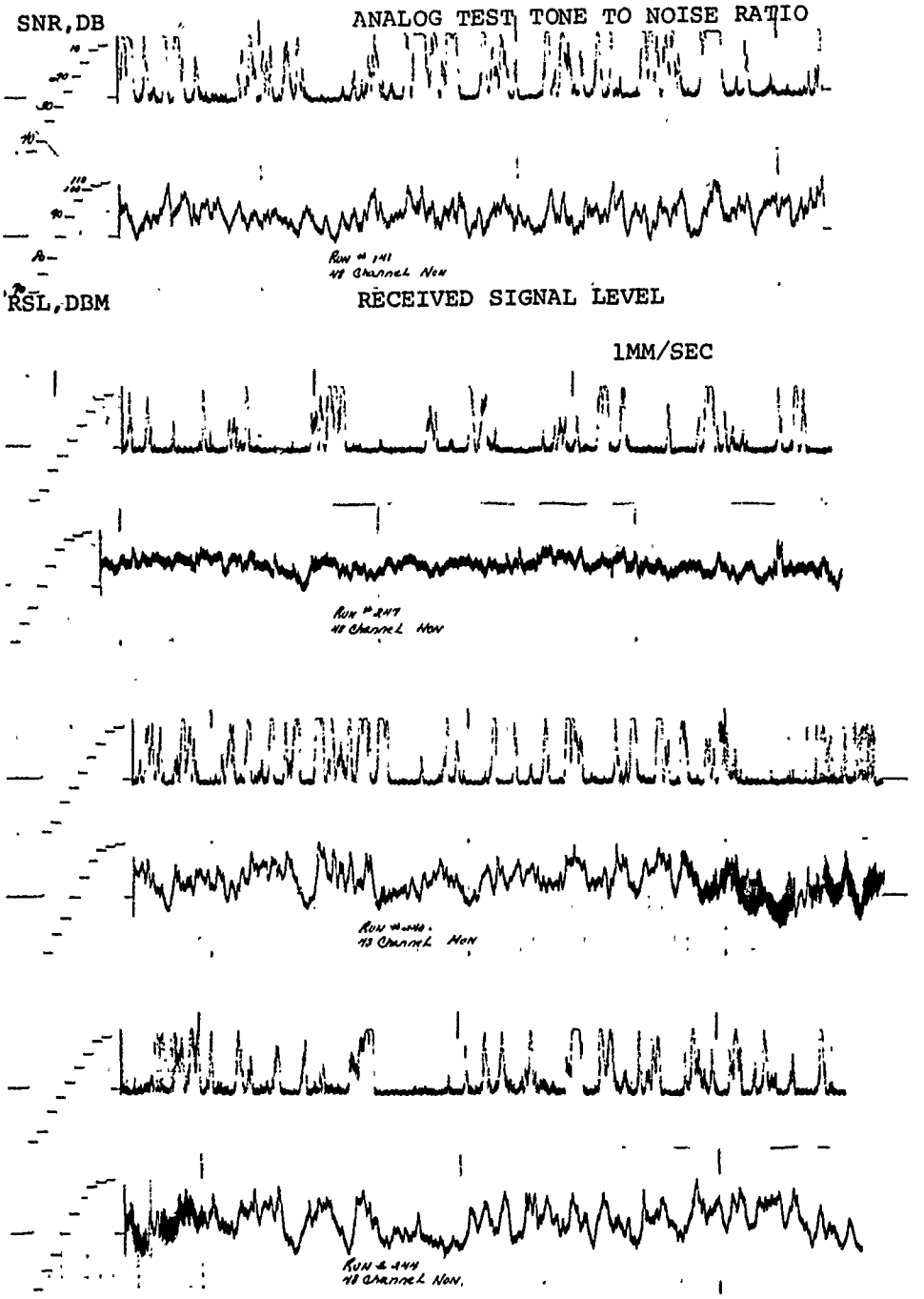

STRIP CHART MEASUREMENTS - 5
FIGURE 5-16

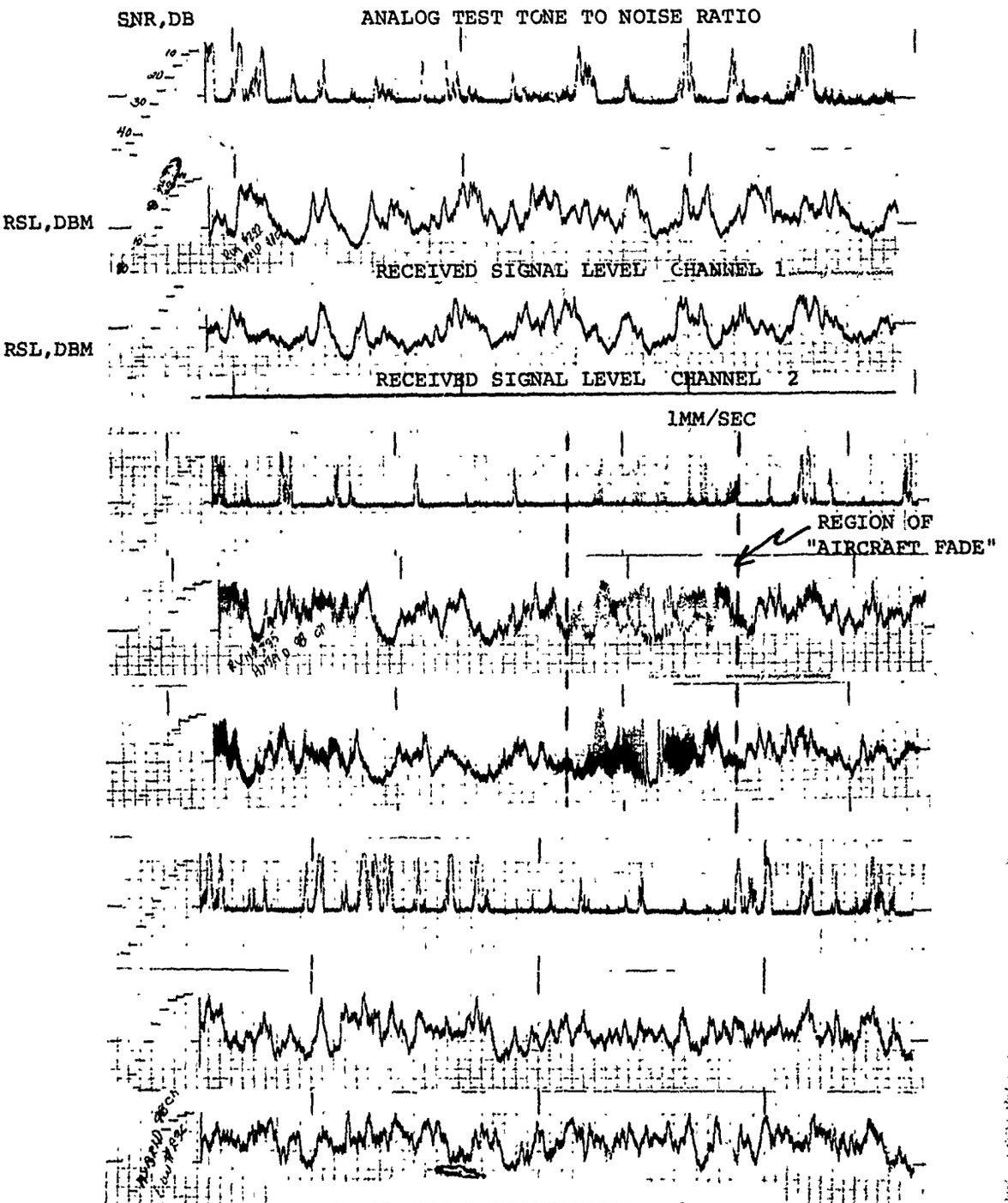

STRIP CHART MEASUREMENTS - 6
FIGURE 5-17

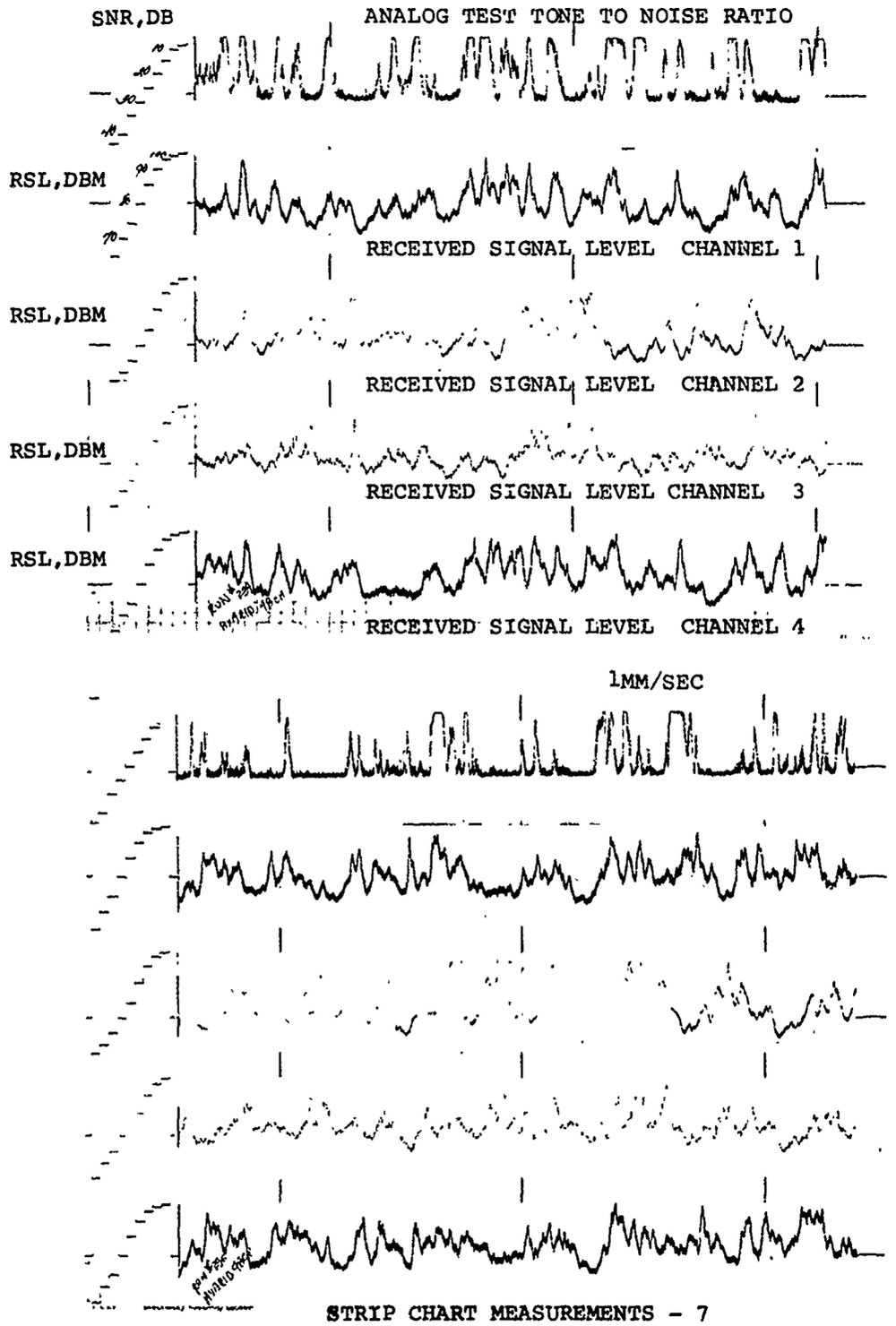

STRIP CHART MEASUREMENTS - 7
FIGURE 5-18

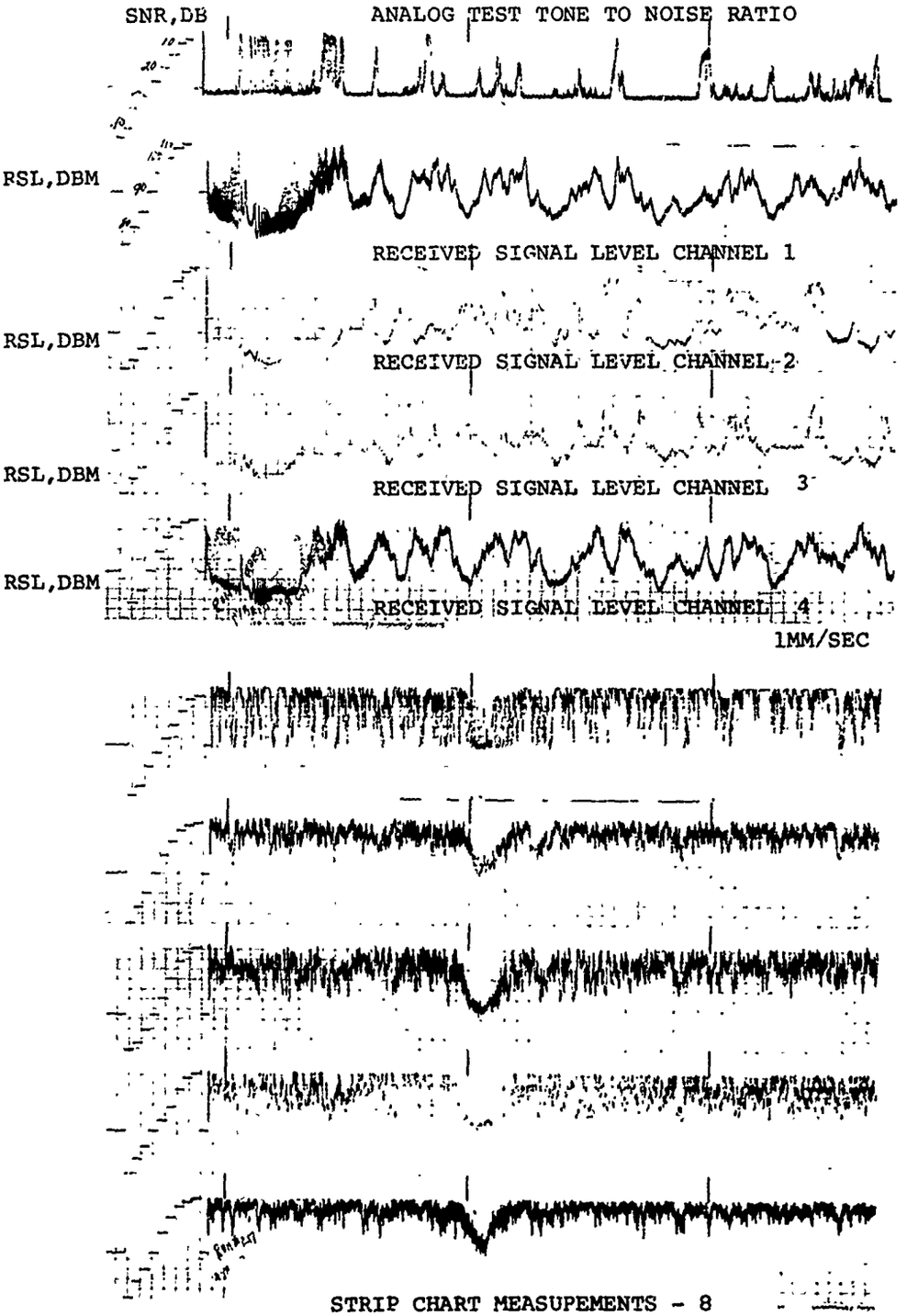

STRIP CHART MEASUPEMENTS - 8
FIGURE 5-19

MISSION
of
Rome Air Development Center

RADC plans and conducts research, exploratory and advanced development programs in command, control, and communications (C^3) activities, and in the C^3 areas of information sciences and intelligence. The principal technical mission areas are communications, electromagnetic guidance and control, surveillance of ground and aerospace objects, intelligence data collection and handling, information system technology, ionospheric propagation, solid state sciences, microwave physics and electronic reliability, maintainability and compatibility.